Publication No. R76-37

Order No. 554

INELASTIC DYNAMIC ANALYSIS OF BUILDING FRAMES

by
TAREK S. AZIZ

Supervised by
José M. Roesset

DEPARTMENT
OF
CIVIL
ENGINEERING

SCHOOL OF ENGINEERING
MASSACHUSETTS INSTITUTE OF TECHNOLOGY
Cambridge, Massachusetts 02139

August 1976

Sponsored by the National Science Foundation
Division of Advanced Environmental Research
and Technology
Grant GI-43106

Additional Copies May be Obtained from

National Technical Information Service
U.S. Department of Commerce
5285 Port Royal Road
Springfield, Virginia 22151

Massachusetts Institute of Technology
Department of Civil Engineering
Constructed Facilities Division
Cambridge, Massachusetts 02139

INELASTIC DYNAMIC ANALYSIS OF BUILDING FRAMES

by

Tarek S. Aziz

Supervised by

José M. Roesset

August 1976

Sponsored by National Science Foundation
Division of Advanced Environmental Research and Technology
Grant GI-43106

Research Report R76-37 Order No. 554

ABSTRACT

The nonlinear dynamic behavior of building frames is considered. The study covers basic points associated with inelastic dynamic analysis procedures. A formulation for the inelastic analysis of a building frame is presented. The formulation is general enough to take into consideration different nonlinearities which might occur in a building frame on a selective basis. Two types of nonlinearities are studied: those due to material behavior and those due to geometry changes. The importance of each nonlinear effect is studied separately and those effects which might be more important than others are pointed out. Among the different effects studied are the P-Δ and stability effects, the presence of gravity loads, axial deformations in the columns, joint size and nonlinear joint behavior, damping, and nonlinear soil-structure interaction.

Comparisons are made between different complex, intermediate, and simple models for inelastic dynamic analysis. From the studies performed, it would appear that for typical building frames a generalized bending model including all the nonlinear effects will yield results which are realistic and physically reasonable. Complex models can be theoretically more exact, but they are also more sensitive to numerical errors. For the cases studied, use of these complex and expensive models does not seem justified.

PREFACE

This report is based on a thesis written by Tarek Saleh Abdel Aziz in partial fulfillment of the requirements for the degree of Doctor of Science at M.I.T. The research was supervised by José M. Roesset, Professor of Civil Engineering, and sponsored by the National Science Foundation, Division of Advanced Environmental Research and Technology, under Grant GI-43106. It is the first of a series of reports describing research conducted under this Grant.

TABLE OF CONTENTS

LIST OF TABLES

LIST OF FIGURES

CHAPTER I

ANALYSIS OF NONLINEAR INELASTIC STRUCTURES

1.1 GENERAL

During the last decade a number of major developments have taken place in the area of inelastic analysis and design. The tremendous growth of research interest has resulted in a considerable amount of knowledge about the analysis and behavior of structures in the inelastic range. However, inelastic design has not as of today (1974) been fully recognized in the specifications of many countries, especially those provisions for seismic design. Inelastic design theory is for many applications a substantial improvement upon allowable stress theory where stress rather than load capacity is emphasized. The research on inelastic analysis and design has resulted in some changes in the basic design philosophy of structures. It has necessitated a more precise definition of the limits of usefulness of a structure and brought attention to the potential advantages of using different values of the load factor for different types of load. Even if the resulting savings in materials and design time have not been substantial, inelastic analysis and design is still necessary for a better understanding of the true behavior of structures.

For the aseismic design of structures it is being increasingly realized that inelastic deformations can happen and should be permit-

ted to produce economical and safe designs. Over a period of time a generally accepted design philosophy has emerged. It is based on the premise that the structure should remain elastic during small earthquakes, which occur frequently; should undergo "limited plastic deformation"during moderate size earthquakes; and may undergo large plastic deformations, without collapse, during infrequent large earthquakes. Design within the framework of this philosophy requires a detailed investigation of the inelastic behavior of structures under dynamic loading.

Current design procedures most probably result in satisfactory behavior under small earthquakes, but it is not yet generally possible to accurately predict the response of a structure in the inelastic range, and thus the execution of the second part of the design philosophy, i.e., that structures should resist very strong seismic disturbances without total collapse, is still subject to uncertainty.

The increasing cost of urban property is on the other hand making the use of highrise buildings in regions of high seismicity an economic necessity. The average highrise building today has virtually eliminated redundancy. The concrete exterior walls have disappeared in many cases in favor of curtain walls. Interior permanent walls are now lightweight construction, and partitions are kept floating most of the time. There is little or no uncalculated strength and the basic structural frame is thus required to carry the entire seismic load.

1.2 DYNAMIC COLLAPSE OF A STRUCTURAL SYSTEM

A major research effort has been directed to the application of ultimate design concepts to the design of building frames in which instability may affect the load-carrying capacity. Experiments have been conducted on full-scale braced and unbraced multistory frames to study their maximum load-carrying capacity under static loading. All tests under static loading showed conclusively that unbraced frames are likely to fail by overall instability before the formation of a plastic mechanism, and that any rational analysis and design procedure should attempt to include this effect.

Due to this effect the load-carrying capacity of a frame may become dependent on the resulting deflections. This kind of interdependence arises frequently in unbraced frames, and it would make a direct design almost impossible.

On the other hand, there have been some attempts in understanding the collapse mechanism of a multistory building under dynamic loading. However, there are still many unexplored parameters which act as contributing factors in causing the collapse of multistory building frames.

Investigation of the deterioration process and the dynamic collapse behavior of an actual structure can only be done if both gravity effects (the so-called P-Δ effect) and the strain hardening effects at least are taken into account in the formulation. The latter effect, favorable in the sense that it results in stable

restoring-force characteristics, may be considerably decreased or cancelled by the former.

1.3 THE PROBLEM

The problem considered here is the analysis and behavior of nonlinear inelastic planar frames. The structure is characterized by the fact that generalized distortions of the individual members are nonlinear functions of the applied generalized loads. The main reasons for nonlinearities are stability and plasticity.

Various conventional methods for determining the forces in the members and displacements of the joints of a structure are available. However, these methods depend upon a linear relationship between stress and strain. This relationship exists only when none of the stresses are above the proportional limit, and are not applicable if the stresses in any part of the structure exceed it.

1.4 HISTORICAL BACKGROUND

Nonlinear behavior of structures under dynamic loading has been a topic of interest for years, and the subject of considerable research throughout the past decade. Work in this area has proceeded basically along two main lines:

(a) In-depth study of the dynamic behavior of various simple, one-degree-of-freedom systems, to increase understanding of the effects of softening and hysteretic dissipation of energy on the response of different models, the effect of gravity loads, etc., both from a deterministic point of view and a probabilistic point of view. Some of the early papers on the subject focused on the inelastic response of single-degree-of-freedom systems with elasto-plastic force deformation relationships. Among such contributions is the work of Penzien[46] and Veletsos and Newmark[51], which advanced our knowledge on inelastic behavior and ductility requirements for simple systems.

Later systems with bilinear, trilinear or more general force deformation relationships were studied. Among these studies is the work of Jennings[34, 35], on Ramberg Osgood systems including as particular cases elastic and elasto-plastic behavior, and the work of Veletsos.[50] Hanson[30] studied the inelastic dynamic response of mild steel structures and concluded that their force displacement relationship could be represented by an expression of the type suggested by Jennings.

Husid[33] examined the effect of gravity loads (P-Δ effect) on the response of an elasto-plastic one-degree-of-freedom system. He concluded that the effect was significant and was characterized by a plastic drift. The systems he studied were, however, unrealistic for actual one-degree-of-freedom models, and the extrapolation to

actual structures is difficult. It would seem also that the results are sensitive to the assumed force deformation relationship. The possible importance of this effect is not closely known, and it is the subject of some controversy at the present time.

(b) Studies on multi-degree-of-freedom systems and particularly plane, ductile frames. Models with different degrees of complexity have been developed for these analyses.

Clough and Benuska[16] performed a study for HUD. The model they presented can be considered as intermediate as far as complexity is concerned. Plastic hinges are assumed to occur only at the ends of each member, with a bilinear moment-curvature relationship. Such effects as the spreading of yielding, nonlinear geometry (P-Δ effect), variation in axial stiffness with progressive yielding and axial bending coupling are neglected. As a matter of fact, even the effect of axial load on the moment capacity of a section was not explicitly considered.

Goel[25, 26] used a model which consists of an equivalent single bay, multistory, rigidly jointed frame that is symmetrical about its vertical centerline. The conversion is equivalent to assuming that all joints at one floor level of the original structure deflect and rotate by equal amounts at all times during the response. The girders in his model follow the nonlinear moment-curvature behavior as defined by the Ramberg-Osgood function. Improvements in Clough and Goel's work have been introduced by Anderson[4, 5, 6], among others.

These improvements include typically consideration of an interaction type formula to determine moment capacity as a function of axial load, different functions for the moment-curvature relationship, and inclusion of P-Δ effects. Lionberger and Weaver[42] considered also the effect of finite joint sizes and nonrigid joints. Bertero[12] presented a simplified formulation of panel zone mechanisms in which he assumed that the single component of panel zone distortion is a shear distortion by virtue of which the rotation of the columns and the rotation of the girders at the joint need no longer be identical. These assumptions might be reasonable for panel zones in interior columns, where both girders framing into the joints are approximately of the same depth. Their extension to exterior columns and top-story joints had to be accepted without experimental substantiation. All these modifications are relatively minor from the point of view of complexity and time of computation.

More complex models, attempting to reproduce some of the other effects and in particular the spreading of yielding and its influence on both bending and axial stiffness, have been used by different authors. Baron and Venkateson[9] studied the inelastic dynamic response of a prismatic segment by tracing the stress-strain history of various fibers at discrete cross sections. The same model had been used for one-story one-bay frames by Perez[47] and was extended to multistory frames by Latona.[40] Latona verified the validity of the model for predicting elastic behavior and elastic stability, but

could not verify its ability to predict inelastic behavior.

The author[8] presented a mathematical model for the analysis of frames which was used to study the incremental static analysis of steel frames loaded to collapse. In this model both the effects of local and overall instability are included, as well as all the nonlinear effects. The model of course is expensive compared to the bending or the interaction models.

At the other end of the spectrum, Anagnostopoulos[3] formulated a simple model which is very economical and which could be used for the approximate nonlinear analysis of a complete building. The model is attractive, since the building is reproduced as a system of different nonlinear springs in space, each spring corresponding to a story of a structural element. Application of the model is, of course, restricted to a certain class of typical buildings. Average effects for a story of a given structural component are studied, rather than the values for a particular joint or member. Use of this model requires, however, preliminary computations and a great deal of engineering judgement to select the most appropriate spring constants for each one.

Table 1.1 presents a short summary of these models, the effects they include, and the type of structures which were analyzed.

Table 1.1

Summary of Models for Nonlinear Analysis of Buildings

Intermediate Models	Solution Scheme, Effects Attempted to Include, and Structures Analyzed.
CLOUGH & BENUSKA	Only point hinges with bilinear moment-curvature relationship. Plane frames and shear walls.
GOEL & HANSON	Point hinges with Ramberg-Osgood moment-curvature relationship and interaction-type formulation for axial loads. P-Δ effects. Yield-forced to occur in the girders. One-bay multistory frames.
ANDERSON & BERTERO	Point hinges with bilinear moment-curvature relationship and interaction-type formula for axial loads, P-Δ effects. One-bay multistory frames designed by different philosophies.
Complex Models	
LATONA & ROESSET	Tangent formulation, including spreading of yielding, inelastic axial behavior, axial bending coupling, overall elastic stability.
AZIZ	Secant formulation, including spreading of yielding, inelastic axial behavior, axial bending coupling, local and overall inelastic stability and post-buckling analysis. Static loads only.
Simple Models	
ANAGNOSTOPOULOS & ROESSET	Frames reproduced as close-coupled systems, with one spring per story. Shear walls reproduced as for coupled systems, same as in Clough's model. Total buildings including torsional effects.

1.5 SCOPE OF THE RESEARCH

In Chapter II a general formulation for a mathematical uncoupled bending model is presented. The model developed is capable of taking into consideration all the nonlinear effects in a convenient, systematic way. The solution is developed and implemented in such a way that some of these nonlinear effects can be intentionally neglected as well. Chapter III contains an extensive comparative study of different bending models. The study is carried out in a systematic way to compare the relative importance of different aspects of the problem. Consideration is given to different ductility definitions, soil-structure interaction, the overshooting and the backtracking problems and comparisons with results of other researchers. Analyses for a 10-story frame are presented. In Chapter IV studies for three frames available in the literature were conducted, using the most general bending model developed which includes all the nonlinear effects and the least general bending model which neglects all the nonlinear effects. This study was carried out in conjunction with a parallel study using a simple trilinear story-wise model as implemented by Anagnostopoulos.[3] Chapter VI contains a comparative study for a three-story frame using the generalized bending model and a fiber model. The conclusions and recommendations for future research are presented in Chapter VII.

CHAPTER II

GENERAL FORMULATION OF A MATHEMATICAL UNCOUPLED BENDING MODEL

2.1 GENERAL

Nonlinear behavior of structures under dynamic and static loading has been a topic of interest for years and the subject of considerable research throughout the past decade. Most of the work in the area has proceeded basically along two directions; simple models where one might be interested in the overall behavior, and more elaborate models where one might be interested in local effects. It is useful here to distinguish between two approaches for analysis.

(1) "Elastic-Plastic Analysis," where it is assumed that plastic hinges form at discrete points but the remainder of the structure remains elastic.

(2) "Compatibility analysis," where consideration is given to the zones of partial plastification and the M-P-ϕ and M-P-ε^* relationships are used directly or indirectly.

It is also useful to distinguish between types of analysis which give the following amount of information, especially under incremental static loading:

(1) Loads and deflections of the structure immediately prior to failure.

(2) Behavior of the frame under the full possible range of loading.

2.2 BASIC PHILOSOPHY BEHIND A BENDING MODEL

As mentioned before, "Elastic-Plastic Analysis" is based on the assumption that plastic hinges form at discrete points, but the remainder of the structure remains elastic. This is the basic philosophy behind what will be termed in the following the "Bending Model." This model is considered a generalization for the "Elastic-Plastic Analysis," since the elasto-plastic behavior in the Bending Model (BM) is not a necessary idealization. However, the concept of a point hinge is a basic characteristic of the model. An analysis using a BM can be illustrated as follows:

Consider a frame to have external loads applied to it which are proportionally increasing. The loads might be static or dynamic and the only requirement is that they are defined by a single load factor "λ". The frame will behave entirely elastically until the bending moment at an end of one member is reached. If loading is continued, this section will take no additional bending moment, thus acting as a plastic hinge. On subsequent loading the rest of the frame will still behave elastically and a prediction of a second plastic hinge can be undertaken. Thus the behavior can be traced against the load factor in a static problem or against time in a dynamic problem.

2.3 SINGLE COMPONENT MODEL SCM

The single component model "SCM" is a model in which each member in the structure is treated as a single elastic component

which is connected to the rest of the structure in a way which depends on the levels of end forces. For example, if the level of forces exceeds the plastic limit at the beginning of a member, the member is treated as being released at this end.

The SCM in its simple form as presented above is the basis for the rigid-plastic analysis of structures, and was first suggested by Giberson [22].

2.4 DUAL COMPONENT MODEL DCM

The concept of a dual component model was first introduced by Clough[16](1967). It provides a form of bilinear moment resistance for each member. While it has no obvious physical meaning, it is a mathematical way of arriving at engineering results. In this model the following is done:

Each member is assumed to consist of two components acting in parallel: a basic elasto-plastic component which develops a plastic hinge at either end when the end moment exceeds a specified yield value, M_p, and a second component which remains fully elastic. A typical member is shown in Fig. 2.1(a). It is noted that the fully elastic component is rotated at each end through the total joint angle, θ, while the elasto-plastic component deforms elastically only through the angle, ϕ. The additional joint rotation, α, indicated in these components represents the plastic hinge deforma-

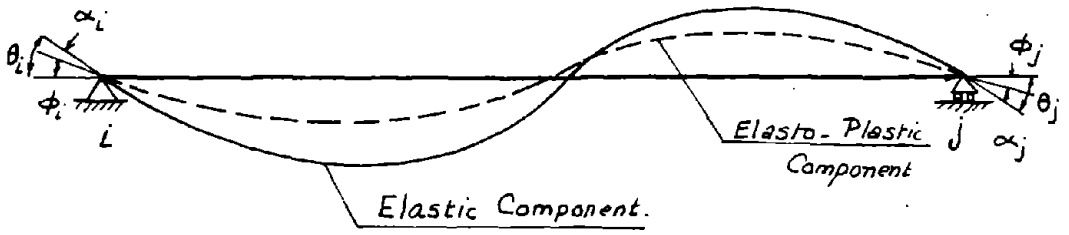

(a) Dual Component Model DCM

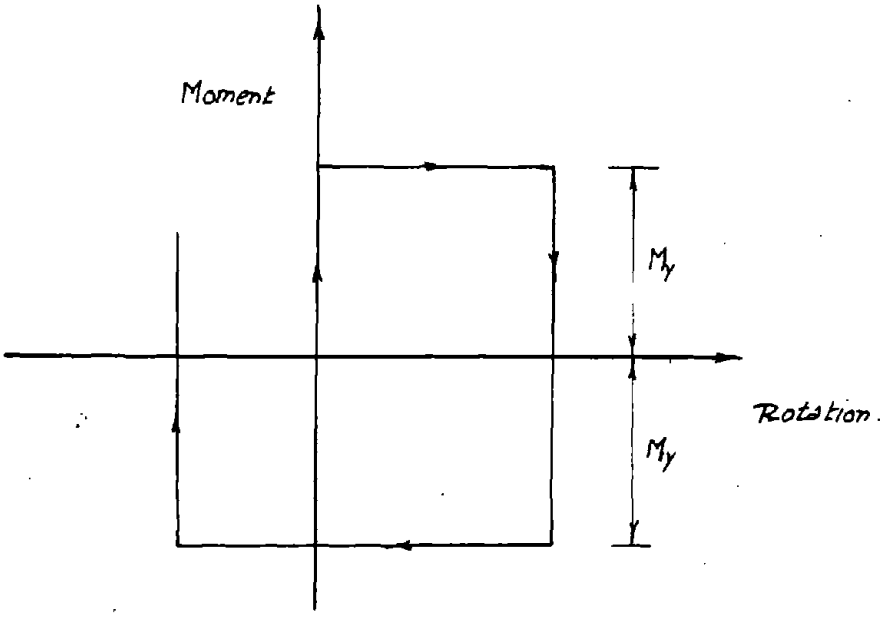

(b) Hinge Characteristics - Elasto-plastic Component

Fig. 2.1 Behavior of a Dual Component Model DCM

tion, which is assumed to have the ideal plastic hinge property depicted in Figure 2.1(b). It should be mentioned here that the total moment continues to increase beyond the yield value, due to the contribution of the elastic component, the amount of this increase can be controlled by using a very flexible elastic component.

In general the incremental end forces can be written in terms of the incremental displacements as follows:

$$\{\Delta F\} = [K]_t \{\Delta u\} \tag{2.1}$$

The tangent stiffness matrix $\underset{\sim}{K}_t$ depends on the status of the member and whether the yield moments at the ends of the member have been exceeded or not. Four different member yield conditions may be defined, for which the tangent stiffness coefficients are:

Case (I) Elastic Member - No Hinges:

$$\underset{\sim}{K}_t = \begin{bmatrix} \frac{EA}{L} & 0 & 0 & \frac{EA}{L} & 0 & 0 \\ 0 & \frac{12EI}{L^3(1+2\beta)} & \frac{6EI}{L^2(1+2\beta)} & 0 & \frac{-12EI}{L^3(1+2\beta)} & \frac{6EI}{L^2(1+2\beta)} \\ 0 & \frac{6EI}{L^2(1+2\beta)} & \frac{4EI}{L}\cdot\frac{(2+\beta)}{2(1+2\beta)} & 0 & \frac{-6EI}{L^2(1+2\beta)} & \frac{2EI}{L}\cdot\frac{(1-\beta)}{1+2\beta} \\ \frac{EA}{L} & 0 & 0 & \frac{EA}{L} & 0 & 0 \\ 0 & \frac{-12EI}{L^3(1+2\beta)} & \frac{-6EI}{L^2(1+2\beta)} & 0 & \frac{12EI}{L^3(1+2\beta)} & \frac{-6EI}{L^2(1+2\beta)} \\ 0 & \frac{6EI}{L^2(1+2\beta)} & \frac{2EI}{L}\cdot\frac{(1-\beta)}{(1+2\beta)} & 0 & \frac{-6EI}{L^2(1+2\beta)} & \frac{4EI}{L}\frac{(2+\beta)}{2(1+2\beta)} \end{bmatrix} \quad (2.2)$$

or

$$\underset{\sim}{K}_t = \begin{bmatrix} S_1 & 0 & 0 & -S_1 & 0 & 0 \\ 0 & S_4 & S_3 & 0 & -S_4 & S_6 \\ 0 & S_3 & S_2 & 0 & -S_3 & S_5 \\ -S_1 & 0 & 0 & S_1 & 0 & 0 \\ 0 & -S_4 & -S_3 & 0 & S_4 & -S_6 \\ 0 & S_6 & S_5 & 0 & -S_6 & S_7 \end{bmatrix} \quad (2.3)$$

where $$\beta = \frac{6EI}{L^2 GA_s} \quad (2.4)$$

and

E = Youngs Modulus of Elasticity

A = Area of the section

I = Moment of inertia of the section

A_s = Shear Area

G = Shear Rigidity Modulus.

L = Length of the Member

$S_1, S_2, S_3, S_4, S_5, S_6$ and S_7 are the stiffness coefficient.

It is worth mentioning that for a member of constant (EI) and constant (EA), $S_6 = S_3$ and $S_7 = S_2$. However, for a member of variable (EI) and (EA) $S_3 \neq S_6$ and $S_7 \neq S_2$.

Case (II) Hinge at End j

$$\underset{\sim}{K}'_t = \begin{bmatrix} S_1' & 0 & 0 & -S_1' & 0 & 0 \\ 0 & S_4' & S_3' & 0 & -S_4' & S_6' \\ 0 & S_3' & S_2' & 0 & -S_3' & S_5' \\ -S_1' & 0 & 0 & S_1' & 0 & 0 \\ 0 & -S_4' & -S_3' & 0 & S_4' & -S_6' \\ 0 & S_6' & S_5' & 0 & -S_6' & S_7' \end{bmatrix} \tag{2.5}$$

where:

$$S_1' = S_1 \tag{2.6}$$

$$S_2' = \beta_1 S_2 + \beta_2 \left(S_2 - \frac{S_5 S_5}{S_7}\right) \tag{2.7}$$

$$S_3' = \beta_1 S_3 + \beta_2 \left(S_3 - \frac{S_5 S_6}{S_7}\right) \tag{2.8}$$

$$S_4' = \beta_1 S_4 + \beta_2 \left(S_4 - \frac{S_6 S_6}{S_7}\right) \tag{2.9}$$

$$S_5' = \beta_1 S_5 \tag{2.10}$$

$$S_6' = \beta_1 S_6 \tag{2.11}$$

$$S_7' = {}_1 S_7 \tag{2.12}$$

Case (III) Hinge at End i:

$$\underset{\sim}{K}_t'' = \begin{bmatrix} S_1'' & 0 & 0 & -S_1'' & 0 & 0 \\ 0 & S_4'' & S_3'' & 0 & -S_4'' & S_6'' \\ 0 & S_3'' & S_2'' & 0 & -S_3'' & S_5'' \\ -S_1'' & 0 & 0 & S_1'' & 0 & 0 \\ 0 & -S_4'' & -S_3'' & 0 & S_4'' & S_6'' \\ 0 & S_6'' & S_5'' & 0 & -S_6'' & S_7'' \end{bmatrix} \tag{2.13}$$

where:

$$S_1'' = S_1 \tag{2.14}$$

$$S_2'' = \beta_1 S_2 \tag{2.15}$$

$$S_3'' = \beta_1 S_3 \tag{2.16}$$

$$S_4'' = \beta_1 S_4 + \beta_2 \left(S_4 - \frac{S_3 S_3}{S_2}\right) \tag{2.17}$$

$$S_5'' = \beta_1 S_5 \tag{2.18}$$

$$S_6'' = \beta_1 S_6 + \beta_2 \left(S_6 - \frac{S_5 S_3}{S_2}\right) \tag{2.19}$$

$$S_1'' = \beta_1 S_7 + \beta_2 \left(S_7 - \frac{S_5 S_5}{S_2}\right) \tag{2.20}$$

Case (IV) Hinges at Both Ends:

$$K_t''' = \begin{bmatrix} S_1''' & 0 & 0 & -S_1''' & 0 & 0 \\ 0 & S_4''' & S_3''' & 0 & -S_4''' & S_6''' \\ 0 & S_3''' & S_2''' & 0 & -S_3''' & S_5''' \\ -S_1''' & 0 & 0 & S_1''' & 0 & 0 \\ 0 & -S_4''' & -S_3''' & 0 & S_4''' & S_6''' \\ 0 & S_6''' & S_5''' & 0 & -S_6''' & S_7''' \end{bmatrix} \quad (2.21)$$

where:

$$S_1''' = S_1 \quad (2.22)$$

and

$$S_i''' = \beta_1 S_i \qquad i \neq 1 \quad (2.23)$$

β_1 and β_2 are defined as follows:

β_1 = strain hardening factor in the model and is given by the slope of its elastic component

and

$$\beta_2 = (1 - \beta_1). \quad (2.24)$$

2.5 A GENERAL SINGLE COMPONENT MODEL GSCM

A General Single Component Model is by definition a model where the member is treated as one integrated part which is connected to the rest of the structure in a certain way. The GSCM has the advantages that many of the nonlinear effects can be introduced easily. It has a very clear physical meaning and its results are directly related to some phenomena familiar to the practicing engineer. Moreover its parameters are derived experimentally or assumed to match the situation faced in practice.

Before deriving the stiffness of GSCM, it is convenient to look at the structure being modeled in a more practical way. The structure consists of a series of members joined to each other by connections. In conventional structural analysis it is assumed that these connections are rigid, which is rarely the case. A typical steel connection is shown in Fig. 2.2a. Under a moment transferred by the member the connection deforms as shown in Fig. 2.2(b) through an angle θ which is the angle of misfit. Realistically the problem might be even more complicated, since the amount of distortion is generally dependent on the axial and shearing forces in the member. However, for all practical purposes it will be assumed that a relation exists between the applied moment from the member "M" and the corresponding distortion "θ". Such relations have been measured experimentally and are reported in different places. A general form of this relation might take the shape

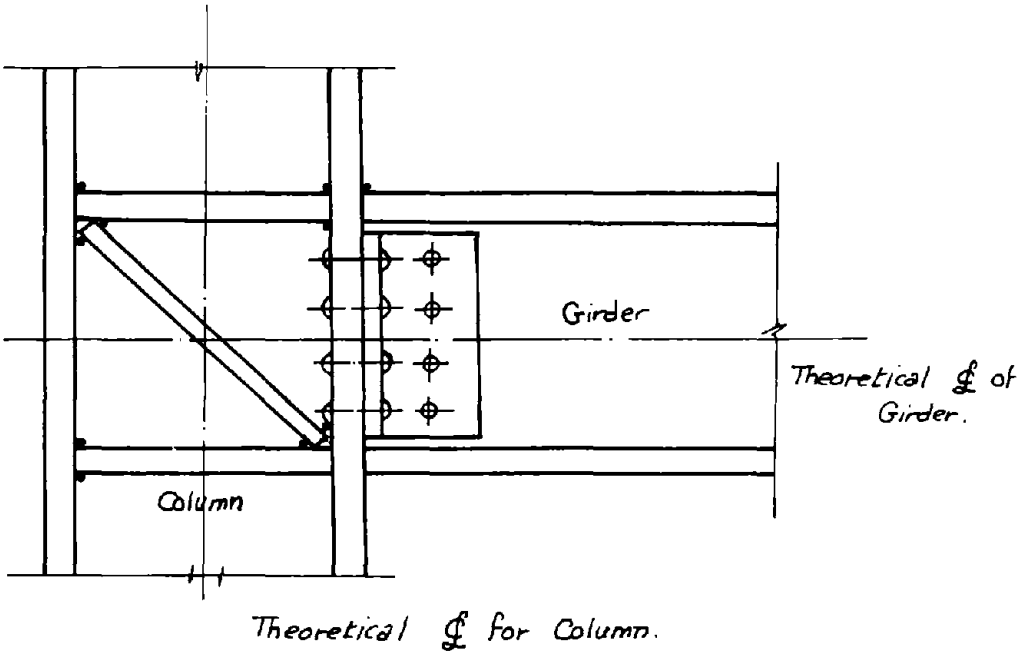

(a) Typical Steel Joint in a Structure.

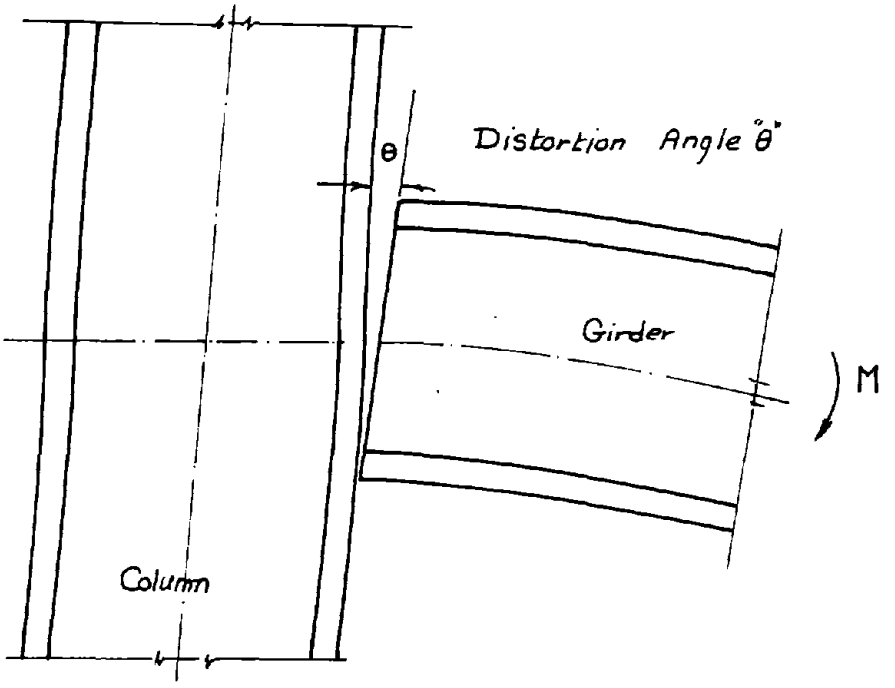

(b) Typical Steel Joint When Distorted.

Fig. 2.2 - Behavior of A Typical Joint

shown in Fig. 2.3a.

The only and basic assumption in GSCM which cannot be relaxed is that such a relation between M and θ exists and is known beforehand. This means that M-θ curves for the joints should be provided as initial data for the problem. These can be obtained from experimental results or by an engineering idealization of the behavior.

The physical meaning of the moment rotation relationship is clear when applied to the behavior of the joint. If, on the other hand, yielding takes place in the member itself, it is necessary to assume or compute a plastification length to define the yield rotation, and further approximations have to be introduced into the analysis.

2.5.1 Theoretical Formulation of GSCM

The stiffness of a member with shear deformation is as given by equation 2.2. Assuming for the time being that only the case of elastic member is considered, and using a sign convention as shown in Fig. 2.3(c), one can write:

$$\{u'\} = \{u\} + [JF]\{F\} \tag{2.25}$$

where $\{u'\} = \begin{bmatrix} u_1' \\ u_2' \\ u_3' \\ u_4' \\ u_5' \\ u_6' \end{bmatrix}$ = Joint displacements vector (2.26)

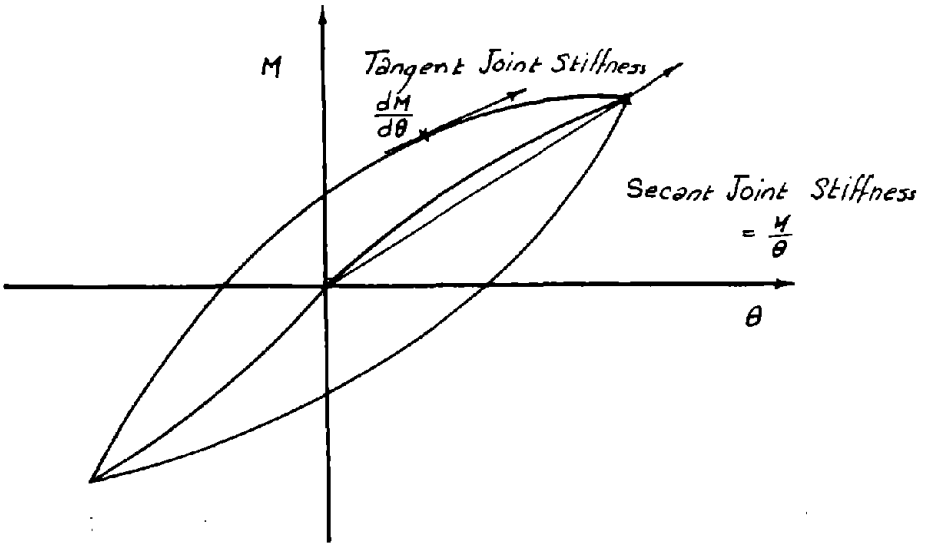

(a) General Behavior of a Joint as defined by a General M-θ Curve.

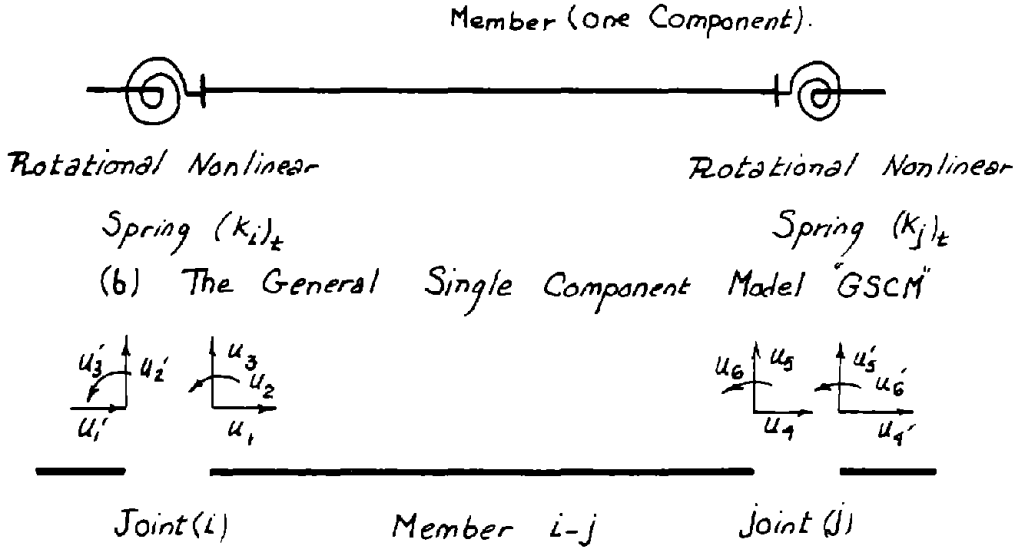

(b) The General Single Component Model "GSCM"

(c) Sign Conventions

Fig. 2.3 - General Single Component Model

and $$\{u\} = \begin{bmatrix} u_1 \\ u_2 \\ u_3 \\ u_4 \\ u_5 \\ u_6 \end{bmatrix}$$ = Member end displacements vector. (2.27)

and $$\{F\} = \begin{bmatrix} F_1 \\ F_2 \\ F_3 \\ F_4 \\ F_5 \\ F_6 \end{bmatrix}$$ = Member end forces vector. (2.28)

[JF] is the joint flexibility matrix given by

$$[JF] = \begin{bmatrix} 0 & 0 & 0 & & & \\ 0 & 0 & 0 & & \underset{\sim}{0} & \\ 0 & 0 & \frac{1}{(K_i)} & & & \\ & & & 0 & 0 & 0 \\ & \underset{\sim}{0} & & 0 & 0 & 0 \\ & & & 0 & 0 & \frac{1}{(K_j)} \end{bmatrix} \quad (2.29)$$

K_i and K_j are the stiffnesses of the two rotational springs. Hence $(\frac{1}{K_i})$ and $(\frac{1}{K_j})$ are the flexibility of the springs, f_i and f_j.

It should be stressed here that it has been arbitrarily assumed that the rest of the terms in [JF] are equal to zero. This

is primarily because rotational springs were used to model the behavior of the joints. Thus one should look at K_i and K_j as being a kind of equivalent stiffness which produces the same rotational distortions at the end joints. K_i and K_j could be either the secant stiffnesses if one is using a secant formulation approach, or the tangent stiffnesses if one is using a tangent formulation approach. There are no major differences in the two formulations and in what follows the tangent approach will be used (although the same equations apply for a secant approach).

The incremental stiffness equations are:

$$\{\Delta F\} = [K]_t \left[\{\Delta u'\} - [JF]_t \{\Delta F\}\right] \tag{2.30}$$

$$\left[[I] + [K]_t[JF]_t\right] \{\Delta F\} = [K]_t\{\Delta u'\} \tag{2.31}$$

or

$$\{\Delta F\} = \left[[I] + [K]_t[JF]_t\right]^{-1} [K]_t \{\Delta u'\} \tag{2.32}$$

$$\{\Delta F\} = [K]_t \{\Delta u\} \tag{2.33}$$

$[K]_t$ = GSCM tangent stiffness matrix

$$= [RM][K]_t \tag{2.34}$$

where

$$[RM] = \text{Reduction Matrix} = \left[[I] + [K]_t[JF]_t\right]^{-1} \tag{2.35}$$

then $$[K]_t = \left[[I] + [K]_t[JF]_t\right]^{-1} [K]_t \tag{2.36}$$

where: $[K]_t$ = Augmented tangent stiffness matrix for the assembly

and: $[JF]_t$ = Tangent flexibility Matrix which has the same form as equation 2.29. Only $(K_i)_t$ and $(K_j)_t$ are substituted for (K_i) and (K_j).

$[I]$ = Unit matrix, i.e. $I_{ij} = \delta_{ij}$.

The following relationships between the incremental joint displacements and the incremental member end displacements exist:

$$\{\Delta u'\} = \left[[I] + [JF]_t[K]_t\right]\{\Delta u\} \tag{2.37}$$

and

$$\{\Delta u\} = \left[[I] + [JF]_t[K]_t\right]^{-1}\{\Delta u'\} \tag{2.38}$$

The above equations are valid for any form of $[JF]_t$ and are thus general in this regard. They are specialized here for the case where [JF] is as given by equation 2.29. Defining $(f_i)_t$ and $(f_j)_t$ to be $\frac{1}{(K_i)_t}$ and $\frac{1}{(K_j)_t}$, respectively:

$$\therefore [I[+[K]_t[JF]_t = \begin{bmatrix} 1 & 0 & 0 & 0 & 0 & 0 \\ 0 & 1 & (f_i)_t S_3 & 0 & 0 & (f_j)_t S_6 \\ 0 & 0 & 1+(f_i)_t S_2 & 0 & 0 & (f_j)_t S_5 \\ 0 & 0 & 0 & 1 & 0 & 0 \\ 0 & 0 & -(f_i)_t S_3 & 0 & 1 & -(f_j)_t S_6 \\ 0 & 0 & (f_i)_t S_5 & 0 & 0 & 1+(f_j)_t S_7 \end{bmatrix} \tag{2.39}$$

Defining D as

$$D = (1+(f_i)_t\ S_2)(1+(f_j)_t\ S_7) - (f_i)_t (f_j)_t\ S_5\ S_5 \tag{2.40}$$

$$\therefore\ [RM] = \left[[I] + [K]_t[JF]_t\right]^{-1} \tag{2.41}$$

$$= \frac{1}{D} \begin{bmatrix} D & 0 & 0 & 0 & 0 & 0 \\ 0 & D & B & 0 & 0 & C \\ 0 & 0 & D' & 0 & 0 & E' \\ 0 & 0 & 0 & D & 0 & 0 \\ 0 & 0 & -B & 0 & D & -C \\ 0 & 0 & E & 0 & 0 & D'' \end{bmatrix} \tag{2.42}$$

where:

$$D' = 1 + (f_j)_t\ S_7 \tag{2.43}$$

$$D'' = 1 + (f_i)_t\ S_2 \tag{2.44}$$

$$B = (f_i)_t\ S_5\ (f_j)_t\ S_6 - (f_i)_t\ S_3\ D' \tag{2.45}$$

$$C = (f_i)_t\ S_5\ (f_j)_t\ S_3 - (f_j)_t\ S_6\ D'' \tag{2.46}$$

$$E = -\ (f_i)_t\ S_5 \tag{2.47}$$

$$E' = -\ (f_j)_t\ S_5 \tag{2.48}$$

and

$$D = D' * D'' - E * E' \tag{2.49}$$

Finally $[K]_t$ is given by $[RM][K]_t$ and is evaluated as

$$\begin{bmatrix} (S_1) & 0 & 0 & -(S_1) & 0 & 0 \\ 0 & (S_4) & (S_3) & 0 & -(S_4) & (S_6) \\ 0 & (S_3) & (S_2) & 0 & -(S_3) & (S_5) \\ -(S_1) & 0 & 0 & (S_1) & 0 & 0 \\ 0 & -(S_4) & -(S_3) & 0 & (S_4) & -(S_6) \\ 0 & (S_6) & (S_5) & 0 & -(S_6) & (S_7) \end{bmatrix} \tag{2.50}$$

where:

$$(S_1) = S_1 \tag{2.51}$$

$$(S_2) = \frac{1}{D}[S_2\, D' + S_5\, E'] \tag{2.52}$$

$$(S_3) = \frac{1}{D}[S_3\, D' + S_6\, D'] \tag{2.53}$$

$$(S_4) = S_4 - S_3\,(S_3)\,(f_i)_t - S_6\,(S_6)\,(f_j)_t \tag{2.54}$$

$$(S_5) = S_5/D \tag{2.55}$$

$$(S_6) = \frac{1}{D}[S_6\, D'' + S_3\, E] \tag{2.56}$$

$$(S_7) = \frac{1}{D}[S_7\, D'' + S_5\, E] \tag{2.57}$$

and as previously mentioned, the member incremental end displacements are related to the joint incremental displacements by the relation:

$$\{\Delta u\} = \left[[I] + [JF][K]_t\right]^{-1} \{\Delta u'\} \tag{2.58}$$

or

$$\{\Delta u\} = \{\Delta u'\} - [JF]_t\, \{\Delta F\} \tag{2.59}$$

It is worth mentioning that for a member which is rigidly jointed, $(f_i)_t$ and $(f_j)_t$ are both zero, and hence [RM] is the unity matrix. I.e., the stiffness matrix of the assembly of a member and two nonlinear springs is the same as the original stiffness matrix of the member by itself.

2.5.2 Effect of Finite Joint Size

So far the stiffness of the member (if a girder) was referred to the centerlines of the adjacent columns, and thus the columns were considered of zero width. When dealing with wide columns of shear walls, the clear length of a girder and its centerline length become very different and some consideration should be given to handle this effect properly. Here this joint size effect is introduced in the analysis through a modified stiffness matrix. Referring to Fig. 2.4 and assuming that the plane cross section of the column or shear wall remains plane after deformation, one can write:

$$(u_2)_i = (u_2)_{i'} + d_i\,(u_3)_{i'} \tag{2.60}$$

$$(u_5)_j = (u_5)_{j'} - d_j\,(u_6)_{j'} \tag{2.61}$$

where $(u_2)_i$ and $(u_5)_j$ are the vertical displacements at the column faces and $(u_2)_{i'}$ and $(u_5)_{j'}$ are the vertical displacements at the centerline of columns.

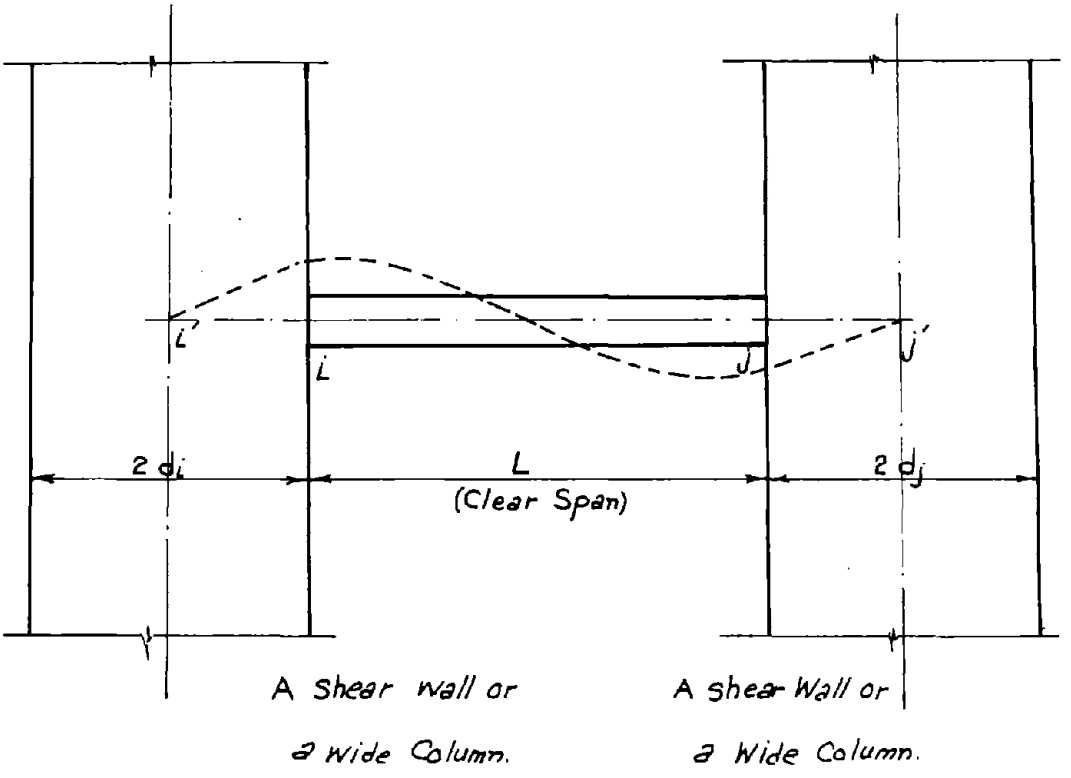

Fig. 2.4 - Effect of Joint Size in Case of Wide Columns or Shear Walls

$$\begin{bmatrix} u_1 \\ u_2 \\ u_3 \\ u_4 \\ u_5 \\ u_6 \end{bmatrix}_{ij} = \begin{bmatrix} 1 & 0 & 0 & 0 & 0 & 0 \\ 0 & 1 & d_i & 0 & 0 & 0 \\ 0 & 0 & 1 & 0 & 0 & 0 \\ 0 & 0 & 0 & 1 & 0 & 0 \\ 0 & 0 & 0 & 0 & 1 & -d_j \\ 0 & 0 & 0 & 0 & 0 & 1 \end{bmatrix} \begin{bmatrix} u_1 \\ u_2 \\ u_3 \\ u_4 \\ u_5 \\ u_6 \end{bmatrix}_{i'j'} \tag{2.62}$$

or

$$\{u\}_{ij} = [G]\,\{u\}_{i'j'} \tag{2.63}$$

$$\{F\}_{ij} = [K]_{ij}\,\{u\}_{ij} \tag{2.64}$$

$$\{F\}_{i'j'} = [G']\,\{F\}_{ij} \tag{2.65}$$

where $[G']$ is given by:

$$[G'] = \begin{bmatrix} 1 & 0 & 0 & 0 & 0 & 0 \\ 0 & 1 & 0 & 0 & 0 & 0 \\ 0 & d_i & 1 & 0 & 0 & 0 \\ 0 & 0 & 0 & 1 & 0 & 0 \\ 0 & 0 & 0 & 0 & 1 & 0 \\ 0 & 0 & 0 & 0 & -d_j & 1 \end{bmatrix} = [G]^T \tag{2.66}$$

Then finally

$$\{F\}_{ij} = [G]^T[K]_{ij}[G]\,\{u\}_{ij'} \tag{2.67}$$

and thus the modified stiffness matrix is given by

$$[K]_{ij'} = [G]^T [K]_{ij} [G] \tag{2.68}$$

Carrying out the multiplication, one can arrive at the stiffness matrix shown in equation 2.69.

$$\{F\}_{ij'} = \begin{bmatrix} (S_1)' & 0 & 0 & -(S_i)' & 0 & 0 \\ 0 & (S_4)' & (S_3)' & 0 & -(S_4)' & (S_6)' \\ 0 & (S_3)' & (S_2)' & 0 & -(S_3)' & (S_5)' \\ -(S_1)' & 0 & 0 & (S_1)' & 0 & 0 \\ 0 & -(S_5)' & -(S_3)' & 0 & (S_4)' & -(S_6)' \\ 0 & (S_6)' & (S_5)' & 0 & -(S_6)' & (S_7)' \end{bmatrix} \{u\}_{ij'} \tag{2.69}$$

where:

$$(S_1)' = (S_1) \tag{2.70}$$

$$(S_2)' = (S_2) + 2(S_3)\, d_i + (S_4)\, d_i^2 \tag{2.71}$$

$$(S_3)' = (S_3) + (S_4)\, d_i \tag{2.72}$$

$$(S_4)' = (S_4) \tag{2.73}$$

$$(S_5)' = (S_5) + (S_6)\, d_i + (S_3)\, d_j + (S_4)\, d_i d_j \tag{2.74}$$

$$(S_6)' = (S_6) + (S_4)\, dj \tag{2.75}$$

$$(S_7)' = (S_7) + 2(S_6)\, d_j + (S_4)\, d_j d_j \tag{2.76}$$

Finally the stiffness equation of GSCM in incremental form can be written as:

$$\{\Delta F\} = [\underline{K}]_t \{\Delta u\} \tag{2.77}$$

where:

$$[\underline{K}]_t = [G]^T[RM][K]_t[G] \tag{2.78}$$

or:

$$[K]_t = [G]^T\left[[I] + [JF]_t[K]_t\right]^{-1}[K]_t[G] \tag{2.79}$$

2.5.3 Stability Effects in GSCM

The main objective of any method of analysis is to predict the behavior of the structure as the load is applied to it. Due to the fact that some of the members of a frame may carry large compressive loads, the elastic and inelastic stability is likely to become important and hence stability effects should be included in the analysis. This could be done by the elastic stability functions discovered first by Timoshenko[57] and tabulated later by Livesley and Chandler[58] in 1956. A similar version of these stability functions has been derived and presented by Roesset.[59] A more general formulation of the inelastic stability functions problem has been presented by Aziz.[8]

In the current study use is made of these stability functions to include both local and global stability. The stiffness of an elastic member modified by stability effects is

$$[K]_t = \begin{bmatrix} S_1 & 0 & 0 & -S_1 & 0 & 0 \\ 0 & S_4*C4 & S_3*C_1 & 0 & -S_4*C_4 & S_6*C_1 \\ 0 & S_3*C_1 & S_2*C_2 & 0 & -S_3*C_1 & S_5*C_3 \\ -S_1 & 0 & 0 & S_1 & 0 & 0 \\ 0 & -S_4*C_4 & -S_3*C_1 & 0 & S_4*C_4 & -S_6*C_1 \\ 0 & S_6*C_1 & S_5*C_3 & 0 & S_6*C_1 & C_7*C_2 \end{bmatrix} \tag{2.80}$$

The functions C_1, C_2, C_3 and C_4 above are dependent on the axial force in the member. Fig. 2.5 shows the shape of these functions and their variation with the axial force P. For a compression member:

$$(aL) = \sqrt{\frac{PL^2}{EI}} \tag{2.81}$$

and

$$C_1 = \frac{a^2L^2(1 - \cos aL)}{\Delta} \tag{2.82}$$

$$C_2 = \frac{(aL) \sin aL - a^2L^2 \cos aL}{\Delta} \tag{2.83}$$

$$C_3 = \frac{a^2L^2 - aL \sin aL}{\Delta} \tag{2.84}$$

$$C_4 = \frac{a^3L^3 \sin aL}{\Delta} \tag{2.85}$$

where

$$\Delta = (1 - \cos aL)^2 - \sin aL(aL - \sin aL) \tag{2.86}$$

For a tension member:

$$(aL) = \sqrt{\frac{PL^2}{EI}} \tag{2.87}$$

$$C_1 = \frac{a^2L^2(\cosh aL - 1)}{\Delta'} \tag{2.88}$$

$$C_2 = \frac{a^2L^2 \cosh aL - aL \sinh aL}{\Delta'} \tag{2.89}$$

$$C_3 = \frac{aL \sinh AL - a^2L^2}{\Delta'} \tag{2.90}$$

$$C_4 = \frac{a^3L^3 \sinh aL}{\Delta'} \tag{2.91}$$

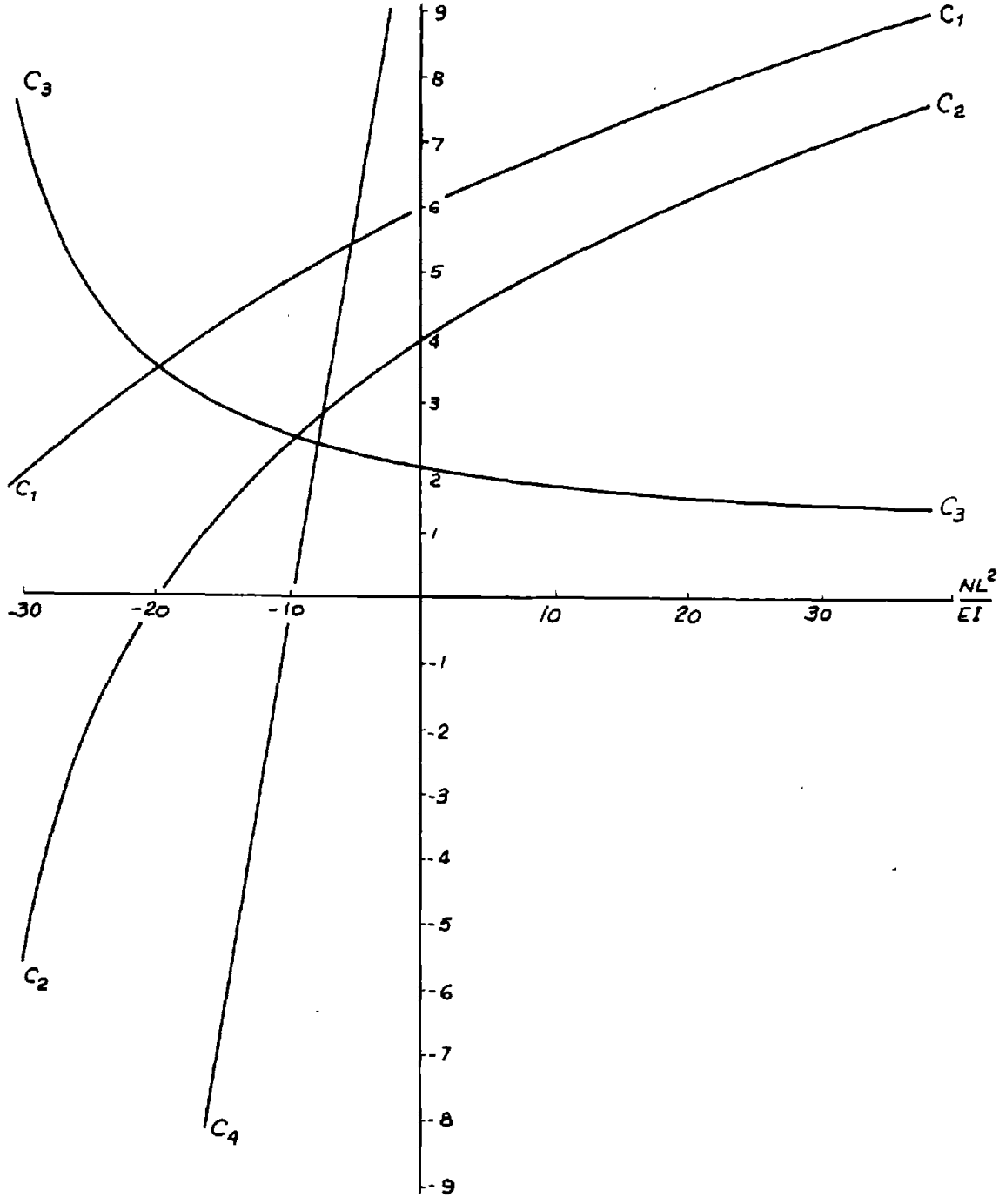

Fig. 2.5 - Stability Functions
(from Reference 59 by Roesset)

where:

$$\Delta' = 2 \sinh aL \left(\frac{aL}{2} - \tanh \frac{aL}{2}\right) \qquad (2.92)$$

Other stability schemes can be used instead of the stability functions. For example, corrective terms can be added to the stiffness matrix or to the member end forces to take into consideration both the local stability and the global stability. Usually it is better to have the correction occurring in the stiffness matrix rather than the member end forces. The major advantage of the stiffness correction is that it doesn't lag a step behind, the way the force correction does. In practice it turns out that this difference of one step may lead to a significant discrepancy between the two methods, especially when there is a great change in the axial forces in the members. For some dynamic problems, this might not be important since the axial load doesn't change very much. In both methods the axial force in the member is the axial force obtained at the end of the previous step. Finally, a mixed scheme can be used where the stiffness matrix is corrected for the axial load, while the force vector is corrected for the change in the axial load. The procedure for correction can be summarized as follows:

(i) Substitute S(4) by $S(4) + \frac{P}{L}$

(ii) Add to the shear at end i the value $\frac{\Delta P}{L}(u_5 - u_2)$

(iii) Add to the shear at end j the value $-\frac{\Delta P}{L}(u_5 - u_2)$

where: P is the axial force in the member,

ΔP is the last change in the axial force from the previous step,

u_2 and u_5 are the lateral displacements at ends i and j respectively, and

S_4 is the transverse diagonal stiffness term in the stiffness matrix of the member.

The latter scheme proved to be as efficient and as accurate as the stability functions described before.

2.5.4 Interaction Effects in GSCM

Interaction effects can be introduced in GSCM easily to provide an interaction model. This model is basically similar to the bending model, but the criterion for the formation of a hinge or its removal is different. The criterion for the bending model is based on the value of the moment, while in the interaction model, it is based on the combination of the values of the bending moments and the axial forces at the ends of the member. If such combination of moment and axial force would produce a point inside the interaction domain, no hinge will be assumed. But if it produces a point on or outside the interaction domain, a hinge with specified behavior should be assumed. Theoretically speaking, introducing interaction effects leads to a coupled model and an iterative procedure should be used to make sure that the combination of the bending moment and axial force leads to a

point on the interaction surface or inside it, but not outside it. However, since in the solution of the dynamic problem the model is stepped through time, many ways can be used and have been used in the current analysis to enforce the previously mentioned condition without having to go through a coupled iterative formulation.

2.5.5 Possible Idealization for Joint Behavior

A basic assumption in GSCM is the fact that the behavior of the joints is known beforehand. Plastic analysis theory is based on the assumption that the behavior of the joints is rigid-plastic. This assumption might not be realistic in types of joints constructed nowadays by typical practices. Many idealizations for the behavior of joints can be assumed, based on experimental data available in the literature.

Among these idealizations for the behavior, the following have been implemented (Fig. 2.6):

1. Idealization (A) - Rigid-Plastic Behavior
2. Idealization (B) - Elastic-Plastic Behavior
3. Idealization (C) - Bilinear Behavior.
4. Idealization (D) - Stiffness Degrading Behavior (parallel unloading branch).
5. Idealization (E) - Stiffness Degrading Behavior (non-parallel unloading branch)
6. Idealization (F) - Stiffness and Strength Degrading Behavior
7. Idealization (G) - Stiffness and Strength Degrading Behavior with physical lower bound on the properties.

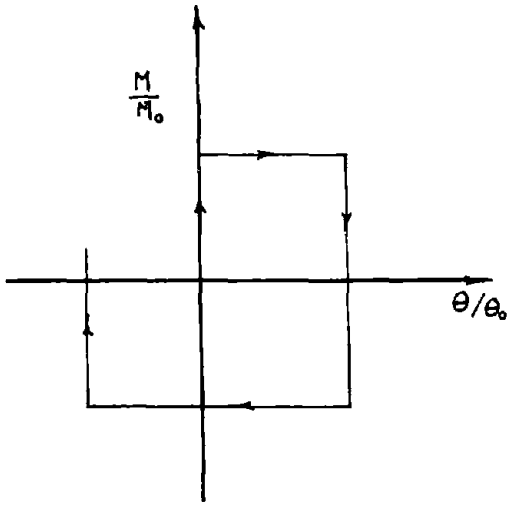

(A) Rigid-Plastic Behavior

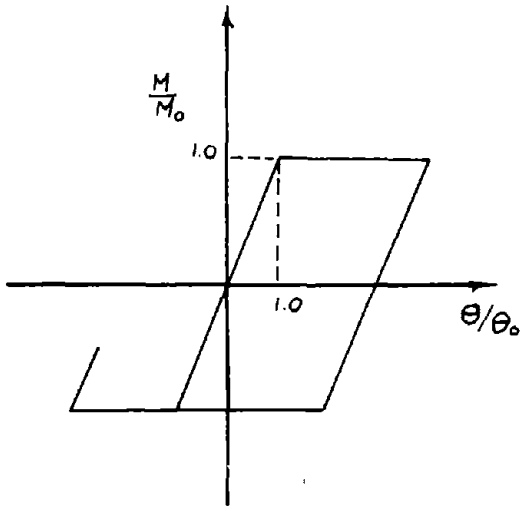

(B) Elastic-Plastic Behavior

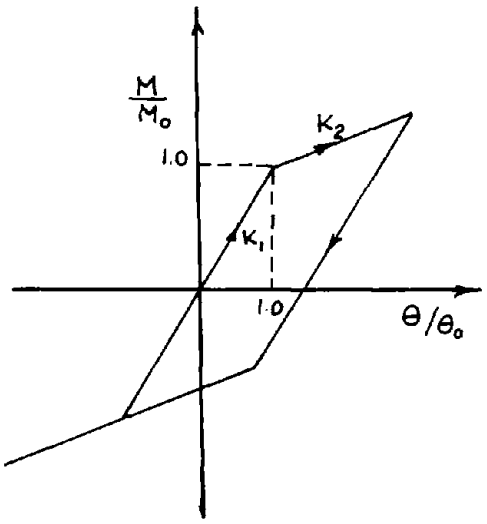

(C) Bilinear Behavior

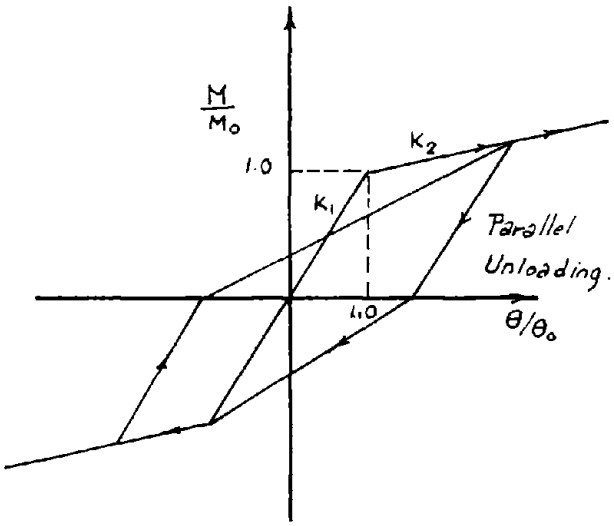

(D) Stiffness Degrading Behavior (Parallel Unloading Branch).

Fig. 2.6 - Possible Idealization for Joints Behabior

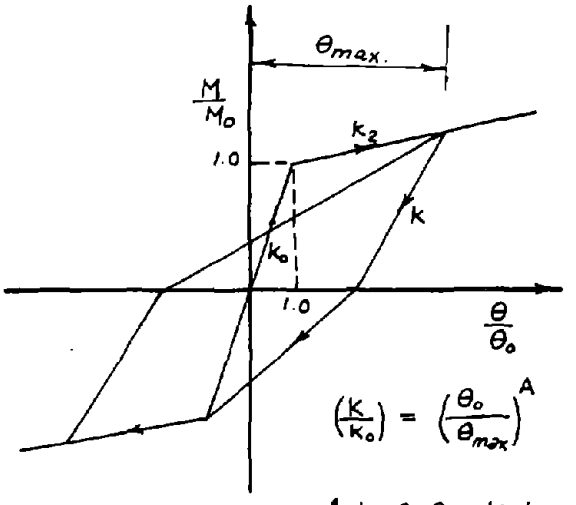

(E) Stiffness Degrading Behavior (Non-parallel Unloading Branch).

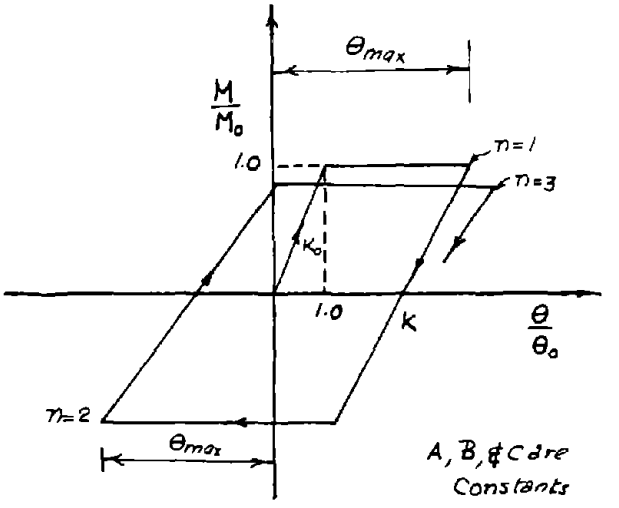

(F) Stiffness and Strength Degrading Behavior (Non-parallel Unloading Branch).

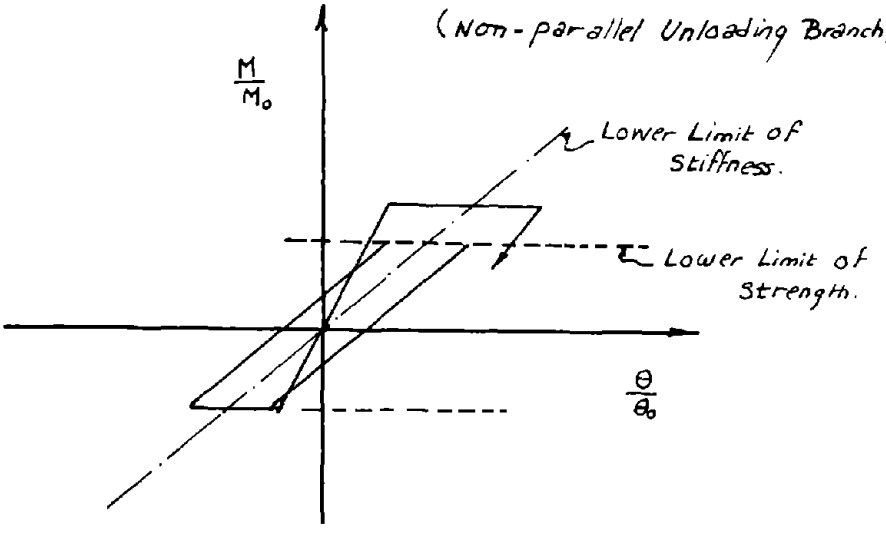

(G) Stiffness and Strength Degrading Behavior With physical Lower Bound on the properties.

Fig. 2.6 - (Continued)

2.6 DEVELOPMENT OF THE SOLUTION SCHEMES

In the previous sections different bending and interaction models have been presented. Different analysis effects were introduced into these models to allow realistic consideration of the true behavior of a building frame. The formulation so far has been general and is thus applicable to both the static and the dynamic case of loading. Here further consideration will be given to the dynamic case, ince the formulation is mainly intended for this type of analysis.

2.6.1 Assumptions in the Formulation

The basic assumptions for the formulation are as follows:

(i) Floor diaphragms are assumed to be completely rigid in their own plane. They are very flexible for out-of-plane deformation.

(ii) The mass of the structure is assumed to be lumped at the floor levels.

(iii) The concepts inherent in a bending model are valid, mainly the concept of a plastic hinge, although the hinge might have an arbitrary behavior as illustrated before.

(iv) The effects of rotatory inertia are neglected for the structural system, although they are considered for the foundation.

(v) Generalized hinges can form at the ends of each girder

or column and gravity loads on the girder elements are represented as initial fixed end forces acting at the nodal points.

(vi) Each nodal point has three degrees of freedom: a horizontal translation, a vertical translation and a rotation.

The formulation includes in addition:

(i) Axial deformation in the columns. However, axial deformations in the girders are neglected since the floor diaphragms are assumed rigid.

(ii) The reduction in frame stiffness due to vertical loads and the change in geometry.

(iii) The effect of axial-flexural interaction on the yield moment of the columns.

2.6.2 Equations of Motion

The equations of motion for a structural system can be written as follows:

$$F_I + F_D + F_R = F_E \tag{2.93}$$

where:

F_I = Inertia force vector

F_D = Damping force vector

F_R = Restoring force vector from the structural system

F_E = Excitation force vector.

For a system excited by a ground acceleration, the above equation becomes:

$$\underset{\sim}{M}\,\ddot{\underset{\sim}{u}} + \underset{\sim}{C}\,\dot{\underset{\sim}{u}} + \underset{\sim}{F}(u) = \underset{\sim}{R} \qquad (2.94)$$

where:

$\underset{\sim}{M}$ = Mass matrix

$\underset{\sim}{u}$, $\dot{\underset{\sim}{u}}$ and $\ddot{\underset{\sim}{u}}$ are relative nodal displacement, velocity and acceleration vectors respectively

$\underset{\sim}{C}$ = Damping matrix

$\underset{\sim}{R}$ = Excitation vector which is equal to $-\underset{\sim}{M}\,\ddot{u}_g$ in case of ground motion where $\ddot{u}_g$ is the input ground acceleration.

$\underset{\sim}{F}(u)$ = Restoring force vector which is dependent on u (displacement vector); it is generally a non-linear function of u.

2.6.3 The Mass Matrix

Generally speaking, the replacement of the distributed mass by a number of concentrated masses reduces the number of degrees of freedom of the system and affects the response of the structure particularly in the higher modes.

In a multi-story building, however, for most practical purposes it is sufficient to consider the mass of each floor as concentrated at the floor level, and the masses of the columns divided between the two floors they connect. This scheme results in a diagonal mass matrix which can be stored as a one-dimensional

array and thus allows a great saving in storage requirements. For all practical problems and typical buildings it was found[60], [61] that such scheme is nearly as accurate as a consistent mass formulation, particularly since a large fraction of the mass is actually contributed by the slab.

2.6.4 Condensing the Stiffness Matrix

In the present study only the lateral modes of vibration are considered. A kinematic condensation followed by a static condensation are used. The kinematic scheme simply imposes the condition that all the joints at a given floor level displace laterally by the same amount. The static condensation scheme assumes negligible inertia loads corresponding to vertical and rotary displacements, and considers the static equations to arrive finally at the lateral stiffness matrix of the structure. The result of both the static and kinematic condensation is that only one degree of freedom per story is retained explicitly, i.e., the lateral displacement of the floor level; however, the effect of all other displacements is retained implicitly, and their values can be obtained from a back substitution process.

2.6.5 The Damping Matrix C

There are several ways by which a convenient damping matrix can be selected. Most of these ways are based on an elastic analysis approach and they are justified because they lead to a mathe-

matical simplification in the elastic range. In the inelastic range there is no major advantage for using any certain form for the matrix $\underset{\sim}{C}$, since the solution is obtained in the time domain. However, since the dissipation of energy reproduced by the matrix $\underset{\sim}{C}$ is assumed to take place whether the structure yields or not, it seems reasonable to consider it constant in both the elastic and inelastic range.

Rayleigh[14] showed that if the damping matrix is a linear combination of the stiffness and mass matrices it will be uncoupled. Caughey[15] showed that a sufficient, though not necessary, condition for the damping matrix to be uncoupled is that it be expressed in the following way:

$$\underset{\sim}{C} = \underset{\sim}{M} \cdot \sum_{\ell=0}^{(N-1)} a_\ell \, [M^{-1} \, K]^\ell \qquad (2.95)$$

where: N = Number of degrees of freedom

and a_ℓ = Undetermined coefficient.

Different observations can be made about the damping matrix $\underset{\sim}{C}$. If the C matrix is chosen proportional to the mass matrix, the modal damping decreases continuously for increasing number of modes. The constant of proportionality is usually chosen to give a prespecified percentage of critical damping in one particular mode (usually the first). If the $\underset{\sim}{C}$ matrix is chosen proportional to the stiffness matrix, the modal damping increases for increasing number of modes.

The constant of proportionality can be chosen to give a prescribed percentage of critical damping in one particular mode.

If the damping matrix is chosen as a combination of the mass matrix and the stiffness matrix, one can have more flexibility in the variation of modal damping over the system's modes, but ultimately the damping will start increasing for high frequencies. Fig. 2.7 shows this particular behavior.

In the present work use has been made of a direct method to arrive at the damping matrix for certain specified modal damping values. The resulting damping matrix has the form:

$$\underset{\sim}{C} = \underset{\sim}{M}\ \underset{\sim}{\Phi}\ \underset{\sim}{\beta}\ \underset{\sim}{\Phi}^T\ \underset{\sim}{M}^T \tag{2.96}$$

where:

$\underset{\sim}{M}$ = Diagonal mass matrix

$\underset{\sim}{\Phi}$ = A matrix whose columns are the eigenvectors of the system (normalized with respect to M)

$= [\Phi_1\ \Phi_2\ \ldots\ldots\ \Phi_n]$

β_i = Percentage of critical damping in the i^{th} mode

ω_i = Circular frequency of the i^{th} mode

$\underset{\sim}{\beta}$ = Diagonal matrix with elements $2\beta_i\omega_i$.

Since the eigenvalue problem has been solved first, the matrix $\underset{\sim}{C}$ can be formed after arriving at the matrices $\underset{\sim}{\beta}$ and $\underset{\sim}{\Phi}$. Thus the method allows the flexibility of having any desired amount of viscous damping in any of the modes.

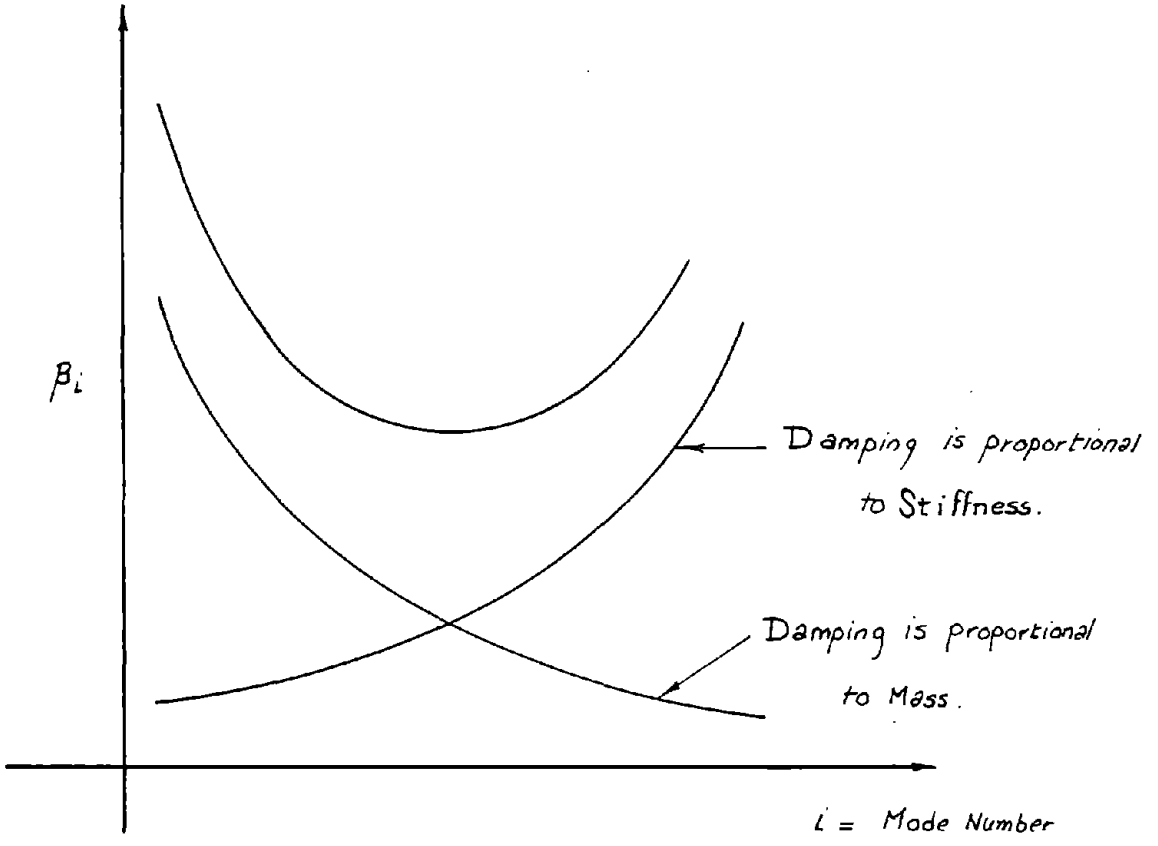

$$\beta_i = \frac{1}{2}\left[\frac{a}{\omega_i} + b\,\omega_i\right]$$

Fig. 2.7 - Rayleigh Type Damping

2.6.6 Numerical Integration Scheme

There are many different procedures available for the numerical determination of dynamic structural response.

In the present study the equations of motion were solved using a step-by-step integration procedure. This procedure, called the "constant velocity method," assumes that the velocities of the system are constant within the time step. Under these assumptions the recurrence formulas for velocities and accelerations are:

$$\dot{\underset{\sim}{u}}_n = \frac{1}{2\Delta t}\left(\underset{\sim}{u}_{n+1} - \underset{\sim}{u}_{n-1}\right) \tag{2.97}$$

and

$$\ddot{\underset{\sim}{u}}_n = \frac{1}{(\Delta t)^2}\left(\underset{\sim}{u}_{n+1} - 2\underset{\sim}{u}_n + \underset{\sim}{u}_{n-1}\right) \tag{2.98}$$

and then

$$\underset{\sim}{u}_{n+1} = \left[\frac{1}{(\Delta t)^2}\underset{\sim}{M} + \frac{1}{2\Delta t}\underset{\sim}{C}\right]^{-1} \cdot \left[\underset{\sim}{R}_n - \underset{\sim}{F}_n + \frac{2}{(\Delta t)^2}\underset{\sim}{M}\,\underset{\sim}{u}_n - \left(\frac{1}{(\Delta t)^2}\underset{\sim}{M} - \frac{1}{2\Delta t}\underset{\sim}{C}\right)\underset{\sim}{u}_{n-1}\right] \tag{2.99}$$

The above matrix equation can be used for the calculation of the displacement vector at time step n+1, in terms of the displacement vectors at steps n and n-1, and the force vector F_n at time step n.

The force vector at time step n is computed easily in a tangent formulation. Since the numerical procedure produces total dis-

placements, the incremental ones are found by substituting the values of two consecutive steps. Then the incremental forces in the different structural components are computed from the tangent stiffness matrix and accumulated to obtain the total forces.

An obvious problem with the "constant velocity method" is that it is not self-starting since at any particular time step n we need the displacements of the two previous steps. This means that in order to start the method one must obtain the displacements of the system at the end of the first step. This was done by using a 4^{th} order Runge-Kutta method which is self-starting. Once the displacements are calculated, velocities and accelerations can be computed from the other equations.

The numerical integration scheme used requires a time step in the order of 1/5 to 1/10 of the smallest natural period, provided that this time step reproduces well the loading. In some problems, where the lowest natural period is very small, this implies an extremely small Δt, should the method remain stable. For most of the cases studied, a Δt of 0.01 sec. was used, which is required to reproduce the earthquake loading. This proved very satisfactory for the type of problems at hand.

CHAPTER III

COMPARATIVE STUDIES OF DIFFERENT BENDING MODELS UNDER DYNAMIC LOADING

3.1 INTRODUCTION

In Chapter III a formulation for the inelastic dynamic analysis of building frames has been presented. This formulation is general enough to take into consideration different nonlinearities which might occur in a building frame on a selective basis. The objective thus is to study the relative importance of each nonlinear effect separately and signal out those effects which might be more important than others.

The type of nonlinearities studied can be grouped into two broad categories: those due to material behavior, and those due to geometry changes. Since the relative importance of each nonlinear effect is dependent on the shape of the building frame studied, some results might not be easily generalized and applied directly to other unusual configurations. Then the objective here is only to demonstrate the relative importance of different effects for some building frames.

The rest of this Chapter will be devoted to discussing further considerations for the bending models. An extensive comparative study for a 10-story 1-bay building frame designed previously by Anderson[5] is presented, and the relative importance of different effects is established for this particular frame.

3.2 DUCTILITY CONSIDERATIONS

3.2.1 General

A widely used measure of the cyclic inelastic behavior of a structure is the so-called ductility factor. The term has been commonly used as a measure of the amount of yielding incurred in a system. Conventionally it is defined as the ratio of the total deformation to the elastic deformation at yield, and it has been variously defined as that ratio for strains, curvatures and deflections. Strictly speaking, a ductility factor has no precise meaning until the method of measuring it has been defined. The value of the ductility factor thus varies widely, depending upon the definition used.

When using the definition based on strains, the ductility factor is almost exclusively dependent on the material properties, while using the definition based on curvatures adds the effects of the shape and structural properties of the cross section. When ductility is defined based on deflections, the entire configuration and response of the structure is incorporated.

A general load-deflection curve is shown in Fig. 3.1. Many characteristic values can be defined for this load-deflection curve as follows:

d_E = Elastic or linear displacement.

d_I = Inelastic or nonlinear displacement

d_R = Recoverable displacement.

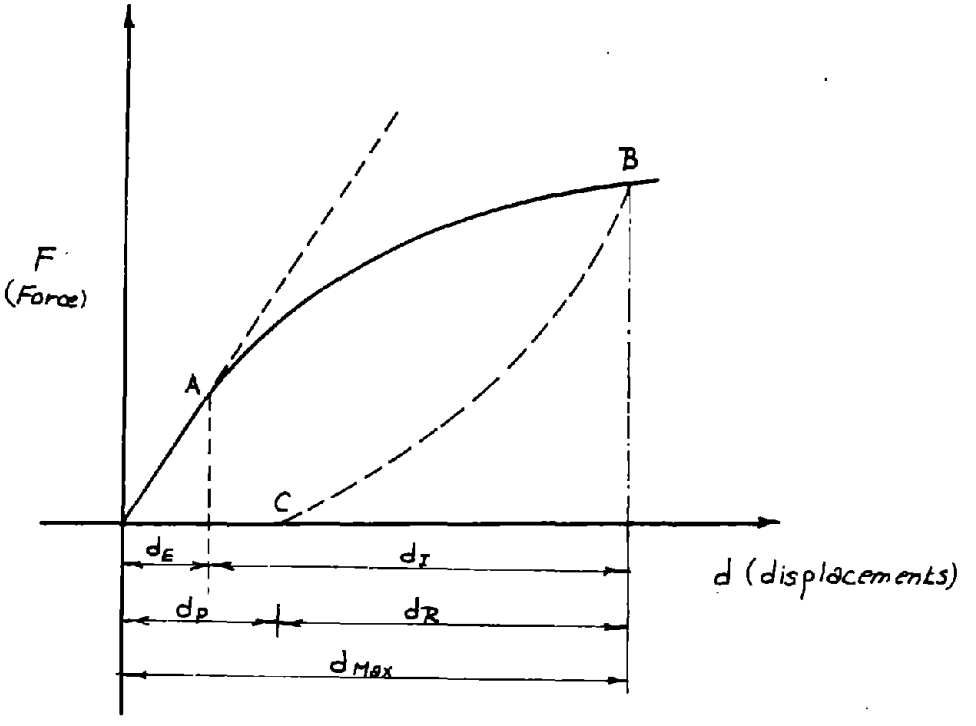

Fig. 3.1 - Ductility Definitions

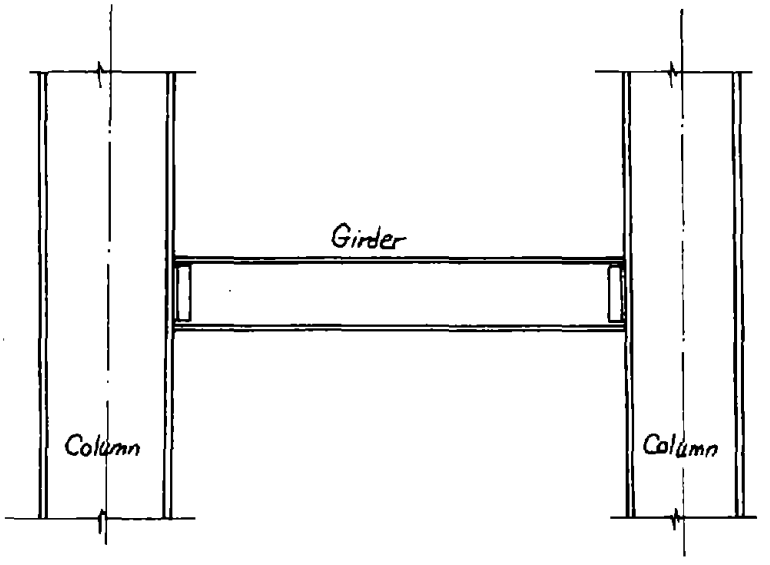

(a) Original Structure

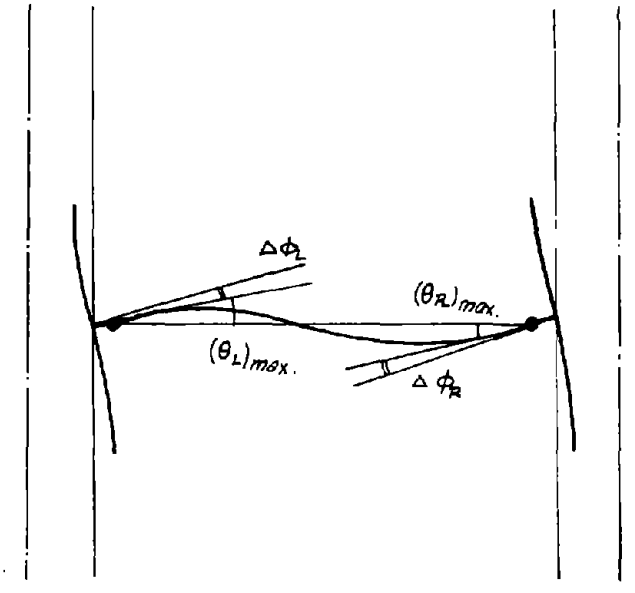

(b) Distorted Mathematical Model

Fig. 3.2 - Ductility Definitions

d_{max} = Maximum displacement

d_p = Permanent displacement.

Ductility then can be defined by the following measures:

$$D_1 = \frac{\text{Max. Displacement}}{\text{Elastic Displacement}} = \frac{d_{Max.}}{d_E} = 1 + \frac{d_I}{d_E} \qquad (3.1)$$

$$D_2 = \frac{\text{Max. Displacement}}{\text{Permanent Displacement}} = \frac{d_{Max.}}{d_P} = 1 + \frac{d_R}{d_P} \qquad (3.2)$$

$$D_3 = \frac{\text{Max. Displacement}}{\text{Recoverable Displacement}} = \frac{d_{Max.}}{d_R} = 1 + \frac{d_P}{d_R} \qquad (3.3)$$

$$D_4 = \frac{\text{Max. Displacement}}{\text{Inelastic Displacement}} = \frac{d_{Max.}}{d_I} = 1 + \frac{d_E}{d_I} \qquad (3.4)$$

$$D_5 = \frac{\text{Permanent Displacement}}{\text{Elastic Displacement}} = \frac{d_P}{d_E} \qquad (3.5)$$

Thus in any analysis using a ductility factor, it is important to bear in mind the definition used. Moreover, it might become very difficult to judge the adequacy of ductility since there is no unique way of measuring it. Probably the most logical measure for ductility in case of a transient response is the ratio of the permanent displacement to the elastic displacement "D_5". However, for a steady-state response a better measure might be the ratio of the maximum displacement and the elastic displacement "D_1". It is not known currently

how damage or cumulative damage is related to ductility. The problem is even more complicated since such relation is not the same when dealing with a joint, a member or the total structure.

Generally speaking, ductility is and will remain for a time one of the most important quantities for evaluating the capability of a structure to resist strong earthquake motions without collapse. It has been defined as discussed before as a ratio of displacements. It could have been defined as ratio between forces as well. Sometimes it is even more meaningful to measure ductility by the amount of energy dissipated per cycle or by an equivalent damping (which dissipates the same amount of energy in each cycle).

3.2.2 Joint Ductility

In the current study joint ductility is measured as the ratio of the maximum joint distortion to the yield distorsion. Strictly speaking, joint ductility is defined only for GSCM, but not for a DCM, and is given by the equation

$$\text{Joint ductility} = \frac{(\Delta\phi)_{\text{Max.}}}{\theta_y} \qquad (3.6)$$

where

$(\Delta\phi)_{max.}$ = Maximum joint distorsion

θ_y = Joint distortion at yield.

3.2.3 Member Ductility

Two definitions of member ductilities have been commonly used and were implemented for the present study. The first one is based on rotation:

$$\text{rotation ductility} = \frac{\text{Max. End Rotation}}{\text{Yield Rotation}} = \frac{\theta_{max.}}{\theta_y} \tag{3.7}$$

$$= 1 + \frac{\text{Plastic Rotation}}{\theta_y} \tag{3.8}$$

To define the yield rotation θ_y it is commonly assumed that hinges will form almost simultaneously at both ends of the member, so that

$$\theta_y = \frac{M_p L}{6EI} \tag{3.9}$$

This assumption is reasonable for the girders when the frame is subjected only to lateral loads, but it becomes questionable when gravity loads are present.

The second definition based on moments assumes that a bilinear relationship exists between moment and curvature, although none of the two models (DCM or GSCM) can enforce directly this type of constitutive relation. Then

$$\text{moment ductility} = 1 + \frac{M_{max} - M_p}{r\, M_p} \tag{3.10}$$

where r is the second slope of the model.

Both definitions are equivalent in the particular case of a member loaded with equal and opposite end moments. For other cases they will both include approximations which have not been thoroughly studied. The validity of the definitions is even more questionable when dealing with members under a variable axial load (columns). This is a subject which needs further research but which is beyond the scope of the present work.

Finally, it is stressed again that ductility is not a unique quantity, but depends on the way of measuring it. This means that comparing the results of different analyses should not be done unless both use the same definition. The problem will be discussed later when comparisons are made with other researchers' published work.

3.3 SOIL-STRUCTURE INTERACTION CONSIDERATIONS

In reality, most structures are situated on flexible foundations, and recorded observations have shown that the response of a structure might be influenced by its foundation medium.

Several methods and mathematical models have been prepared to represent the flexible foundation medium. Whatever model is used, the amplification and attenuation effects of the supporting soil should be properly accounted for in the earthquake response analysis of the soil-building system.

Here the soil-structure interaction is treated by an equivalent lumped nonlinear model for the soil. The initial properties of the soil model can be determined from the elastic half-space or the elastic layered half-space, which are commonly used in the classical problem of vibration of plates resting on elastic foundation. For example, by utilizing Bycroft's[63] elasticity solutions for a dynamically loaded continuum, frequency -dependent stiffness and associated damping coefficients that characterize the dynamic proper-

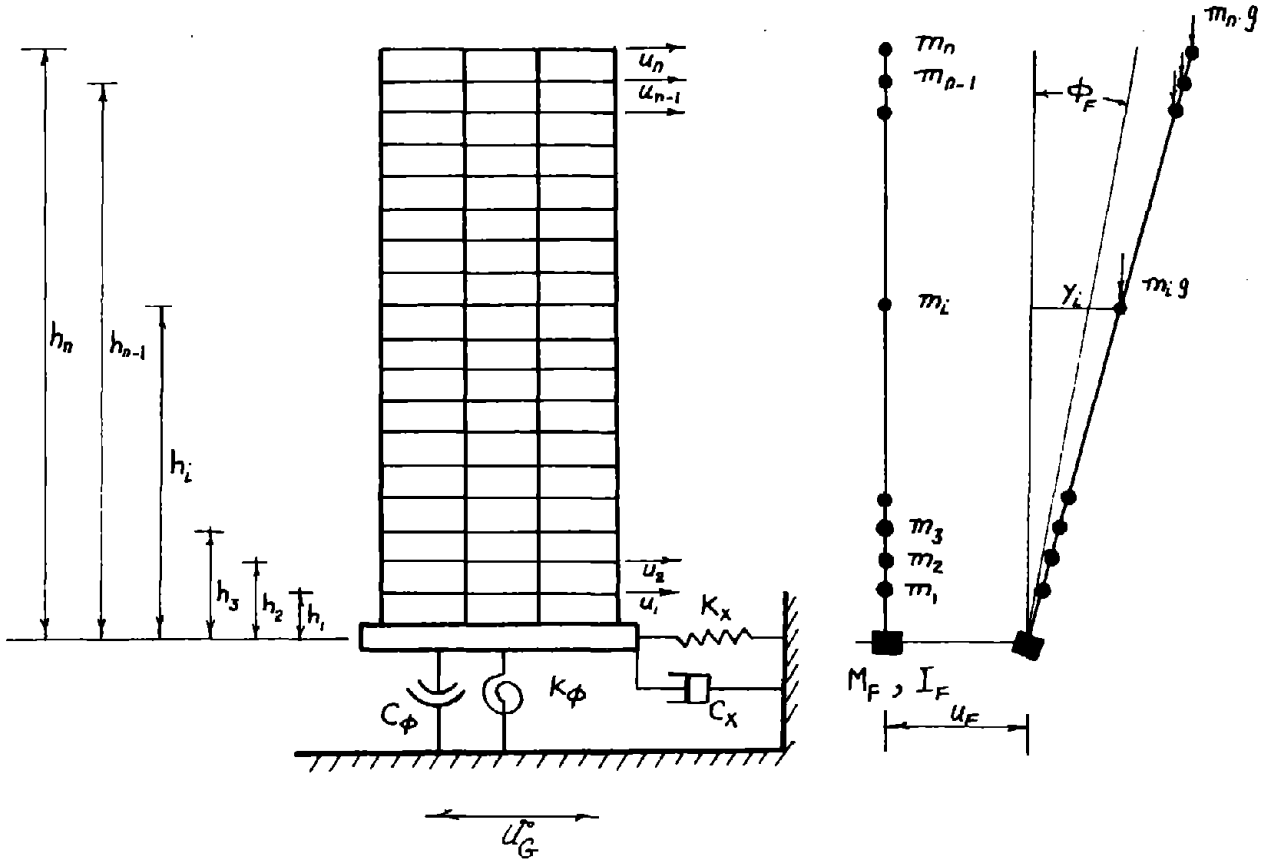

Fig. 3.3 - Soil-Structure Interaction Model for a High-rise Building

ties of the medium can be determined. (See for example Whitman and Richart.)[55] Later Parmelee, Perelman and Lee[62] have shown that the stiffness and associated damping characteristics of the foundation medium can be assumed to be constant and are determined by the physical properties of the soil-structure system. Thus for the purpose of this study it will be assumed that by an evaluation and analysis of the underlying soil, appropriate springs, masses and damping values have been determined to simulate the initial behavior of the soil.

Using such properties, the equations of motion for the coupled soil-structure system can be derived as follows:

Equations of Motion for the Structure

$$[m]\{\ddot{Y}\} + [c]\{\dot{u}\} + [k]\{u\} = 0 \qquad (3.11)$$

where [m], [c] and [k] are the mass, damping and lateral stiffness matrices respectively, and

$$Y = \begin{bmatrix} Y_1 \\ Y_2 \\ Y_3 \\ \vdots \\ Y_n \end{bmatrix} = \text{Total horizontal displacements of each floor.}$$

and is given by:

$$\{Y\} = \{u\} + [h]\{J\}\phi_F + \{J\}u_F + \{J\}u_G \qquad (3.12)$$

or:

$$\{Y\} = \{u'\} + \{J\}u_G \qquad (3.13)$$

where

$$[h] = \begin{bmatrix} h_1 & & & \\ & h_2 & & \underset{\sim}{0} \\ & & \ddots & \\ \underset{\sim}{0} & & & h_n \end{bmatrix}_{n \times n} \tag{3.14}$$

and

$$J = \begin{bmatrix} 1 \\ 1 \\ \vdots \\ 1 \end{bmatrix}_{n \times 1} \tag{3.15}$$

u_F and ϕ_F are the horizontal displacement and rotation of the foundation respectively. u' is the total displacement vector with respect to the foundation.

$$\therefore \quad [m]\{\ddot{u}\} + [m][h]\{J\}\ddot{\phi}_F + [m]\{J\}\ddot{u}_F + [m]\{J\}\ddot{u}_G + [c]\{\dot{u}\} + [k]\{u\} = 0 \tag{3.16}$$

Base Shear and Overturning Moment

The base shear and the overturning moment exerted by the structure on the foundation are given as follows:

$$B.S. = \sum_{i=1}^{n} F_i = \sum_{i=1}^{n}\sum_{j=1}^{n} k_{ij} u_j + \sum_{i=1}^{n}\sum_{j=1}^{n} c_{ij} \dot{u}_j$$

$$= \underset{\sim}{J}^T \underset{\sim}{k}\, \underset{\sim}{u} + \underset{\sim}{J}^T \underset{\sim}{c}\, \dot{\underset{\sim}{u}} \tag{3.17}$$

$$O.T.M. = \sum_{i=1}^{n} F_i h_i = \sum_{i=1}^{n} h_i \sum_{j=1}^{n} k_{ij} u_j + \sum_{i=1}^{n} h_i \sum_{j=1}^{n} c_{ij} \dot{u}_j$$

$$= \underset{\sim}{h}^T \underset{\sim}{k} \underset{\sim}{u} + \underset{\sim}{h}^T \underset{\sim}{c} \dot{\underset{\sim}{u}} \tag{3.18}$$

In tensorial notation:

$$B.S. = \delta_{ii} k_{ij} u_j + \delta_{ii} c_{ij} \dot{u}_j \tag{3.19}$$

$$O.T.M. = \delta_{ii} h_i k_{ij} u_j + \delta_{ii} h_i c_{ij} \dot{u}_j \tag{3.20}$$

Total Moment on the Base

If gravity loads are included in the analysis, an expression for the total moment can be written as follows:

$$T.M. = O.T.M. + \text{Moment due to vertical loads} \tag{3.21}$$

$$= O.B.M. + g\,[m]\,\{\underset{\sim}{Y} - \underset{\sim}{J} u_F - \underset{\sim}{J} u_g\} \tag{3.22}$$

$$= O.T.M. + g\,[m]\,\{u\} + g\,[m]\,[h]\,\{J\}\,\phi_F \tag{3.23}$$

$$\therefore T.M. = \underset{\sim}{h}^T \underset{\sim}{k} \underset{\sim}{u} + \underset{\sim}{h}^T \underset{\sim}{c} \dot{\underset{\sim}{u}} + g \underset{\sim}{m} \underset{\sim}{u} + g \underset{\sim}{m} \underset{\sim}{h} \underset{\sim}{J} \phi_F \tag{3.24}$$

Equations of Motion for the Foundation

The equations of motion at the foundation are given as follows:

$$M_F \ddot{Y}_F + k_x u_F + c_x \dot{u}_F - B.S. = 0 \tag{3.25}$$

$$I_F \ddot{\phi}_F + k_\phi \phi_F + c_\phi \dot{\phi}_F - T.M. = 0 \tag{3.26}$$

Equations of Motion for the Coupled System

Choosing the unknowns to be the total displacements with respect to the foundation, the coupled equations of motion take the form:

$$\underset{\sim}{m}\,\ddot{\underset{\sim}{u}} + \underset{\sim}{c}\,\dot{\underset{\sim}{u}} + \underset{\sim}{k}\,\underset{\sim}{u} = -\,\underset{\sim}{J}\,\ddot{u}_G \tag{3.27}$$

where

$$\underset{\sim}{m} = \begin{bmatrix} m_1 & & & & & & \\ & m_2 & & & & & \\ & & m_3 & & & \underset{\sim}{0} & \\ & & & \ddots & & & \\ & & & & m_n & & \\ & \underset{\sim}{0} & & & & m_F & \\ & & & & & & I_F \end{bmatrix} \tag{3.28}$$

and

$$\underset{\sim}{k} = \begin{bmatrix} \underset{\sim}{k} & -\underset{\sim}{k}\,\underset{\sim}{J} & -\underset{\sim}{k}\,\underset{\sim}{h} \\ -\underset{\sim}{J}^T\underset{\sim}{k} & k_x+\underset{\sim}{J}^T\underset{\sim}{k}\,\underset{\sim}{J} & \underset{\sim}{J}^T\,\underset{\sim}{k}\,\underset{\sim}{h} \\ -\underset{\sim}{h}^T\underset{\sim}{k} & \underset{\sim}{h}^T\,\underset{\sim}{k}\,\underset{\sim}{J} & k_\phi+\underset{\sim}{h}^T\,\underset{\sim}{k}\,\underset{\sim}{h} \end{bmatrix} \tag{3.29}$$

$$\underset{\sim}{c} = \begin{bmatrix} \underset{\sim}{c} & -\underset{\sim}{c}\,\underset{\sim}{J} & -\underset{\sim}{c}\,\underset{\sim}{h} \\ -\underset{\sim}{J}^T\underset{\sim}{c} & c_x+\underset{\sim}{J}^T\underset{\sim}{c}\,\underset{\sim}{J} & \underset{\sim}{J}^T\,\underset{\sim}{c}\,\underset{\sim}{h} \\ -\underset{\sim}{h}^T\underset{\sim}{c} & \underset{\sim}{h}^T\,\underset{\sim}{c}\,\underset{\sim}{J} & c_\phi+\underset{\sim}{h}^T\,\underset{\sim}{c}\,\underset{\sim}{h} \end{bmatrix} \tag{3.30}$$

$$\underset{\sim}{u} = \begin{bmatrix} \{\underset{\sim}{u}'\} \\ u_F \\ \phi_F \end{bmatrix} \tag{3.31}$$

where $\underset{\sim}{u}'$ are the total displacements relative to the foundation.

$$\underset{\sim}{J} = \begin{bmatrix} 0 \\ 0 \\ 0 \\ 0 \\ 0 \\ M_F \\ 0 \end{bmatrix} \begin{matrix} \\ \\ \\ \\ \\ \} n \\ \} 2 \end{matrix} \tag{3.32}$$

and

$$\underset{\sim}{h} = \begin{bmatrix} h_1 \\ h_2 \\ . \\ . \\ . \\ h_n \end{bmatrix} \qquad \text{and } m = \begin{bmatrix} m_1 \\ m_2 \\ . \\ . \\ . \\ m_n \end{bmatrix} \tag{3.33}$$

Including gravity effects in the soil model can be done by either of two methods:

(i) Modifying the elements in the stiffness matrix by the structural weights as shown below:

$$\underset{\sim}{k}_G = \begin{bmatrix} \underset{\sim}{k} & -\underset{\sim}{k}\,\underset{\sim}{J} & -\underset{\sim}{k}\,\underset{\sim}{h} \\ -\underset{\sim}{J}^T\underset{\sim}{k} & k_x+\underset{\sim}{J}^T\,\underset{\sim}{k}\,\underset{\sim}{J} & \underset{\sim}{J}^T\,\underset{\sim}{k}\,\underset{\sim}{h} \\ -\underset{\sim}{h}^T\underset{\sim}{k}-g\underset{\sim}{m}^T & \underset{\sim}{h}^T\,\underset{\sim}{k}\,\underset{\sim}{J} + g\,\underset{\sim}{m}^T\underset{\sim}{J} & k_\phi+\underset{\sim}{h}^T\underset{\sim}{k}\,\underset{\sim}{h} \end{bmatrix} \qquad (3.34)$$

(ii) Adding to the excitation vector a gravity excitation vector given by:

$$\underset{\sim}{I} \cdot g\,\underset{\sim}{m}^T\,(\underset{\sim}{u}' - \underset{\sim}{J}\,u_F)$$

where

$$\underset{\sim}{I} = \begin{bmatrix} 0 \\ 0 \\ 0 \\ \vdots \\ 0 \\ 0 \\ 1 \end{bmatrix} \begin{matrix} \} n \\ \\ \\ \\ \\ \} 2 \end{matrix} \qquad (3.35)$$

u' and u_F are the values obtained at the previous time step.

The latter scheme is more economical and faster, and is used in the study.

3.4 THE OVERSHOOTING AND THE BACKTRACKING PROBLEMS: EFFECT OF TIME STEP OF INTEGRATION

The overshooting and backtracking problem is the major disadvantage of using a tangent formulation as implemented here. The state of yield for each component in the structural system is determined only once at the beginning of each time increment, then the initial value problem is progressed through either the load domain or the time domain. In structural systems which have a well-defined yield point, whether this yield point is at the stress-strain level or at the total behavior level, "overshooting" and backtracking take place. The phenomenon is best illustrated as shown in Fig. 3.4. Whenever the component yields, the yield level is overshot by a small amount upon entering the nonlinear state. Upon returning to the nonlinear state, the behavior is backtracked for one domain step.

A similar effect might be introduced by modifying the yield capacity at the ends of a member for a given interaction surface as the analysis progresses.

In the current work the problem of overshooting and backtracking was studied to establish the most convenient time increment to be used in the analysis. Since recently most of the historical records of earthquakes have been reprocessed at California Institute of Technology, it was decided to use the first 6 sec. of the most recent version of the Imperial Valley 1940 N-S earthquake record (El Centro). The initial time step for this record is 0.02 seconds; thus

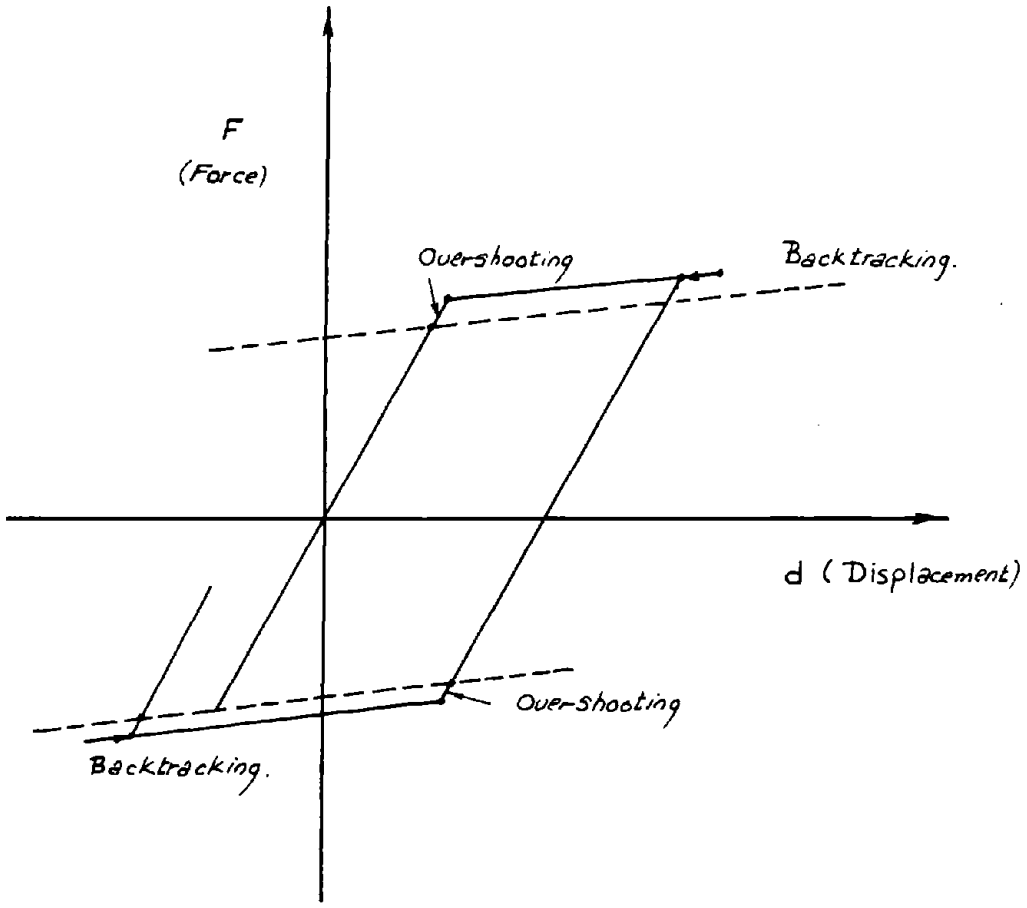

Fig. 3.4 - The Overshooting and the Backtracking Phenomena

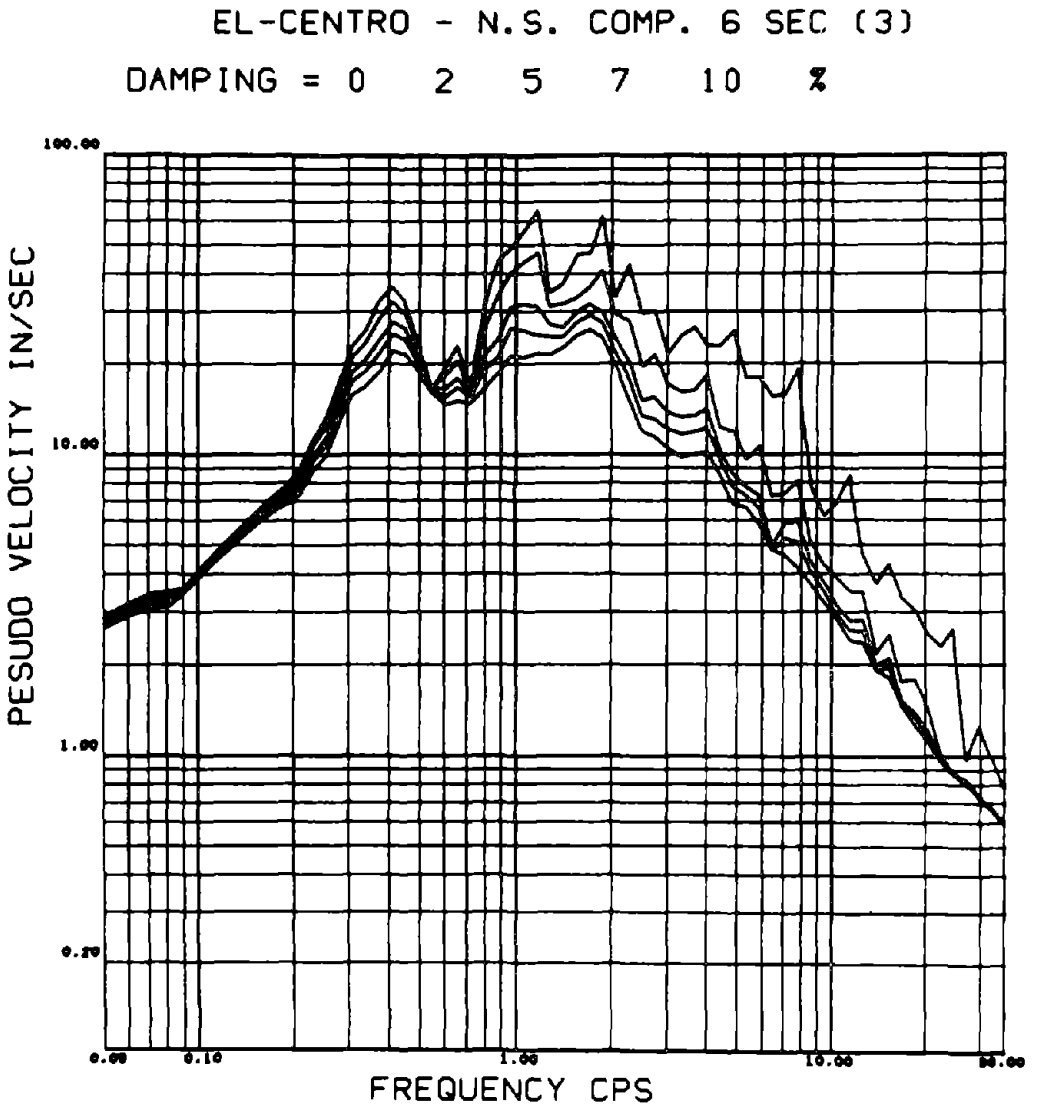

Fig.3.5 - Response Spectra - Imperial Valley (El Centro)
N.S. Component 1940 (ΔT = 0.02 Sec.)

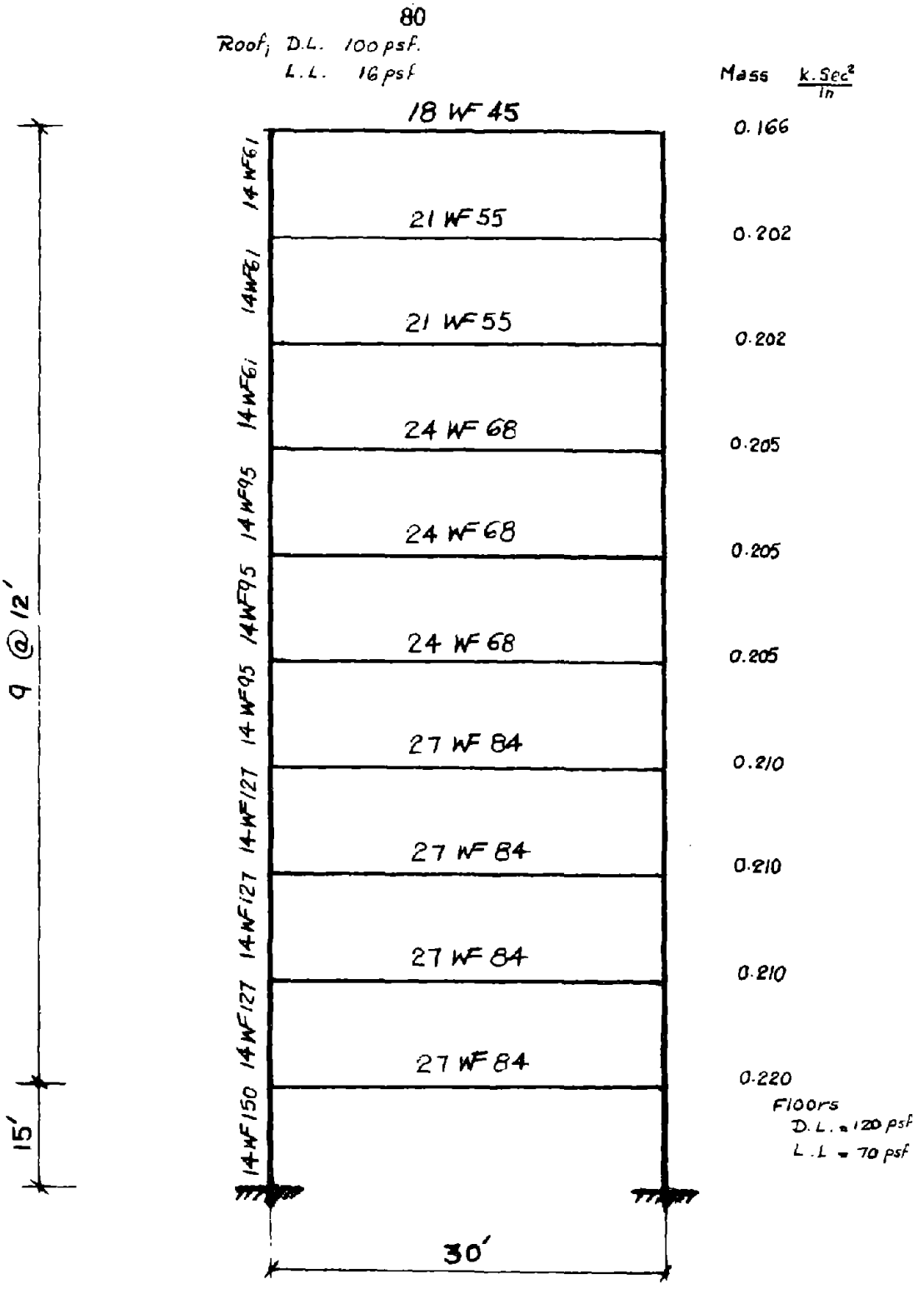

Fig. 3.6 - 10-Story 1-Bay Frame Designed by Anderson & Bertero

two other records were obtained by redigitizing the original record at 0.01 sec. and 0.005 sec. From the mathematical point of view, the three digitized records are identical and they form a minimizing sequence. Response spectra for the original record are shown in Fig. 3.5 for different damping values. The 10-story 1-bay frame shown in Fig. 3.6, which was previously designed by Anderson, was subjected to the three records mentioned above. A 5% damping proportional to the mass, and a DCM with 5% second slope were used. Gravity effects were introduced by appropriate initial static forces and stability was introduced by the stability functions presented before. The interaction formula of AISC for axial-bending strong axis interaction was used.

The results of the study are shown in Figs. 3.7 through 3.17. From the results presented, the following conclusions can be reached:

1. As far as the relative displacements of the structure are concerned, using a Δt of 0.02 leads to a small error which is larger for the lower stories than the upper stories of the building. The error is always positive.

2. The error in the interstory displacements is generally of the same order as the error in the floor displacements.

3. The story forces are the most affected among all response parameters, since high-frequency components are expected to contribute more to this parameter. However, this phenomenon does not seem to affect the other response parameters.

4. The error in the story shears is more for the upper stories and is relatively less for the lower stories.

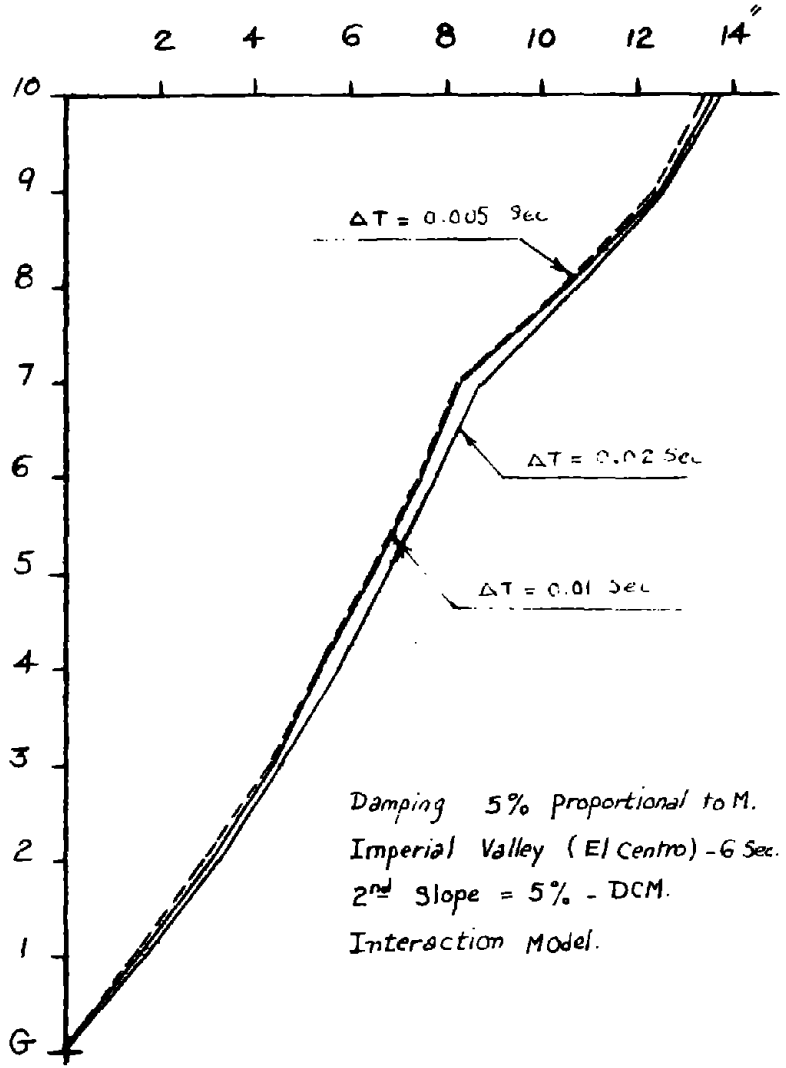

Fig. 3.7 - Effect of Time Increment on Floor Displacements

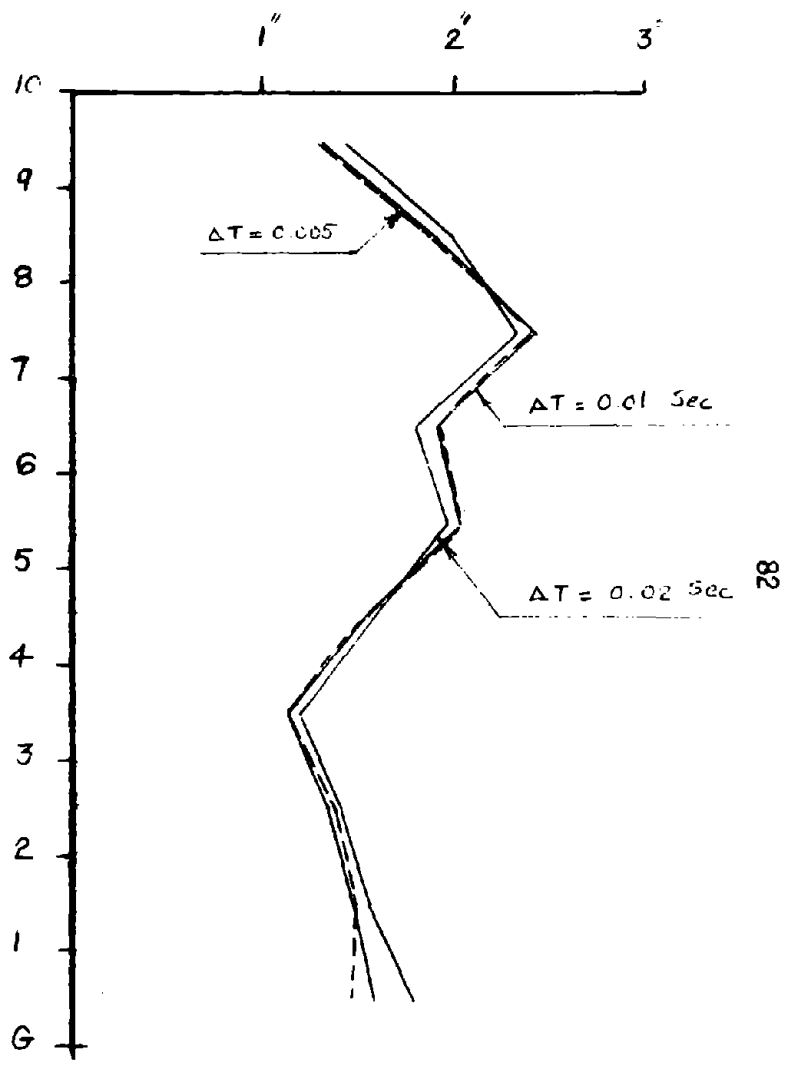

Fig. 3.8 - Effect of Time Increment on Interstory Displacements

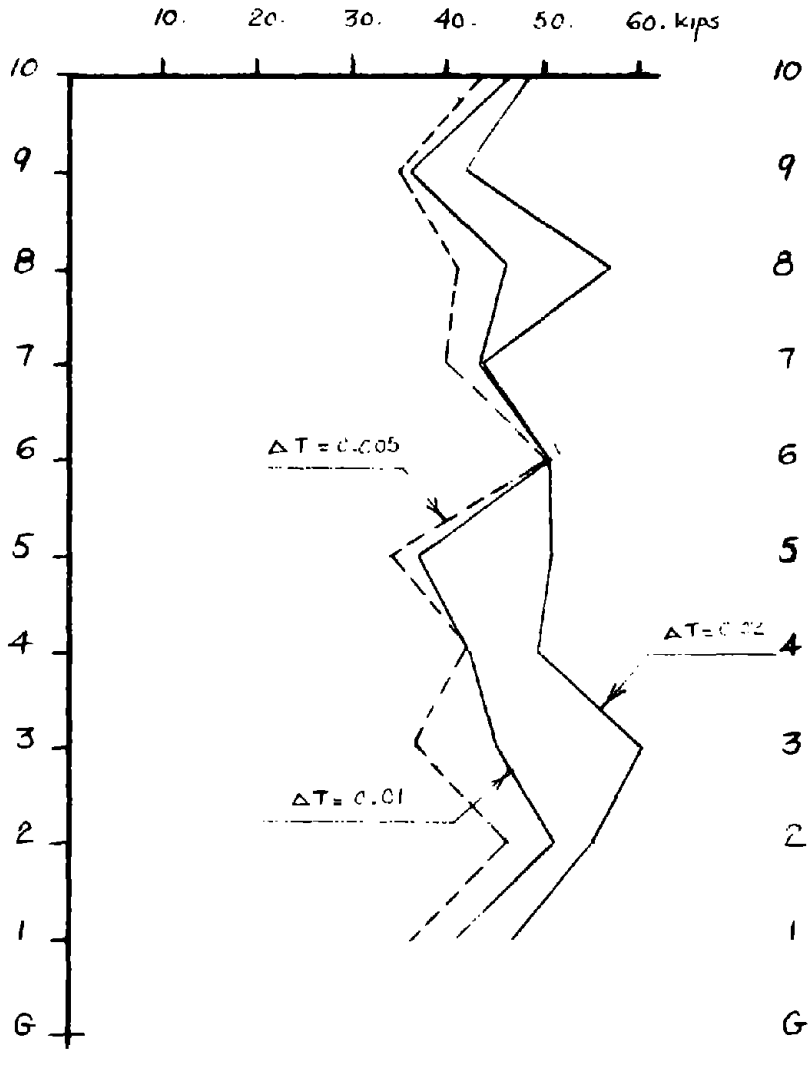

Fig. 3.9 - Effect of Time Increment on Story Forces

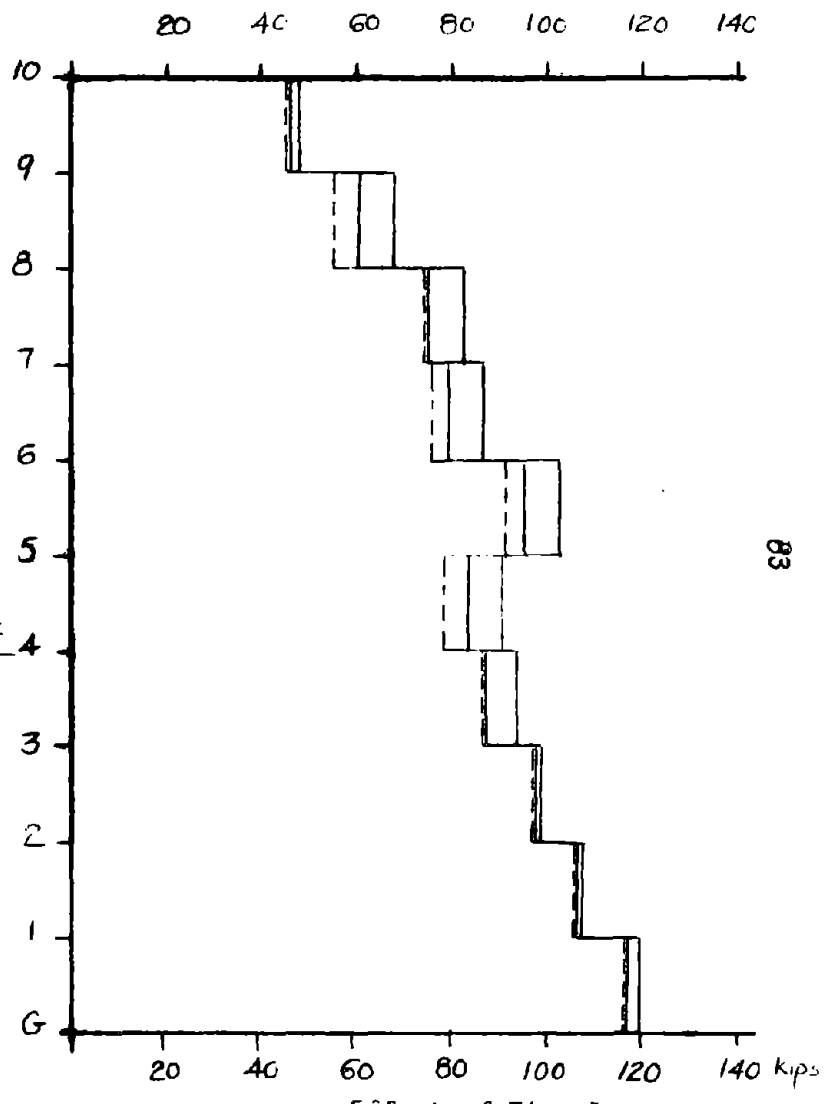

Fig. 3.10 - Effect of Time Increment on Story Shears

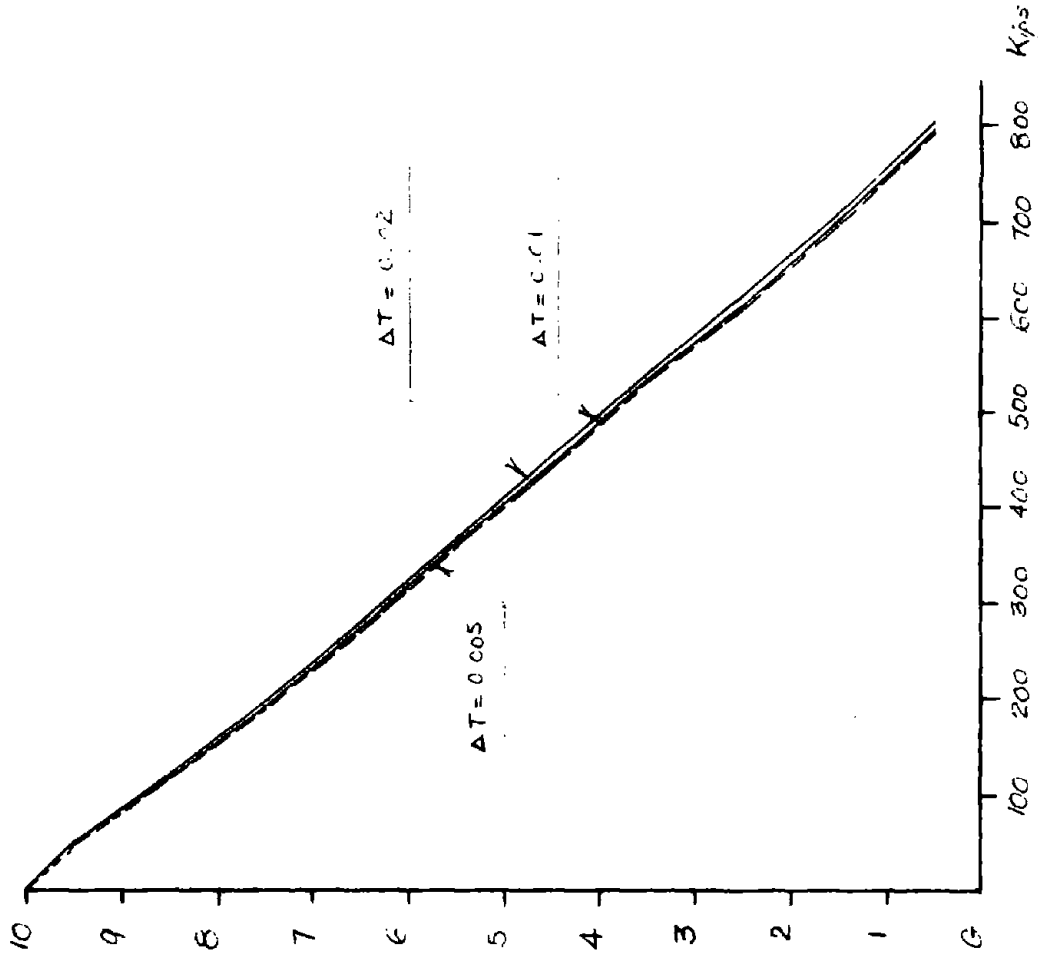

Fig. 3.11 - Effect of Time Increment on the Maximum Column Axial Forces

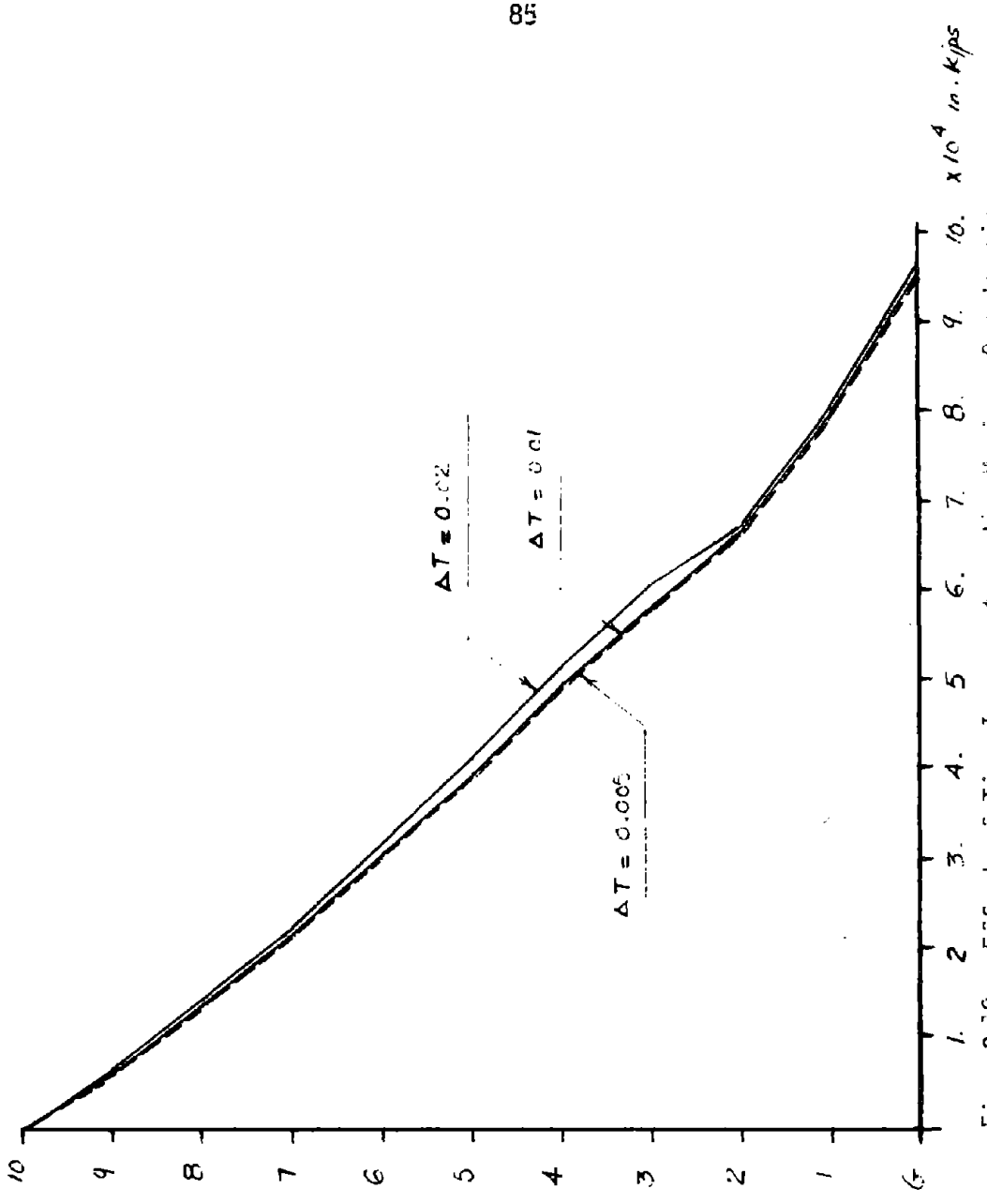

Fig. 3.12 - Effect of Time Increments on the Maximum Overturning Moment

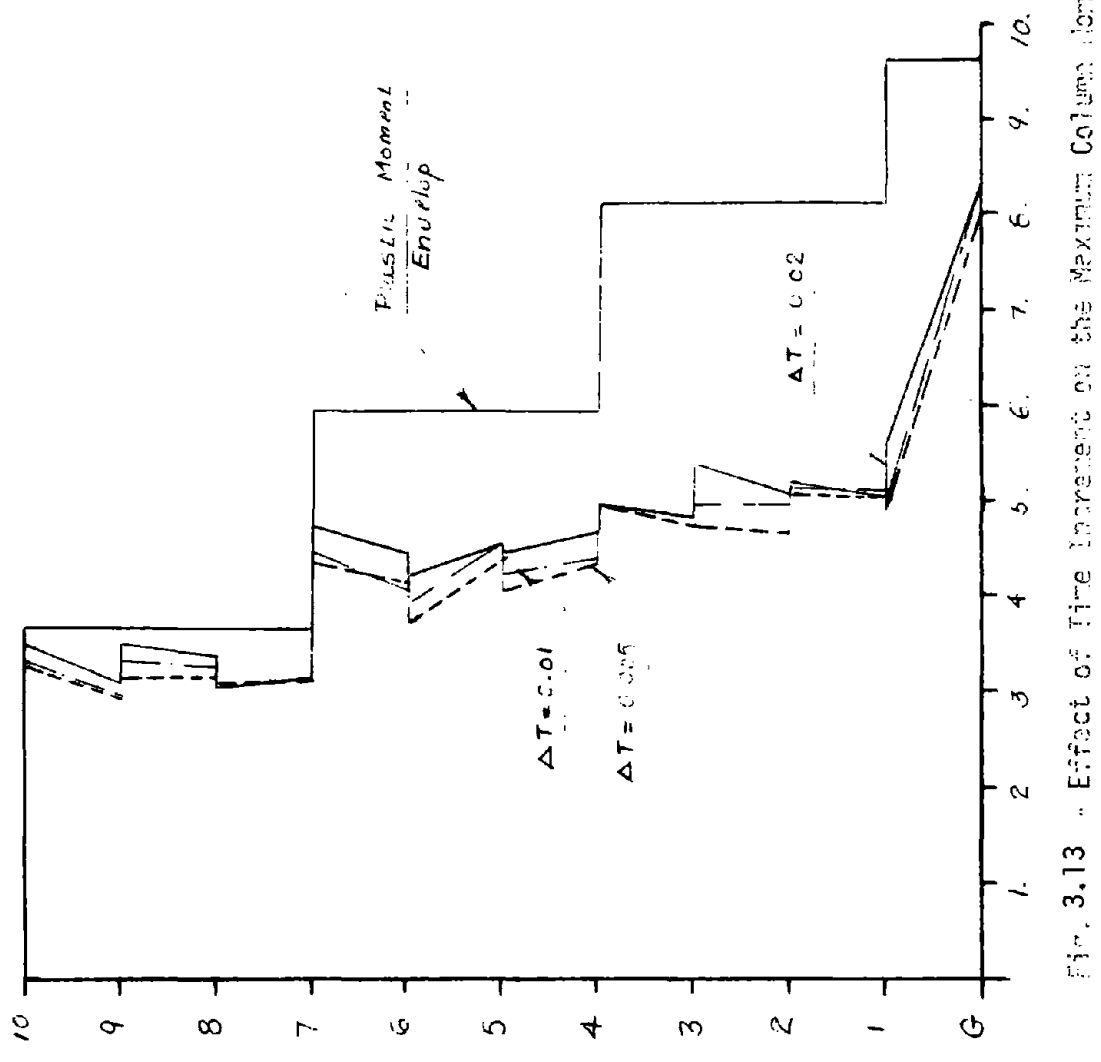

Fig. 3.13 - Effect of Time Increment on the Maximum Column Moments

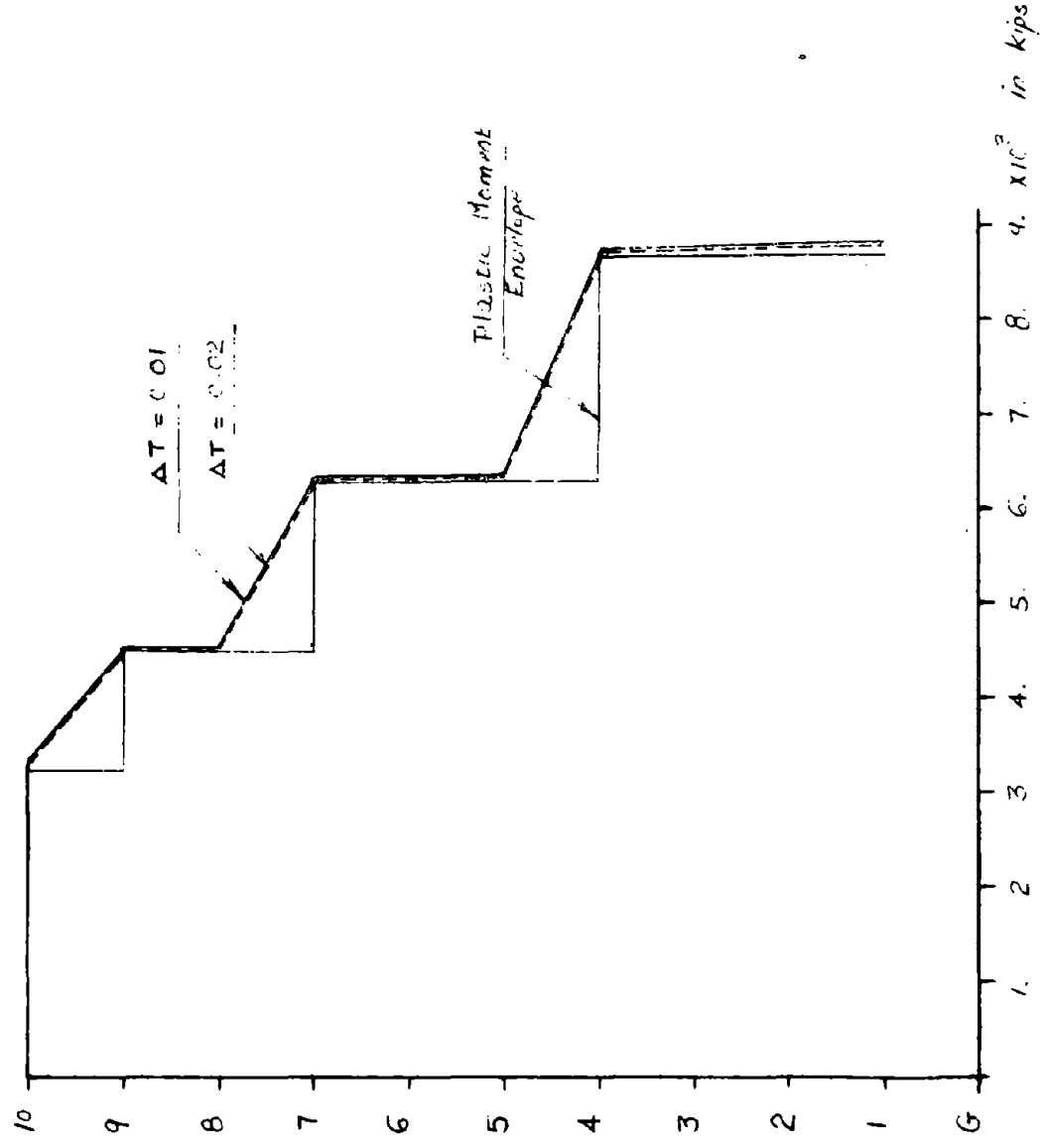

Fig. 3.19 - Effect of Time Increment on the Maximum Girder Moments

5. Axial forces in the columns are not affected by the time increment for the range of time increments studied, while the overturning moment is slightly affected.

6. The individual member forces are slightly affected. The columns are affected more than the girders, because they experience interaction and other nonlinear effects.

7. Column ductilities and girder ductilities are affected by the increment size, although some locations in the building did not show any effect.

8. Using an increment size of 0.01 sec. is both economical and accurate, and thus all the following analyses will be done using such time increment. Decreasing the time increment below 0.01 sec. does not lead to any significant or justified increase in accuracy. This is easily concluded by comparing the response curves for increment size of 0.01 sec. versus 0.005 sec., which tend to be very close to each other.

9. The constant velocity method which was used to solve the equations of motion might offer some advantages over other integration schemes particularly in the inelastic range. The time interval of integration should be small enough to both represent the earthquake loading accurately and also to avoid any excessive overshooting or backtracking.

10. Generally speaking, a minimizing sequence exists for most of the response parameters, which suggests that one can obtain an upper bound of these response parameters by using a well-chosen increment size. Strictly speaking, this upper bound is not observed in the individual member forces, since the results oscillate around the real solution. This could be attributed to the special nature of the overshooting and the backtracking phenomenon encountered here.

3.5 COMPARATIVE STUDIES FOR DIFFERENT BENDING MODELS

3.5.1 Comparisons with Results by Anderson

To verify the correctness of the computer program developed, the 10-story 1-bay frame shown in Fig. 3.6 was studied. The earthquake excitation used was the N-S component of El Centro, 1940. It is worth mentioning that there are at least two versions of this component in addition to the new version reprocessed recently by California Institute of Technology. The response spectra of these two versions are shown in Figs. 3.15 and 3.16. In Fig. 3.17 the three spectra for 5% damping are plotted on top of each other. It is evident that although the three records are very similar, they can differ at a specific frequency by as much as 30 - 50%, especially for frequencies between 0.5 to 0.7 cps. In the current study the second version of El Centro, which came originally from California, was used.

Fig. 3.18 shows the response of the frame to the three different versions of El Centro (as obtained with the present computer program) and the results of Anderson. It can be seen that the solution with the California version of El Centro, labeled current study, is in very good agreement with Anderson's. Differences of up to 30% do, however, exist between the displacements resulting from the three versions of supposedly the same earthquake.

3.5.2 Single Component Model versus Dual Component Model

In the previous Chapter the GSCM and DCM models were discussed.

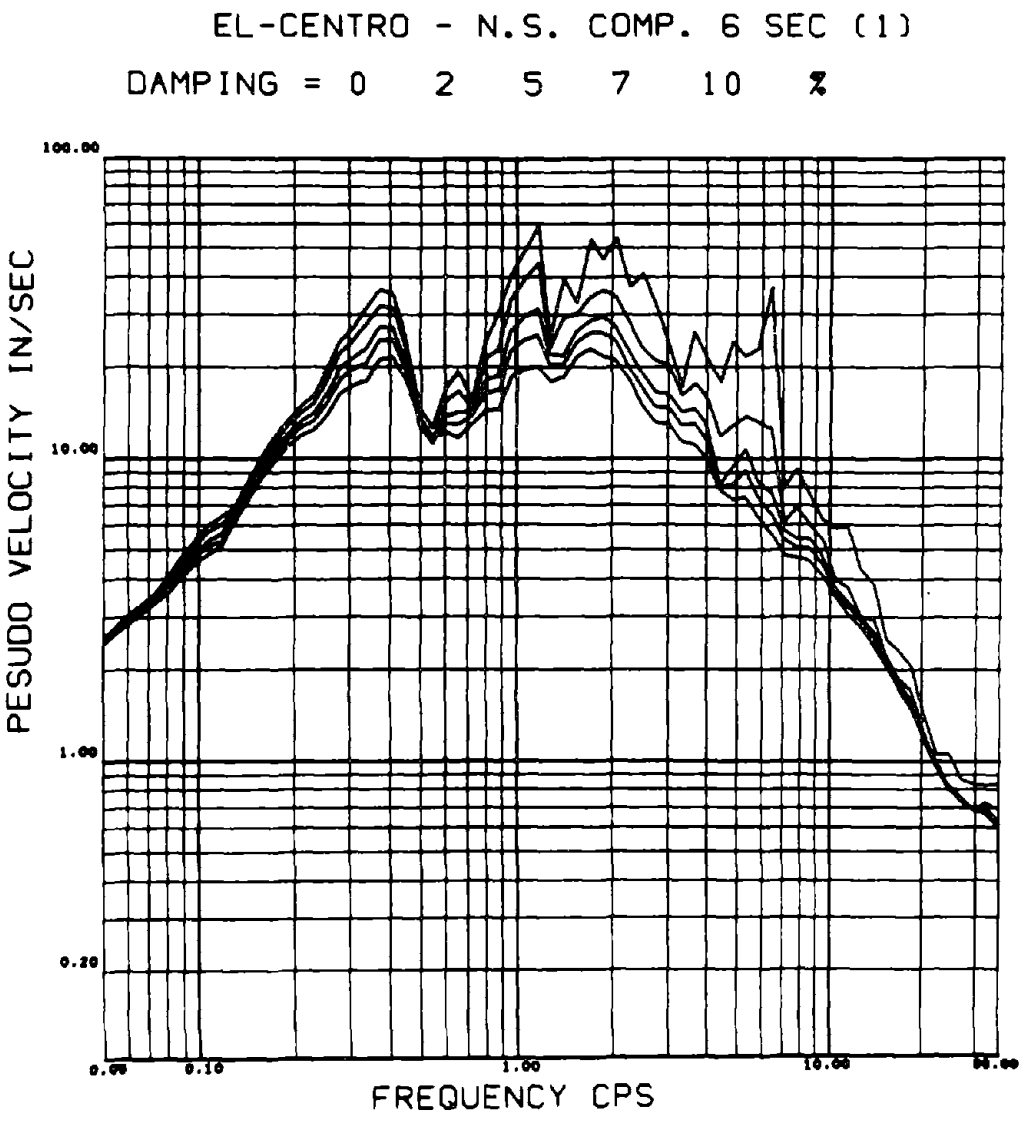

Fig. 3.15 - El Centro N.S. Component 1940 - Version #1

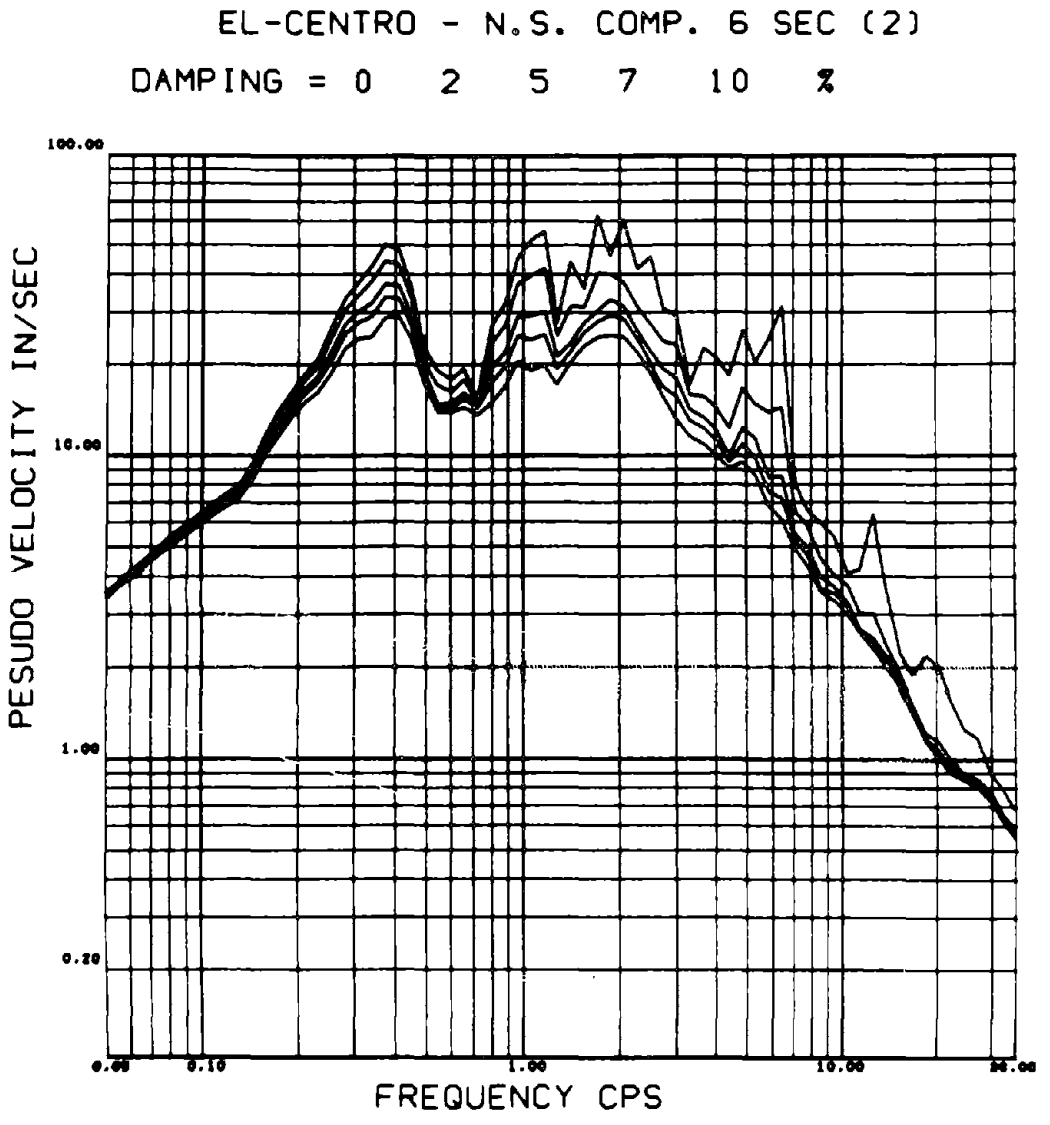

Fig. 3.16 - El Centro N.S. Component 1940 - Version #2

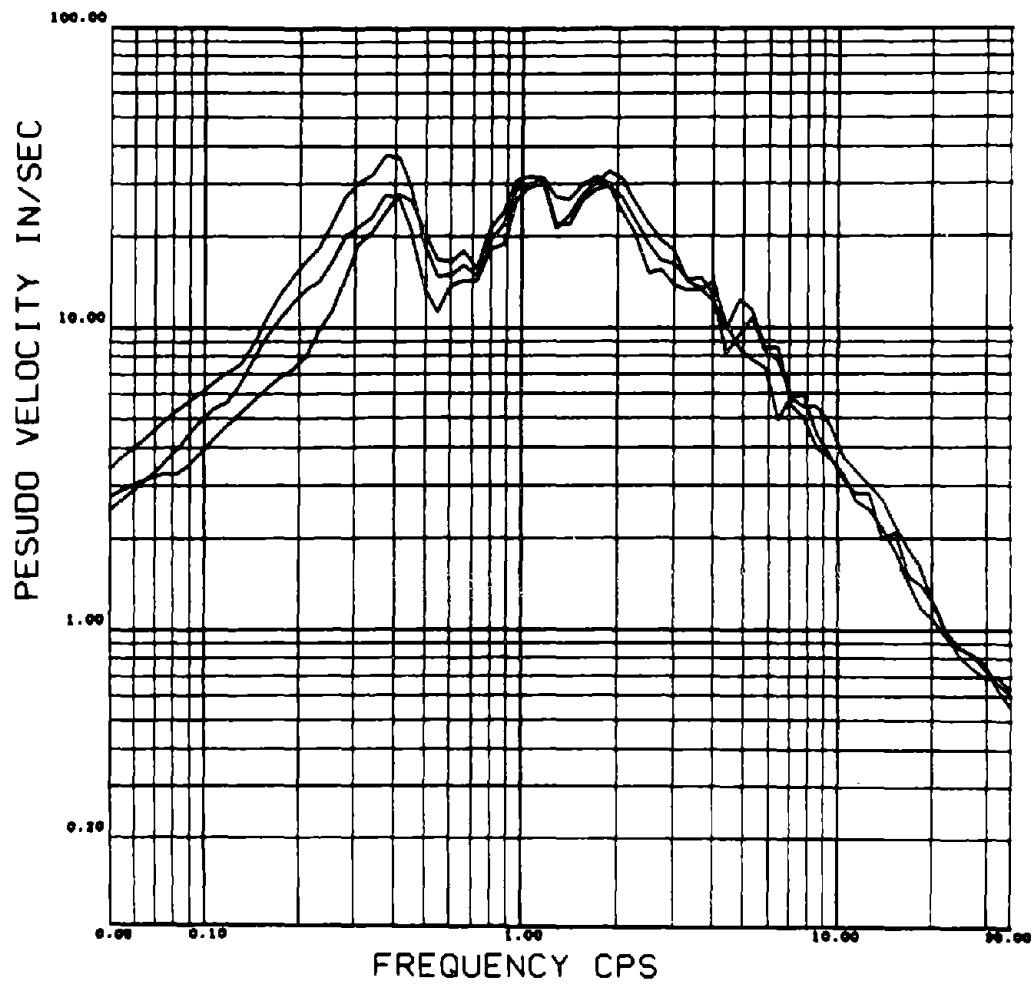

Fig. 3.17 - Nominal El Centro Spectra at 5% Damping

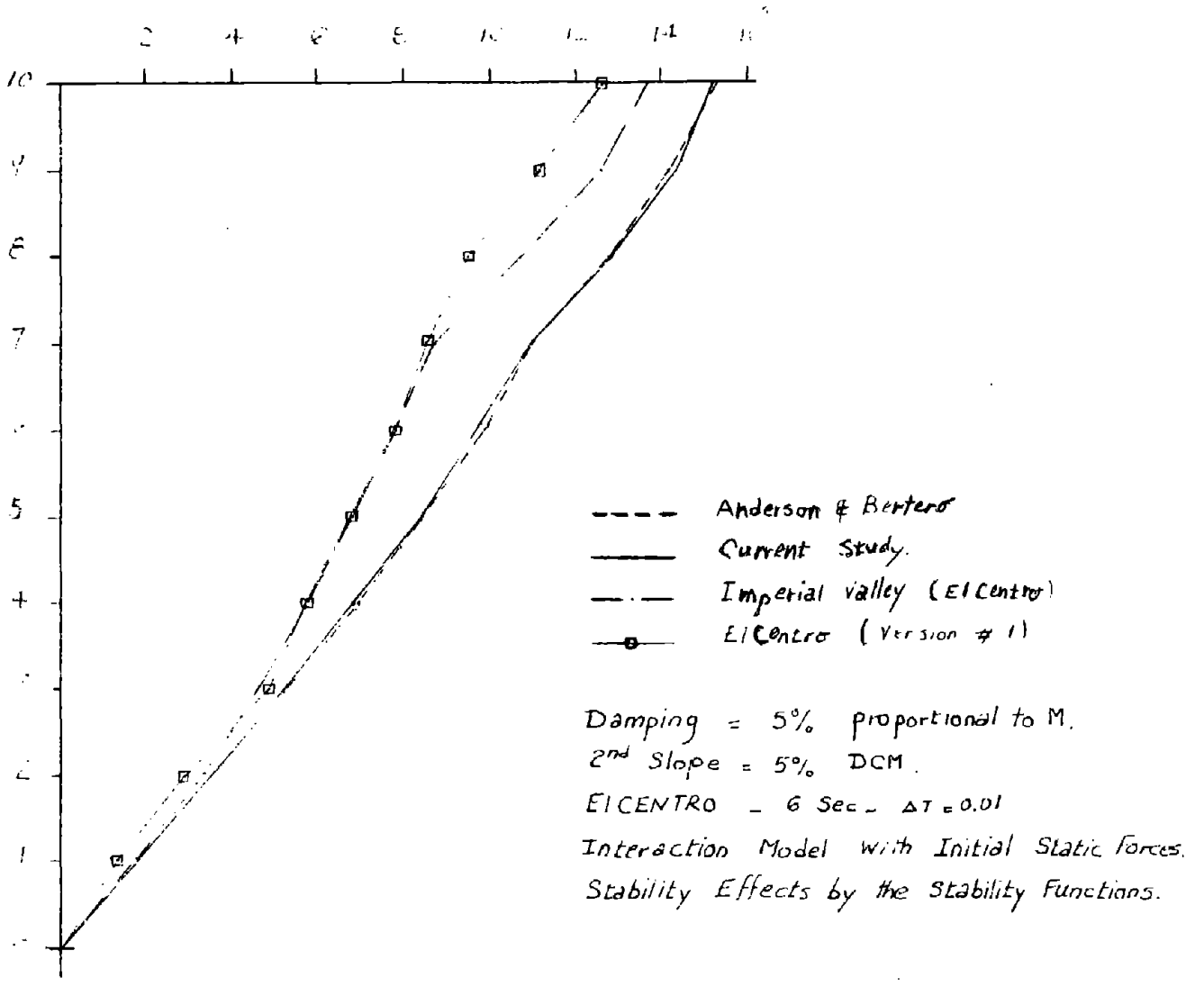

Fig. 3.18 - Comparisons with Results by Anderson - Maximum Displacements

Theoretically speaking, there is no simple way to match the response of a GSCM with that of a DCM. The number of conditions which should be satisfied is more than the number of variables to be chosen (which are mainly the strain hardening factors). Figs. 3.19 and 3.20 show a case study of the 10-story 1-bay frame with the following models:

1. A DCM with 5% strain hardening.
2. A GSCM (Bilinear in nature) with a 0.01% strain hardening.
3. A GSCM (Bilinear in nature) with a 0.001% strain hardening.

The case study suggests the following:

1. The bilinear GSCM gives in general similar results to the DCM in the cases where both of them can be used.

2. The results of the analysis are not substantially affected by the strain hardening factor used within the range considered. Any reasonable value of the correct order is sufficient from the practical point of view for the cases studied.

3. Although there is no theoretical way to get perfect match between a GSCM and a DCM, the results obtained were close from the practical point of view.

3.5.3 Effect of Stability Schemes

As discussed before in Chapter II, two stability schemes can be used; the first is based on the stability functions, and the other on corrective terms added to the stiffness matrix. Both schemes were used here and compared. The results of the comparison

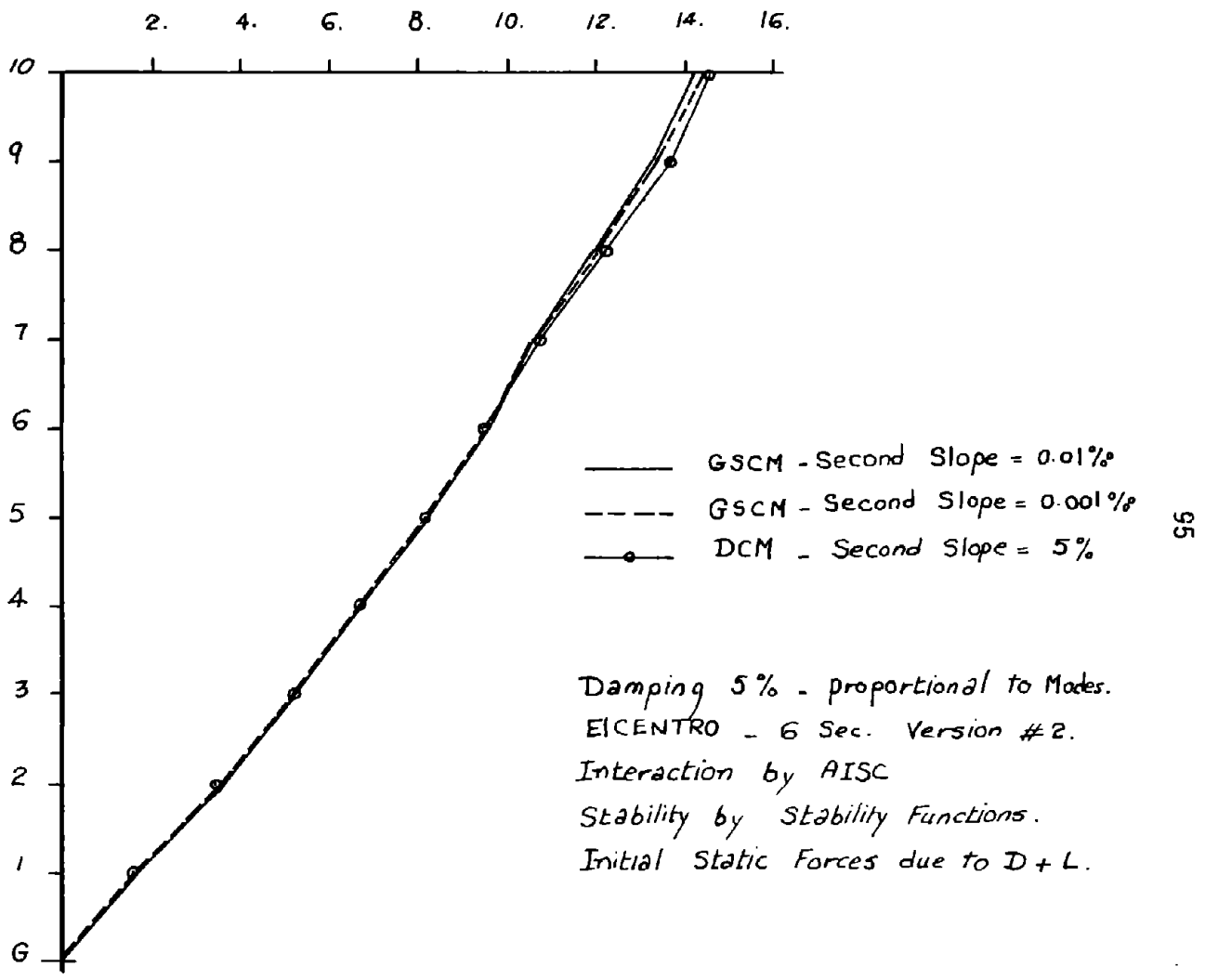

Fig. 3.19 - GSCM versus DCM - Maximum Displacements

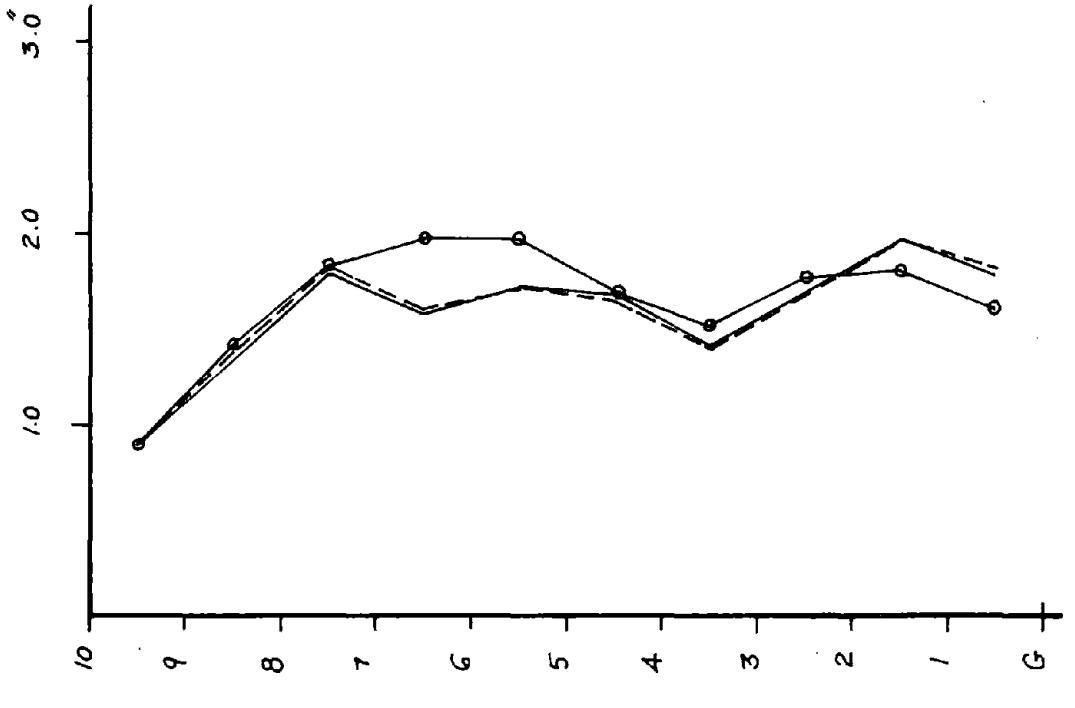

Fig. 3.20 - GSCM versus DCM - Maximum Interstory Displacements

are shown in Figs. 3.21 and 3.22. From a study of the different response parameters it was concluded that the two schemes give almost identical results. There is no advantage of using one or the other. However, if the stability functions were used in the conventional way, the cost of analysis might increase. In the current study look-up files which contain the different stability functions were created in data blocks. This scheme of storing and retrieving the stability functions proved to be as economical and accurate as the other stability schemes, and thus was used throughout most of the rest of this work.

3.5.4 P-Δ Effects

The relative importance of the P-Δ effects in the analysis is studied in Figs. 3.23 through 3.34. The figures represent results obtained when the P-Δ effects are properly taken into consideration or intentionally neglected. Also Figs. 3.35 and 3.36 represent the time history of the roof displacement and the time history of the axial force in the first-story column. Based on these Figures the following can be concluded for the case studied:

1. The P-Δ effects tend to increase both the displacements of the frame and the interstory displacements. They seem to reduce the story shears and they have little effect on the story forces.

2. The P-Δ effects tend to increase the ductility requirements for both columns and girders. The increase is more pronounced for the lower stories.

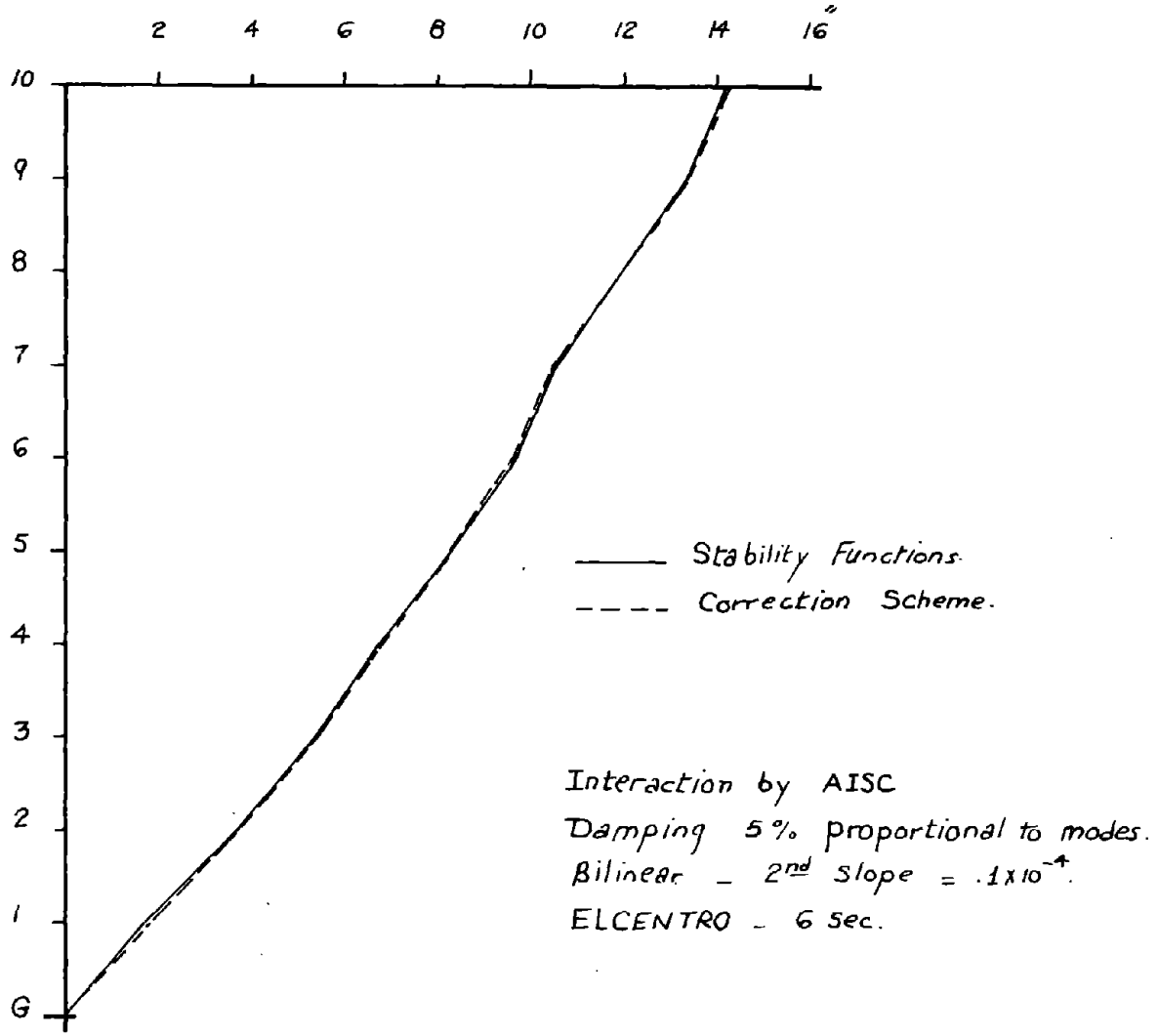

Fig. 3.21 - Effect of Stability Scheme on Maximum Displacements

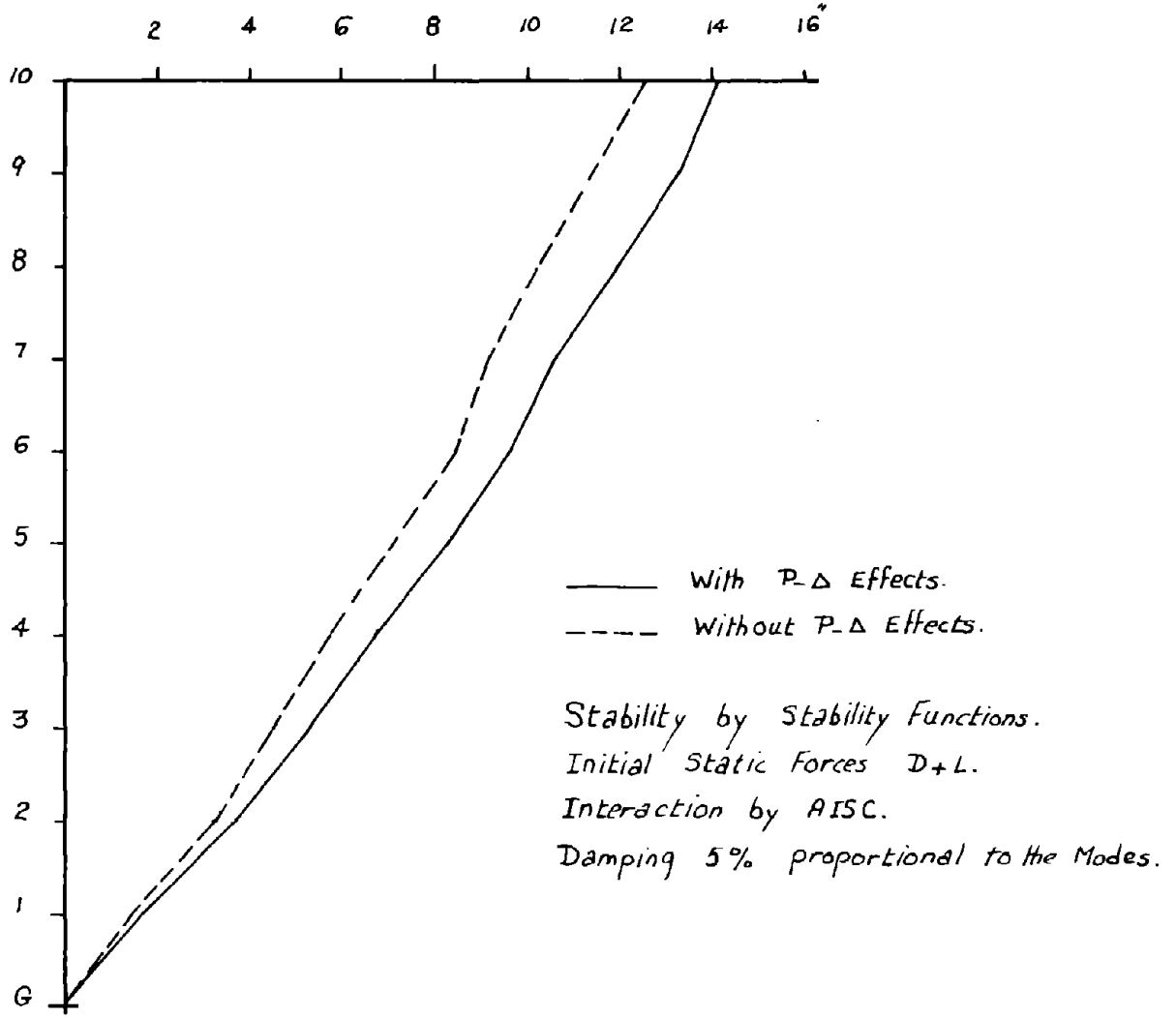

Fig. 3.22 - P-Δ Effects - Maximum Displacements

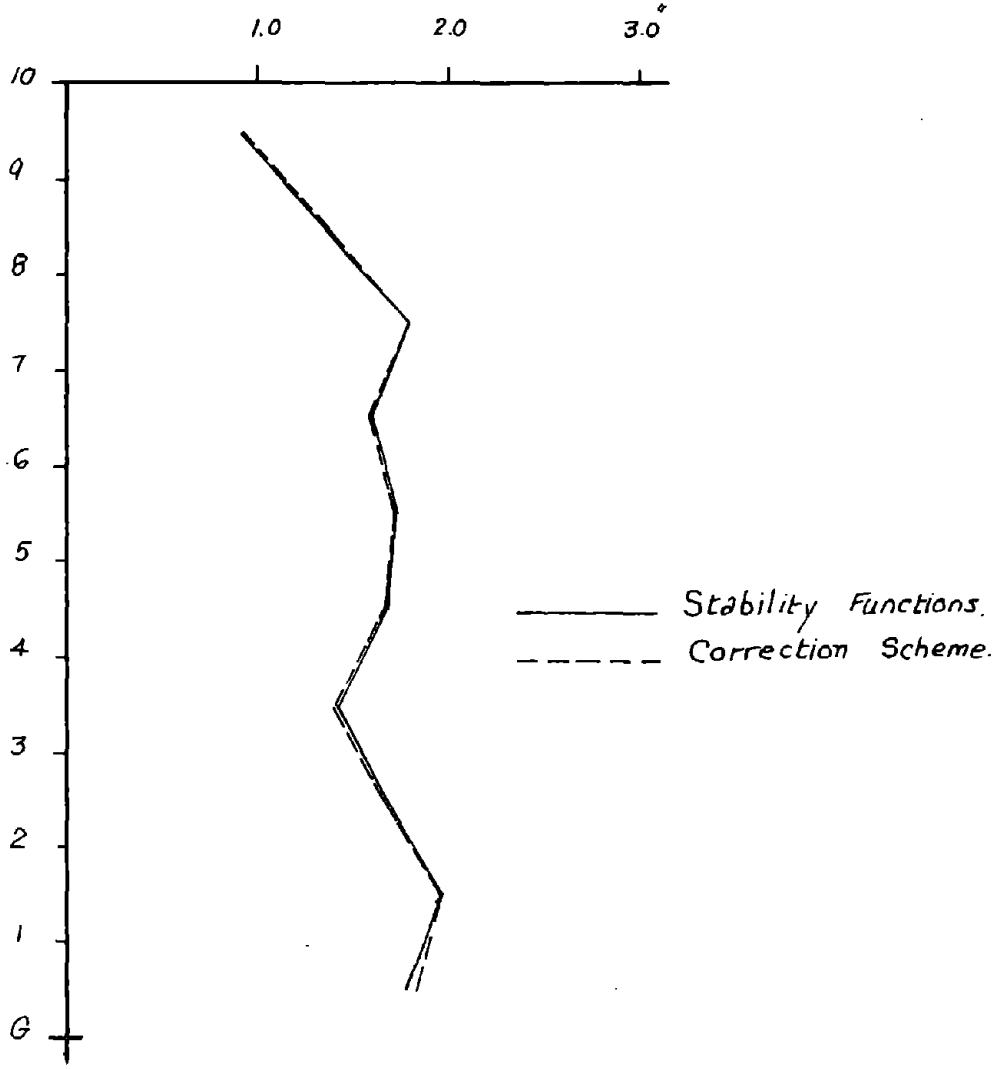

Fig. 3.23 - Effect of Stability Scheme on Maximum Interstory Displacements

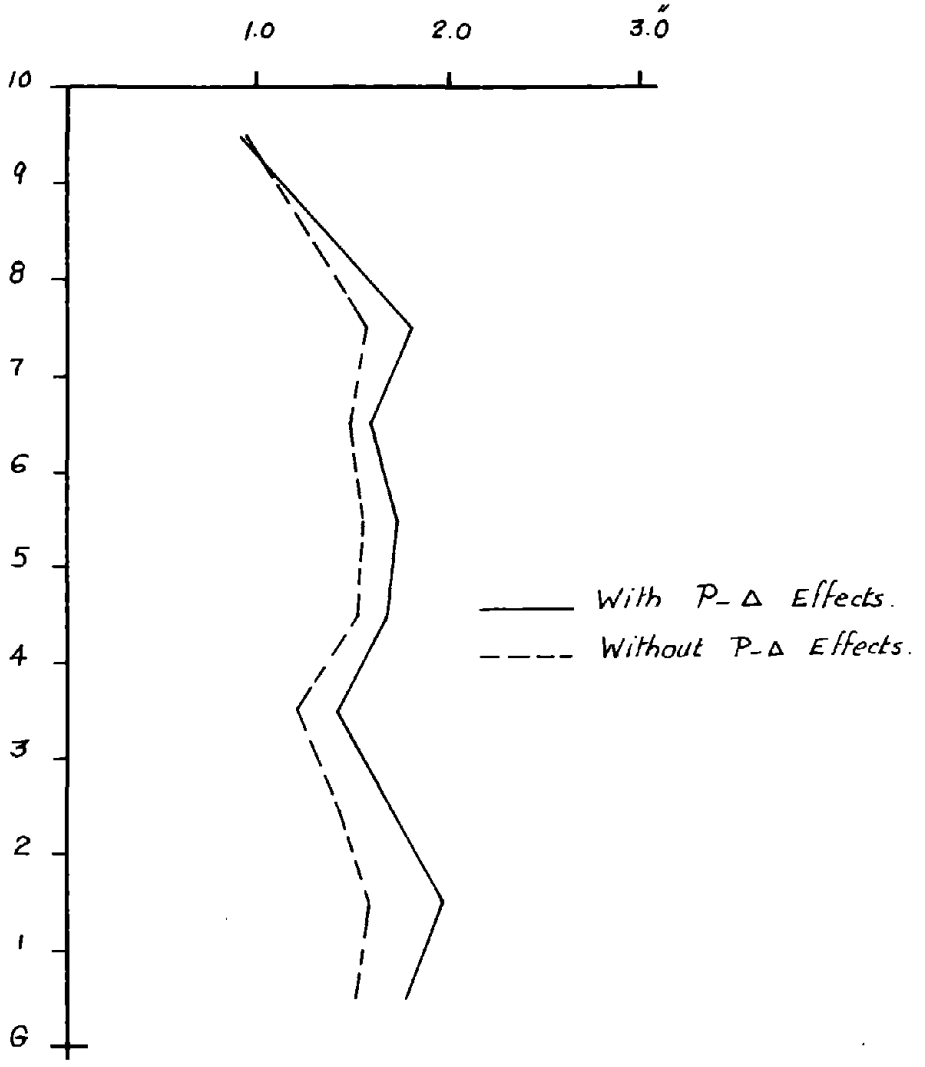

Fig. 3.24 - P-Δ Effects - Maximum Interstory Displacements

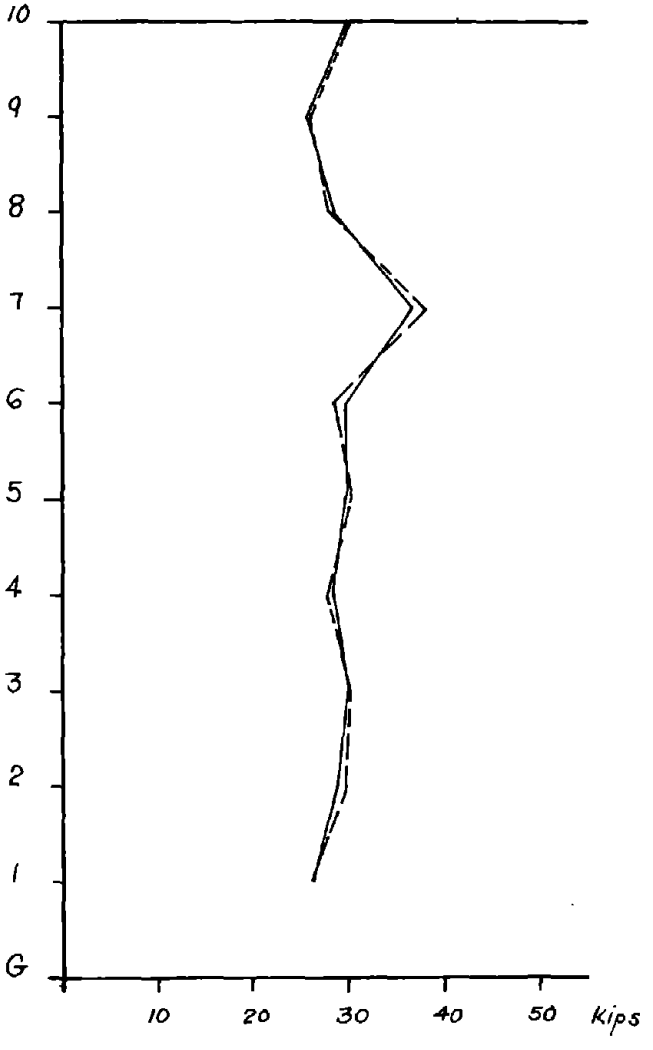

Fig. 3.25 - P-Δ Effects - Maximum Story Forces

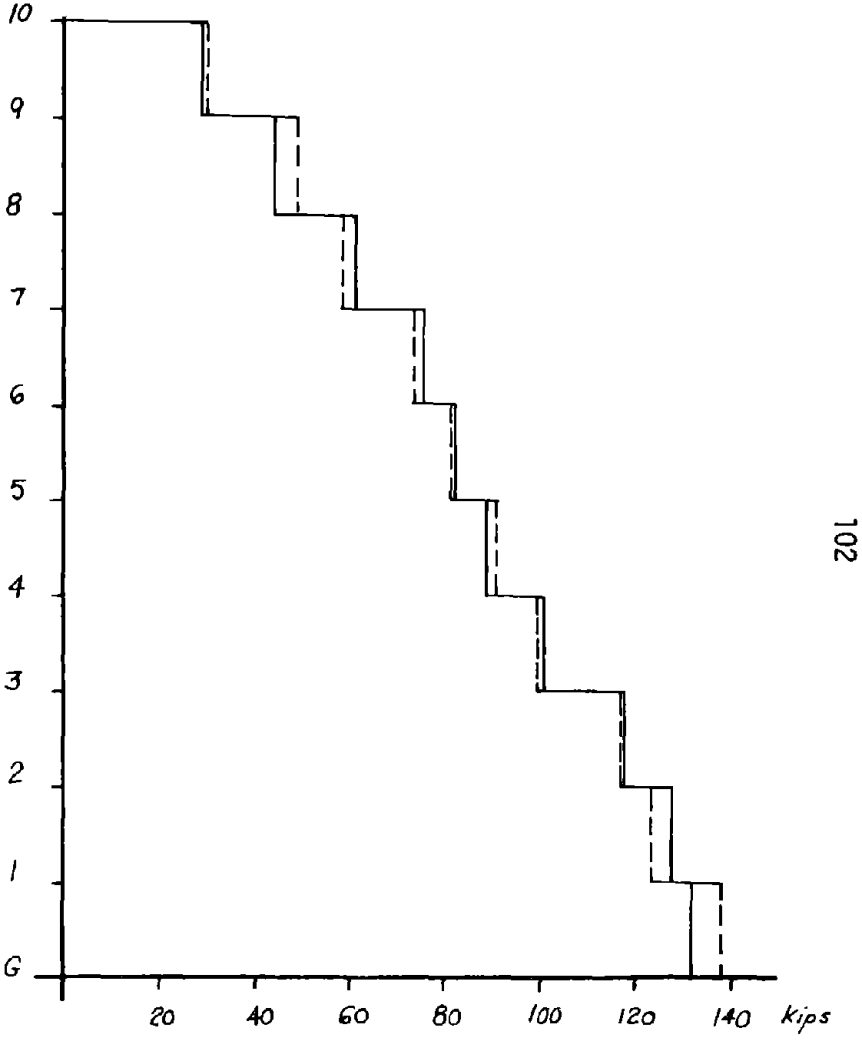

Fig. 3.26 - P-Δ Effects - Maximum Story Shears

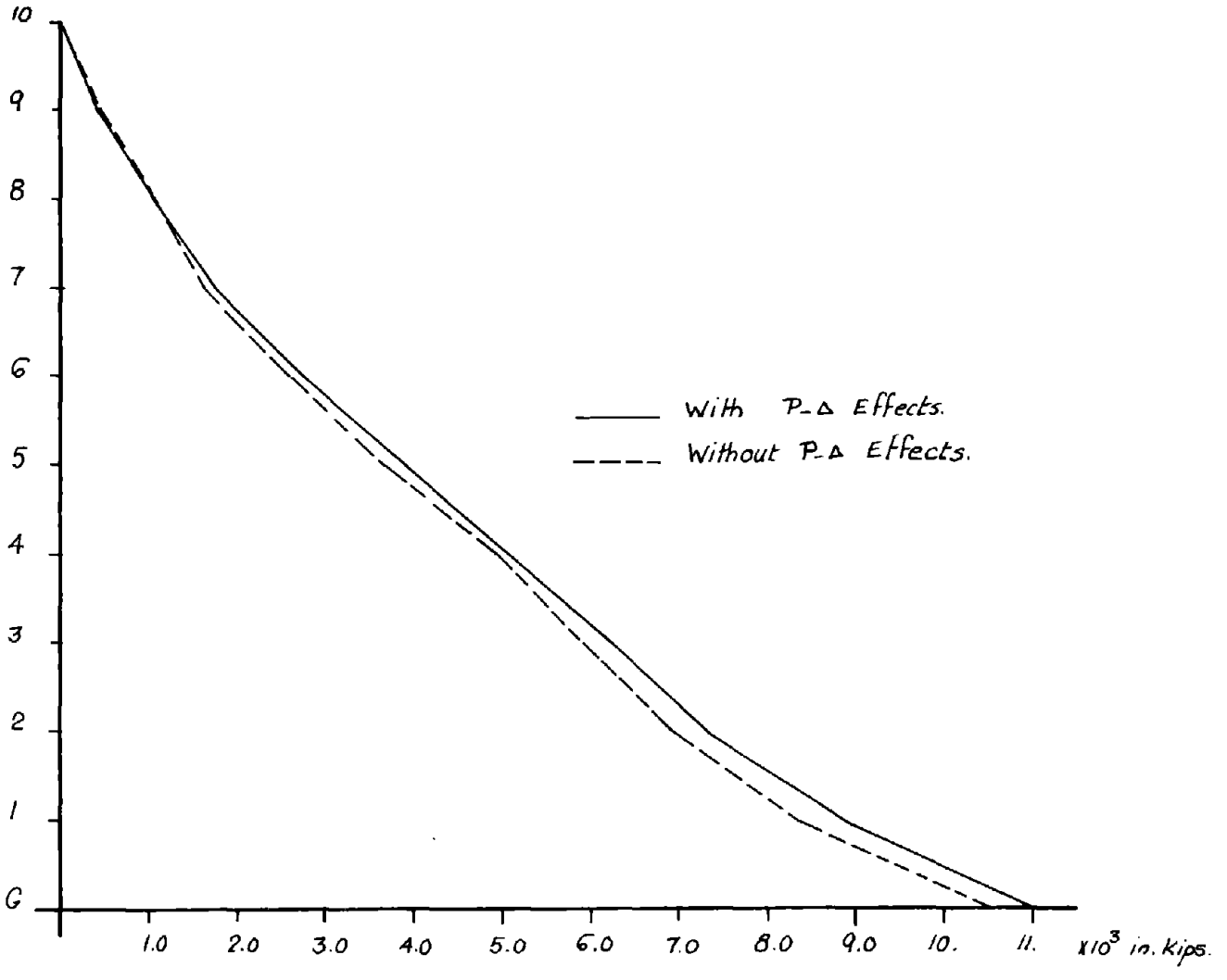

Fig. 3.27 - P-Δ Effects - Maximum Overturning Moment

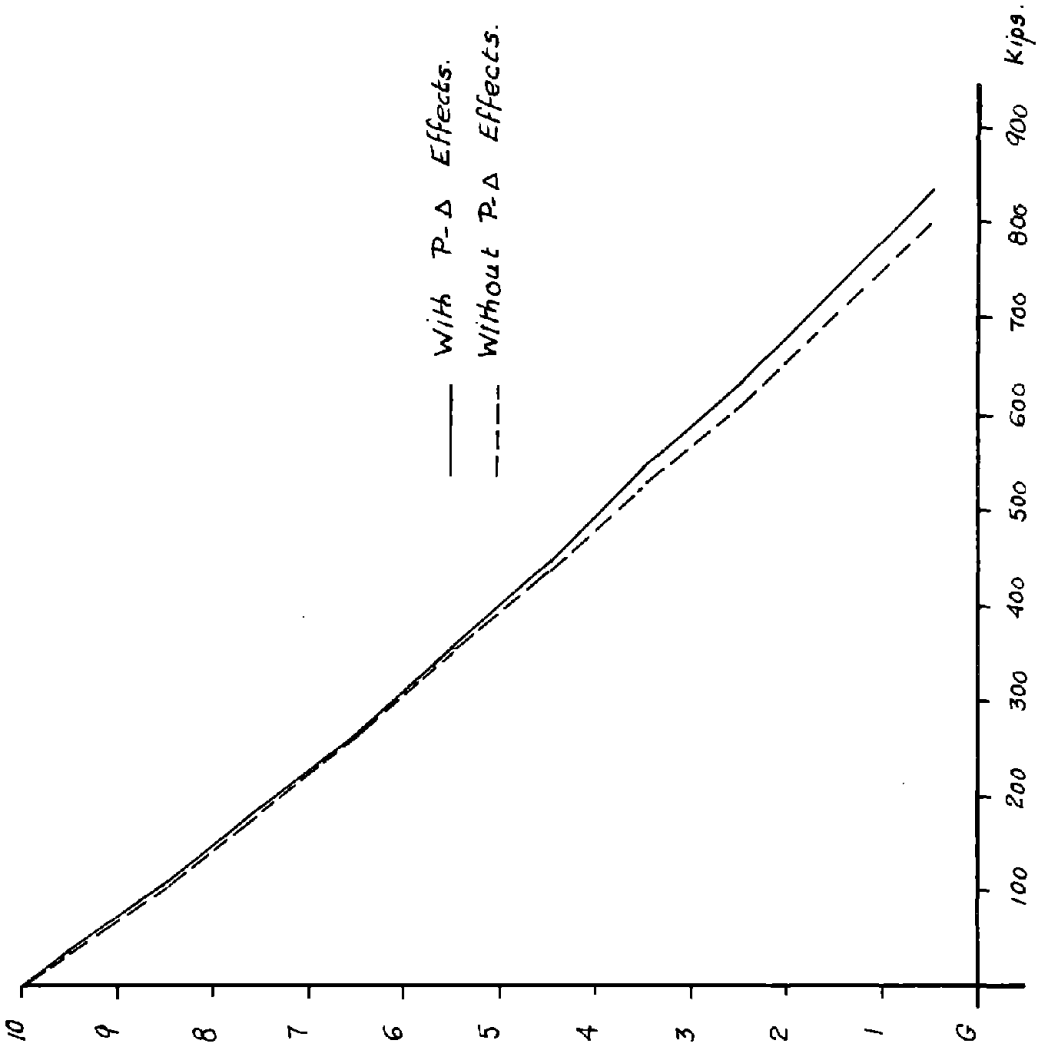

Fig. 3.28 - P-Δ Effects - Maximum Axial Forces in Columns

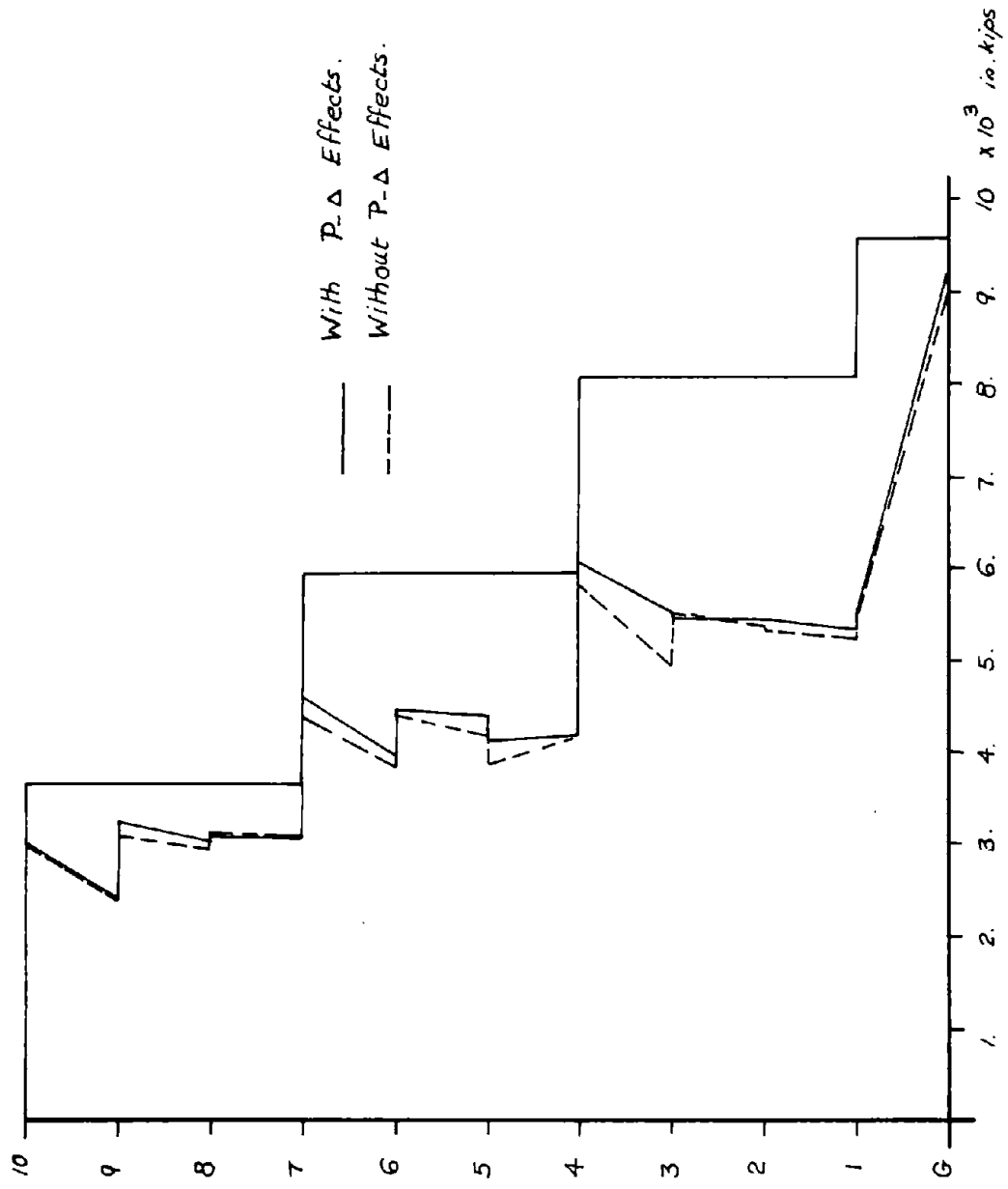

Fig. 3.29 - P-Δ Effects - Maximum Column Moments

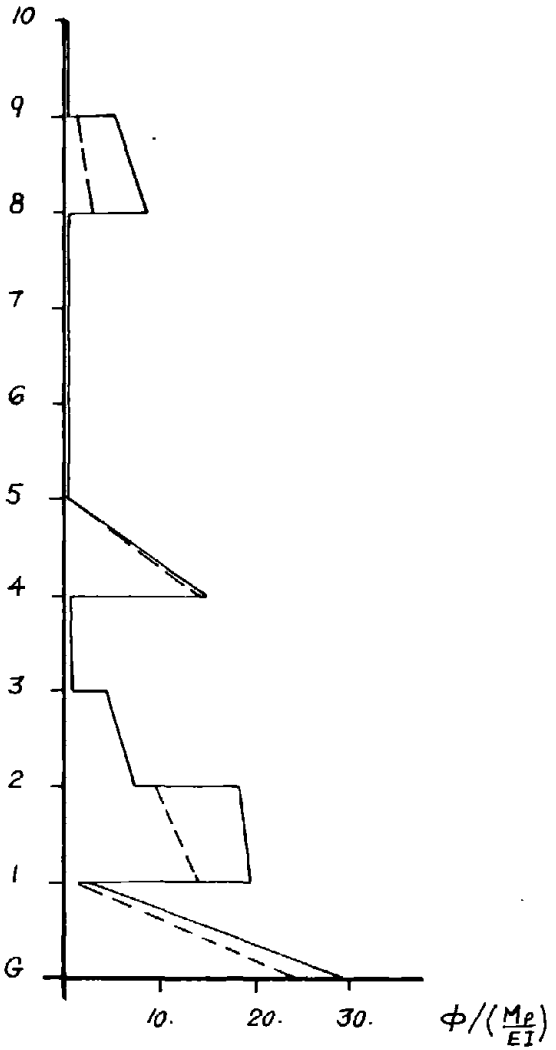

Fig. 3.30 - P-Δ Effects - Maximum Joint Rotations in Columns

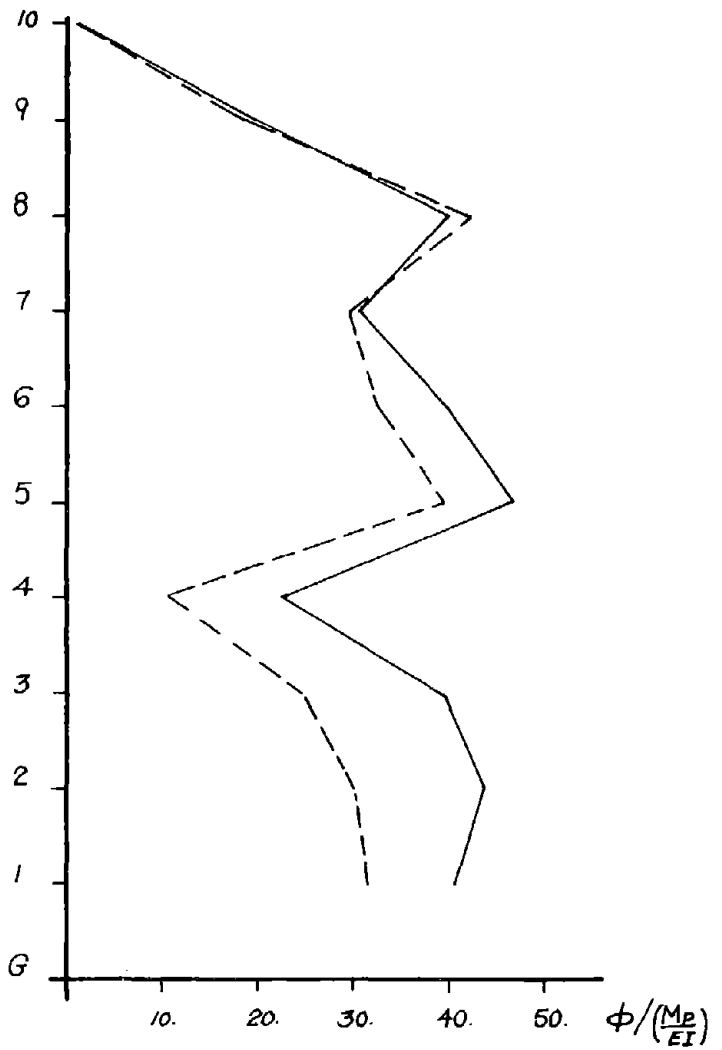

Fig. 3.31 - P-Δ Effects - Maximum Joint Rotations in Girders

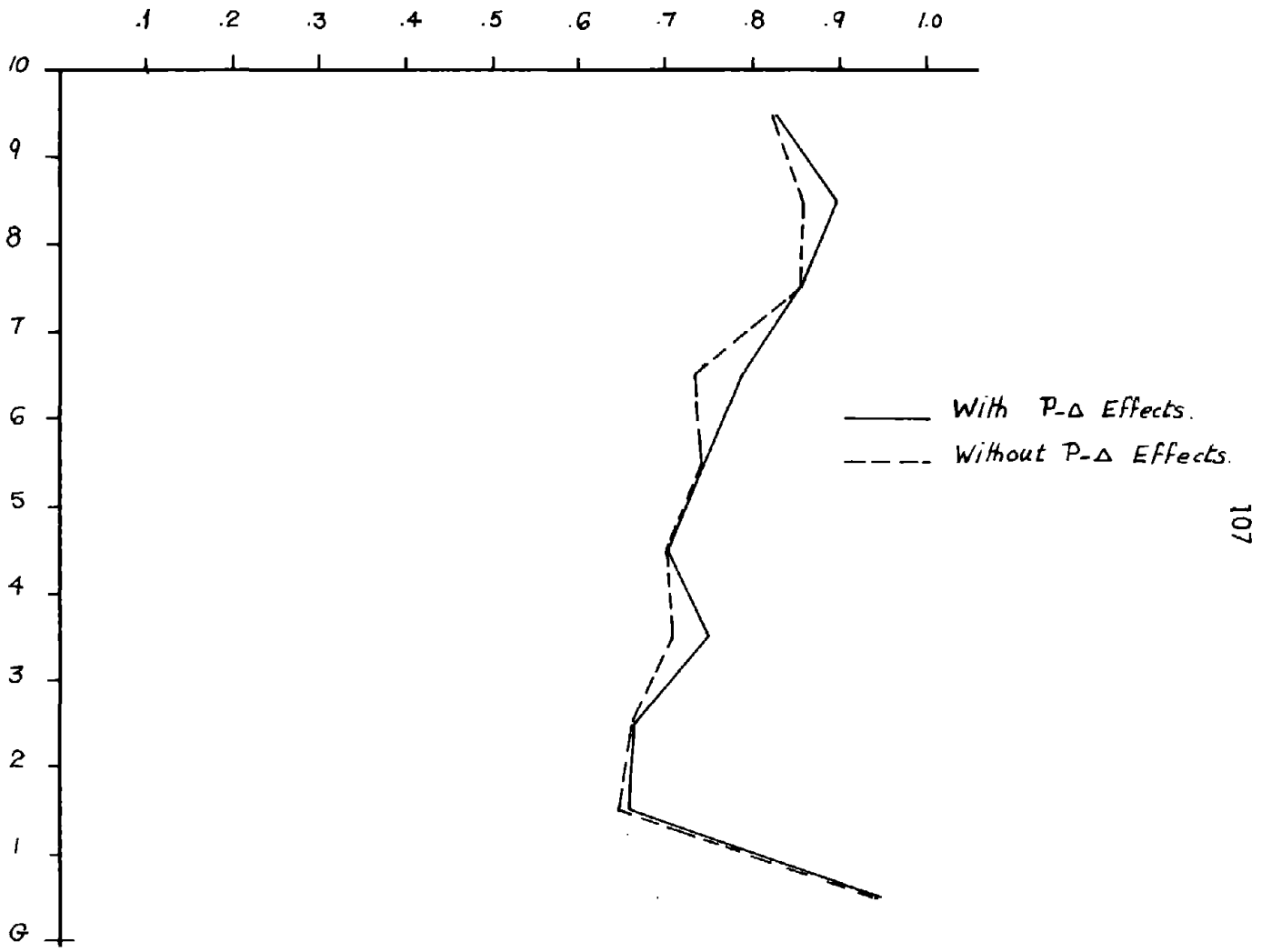

Fig. 3.32 - P-Δ Effects - Maximum Moment Ratios in Columns

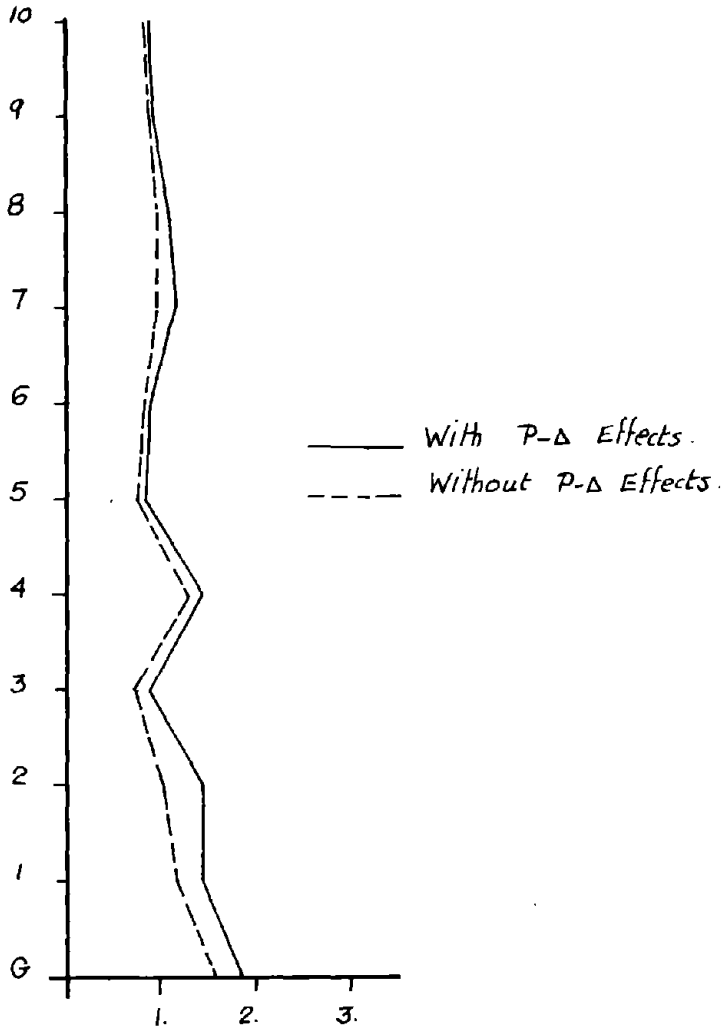

Fig. 3.33 - P-Δ Effects - Maximum Column Ductilities

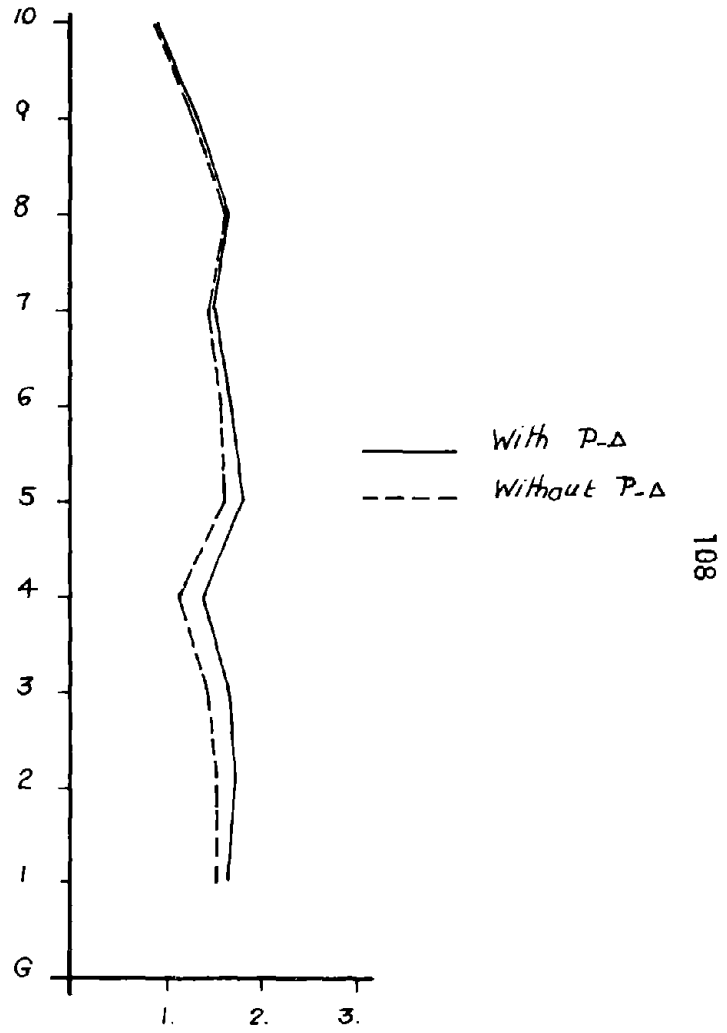

Fig. 3.34 - P-Δ Effects - Maximum Girder Ductilities

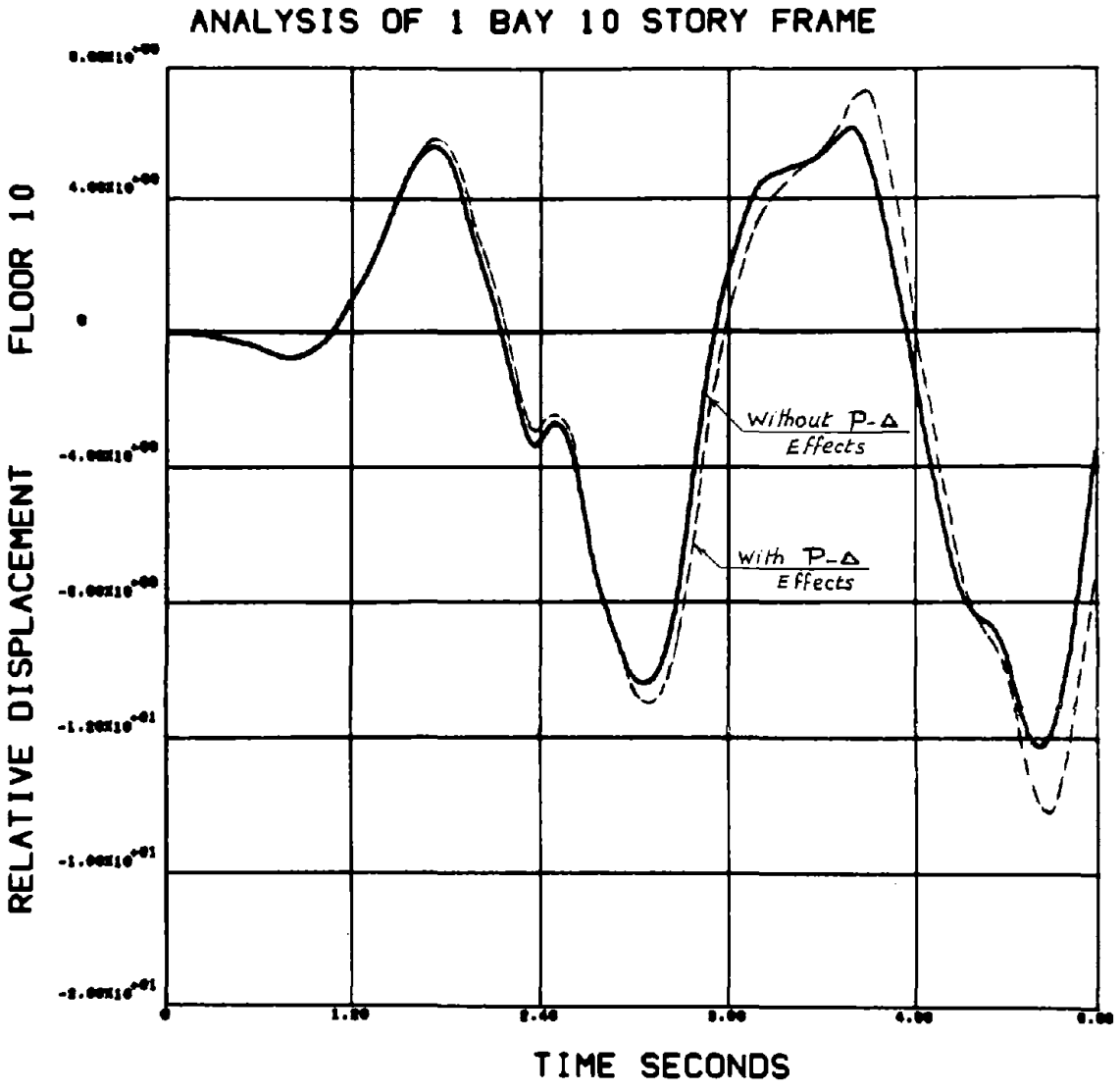

Fig. 3.35 - P-Δ Effects on Roof Displacements

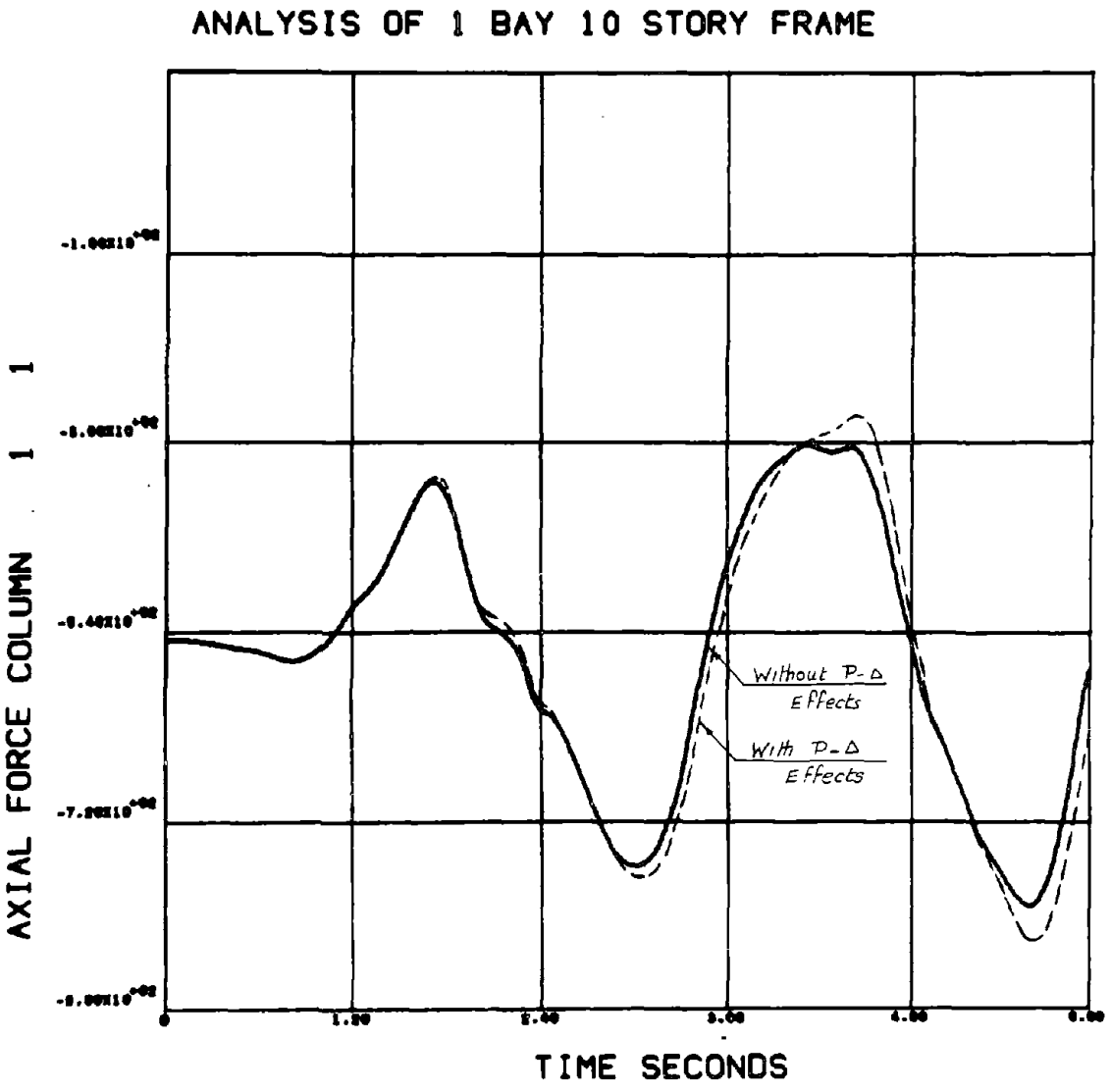

Fig. 3.36 - P-Δ Effects on the Axial Force in the Bottom Column

3. The P-Δ effects tend to increase joint distortions and member forces, but they might not cause physical collapse of the structure considered. Neglecting the P-Δ effects in the analysis is in this case unconservative.

4. The P-Δ effects are generally not as serious as they seem to be, and in a code-type approach for design, equivalent static forces might be determined to introduce such effects in the analysis. Currently codes are evolving, and it might be possible through extensive studies for typical building frames to push this approach forward in a rational way.

3.5.5 Gravity Loads Effects

The presence of gravity loads can affect the behavior of a building frame under seismic action in several ways: Gravity loads on the structure may reduce substantially the elastic range under lateral loads due to earlier formation of inelastic action. Since the effective yield moments of the columns depend on the axial-flexural interaction, it is expected that gravity loads have more significant effects on these members. The problem is magnified by the additional moments introduced due to the P-Δ effects.

For the purpose of this study, gravity loads are adequately represented by initial static forces acting at the ends of the different members.

To demonstrate the effect of gravity loads on the response, the following analyses are made.

1. Analysis where gravity loads are accounted for and the axial flexural interaction is properly considered by a given interaction surface.

2. Analysis where gravity loads are considered but the axial-flexural interaction is taken into consideration by reducing the plastic moment capacities under the static loads only.

3. Analysis where gravity loads are considered, but no axial-flexural interaction is considered.

4. Analysis where gravity loads are considered as axial forces in the columns only and axial-flexural interaction is not considered.

5. Analysis where gravity loads are completely neglected.

Figures 3.37 through 3.45 demonstrate the results obtained for the above five different analyses. From these results the following conclusions can be derived.

1. Gravity effects can introduce a considerable reduction in the overall stiffness of the structure and its elastic limit.

2. Considering gravity loads leads to larger ductility requirements for both the girders and the columns. The effect is more pronounced for the columns than for the girders.

3. It seems that as far as the overall behavior is concerned, using a bending model with reduced plastic moments due to the static initial axial forces in the columns gives results very similar to those of a more accurate interaction model.

4. Introducing axial-flexural interaction in the case studied leads to an increase in displacements and to a reduction in forces. It also leads to an increase in ductility requirements—in particular—for the columns.

Figures 3.46 and 3.47 demonstrate the effect of introducing

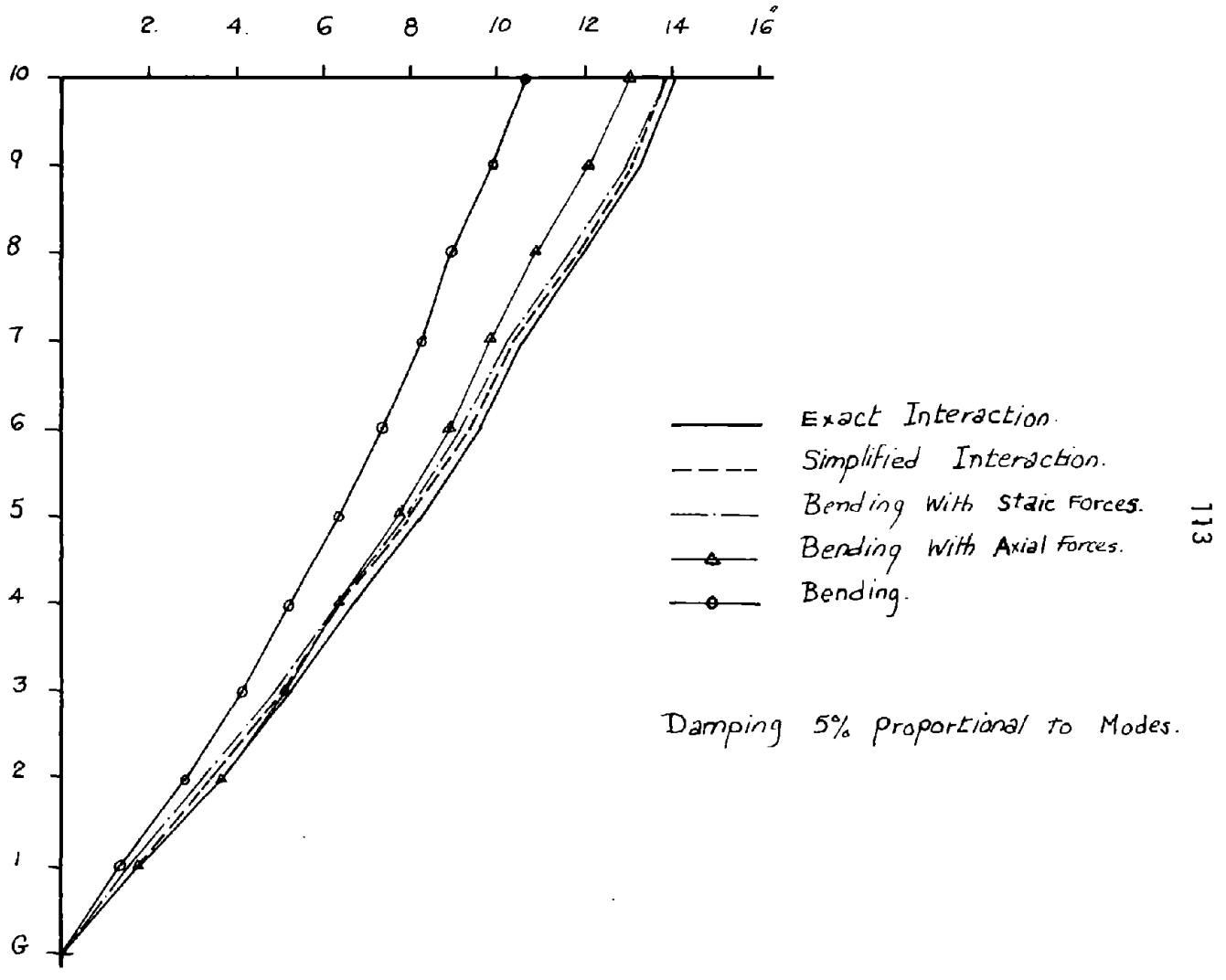

Fig. 3.37 - Effect of Gravity Loads on the Maximum Displacements

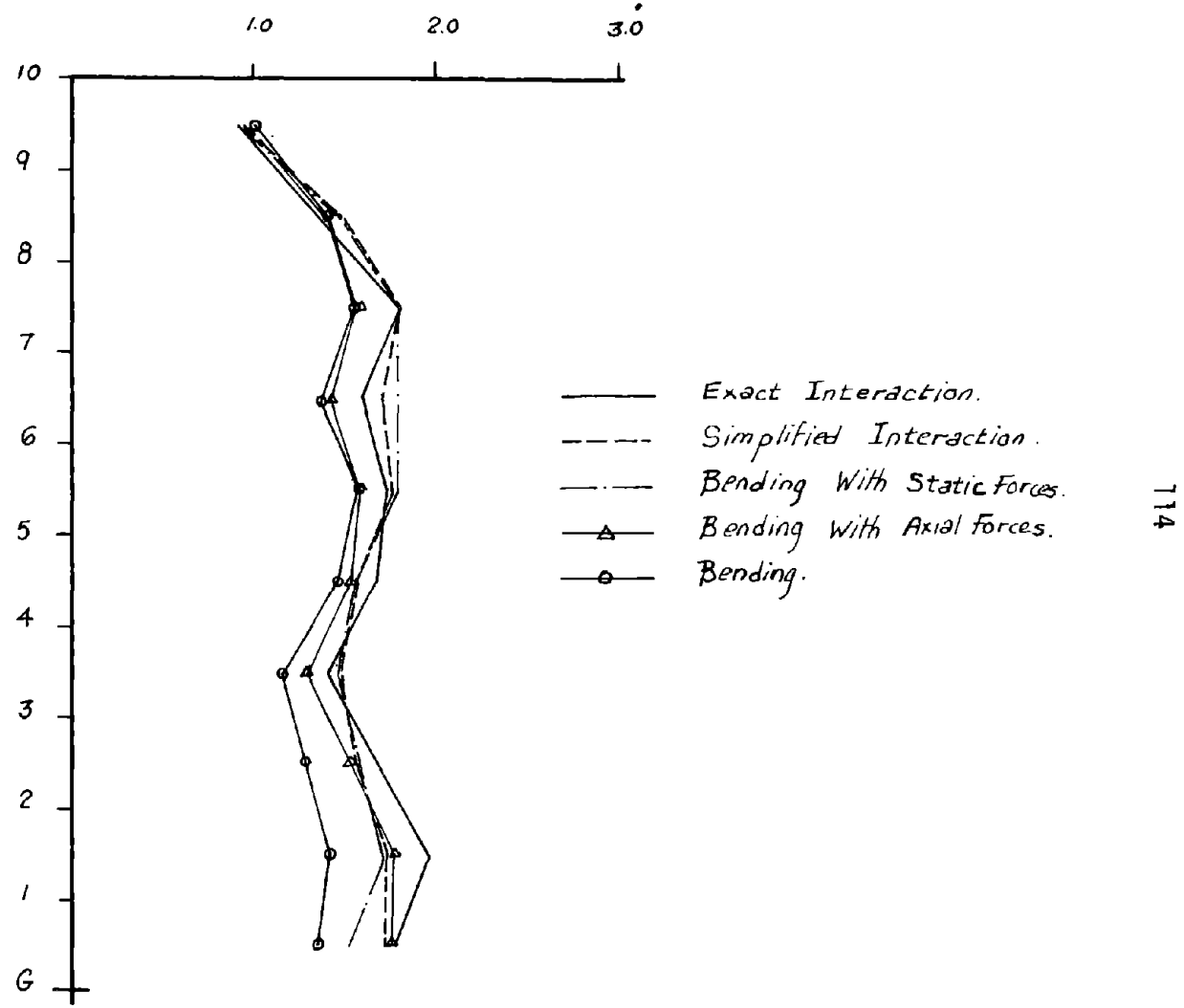

Fig. 3.38 - Effect of Gravity Loads on the Maximum Interstory Displacements

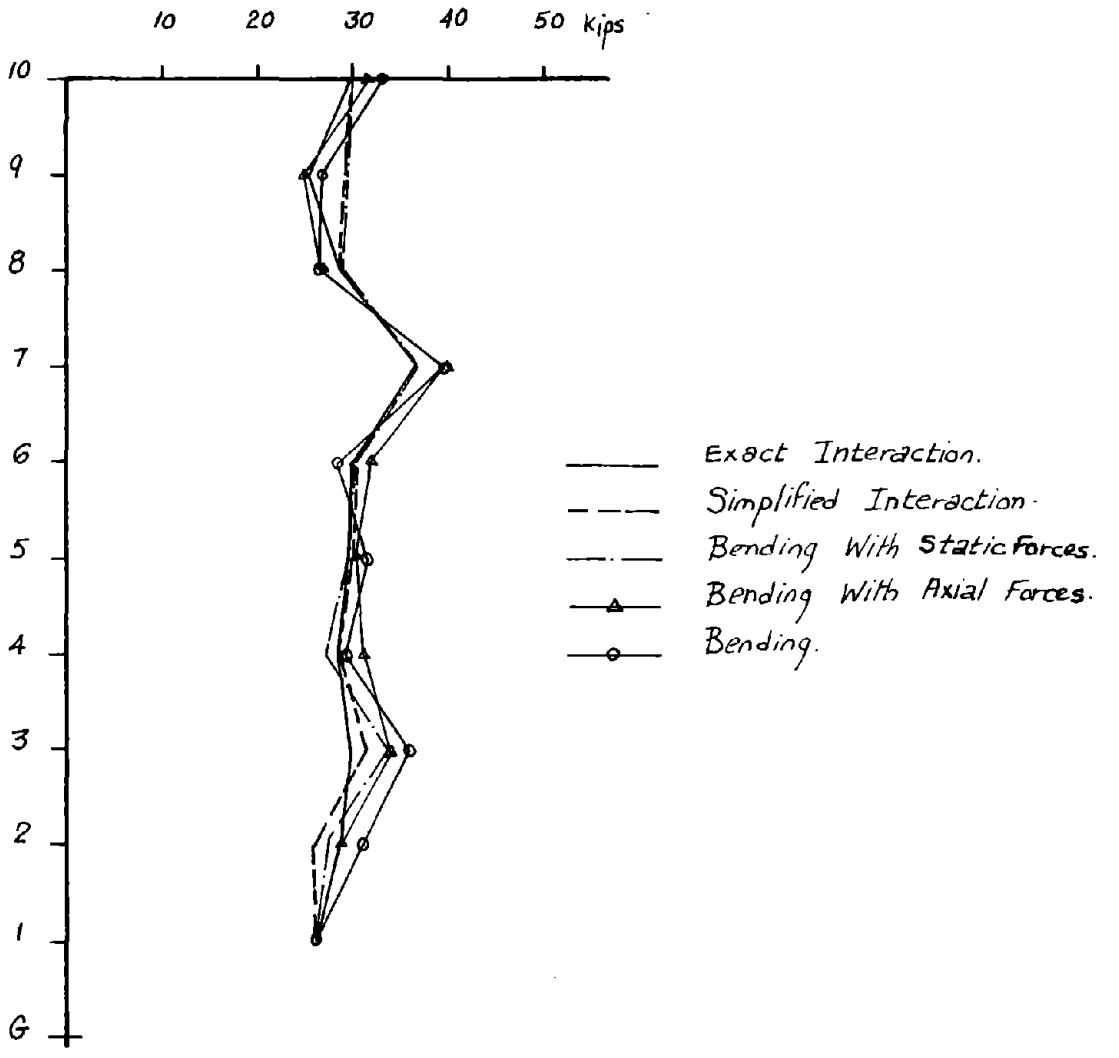

Fig. 3.39 - Effect of Gravity Loads on the Maximum Story Forces

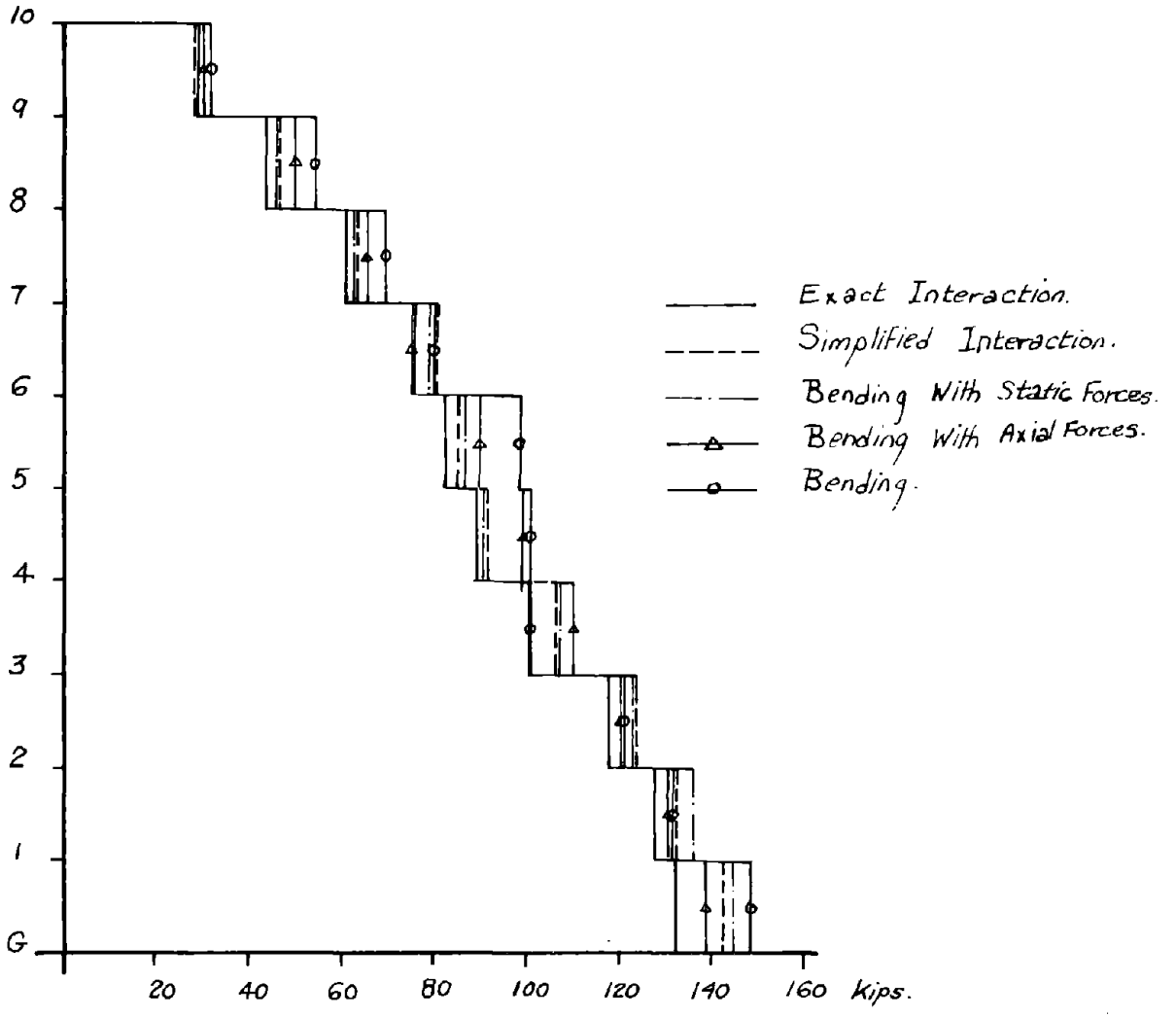

Fig. 3.40 - Effect of Gravity Loads on the Maximum Story Shears

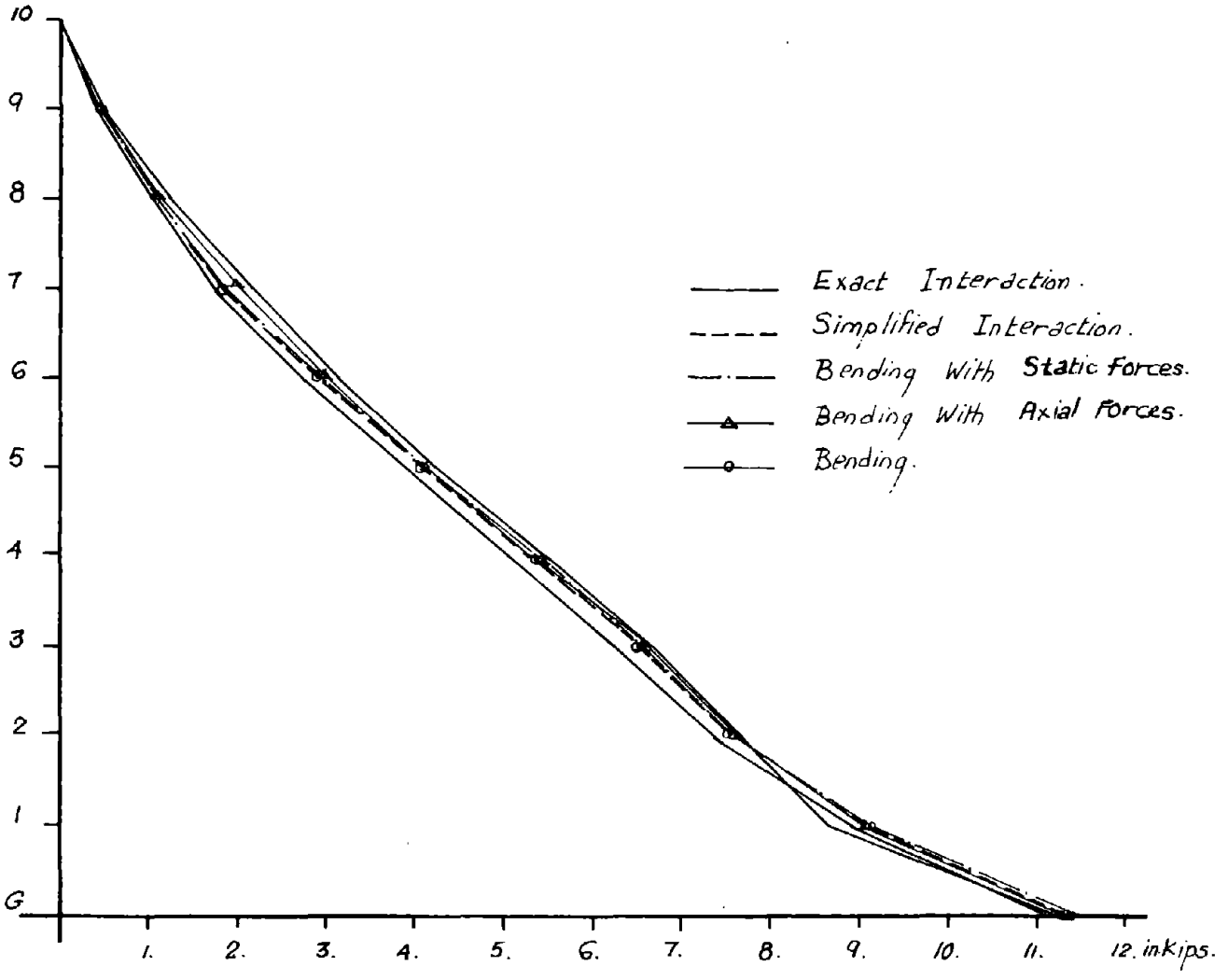

Fig. 3.41 - Effect of Gravity Loads on the Maximum Overturning Moments

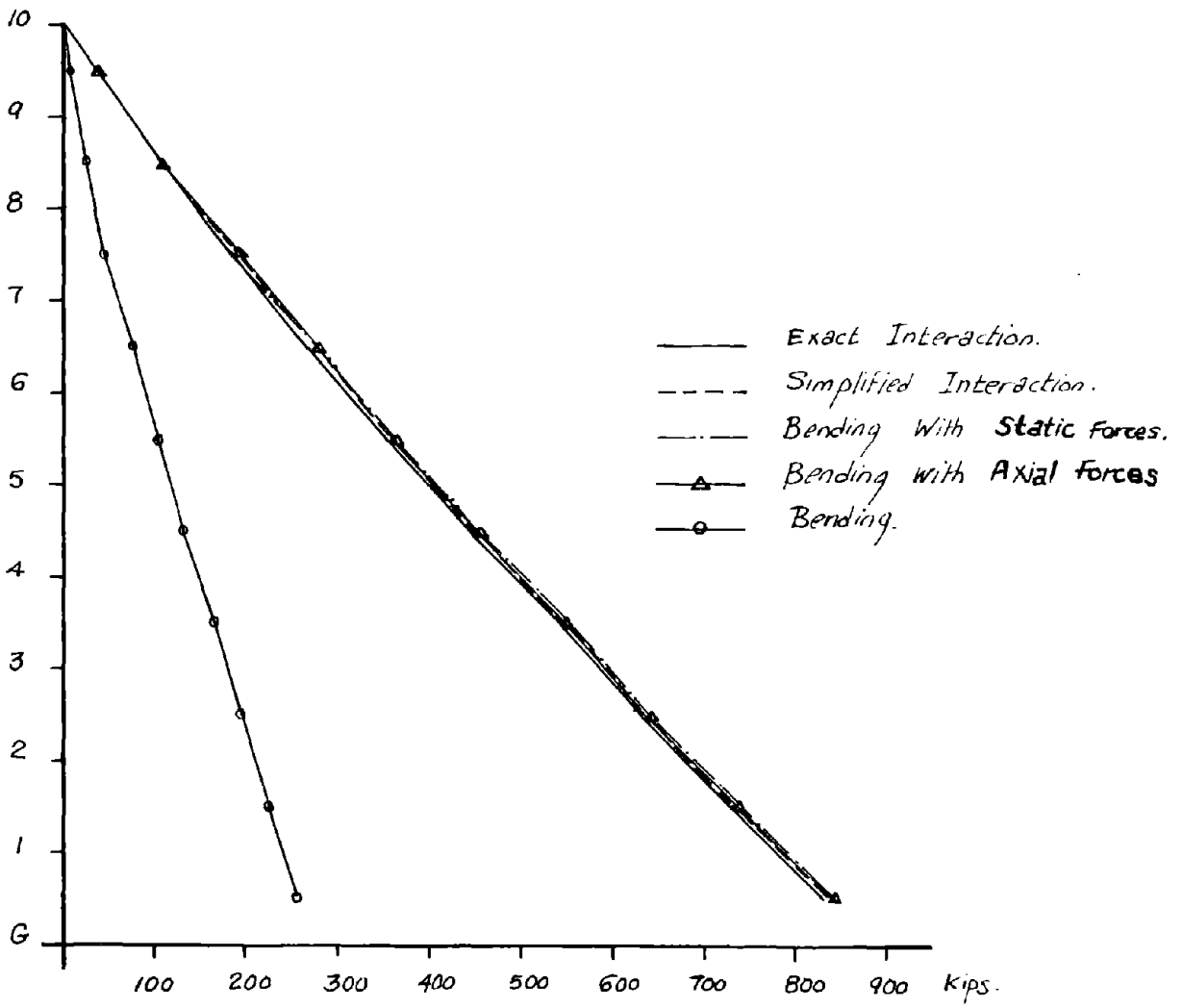

Fig. 3.42 - Effect of Gravity Loads on the Maximum Axial Forces in the Columns

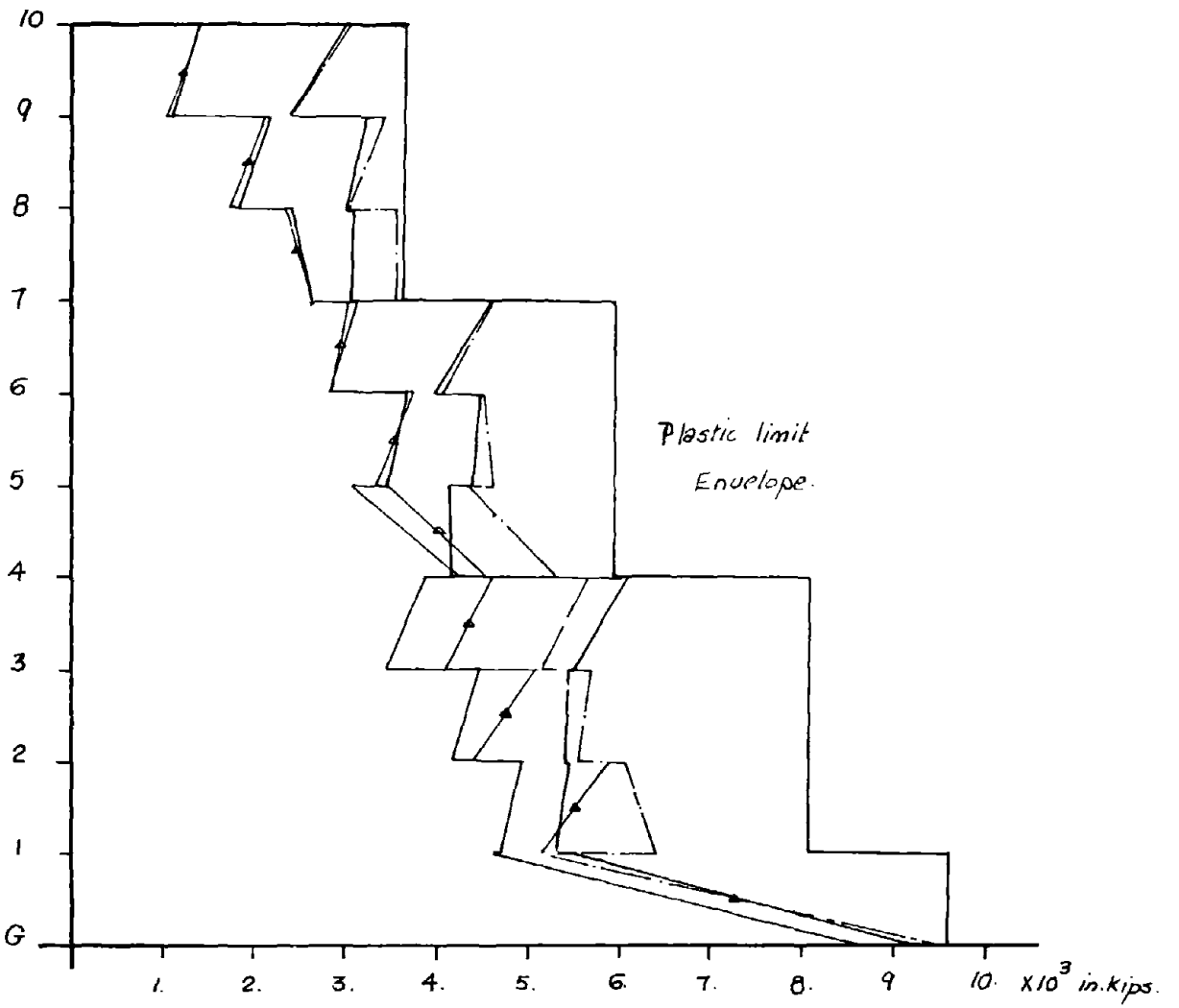

Fig. 3.43 - Effect of Gravity Loads on the Maximum Column Moments

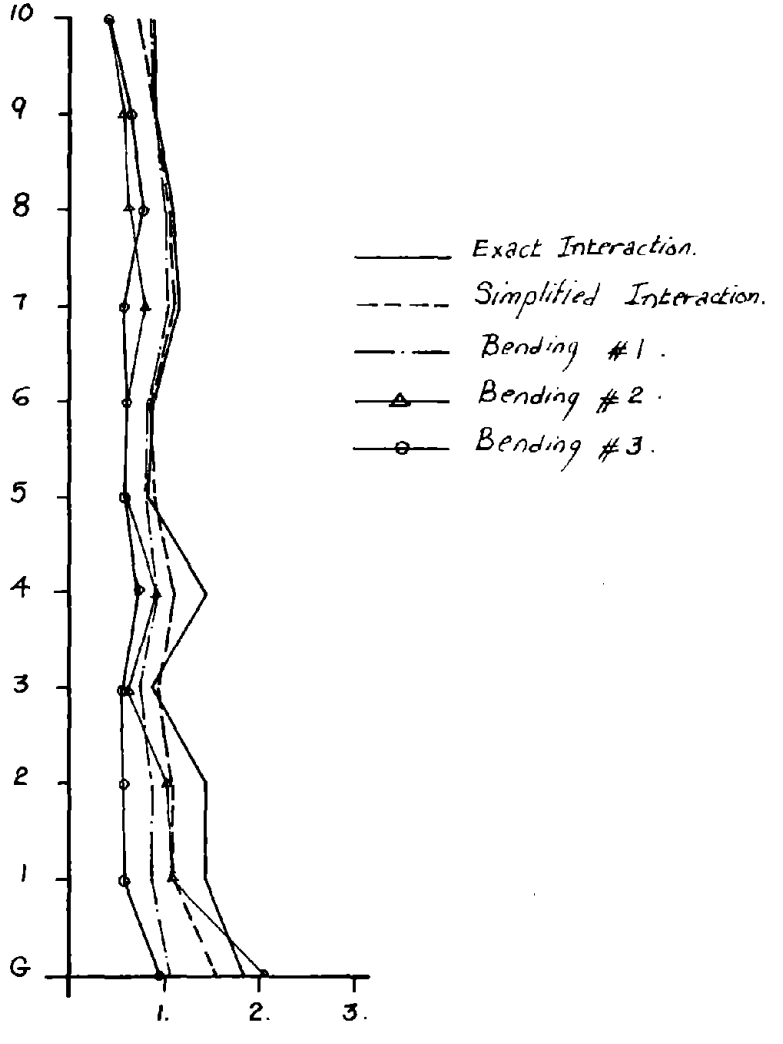

Fig. 3.44 - Effect of Gravity Loads on the Maximum Column Ductilities

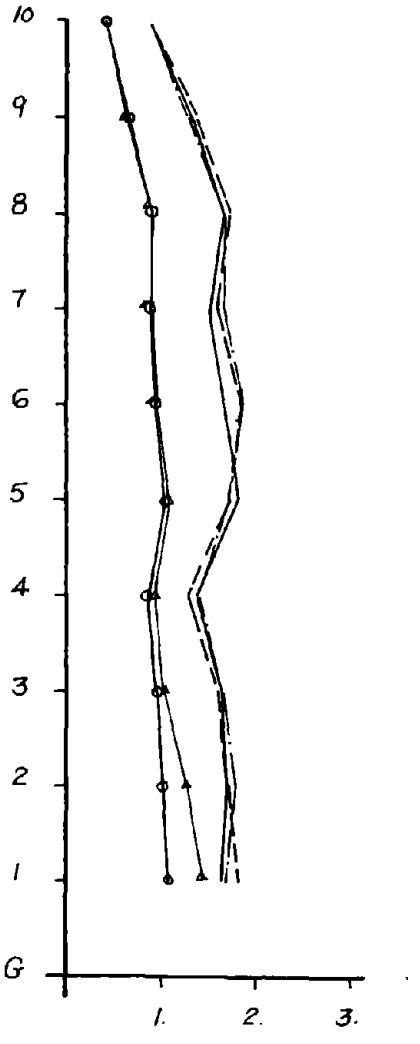

Fig. 3.45 - Effect of Gravity Loads on the Maximum Girder Ductilities

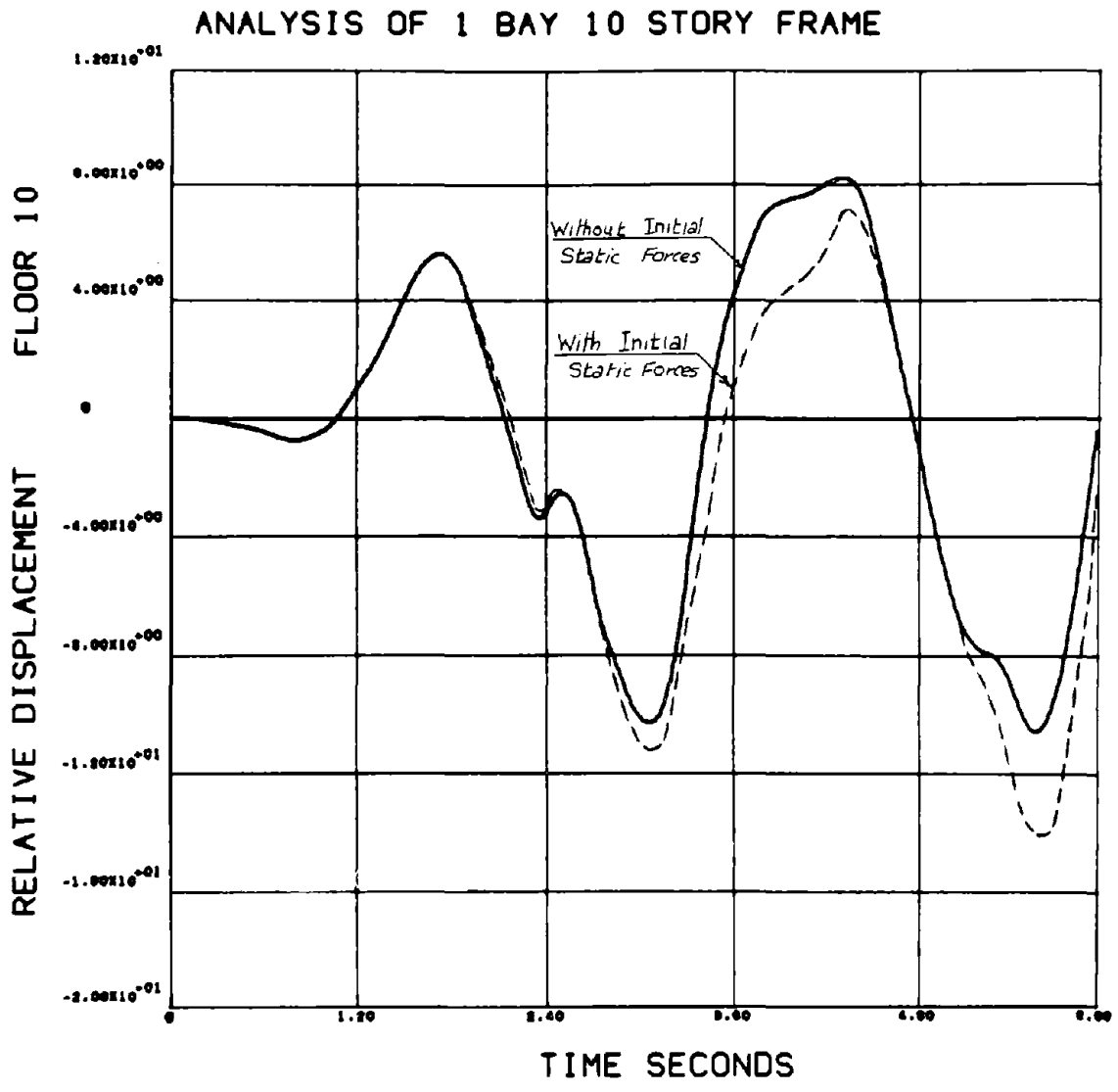

Fig. 3.46 - Effect of Initial Static Forces On Roof Displacement

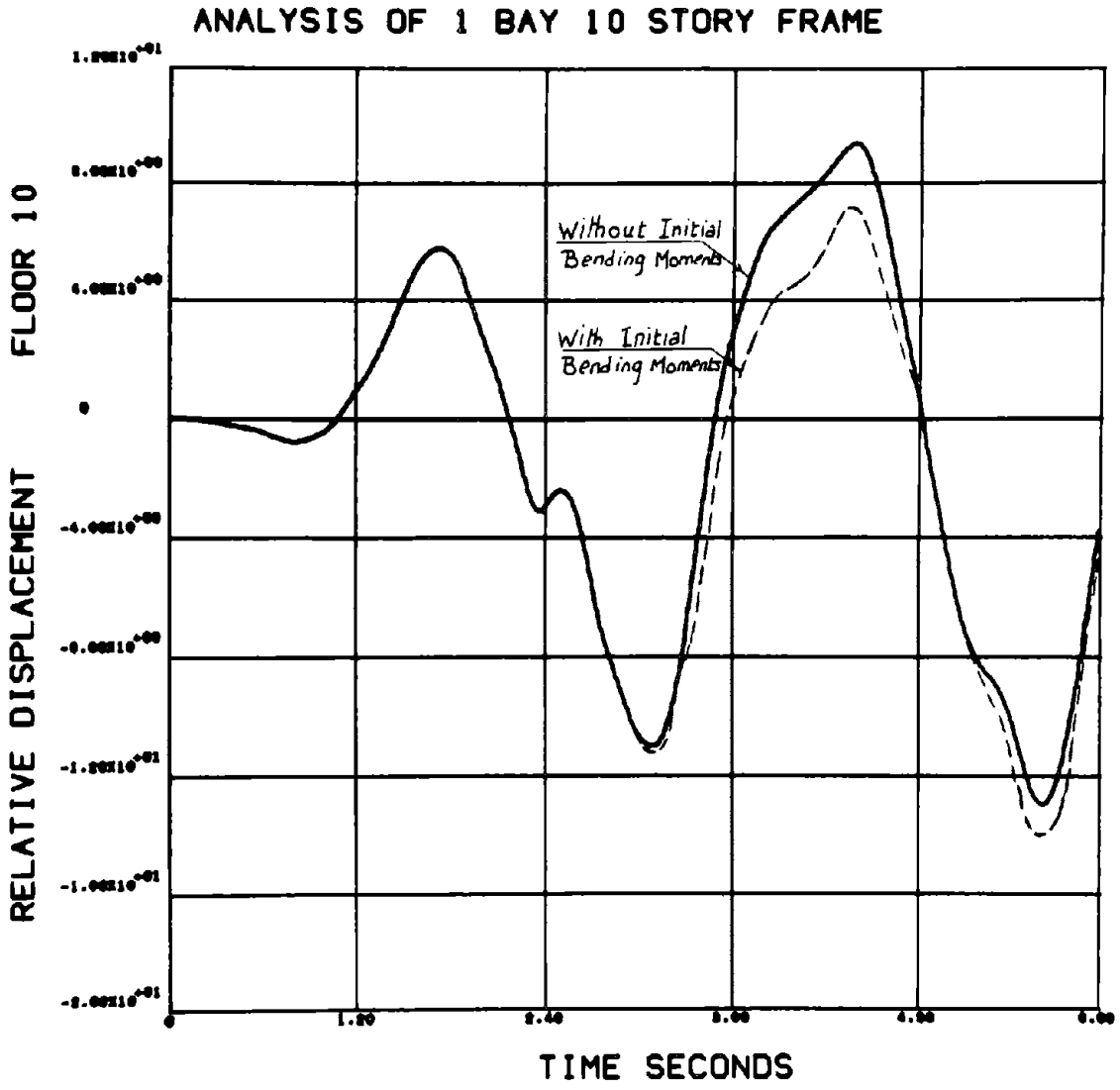

Fig. 3.47 - Effect of Neglecting the Initial Bending Moments on Roof Displacement

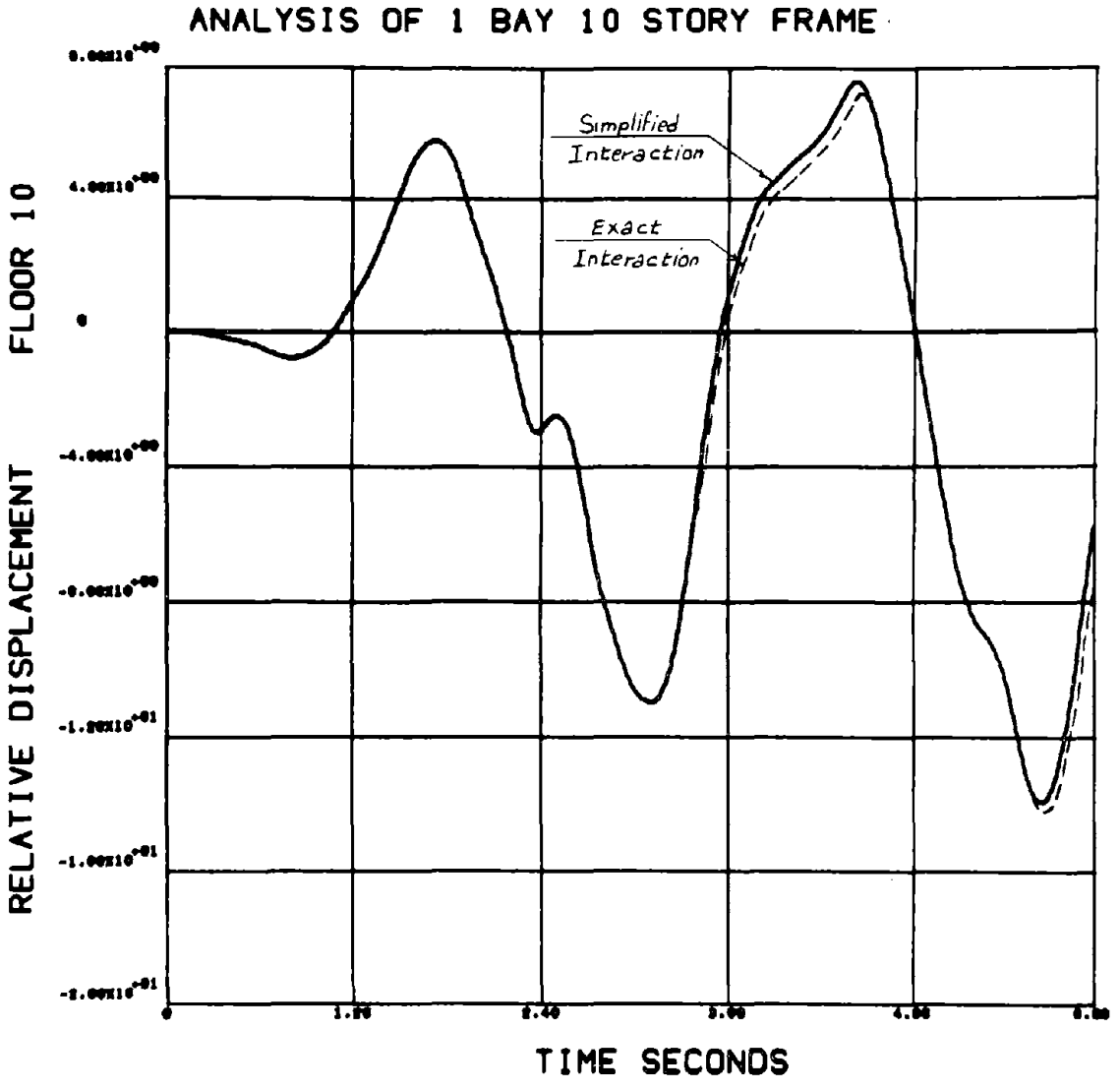

Fig. 3.48 - Roof Displacement for an Exact Interaction Model versus a Simplified Interaction Model

gravity as axial loads only, versus introducing it as axial loads and moments; while Fig. 3.48 demonstrates the effect of reducing the plastic capacity beforehand under the static axial forces versus performing a proper interaction analysis.

Finally, it is worth noticing that accidentally in the case studied when gravity loads are neglected in the analysis, the response is almost elastic, and only slight yielding occurs in the girders.

3.5.6 Effects of Axial Deformations in the Columns

Axial deformations in the columns might affect the analysis in two ways:

1. The axial distortions of the columns lead to an increase in the elastic period of the structure, which in turn might change the response under dynamic loading.

2. The accumulated effect of column distortions leads to an increase in the upper story displacements and also to an increase in the drift and thus to a magnification in the P-Δ effects.

To study the relative importance of axial deformations, a fictitious model with large areas for the columns (10,000 in^2) was compared to the original frame model. Figs. 3.49 through 3.57 demonstrate the relative importance of such effect. The following conclusions can be reached for the case studied.

1. Neglecting axial deformation will lead to a reduction in the fundamental period (smaller in the higher modes).

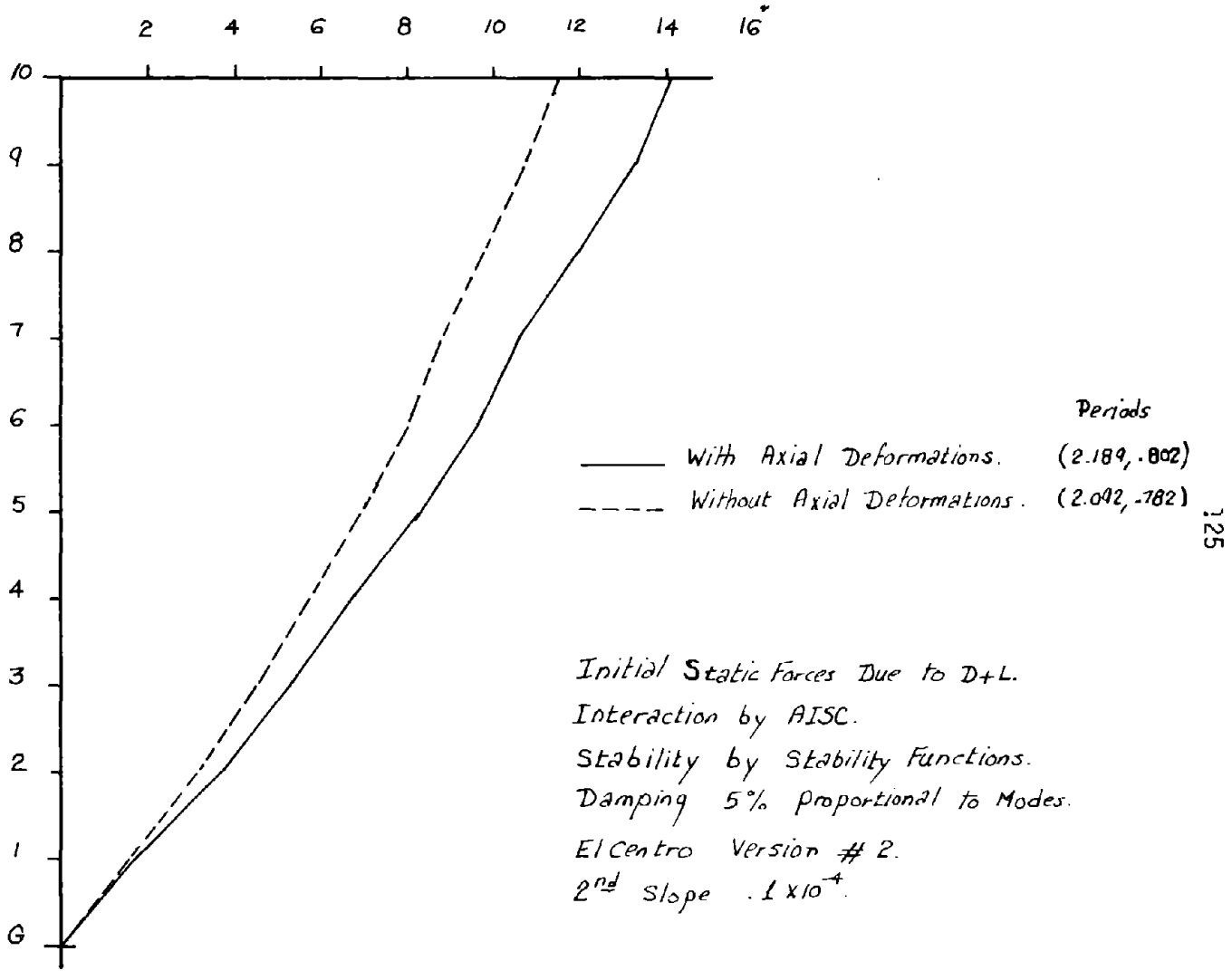

Fig. 3.49 - Effect of Axial Deformations on Maximum Displacements

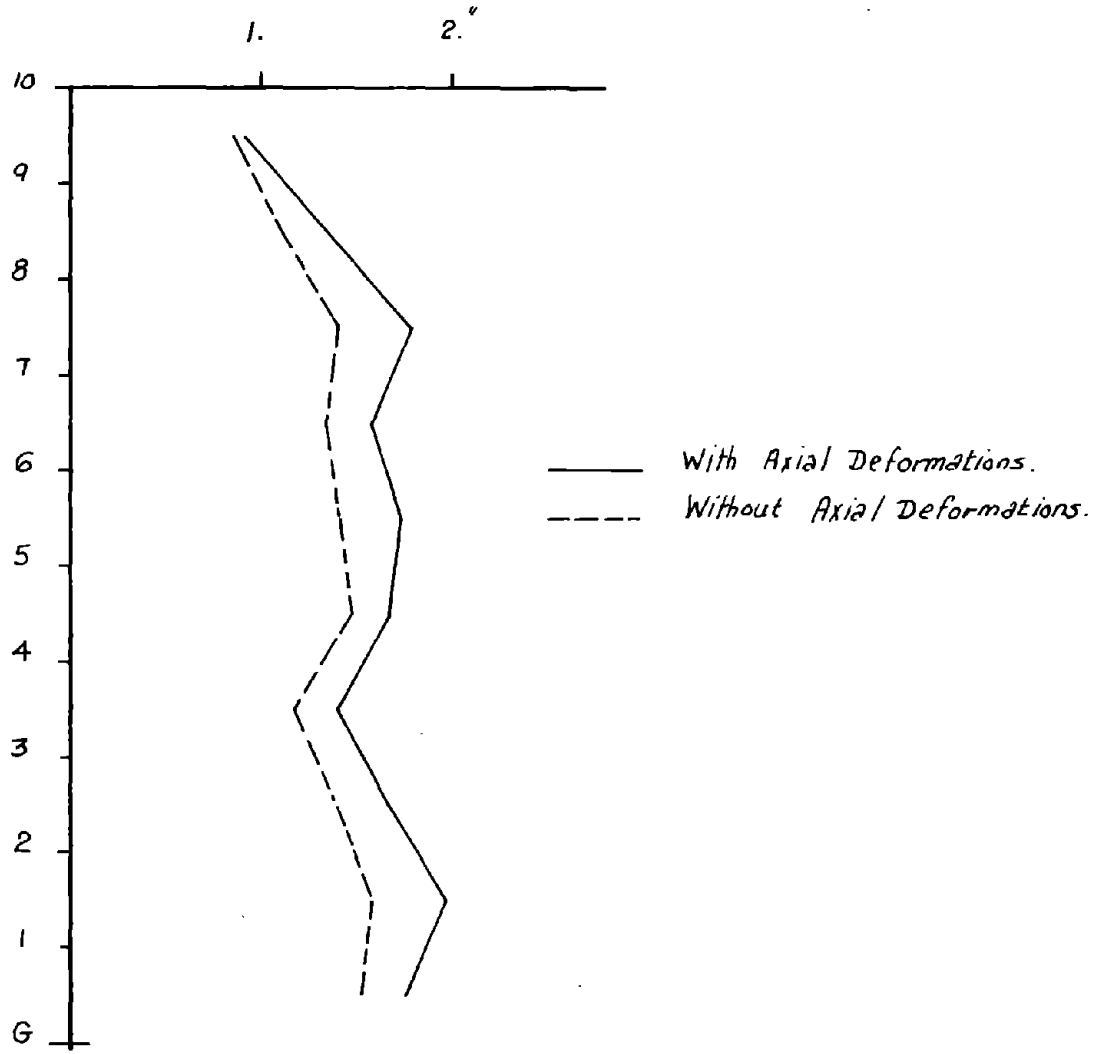

Fig. 3.50 - Effect of Axial Deformations on Maximum Interstory Displacements

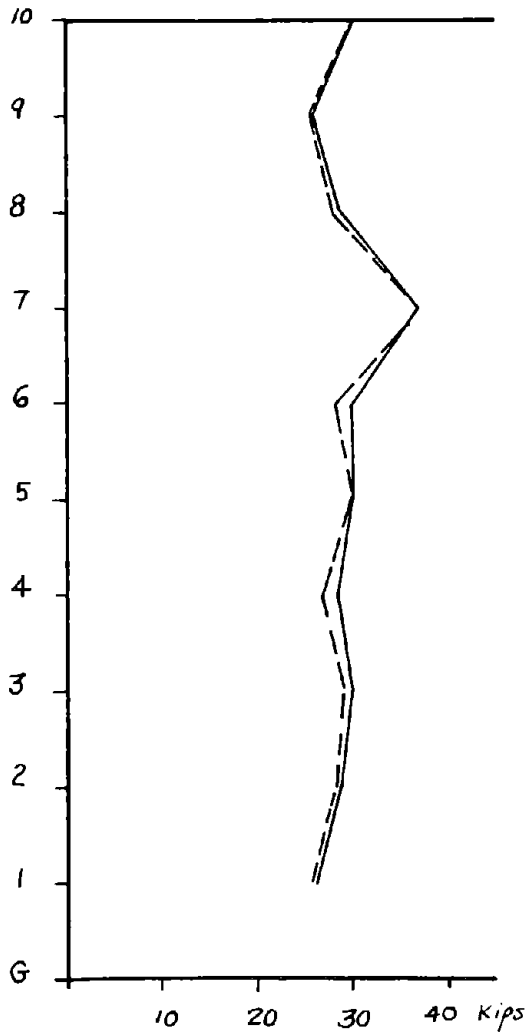

Fig. 3.51 - Effect of Axial Deformations on Maximum Story Forces

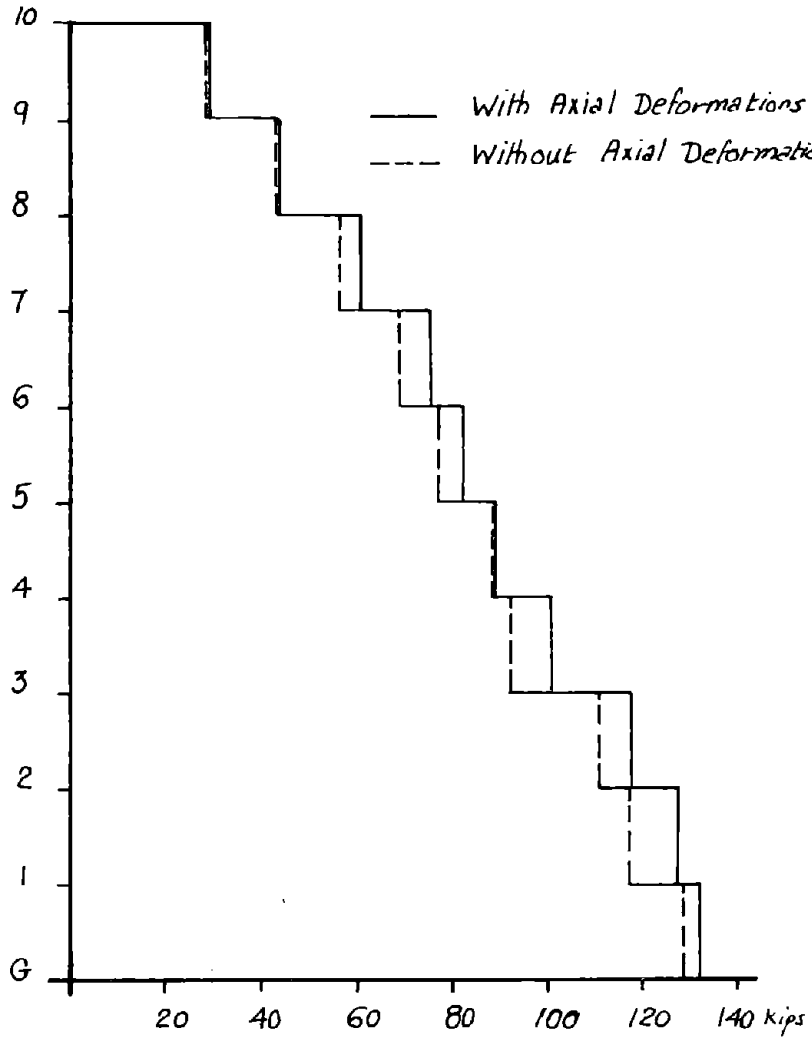

Fig. 3.52 - Effect of Axial Deformations on Maximum Story Shears

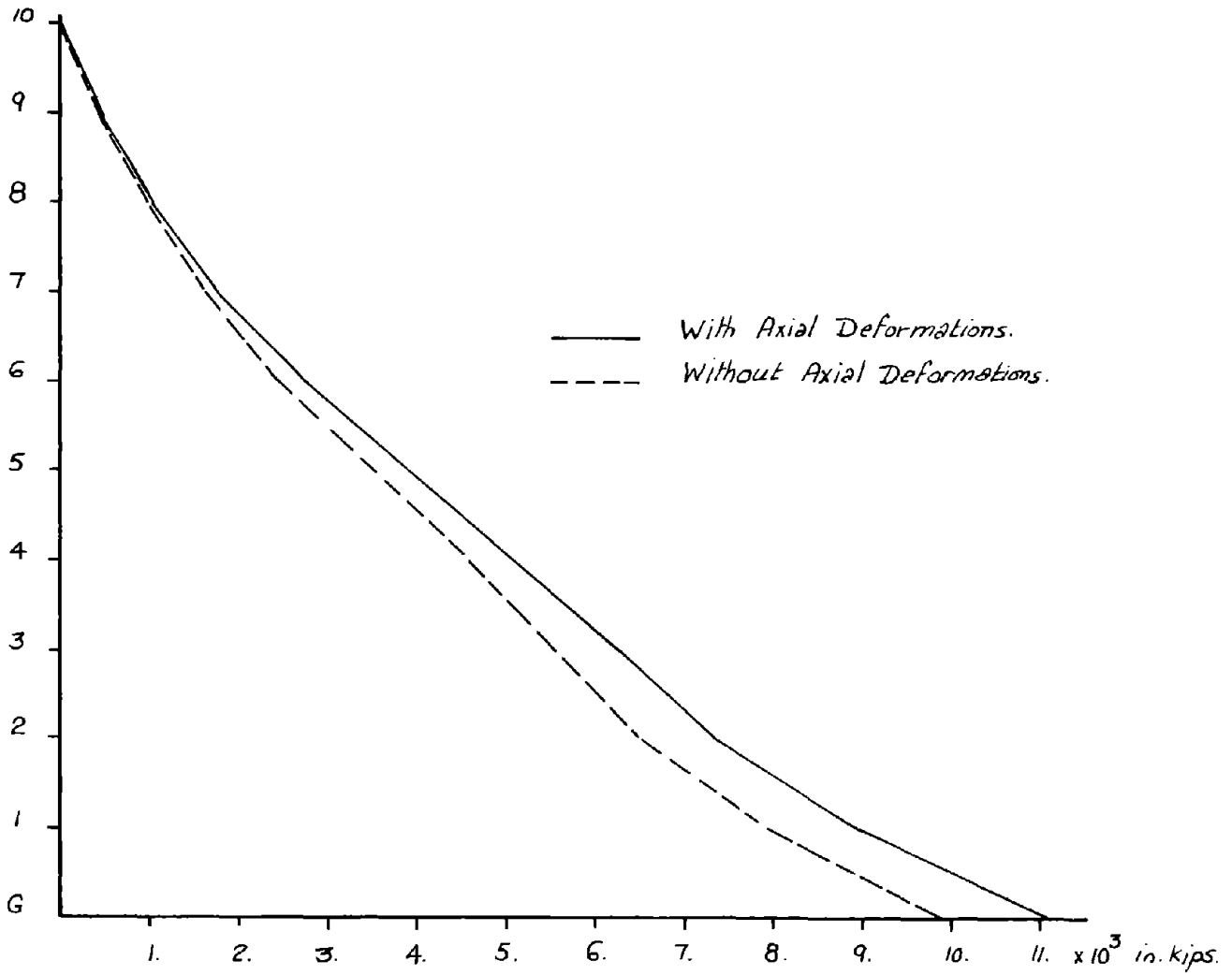

Fig. 3.53 - Effect of Axial Deformations on Maximum Overturning Moments

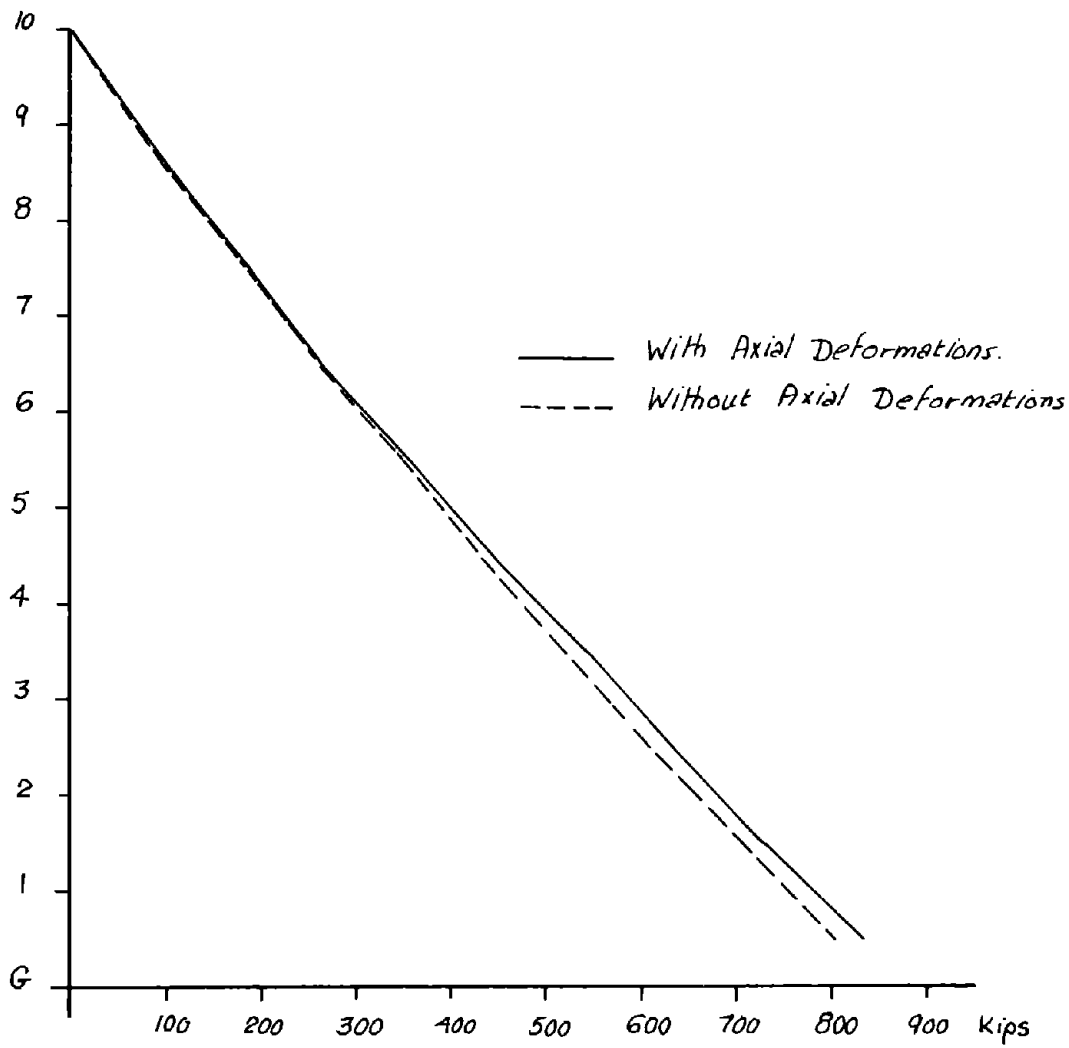

Fig. 3.54 - Effect of Axial Deformations on Maximum Axial Forces in Columns

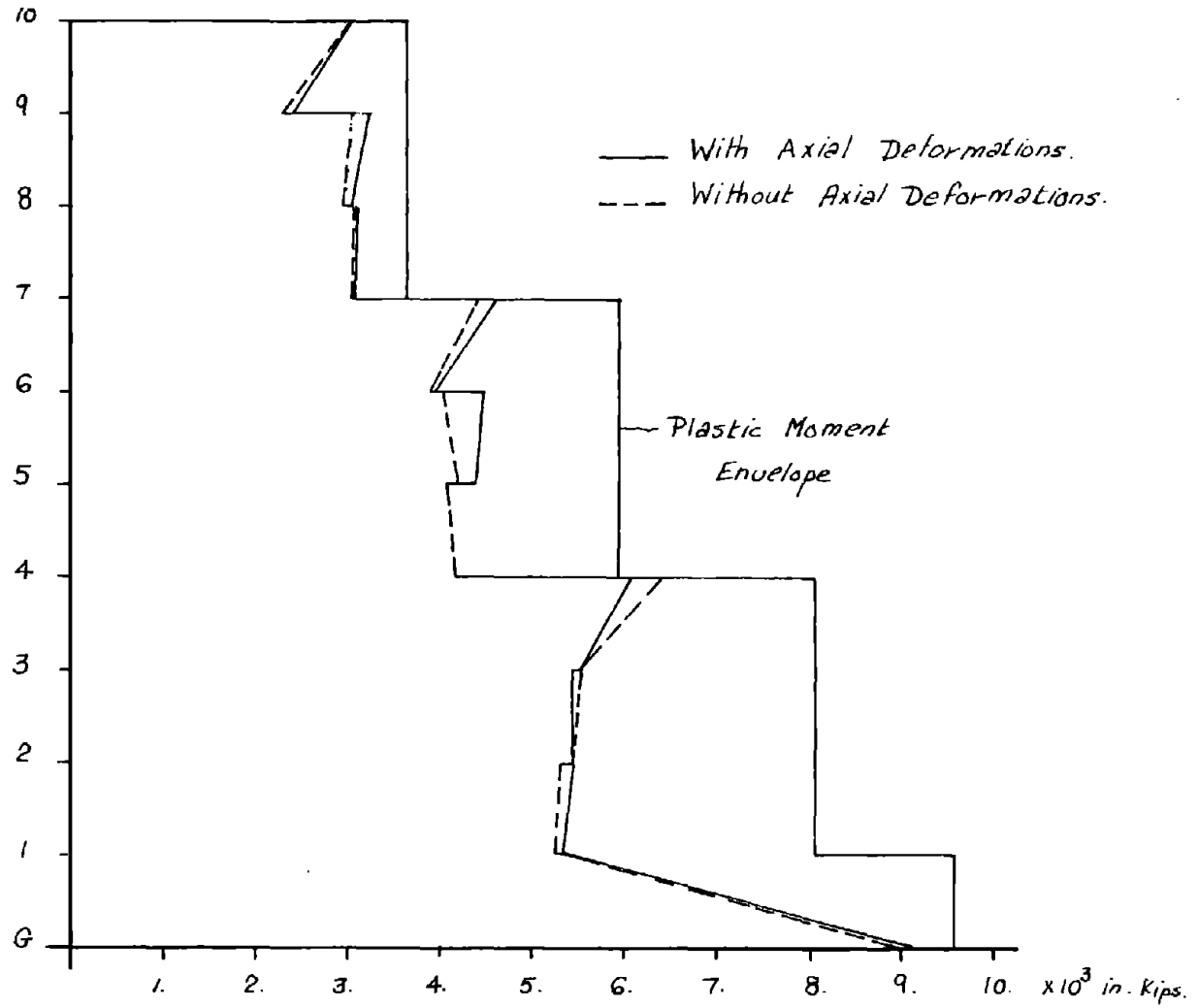

Fig. 3.55 - Effect of Axial Deformations on Maximum Column Moments

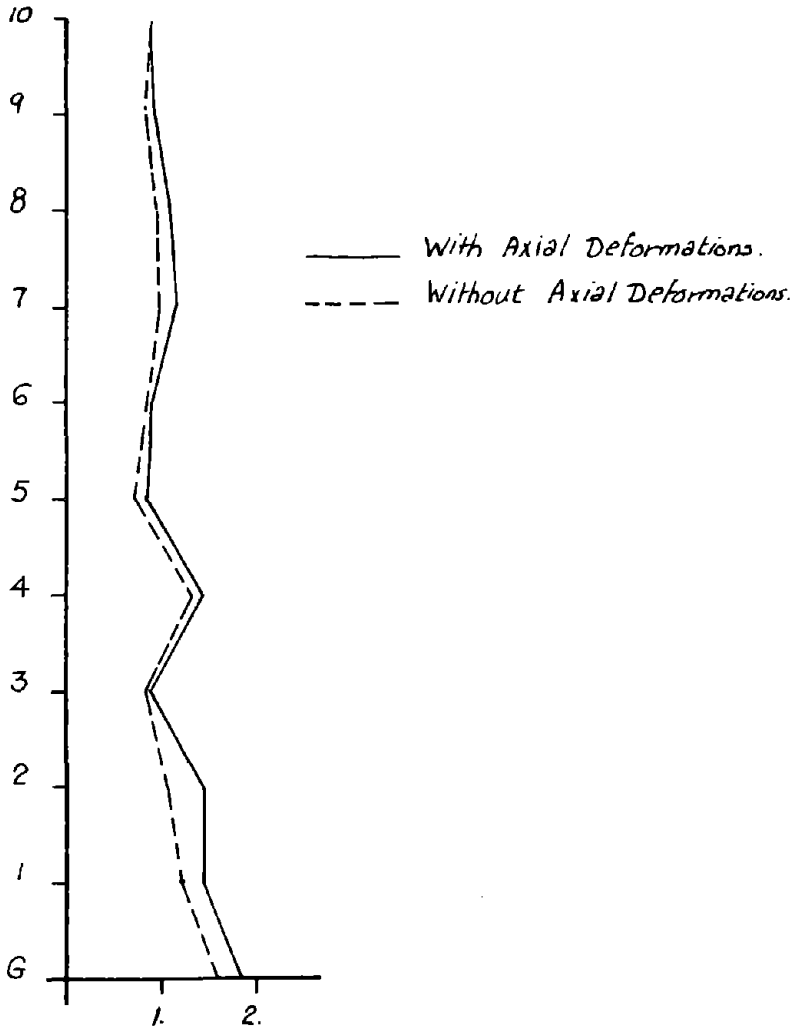

Fig. 3.56 - Effect of Axial Deformations on Maximum Column Ductilities

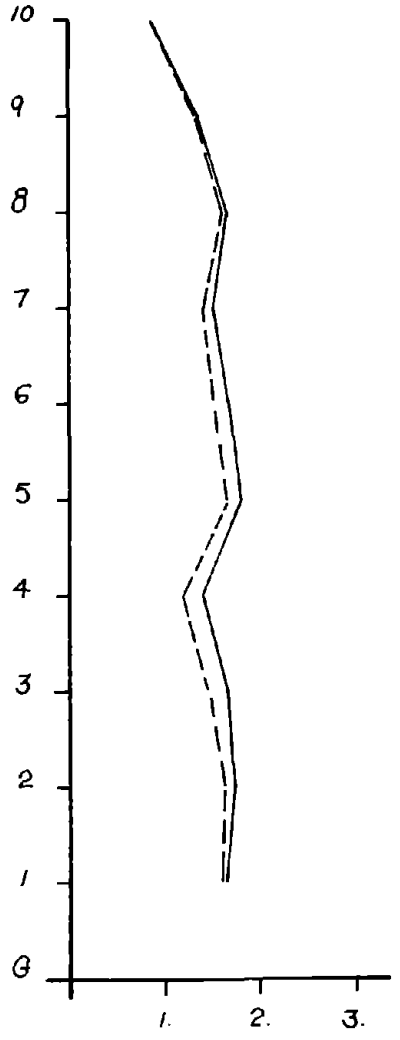

Fig. 3.57 - Effect of Axial Deformations on Maximum Girder Ductilities

2. A substantial increase in story and interstory displacements can occur when axial deformations in the columns are introduced in the analysis, for slender frames.

3. An increase in ductility requirements for both the columns and the girders is observed when axial deformations in the columns are properly taken into account. Also a similar increase in plastic deformations for both the columns and the girders is observed.

3.5.7 Effect of the Length of Plastification Zone

To establish the relative importance of a point hinge assumption versus a finite length plastification zone assumption, a model consisting of the basic frame with an assumed plastification zone of 10" for the columns and 20" for the girders was studied. The effect of assuming such a soft zone in the joints is to increase the fundamental period of the structure from 2.189 sec. to 2.507 sec., since an additional joint flexibility was introduced even in the elastic range. This change in period combined with the change in the inelastic rotational capacity at the ends of each member resulted in an increase in the roof displacement from approximately 14" to 18".

Figs. 3.58 through 3.65 demonstrate such effect. They are self-explanatory. An obvious increase in story displacements, interstory displacements, column and girder ductilities is observed when introducing joint flexibility in the analysis. It might be worth noticing that the story shears did not get affected that much, although an increase in the overturning moment is observed.

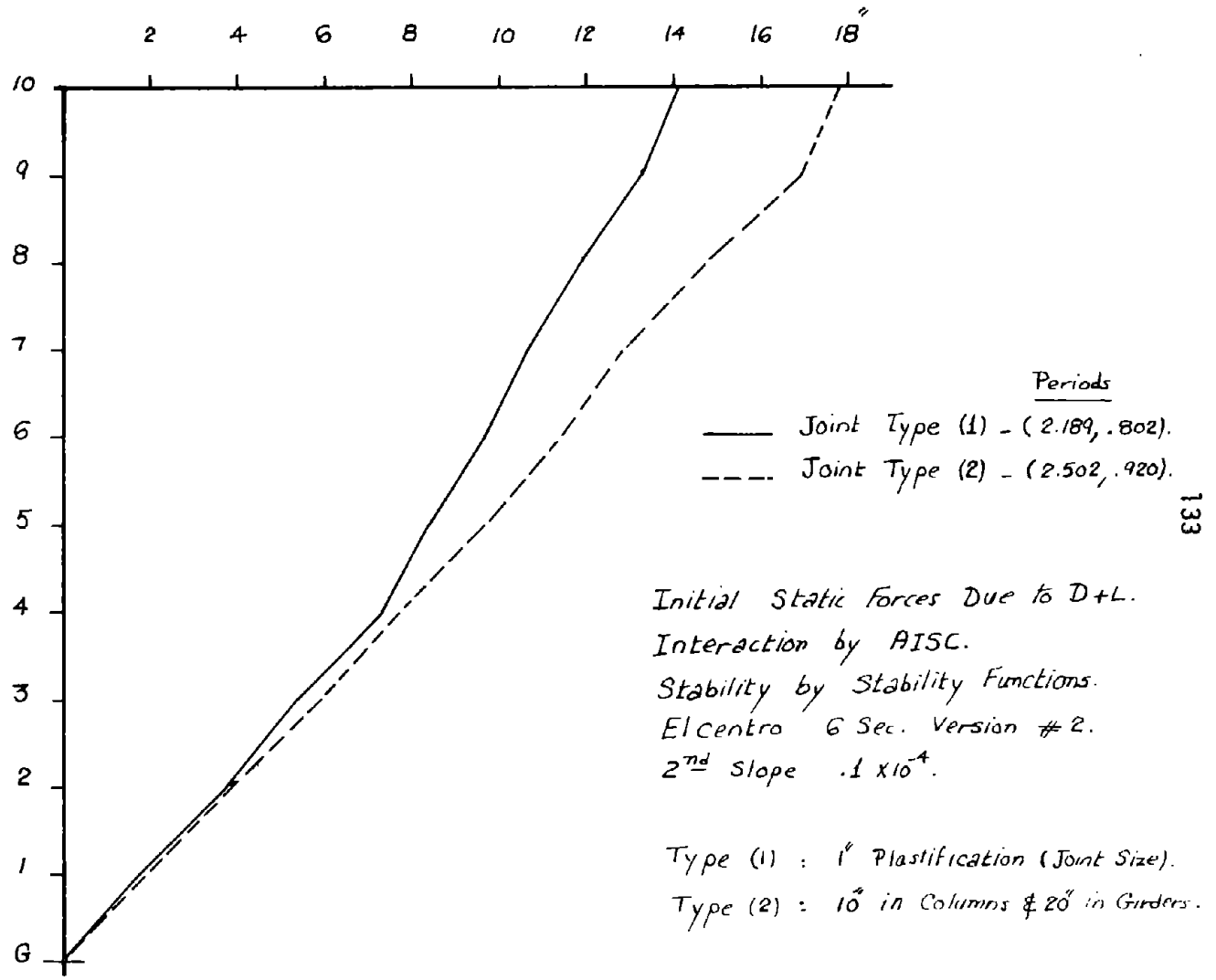

Fig. 3.58 - Effect of Joints Behavior and Length of Plastification Zone on Maximum Displacements

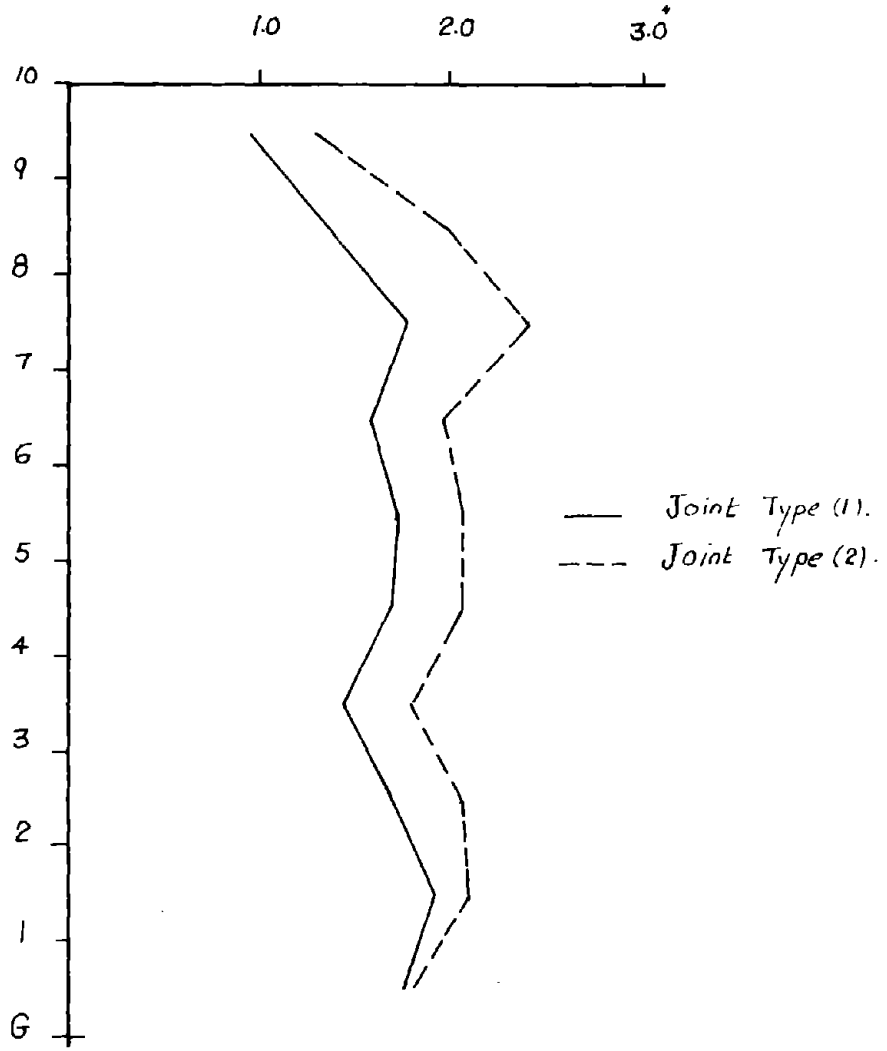

Fig. 3.59 - Effect of Joints Behavior and Length of Plastification Zone on Maximum Interstory Displacements

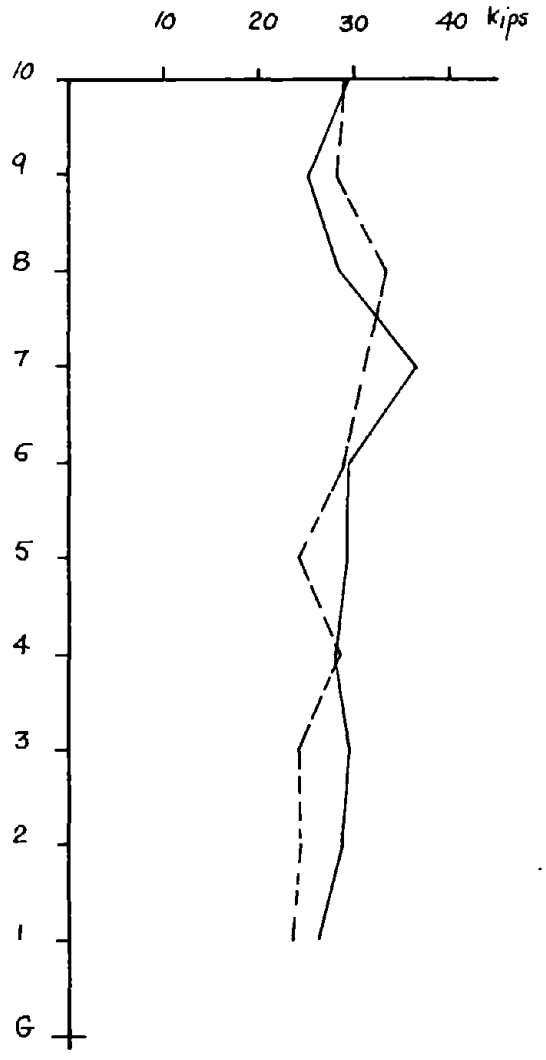

Fig. 3.60 - Effect of Joints on Maximum Story Forces

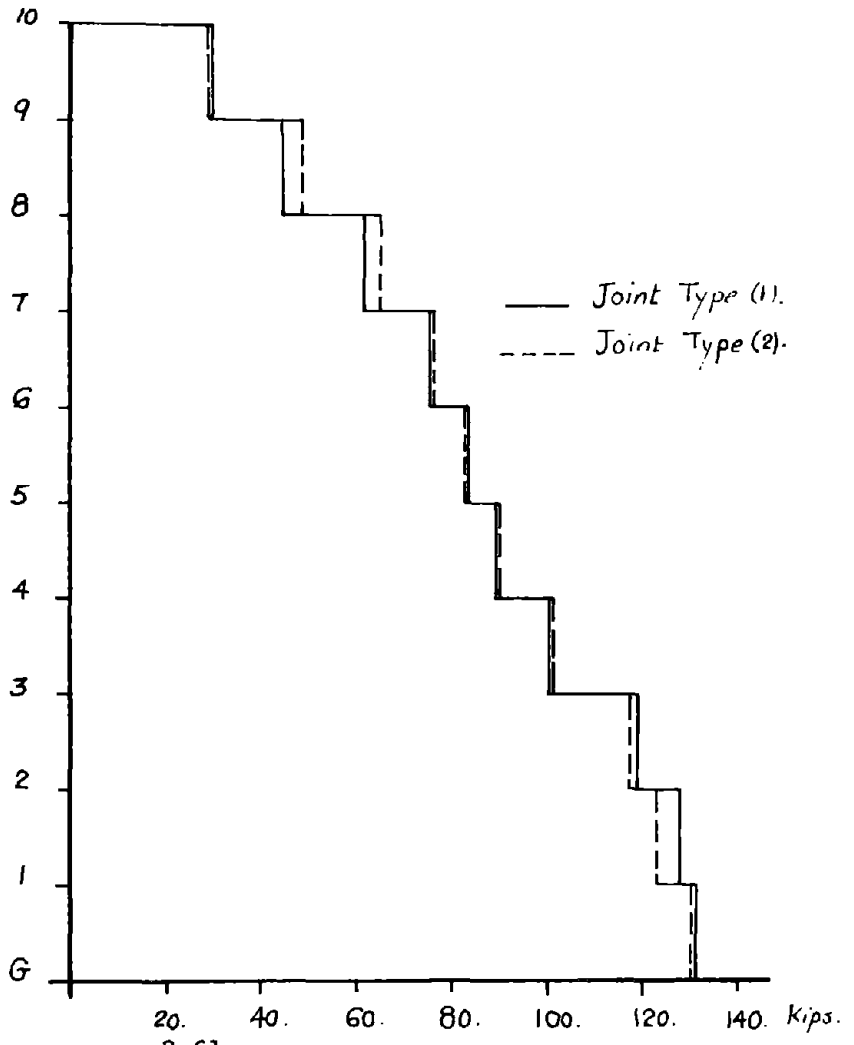

Fig. 3.61 - Effect of Joints on Maximum Story Shears

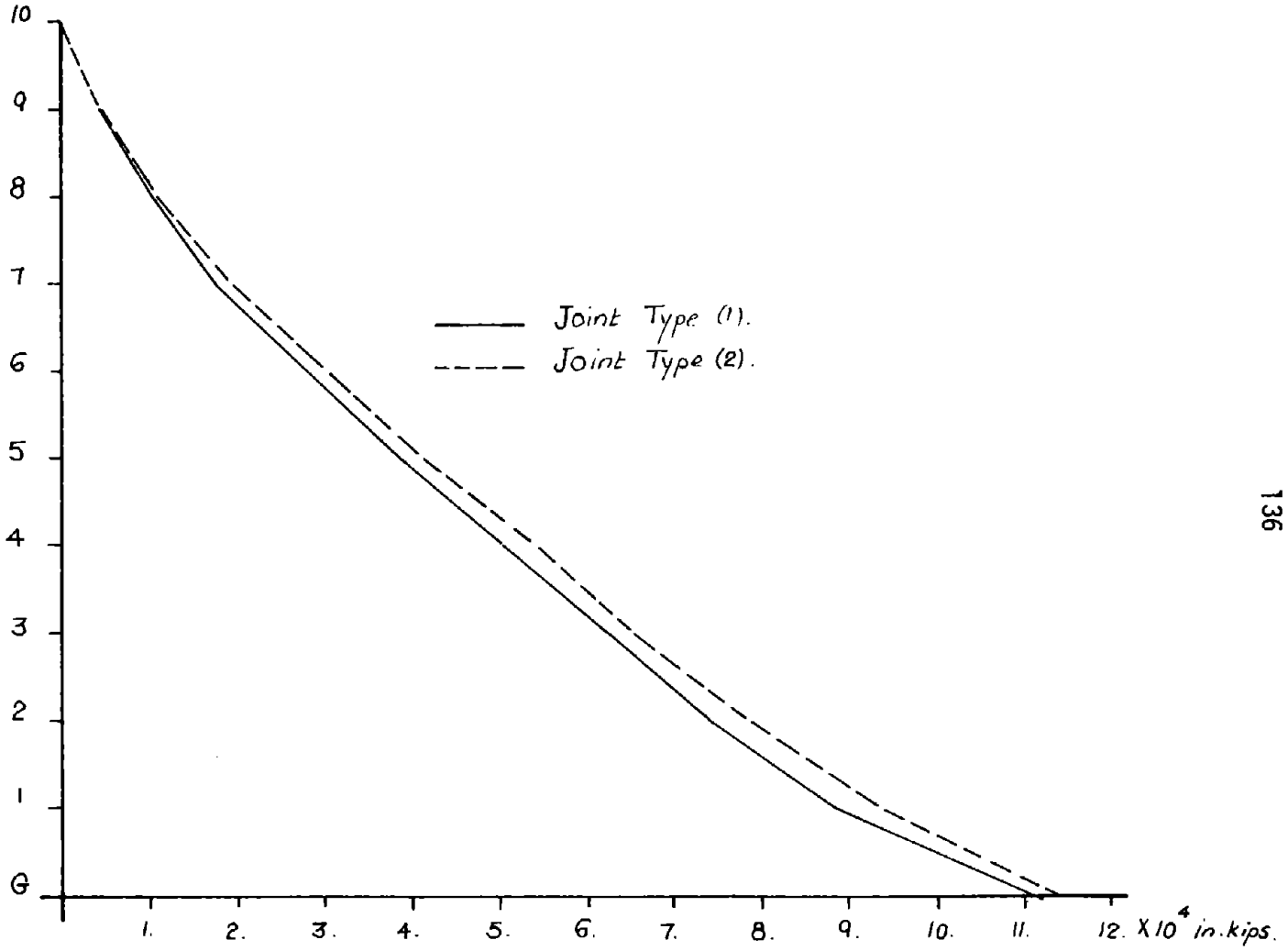

Fig. 3.62 - Effect of Joints on Maximum Overturning Moments

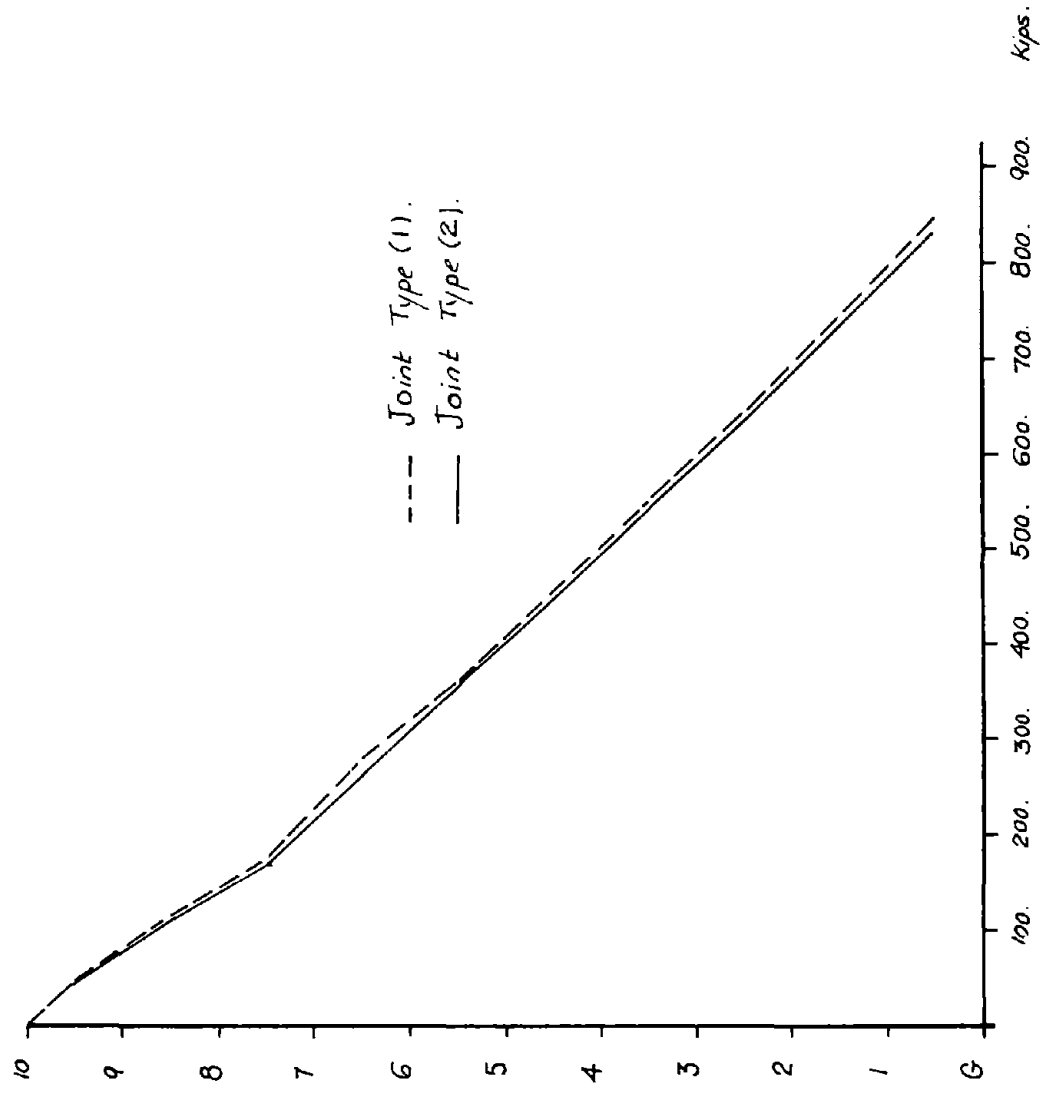

Fig. 3.63 - Effect of Joints on Maximum Axial Forces in Columns

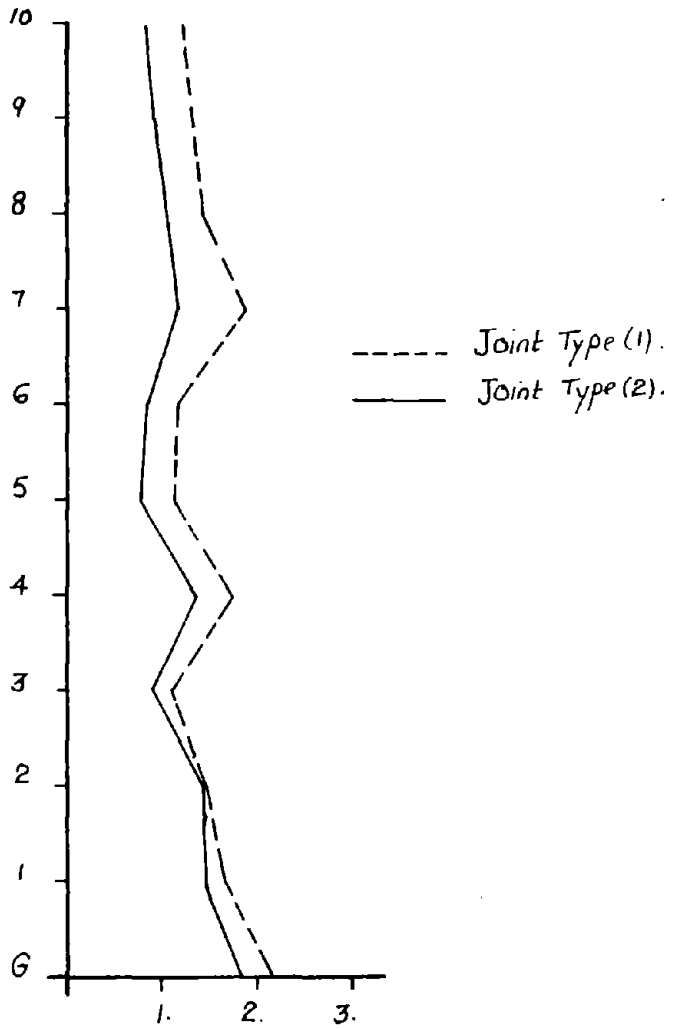

Fig. 3.64 - Effect of Joints on Maximum Column Ductilities

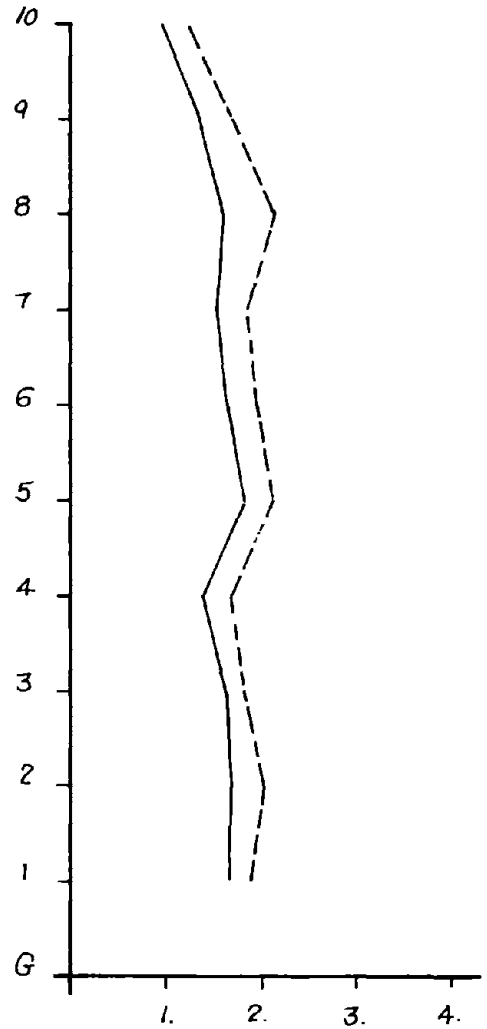

Fig. 3.65 - Effect of Joints on Maximum Girder Ductilities

3.5.8 Effect of Beam-Column Connection Size

In the current analysis the size of beam-to-column connection can be introduced. Three frames with three assumed column widths were studied. The widths chosen were 0, 14" and 30". Figs. 3.66 through 3.76 show the effect of the three widths on the results. From these figures the following can be concluded.

1. Beam column overlap can affect the results of the analysis substantially, since it changes the period of the structure on one hand, and on the other hand it moves the location of the plastic hinge away from the columns, which may be equivalent to an increase in the plastic capacity of the girders.

2. Neglecting the width of the columns in the analysis is generally on the safe side. Introducing it might not be on the safe side, since the joint interior is assumed here to be infinitely rigid. In reality such interior is subjected to large shear deformations which tend to offset the above demonstrated effect.

3. Generally speaking, the effect of the finite size of the joints can be sometimes as important as other effects previously studied (for example, the P-Δ effect). Further research should be directed toward a better understanding of the mechanism of deformation inside the beam column overlap, since such zone might affect the analysis substantially.

3.5.9 Effect of Damping

Damping can be assumed in several different mathematical terms. Figs. 3.77 through 3.88 show the effect of choosing different damping values or damping schemes on the results of the analysis. All the

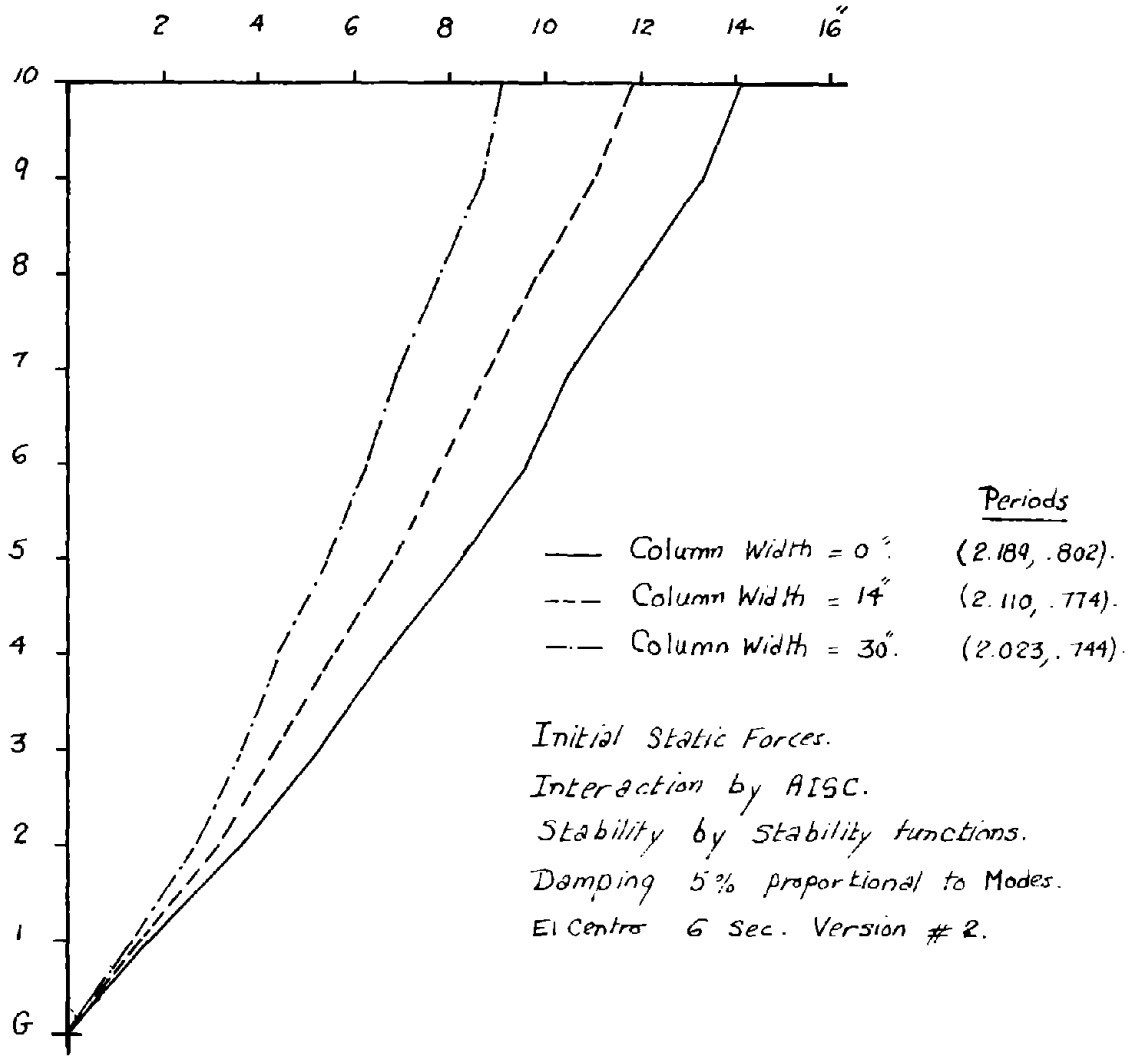

Fig. 3.66 - Effect of Beam-Column Overlap on Maximum Story Displacements

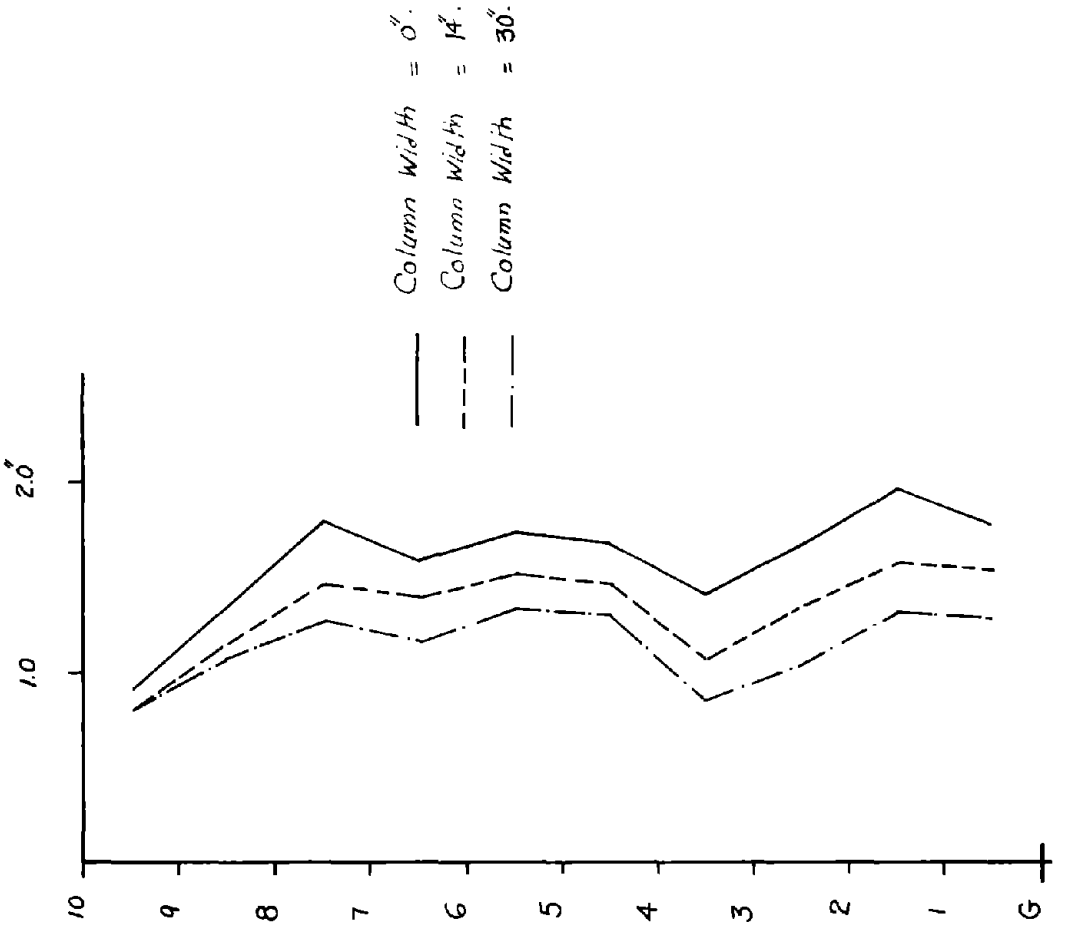

Fig. 3.67 - Effect of Beam-Column Overlap on Maximum Interstory Displacements

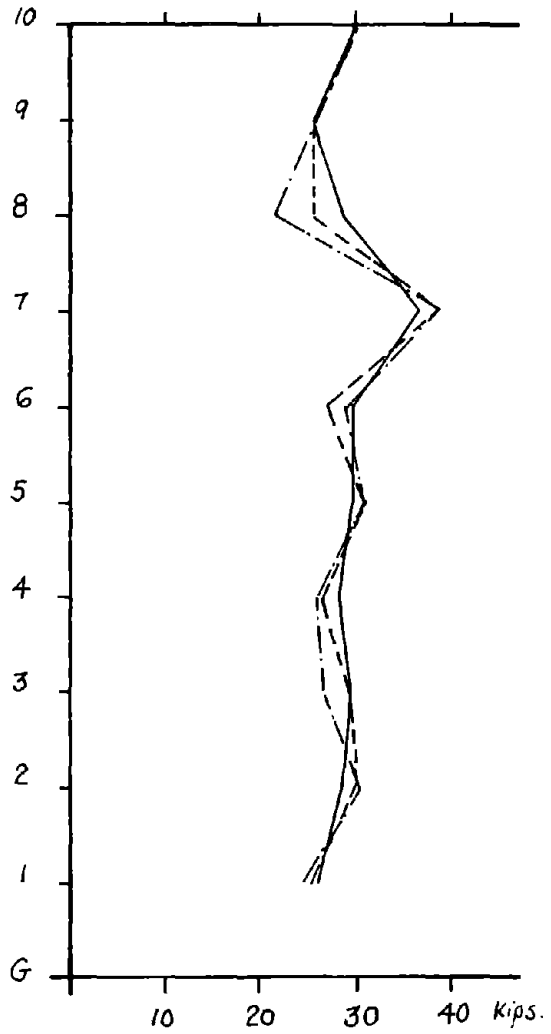

Fig. 3.68 - Effect of Beam-Column Overlap on Maximum Story Forces

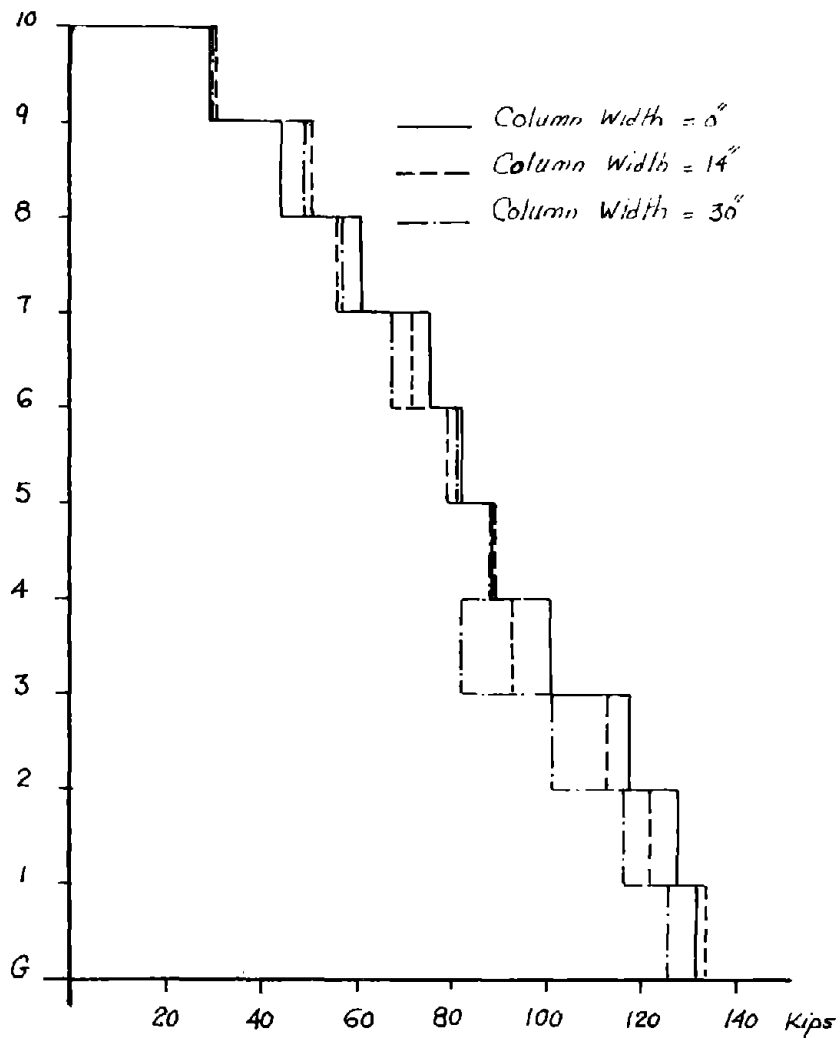

Fig. 3.69 - Effect of Beam-Column Overlap on Maximum Story Shears

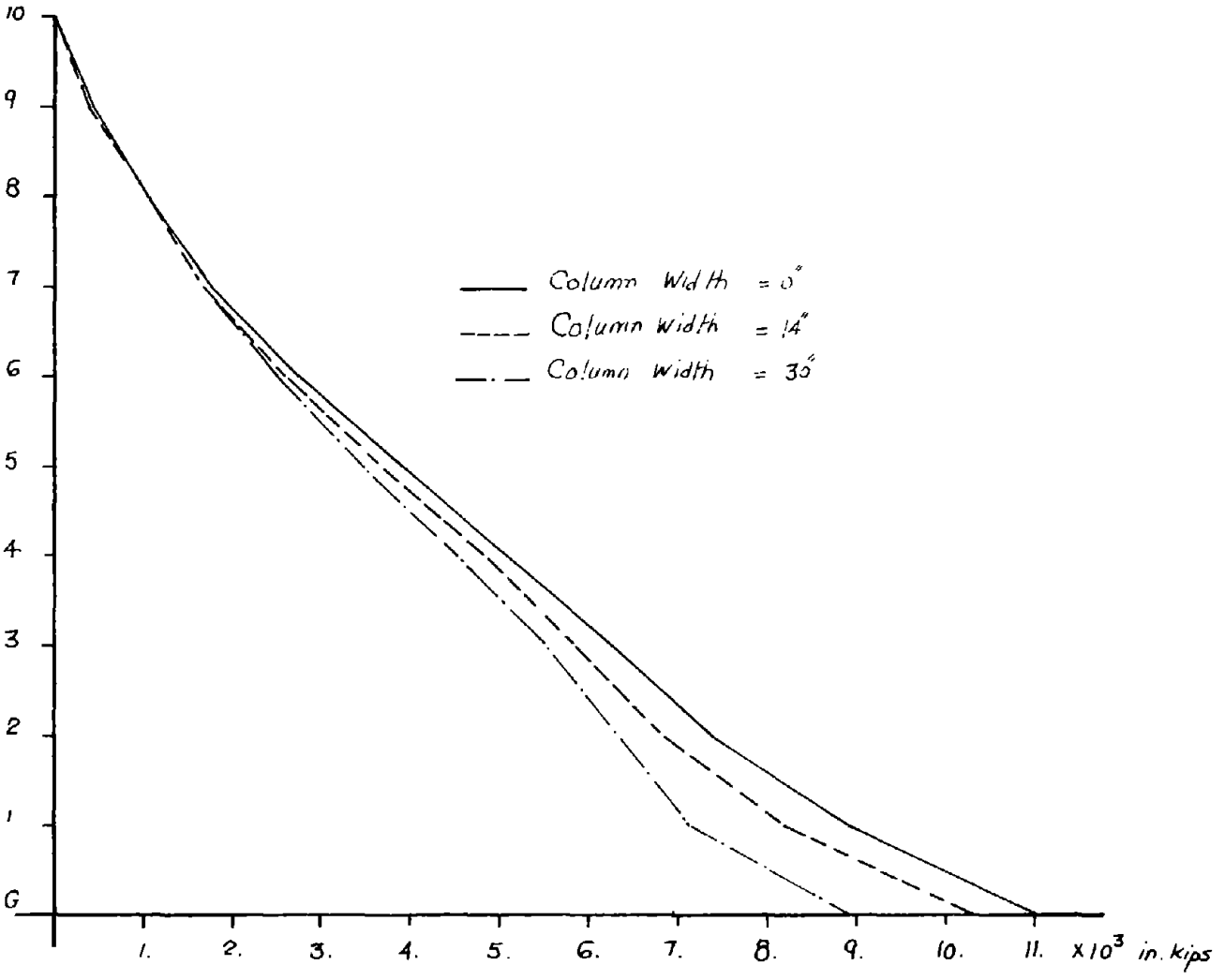

Fig. 3.70 - Effect of Beam-Column Overlap on Maximum Overturning Moments

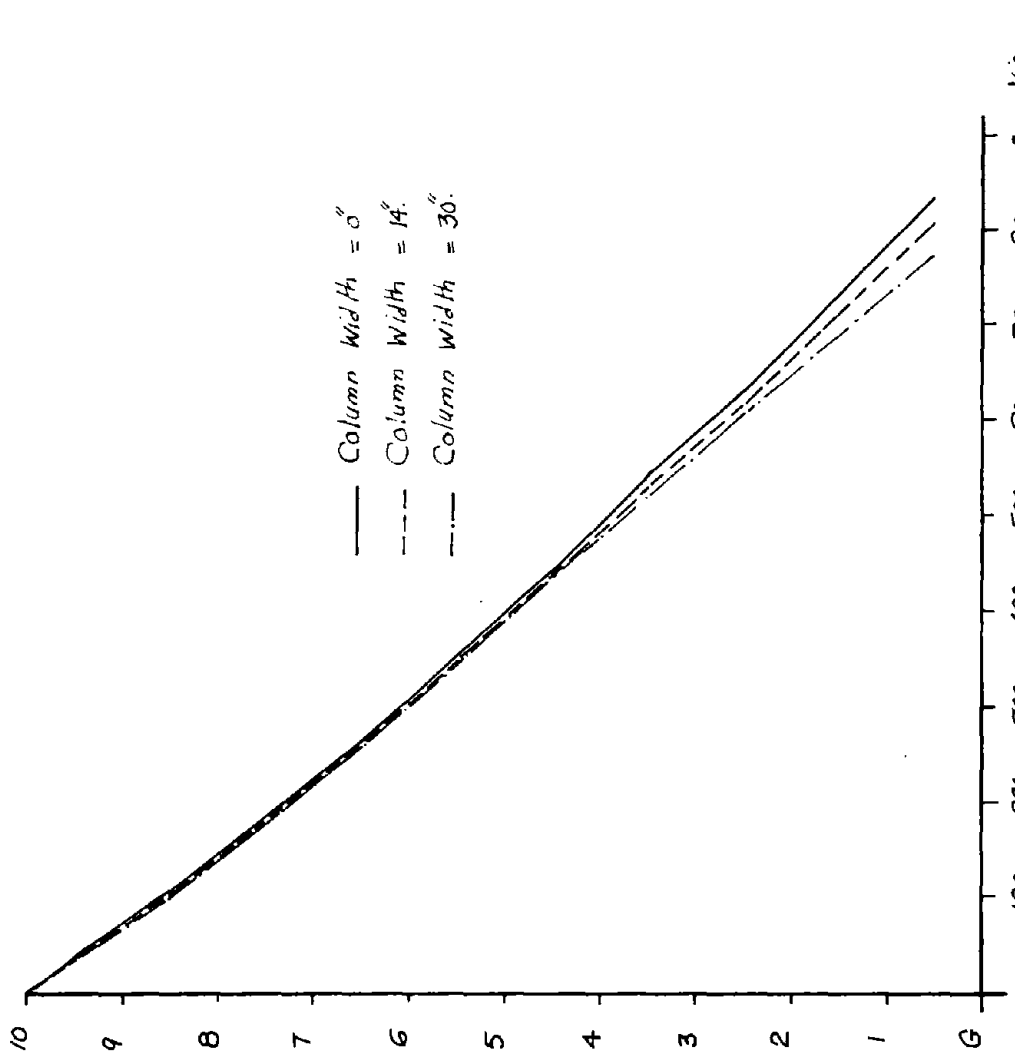

Fig. 3.71 - Effect of Beam-Column Overlap on Maximum Axial Forces on Columns

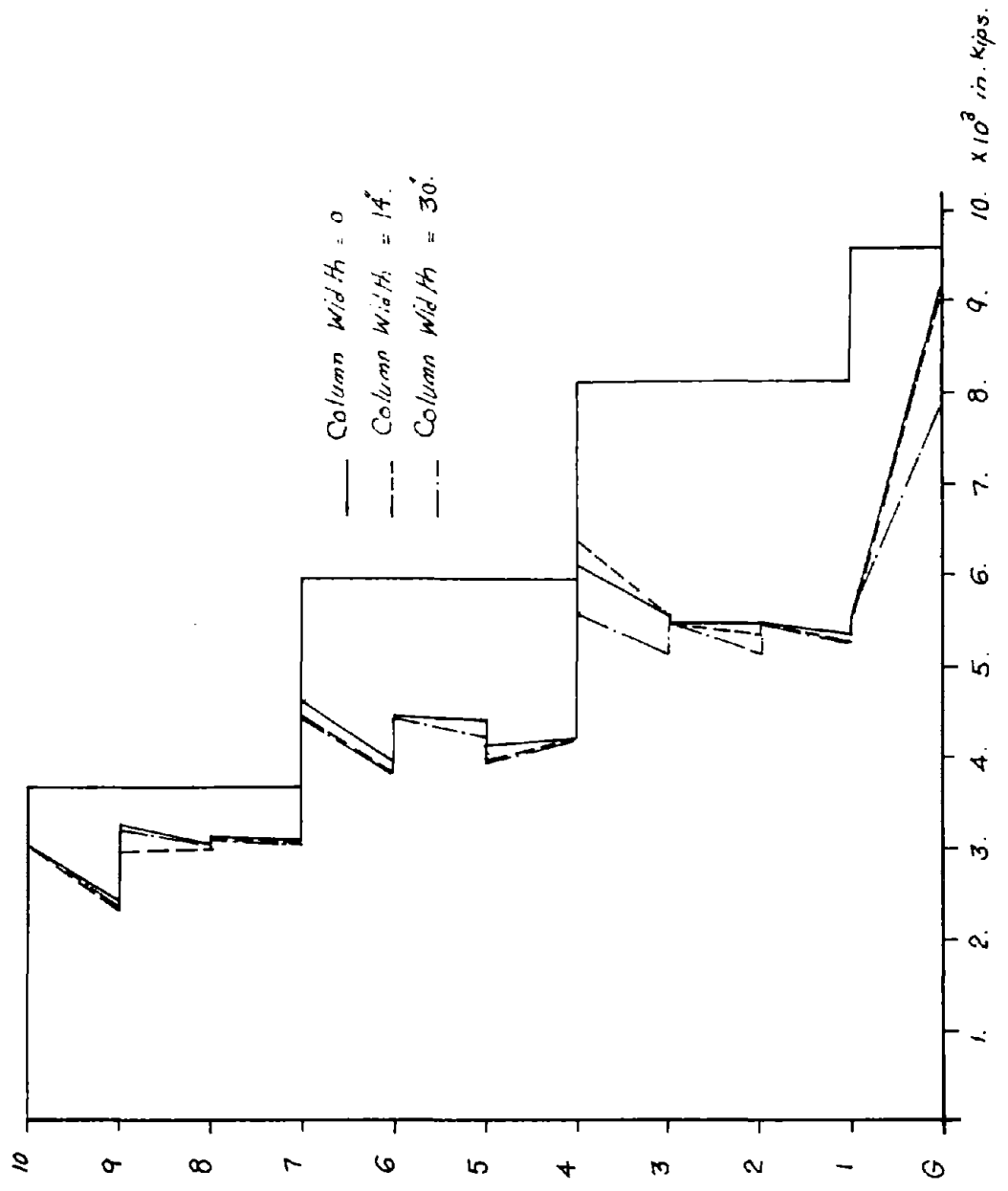

Fig. 3.72 - Effect of Beam-Column Overlap on Maximum Moments on Columns

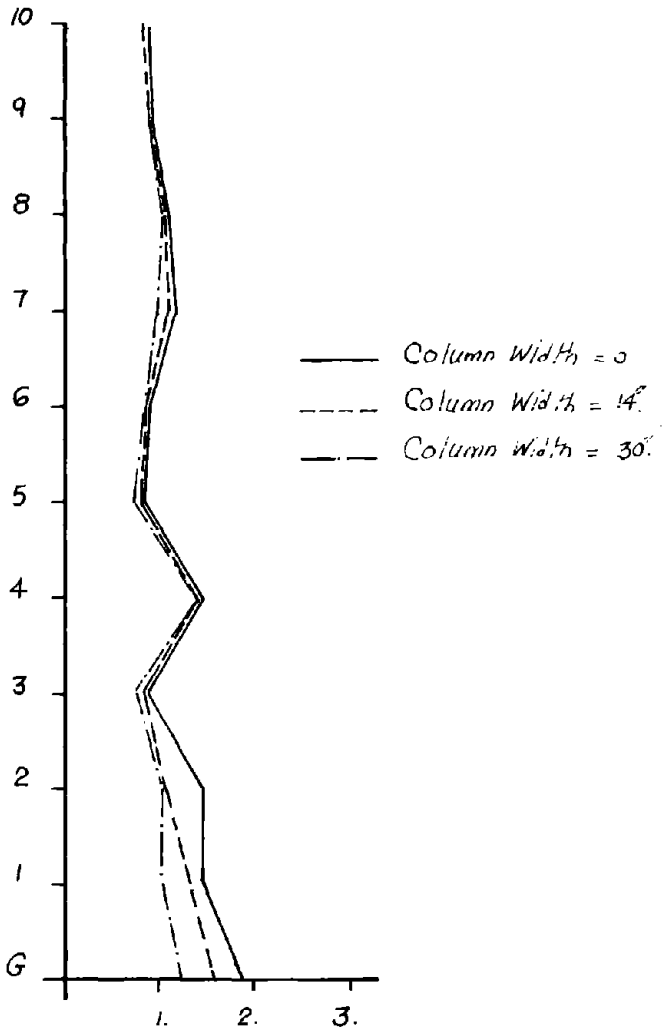

Fig. 3.73 - Effect of Beam-Column Overlap on Maximum Column Ductilities

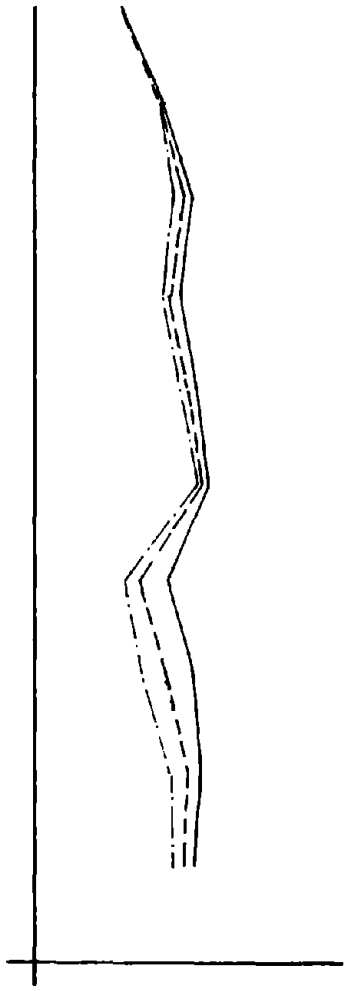

Fig. 3.74 - Effect of Beam-Column Overlap on Maximum Girder Ductilities

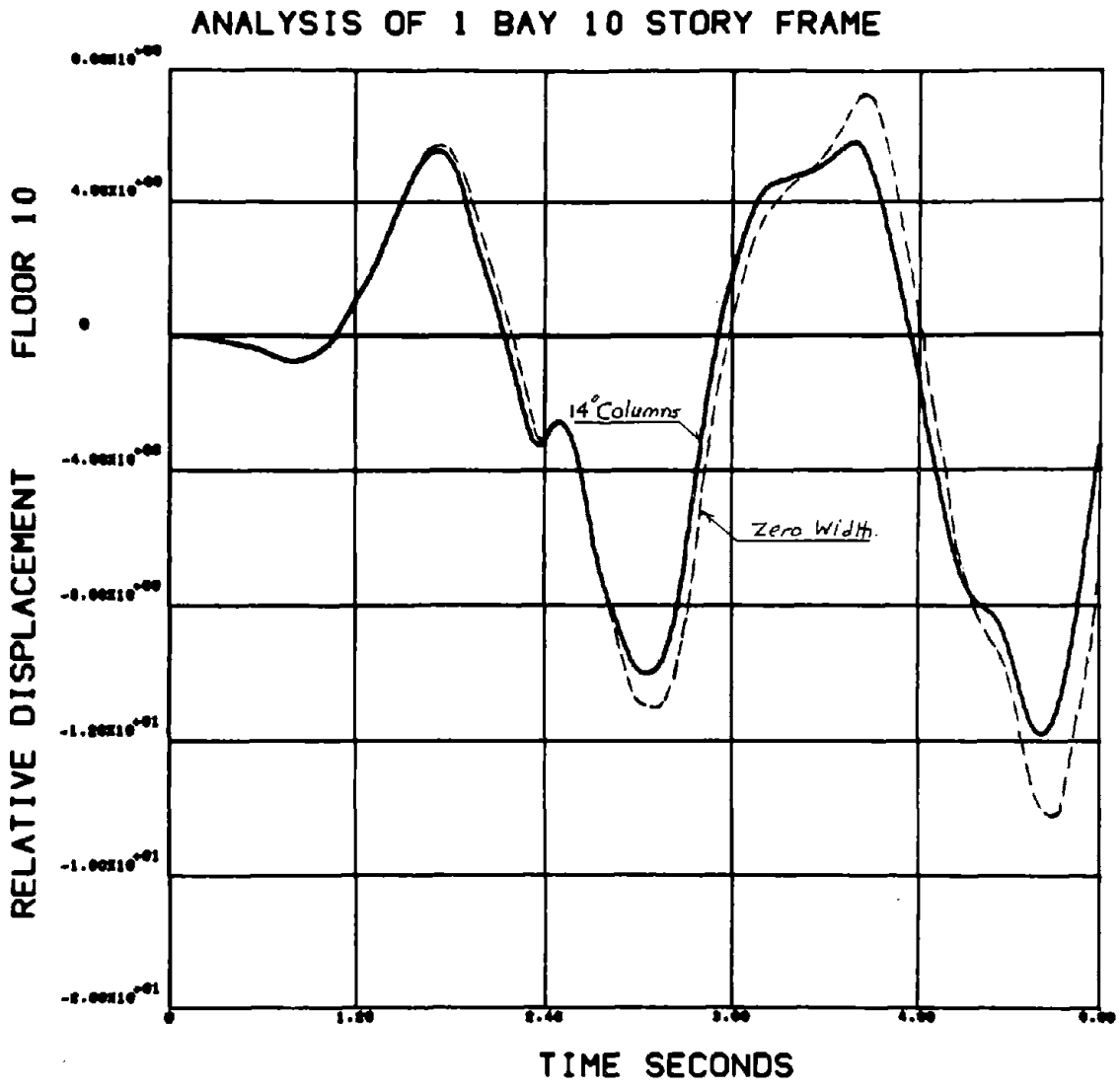

Fig. 3.75 - Effect of Column Width Used in the Analysis on the Roof Displacement

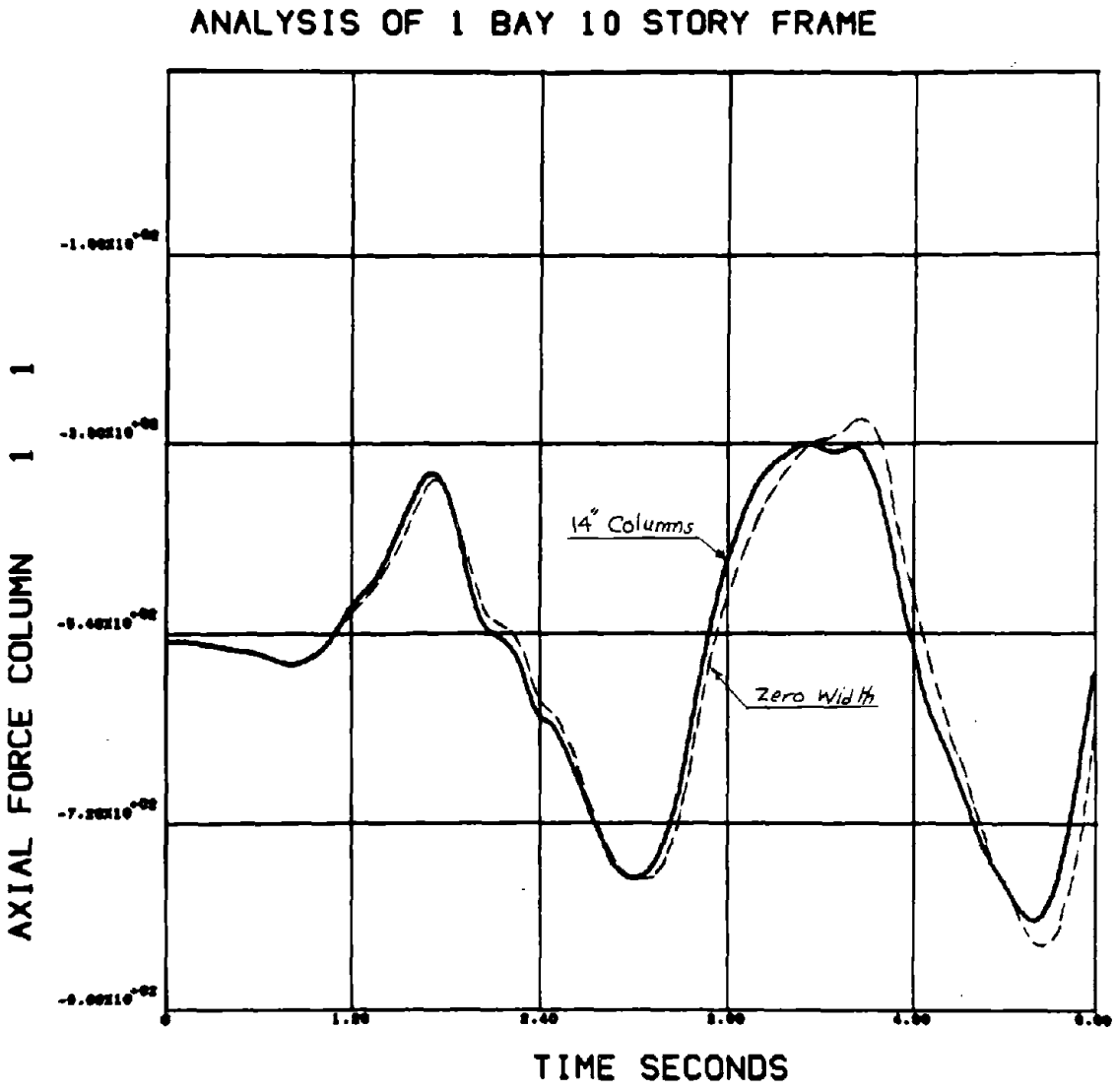

Fig. 3.76 - Effect of Column Width Used in the Analysis on the Axial Force in the Bottom Column

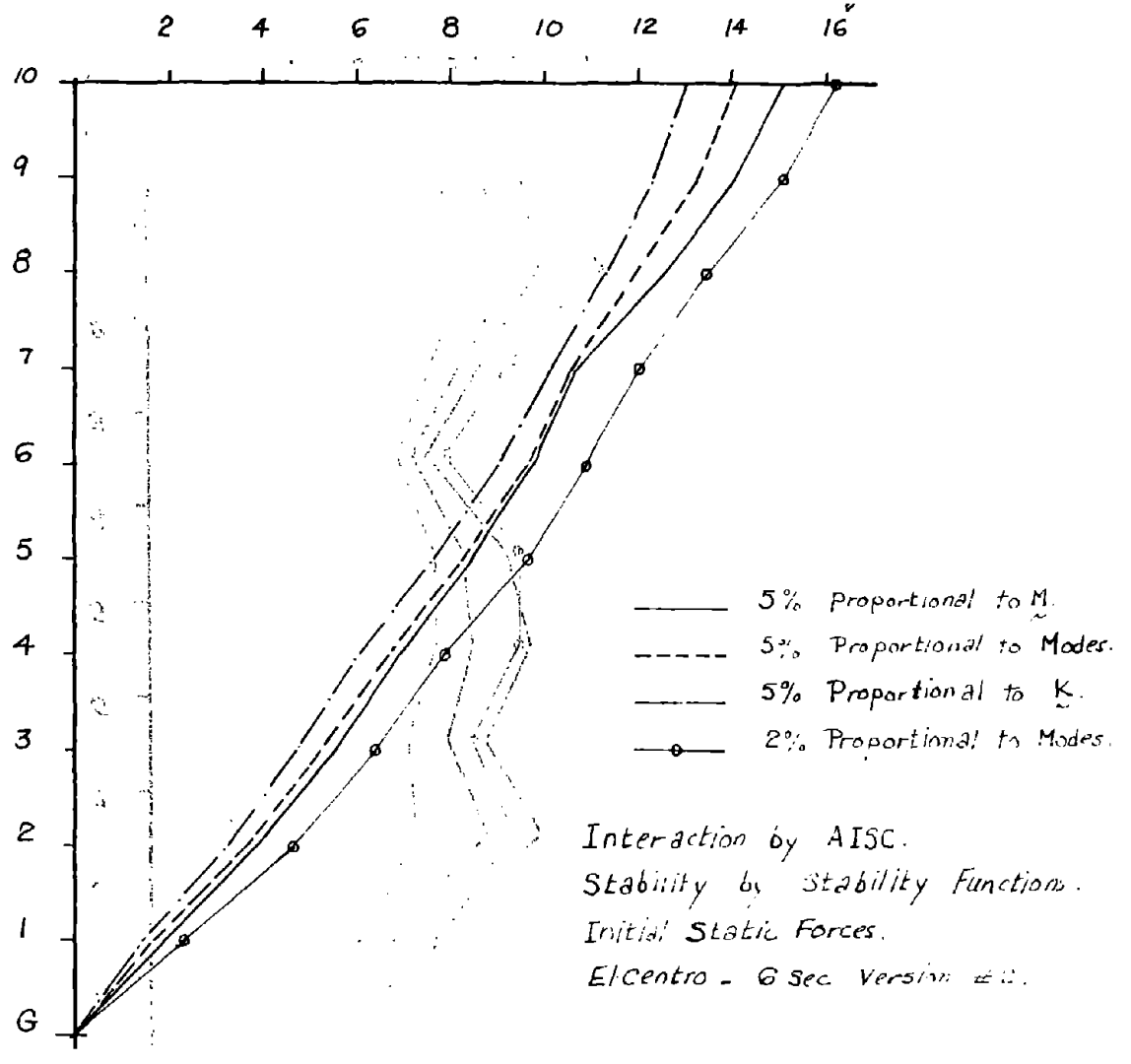

Fig. 3.77 - Effect of Damping on Maximum Story Displacements

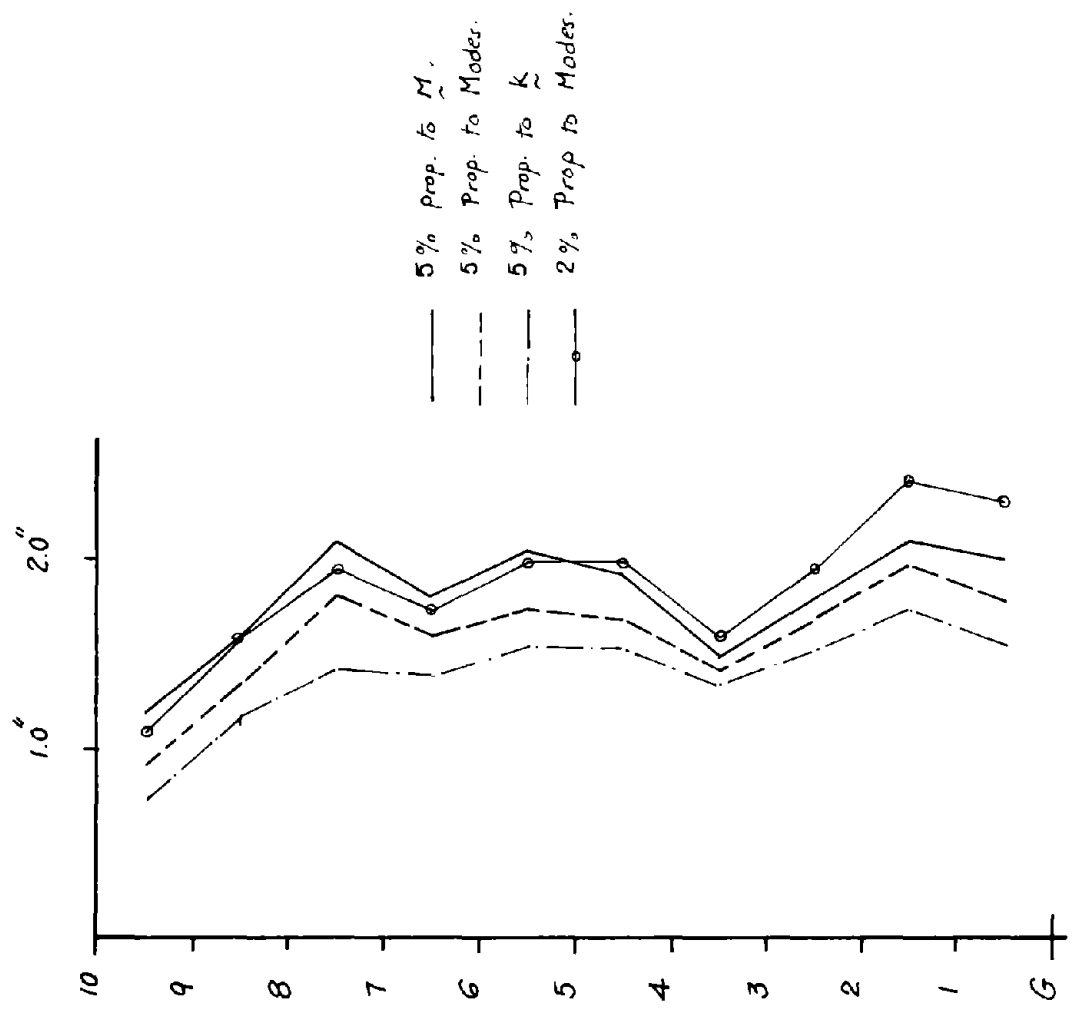

Fig. 3.78 - Effect of Damping on Maximum Interstory Displacements

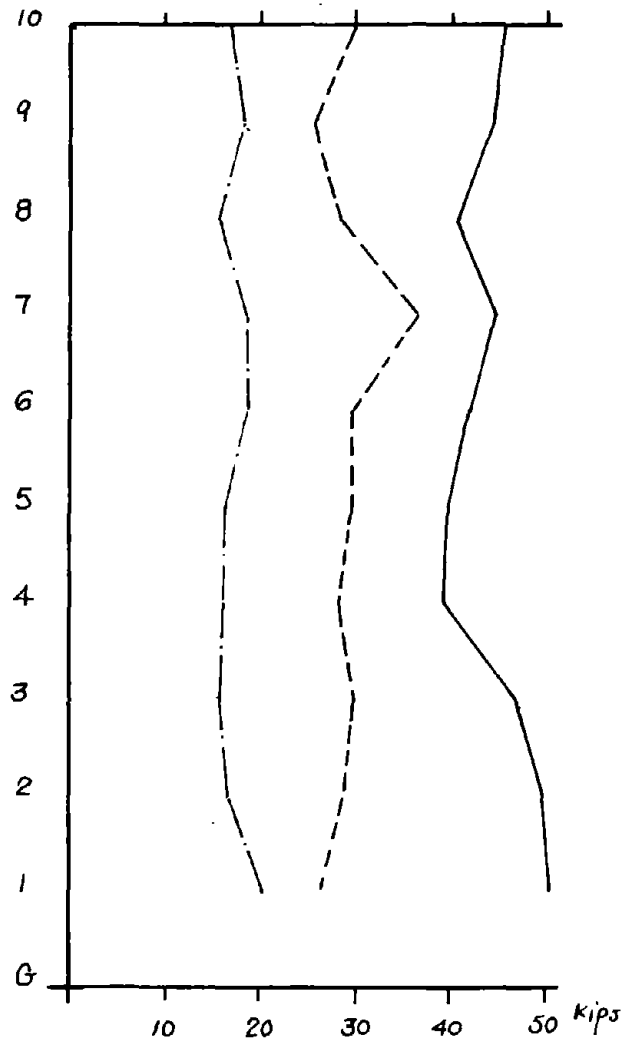

Fig. 3.79 - Effect of Damping on Maximum Story Forces

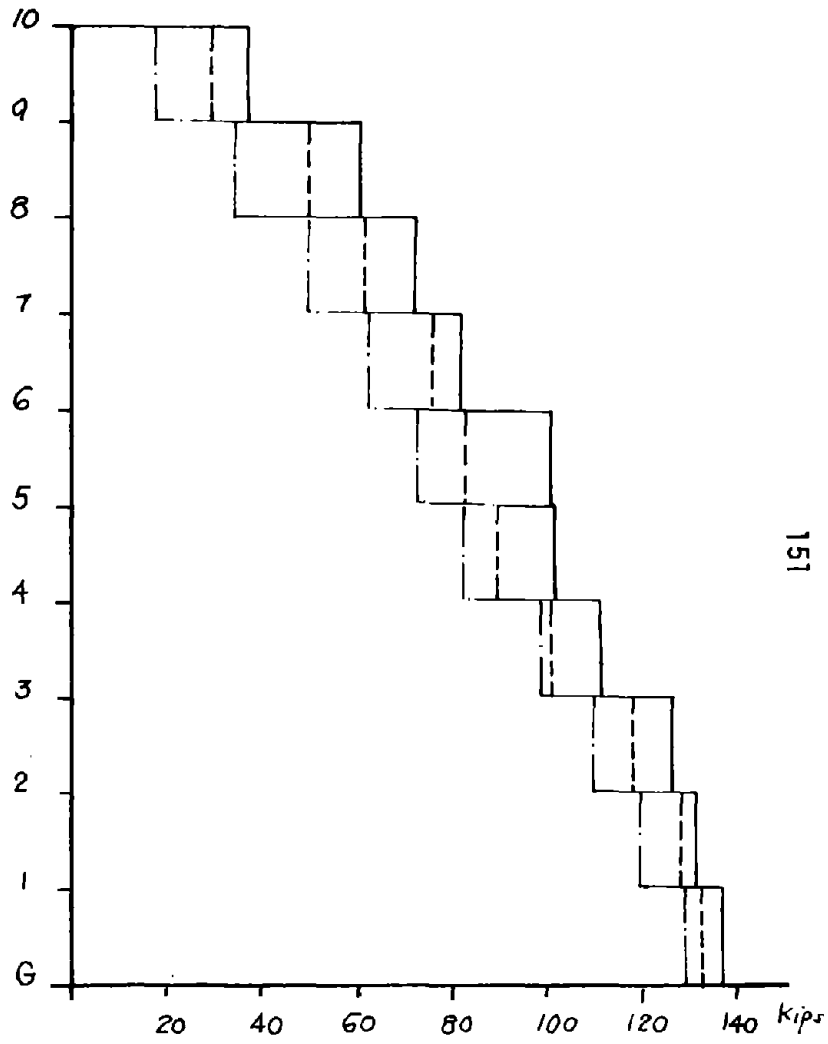

Fig. 3.80 - Effect of Damping on Maximum Story Shears

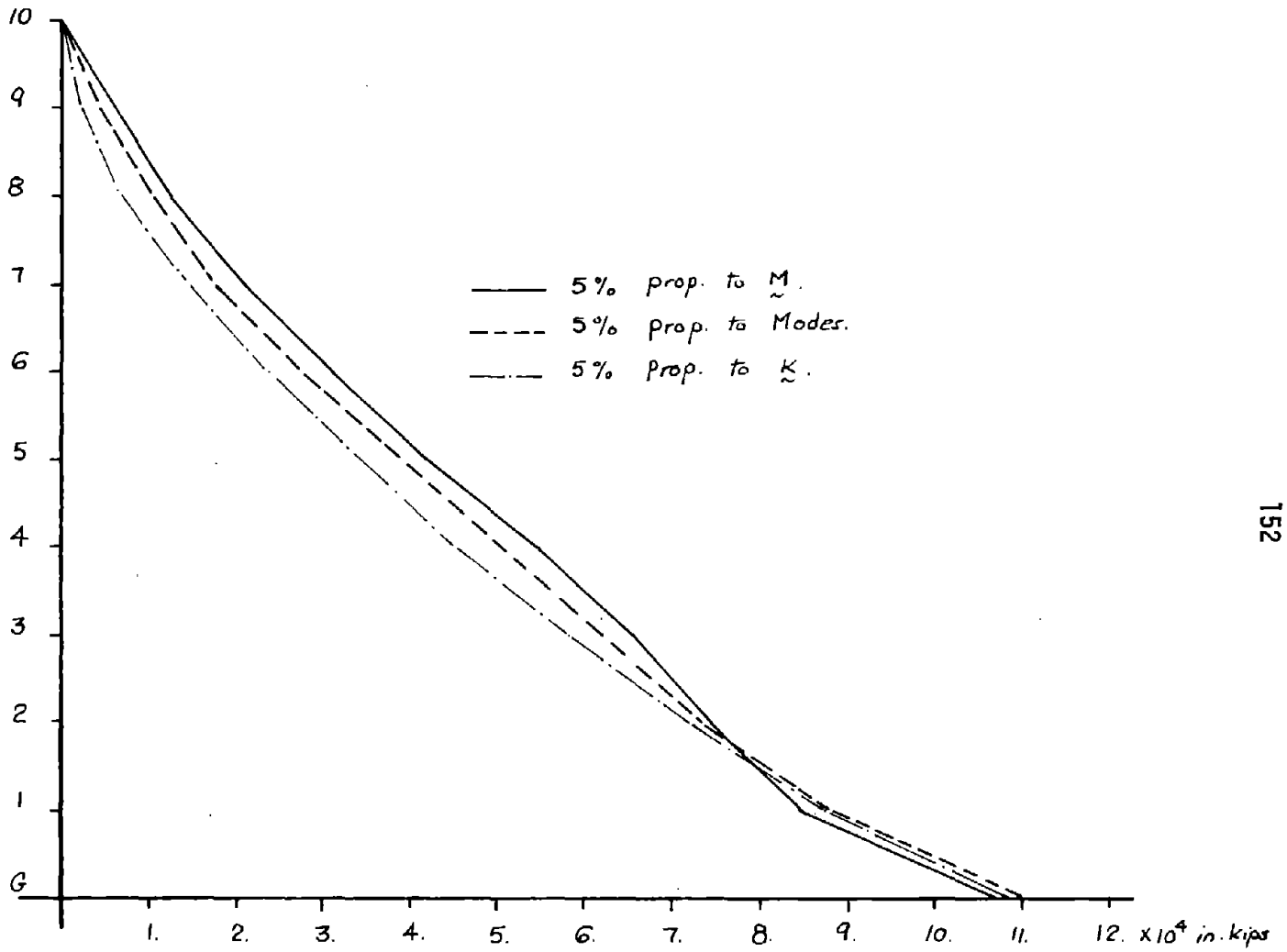

Fig. 3.81 - Effect of Damping on Maximum Overturning Moments

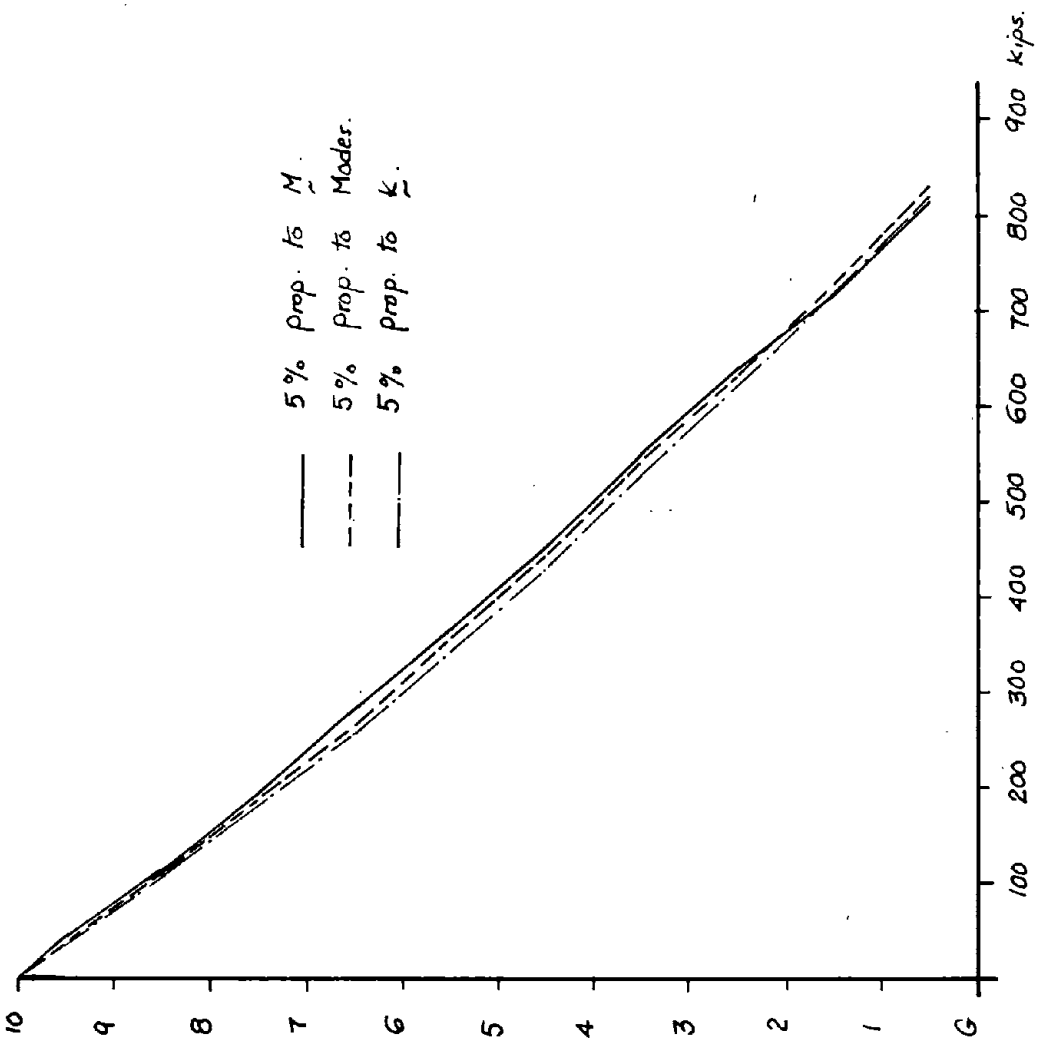

Fig. 3.82 - Effect of Damping on Maximum Column Axial Forces

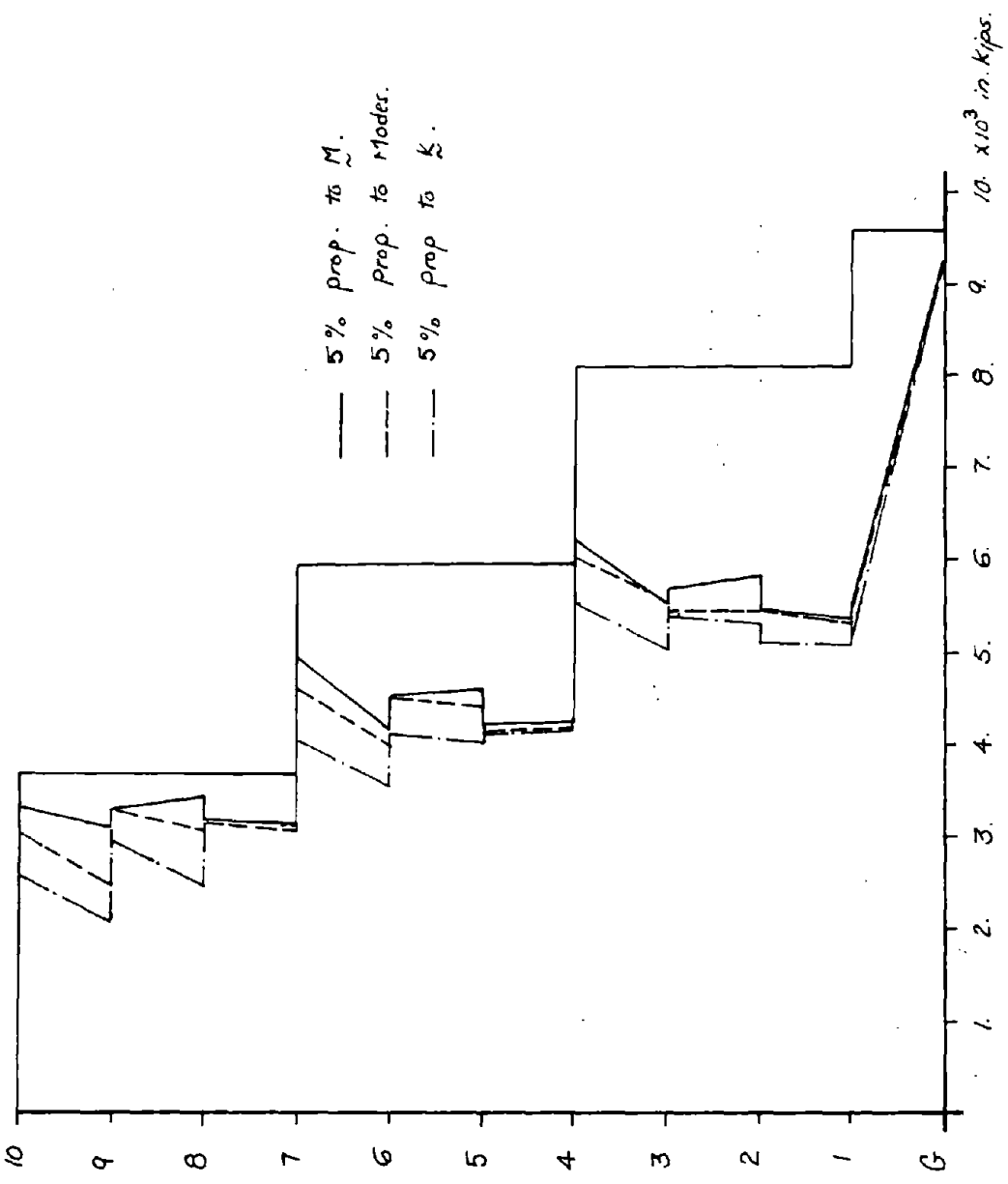

Fig. 3.83 - Effect of Damping on Maximum Column Moments

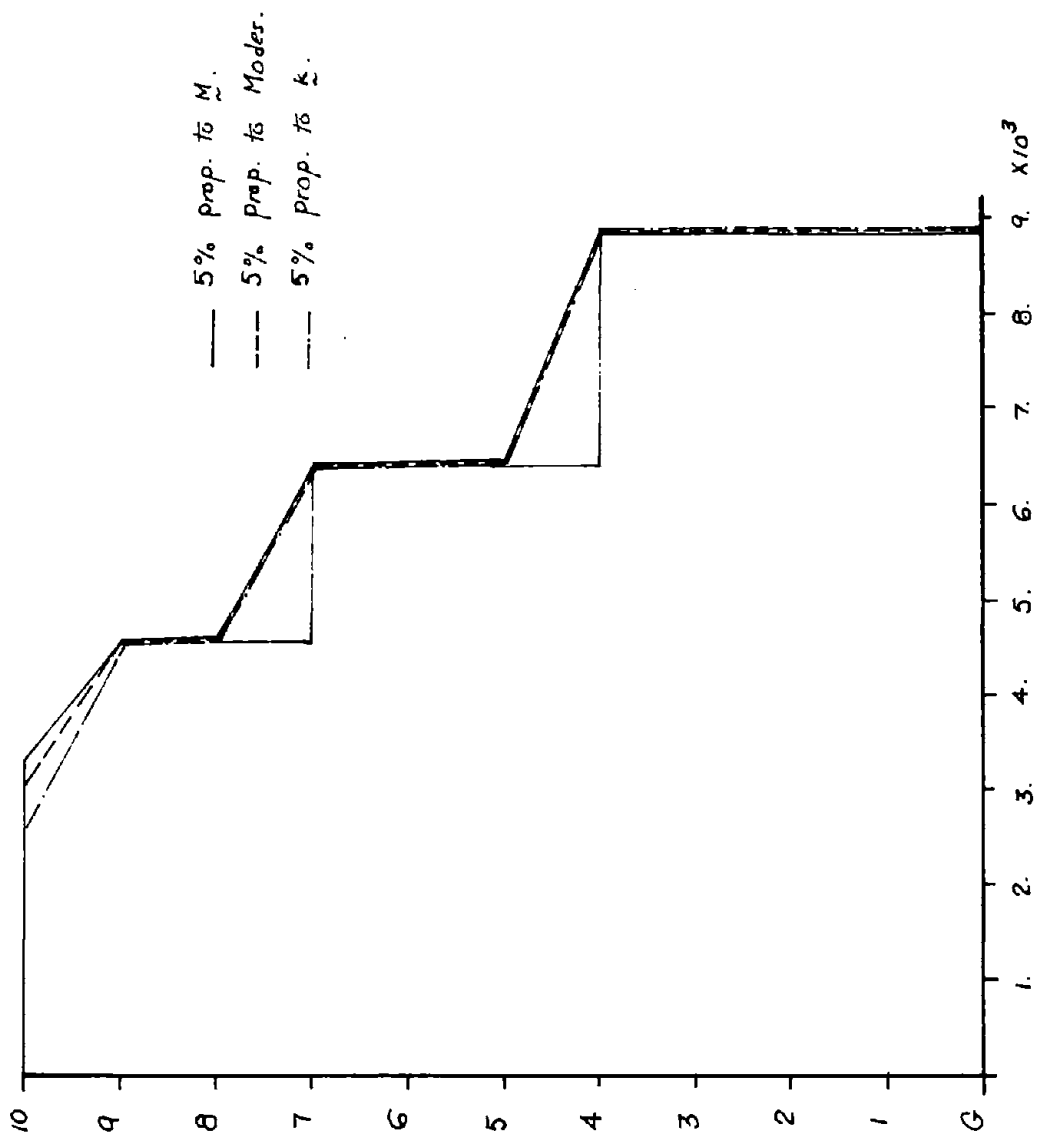

Fig. 3.84 - Effect of Damping on Maximum Girder Moments

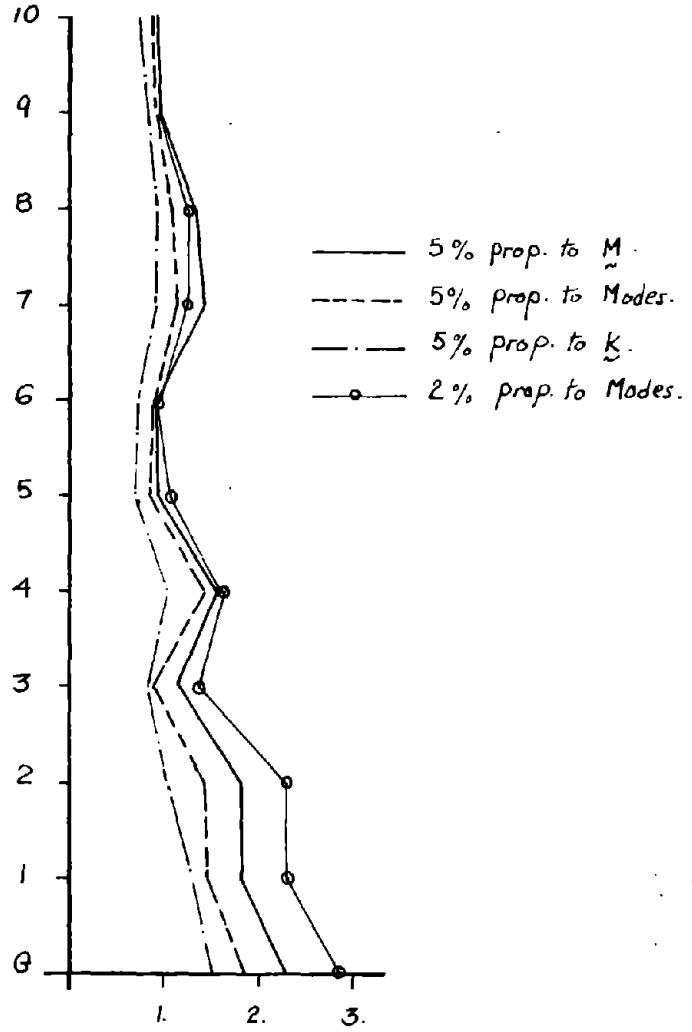

Fig. 3.85 - Effect of Damping on Maximum Column Ductilities

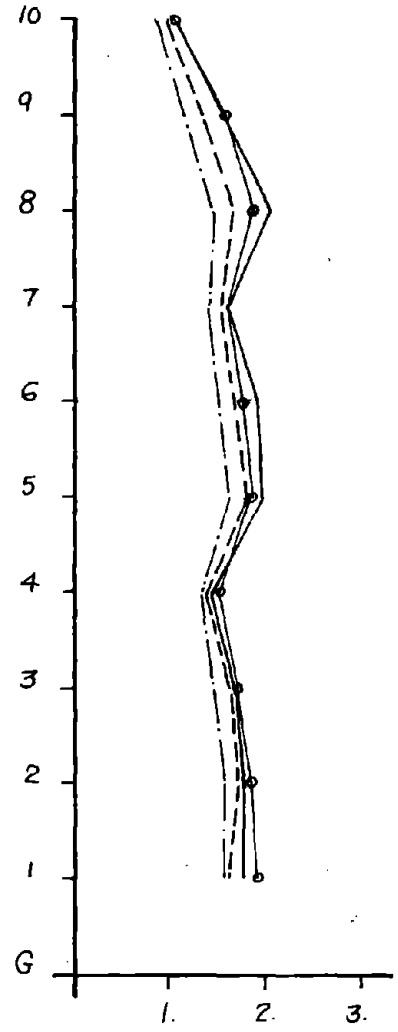

Fig. 3.86 - Effect of Damping on Maximum Girder Ductilities

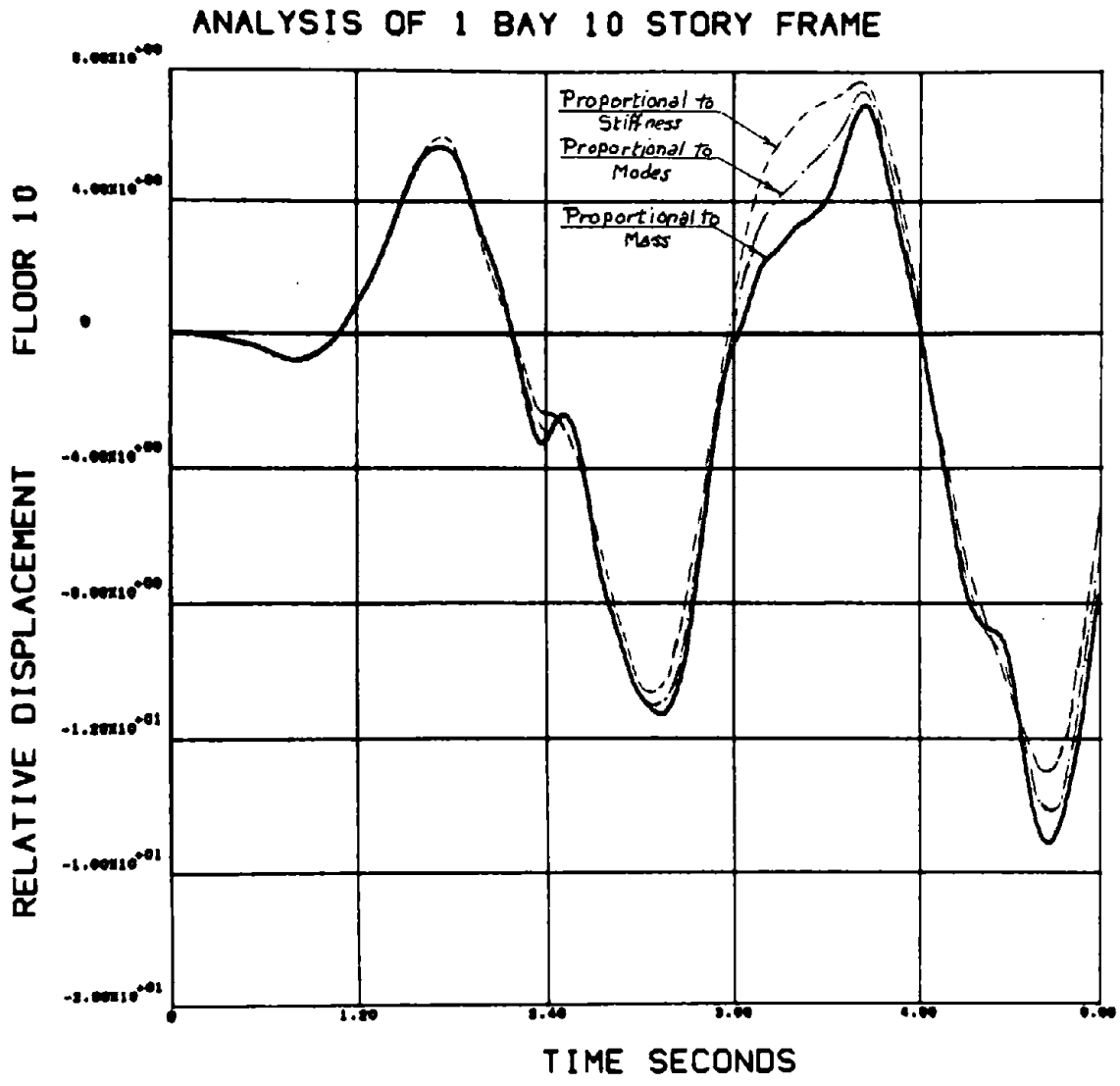

Fig. 3.87 - Effect of Damping on the Roof Displacement

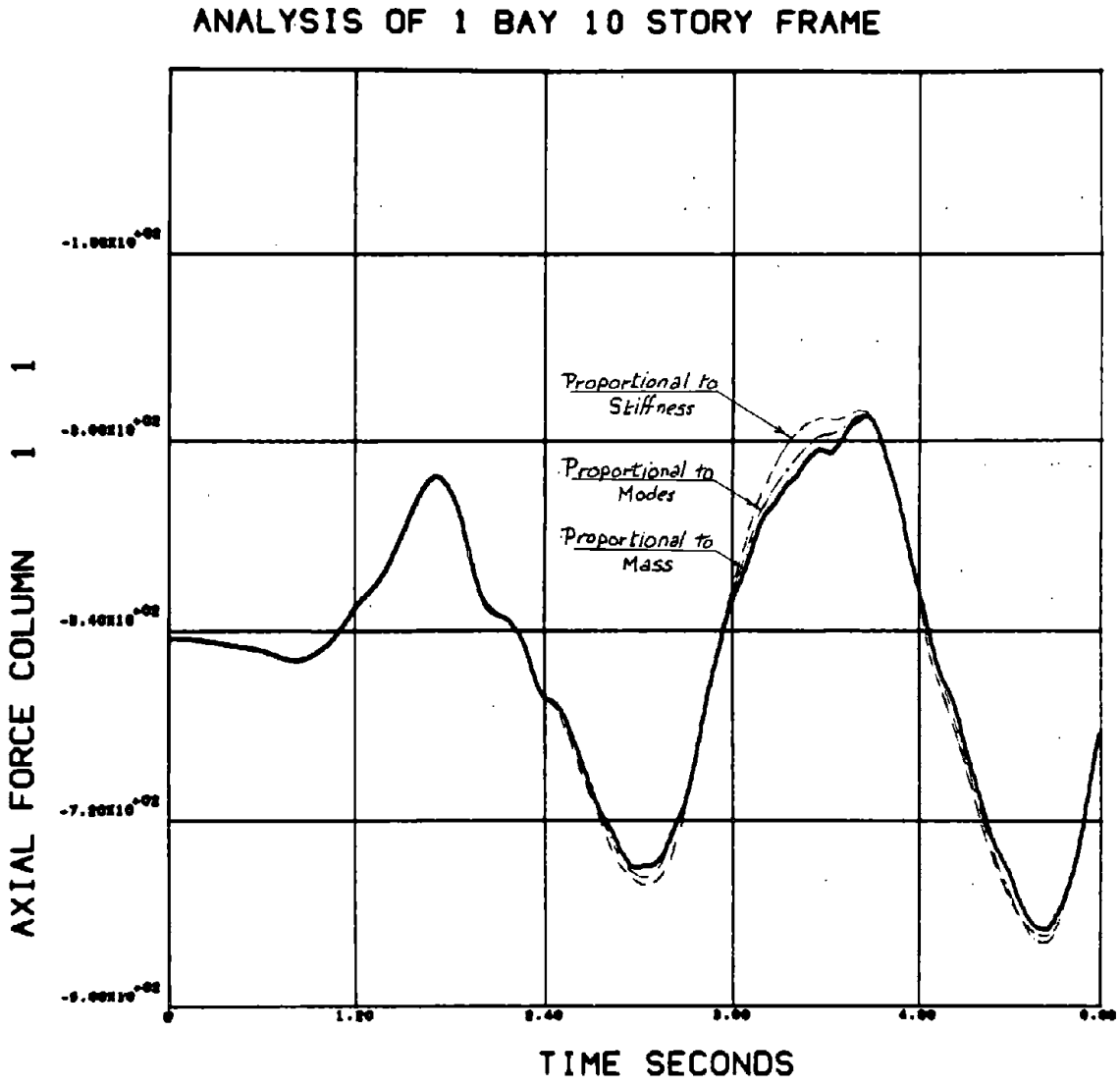

Fig. 3.88 - Effect of Damping on the Axial Force in the Bottom Column

schemes were chosen to give 5% damping in the first mode. From these figures it can be concluded that the effect of the damping scheme used is as important as many of the other nonlinear effects studied before. Further research should be directed to establish both the value and the mathematical form of damping to be used in dynamic analysis.

3.5.10 Soil-Structure Interaction Effects

In performing an analysis for a soil building system, one might face the following situations:

1. An inelastic structure resting on an elastic soil.
2. An elastic structure resting on an inelastic soil.
3. An inelastic structure resting on an inelastic soil.

Four models were compared in the current study. In the first model, soil-structure interaction was completely neglected, and the classic rigid foundation assumption was used; in the second model two elastic springs and two viscous dashpots were introduced to simulate an elastic linear soil; and in the third model, two bilinear springs were introduced to simulate a nonlinear soil with the same viscous soil damping used in the second model. The fourth model is identical to the third model, but a zero value of viscous damping was assumed for the soil.

The initial soil properties were determined for an equivalent circular footing resting on an elastic half-space. These properties

might be typical of many highrise structures constructed nowadays.

Figs. 3.89 and 3.90 demonstrate the effect of elastic soil-structure interaction on the response of the basic frame studied. The response of the other two models happened to lie in between, and are not plotted for clarity purposes. From the results presented, it seems that soil-structure interaction has very little effect on the dynamic response of the frame studied.

3.6 CLOSING REMARKS

In this Chapter an attempt was made to systematically study the different nonlinear effects on a building frame. The study was restricted to a 10-story 1-bay frame designed by Anderson. However, the analysis was automated and implemented in a general computer program to be able to repeat the same approach for any different building frame encountered in practice. Different conclusions were reached with respect to each nonlinear effect, as reported in the corresponding sections.

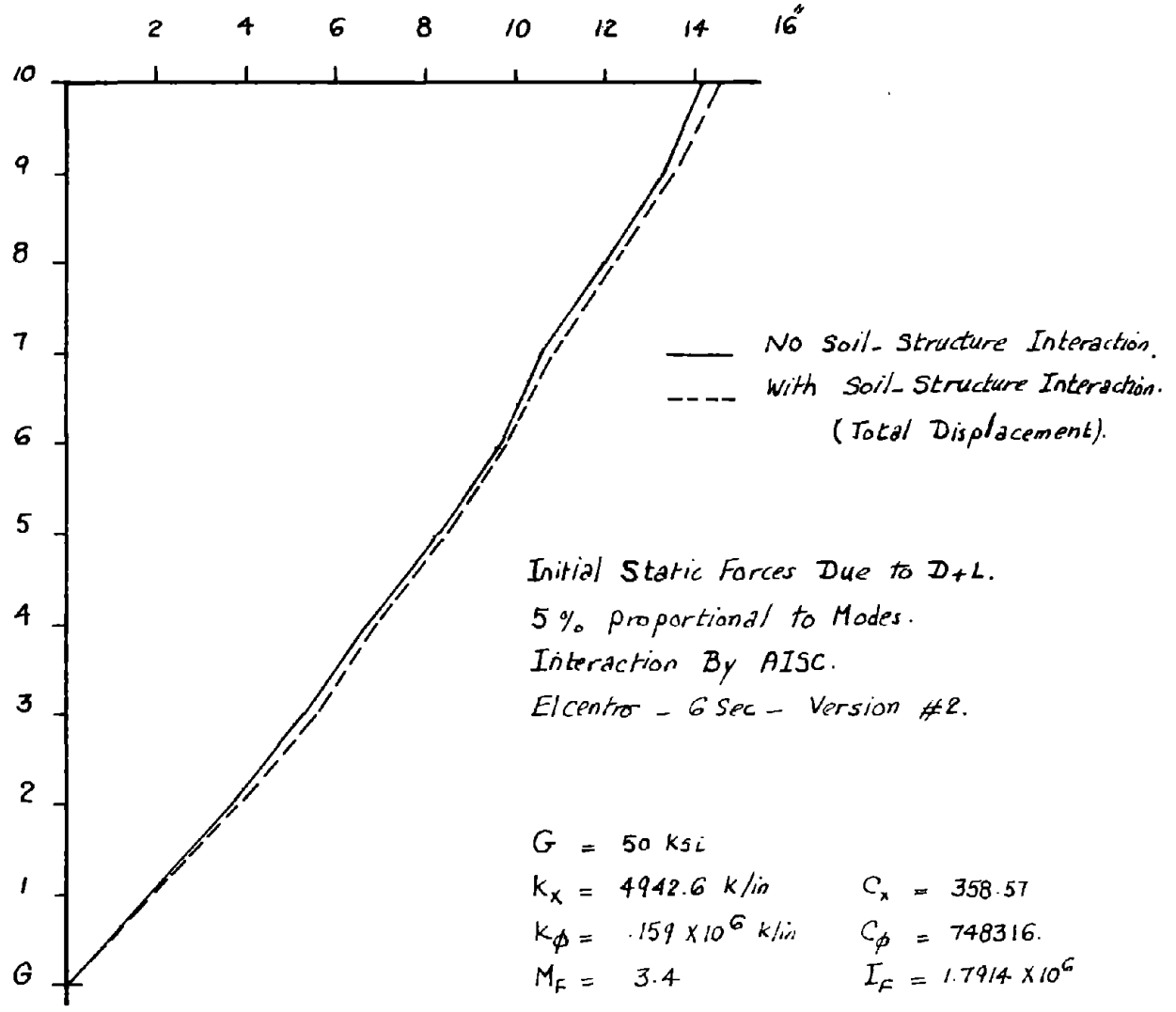

Fig. 3.89 - Effect of Soil-Structure Interaction on the Total Displacements.

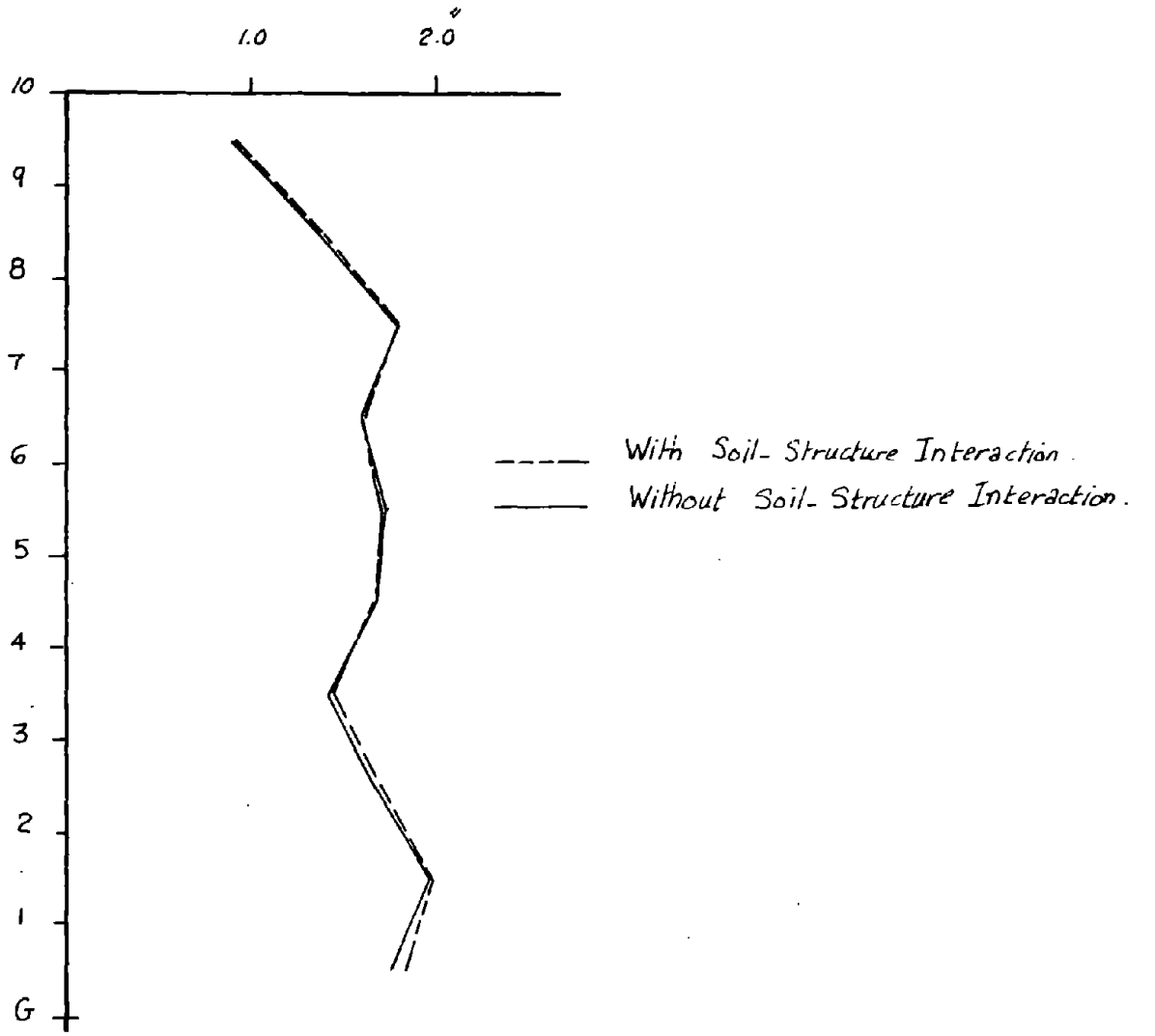

Figure 3.90 - Effect of Soil-Structure Interaction on the Maximum Interstory Displacements

CHAPTER IV

COMPARATIVE STUDIES FOR SIMPLE VERSUS BENDING MODELS

4.1 GENERAL

In Chapter III the 10-story 1-bay frame designed by Anderson was subjected to extensive comparative studies using a generalized bending model. In this Chapter comparisons are made between the prediction of the most general bending model which includes all the nonlinear effects and the prediction of the least general bending model which neglects all the nonlinear effects. Different frames which appeared in the literature will be used as working material for this comparative study. In conjunction with the study, the two models mentioned above will be used as yardsticks for evaluating a very simple approximate model which gained some attraction by other researchers [3,64,65] for its economy and inherent intuitive engineering features.

4.2 APPROXIMATE SIMPLE MODELS (STORY-BY-STORY BEHAVIOR)

The idea of an approximate formulation for the behavior of a building by a series of shear springs has been recognized for many years. The concept involves modeling the building based on its story-by-story behavior and was suggested first for the linear elastic case and proved to be satisfactory for certain classes of structures—mainly those for which axial shortening of the columns is

not important (for example, wide frames). Extending the concepts of story-by-story behavior to the inelastic case was a natural progress in thinking which took place some years later. Anagnostopoulos[3] implemented a formulation in which different types of shear springs between floors are arbitrarily assumed to reproduce the overall behavior. He was motivated by the idea that a set of equivalent nonlinear springs can be determined for each floor, each spring corresponding to one of the components in the building. This type of analysis, of course, is only intended as an approximate tool; it will not yield detailed information about a particular member in a particular frame, but rather will average overall behavior for the various components in each story. Determining the properties of the nonlinear models which would best reproduce the interstory behavior of the structural components is a crucial problem in using a method of this kind. In this Chapter no attempt is made to derive the most appropriate model for each case. Instead a simple model suggested by Anagnostopoulos as an average for steel frames will be used. The model is based on a trilinear relationship between the story shear and the corresponding displacement as shown in Fig. 4.1. The story yield level is determined by the equation

$$F_{y_{max.}} = \text{Min.} \quad 2\,\frac{\Sigma M_{yc}}{h}\,, \quad 2\,\frac{\Sigma M_{yG}}{h}$$

where $F_{y_{max.}}$ = Max. story yield force

h = Story height

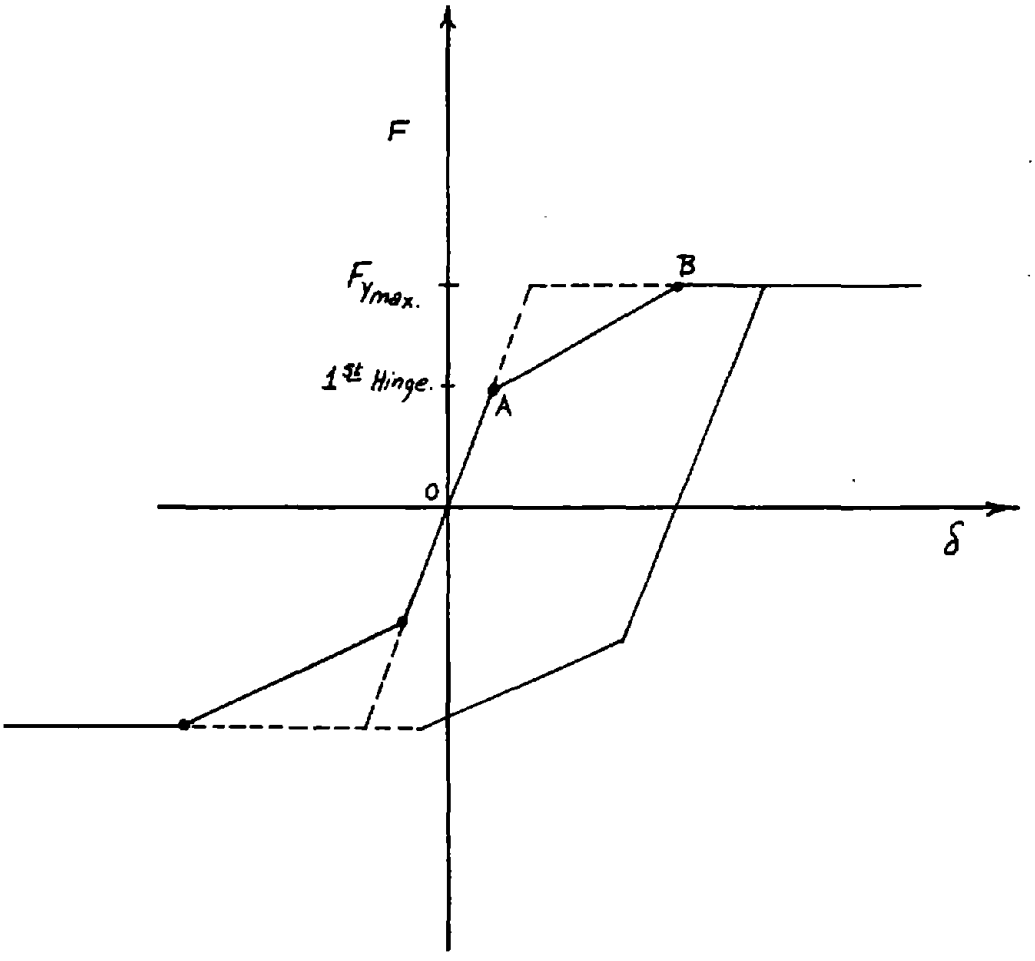

Fig. 4.1 Simple Trilinear Model Used in the Analysis

ΣM_{yc} = Sum of plastic capacities for all columns in the floor.

ΣM_{yG} = Sum of plastic capacities for all girders in the floor.

Two further assumptions were tentatively suggested by Anagnostopoulos and are used here. The first assumption concerns the transition point "A", which is assumed to be at a level of half the story yield force. The second assumption concerns the slope after the other transition point "B", assumed to be 20% of that of "OA".

4.3 CASE STUDY I - ANDERSON'S FRAME (1969)

The frame studied previously in Chapter III is used as the first working specimen to compare the simple model and the two bending models. Two levels of excitation are used. The first type is the N-S component of El Centro 1940 (version #2, first 6 seconds), while the second type is the same record magnified by 1.5. The objective thus is to evaluate the different models under typical design excitation and also under large levels of excitation. Fig. 4.2 shows the maximum story displacements for the three models. Fig. 4.3 shows interstory displacements, and Fig. 4.4, story forces. Fig. 4.5 shows the different ductility predictions. One must keep in mind, however, the difference in the definition used to measure ductilities in both models. It is worth mentioning that the bending models lead to relatively more uniform ductility values than the simple model.

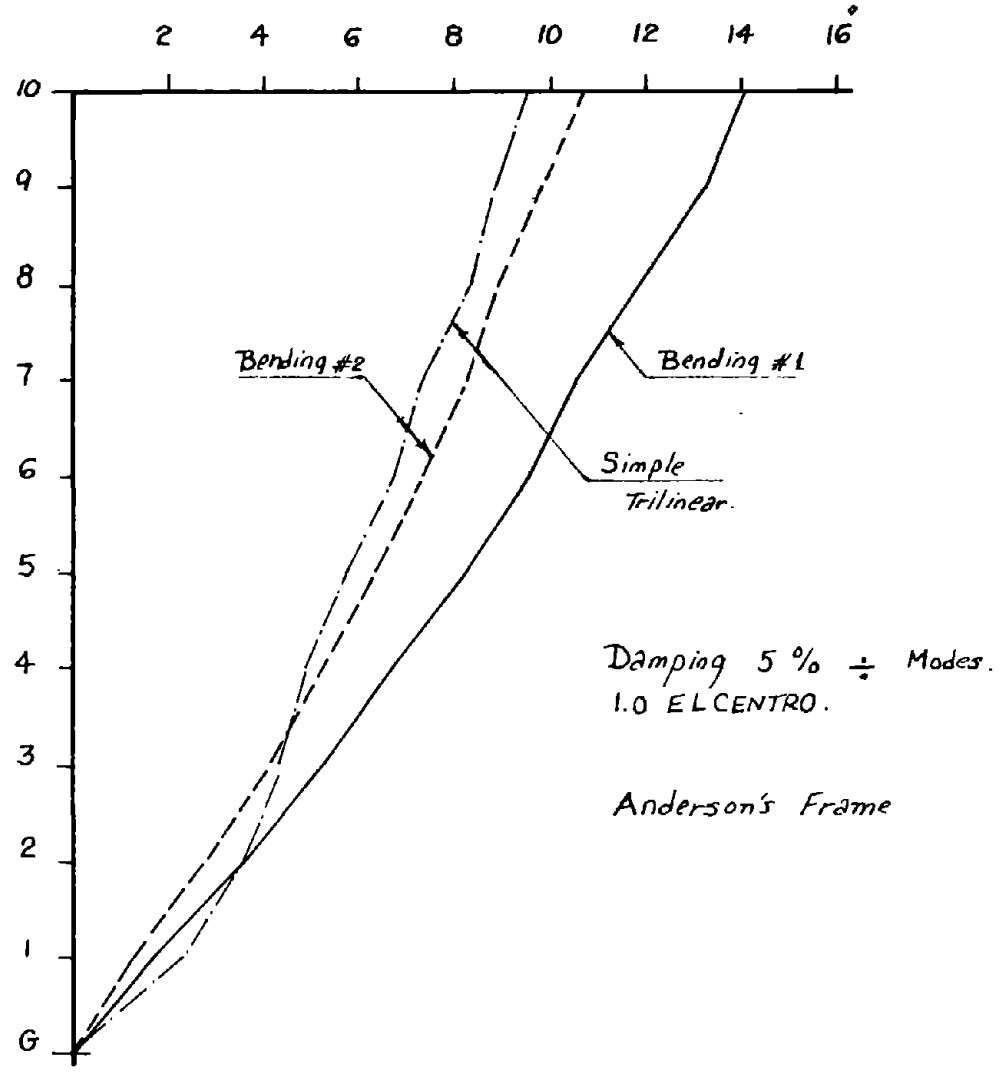

Fig. 4.2 - Maximum Displacements - Simple versus Bending

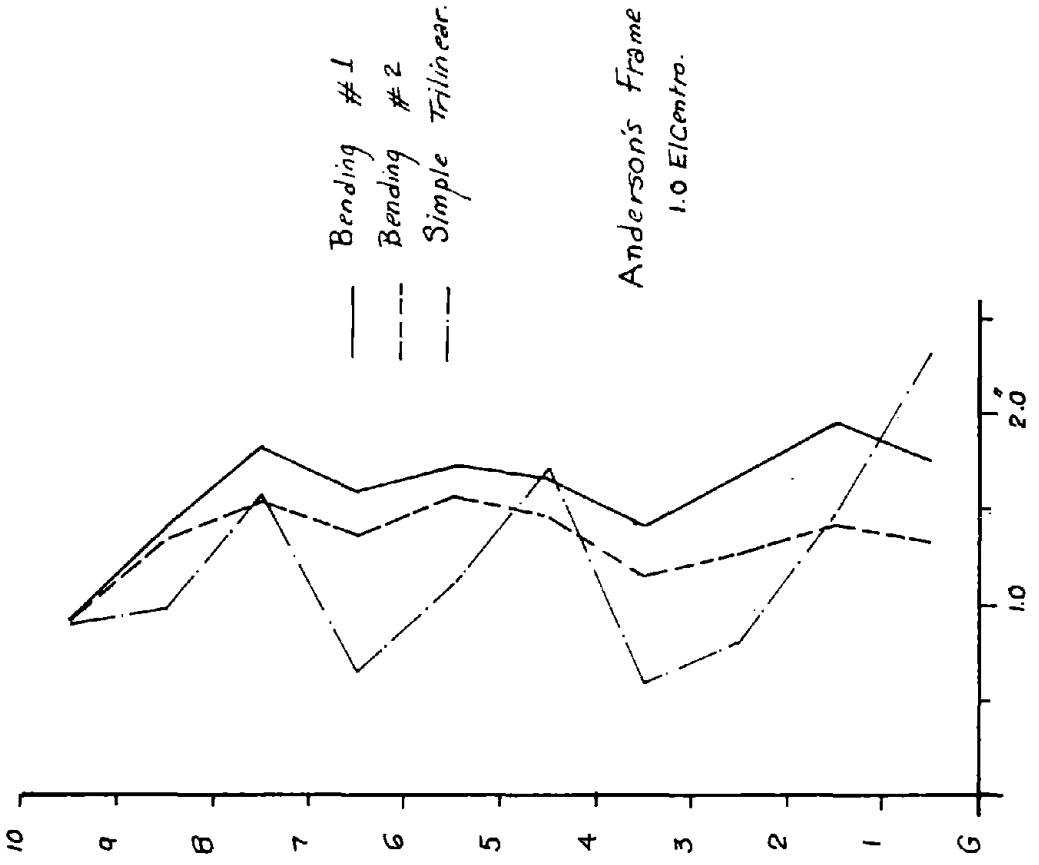

Fig. 4.3 - Maximum Interstory Displacements - Simple versus Bending

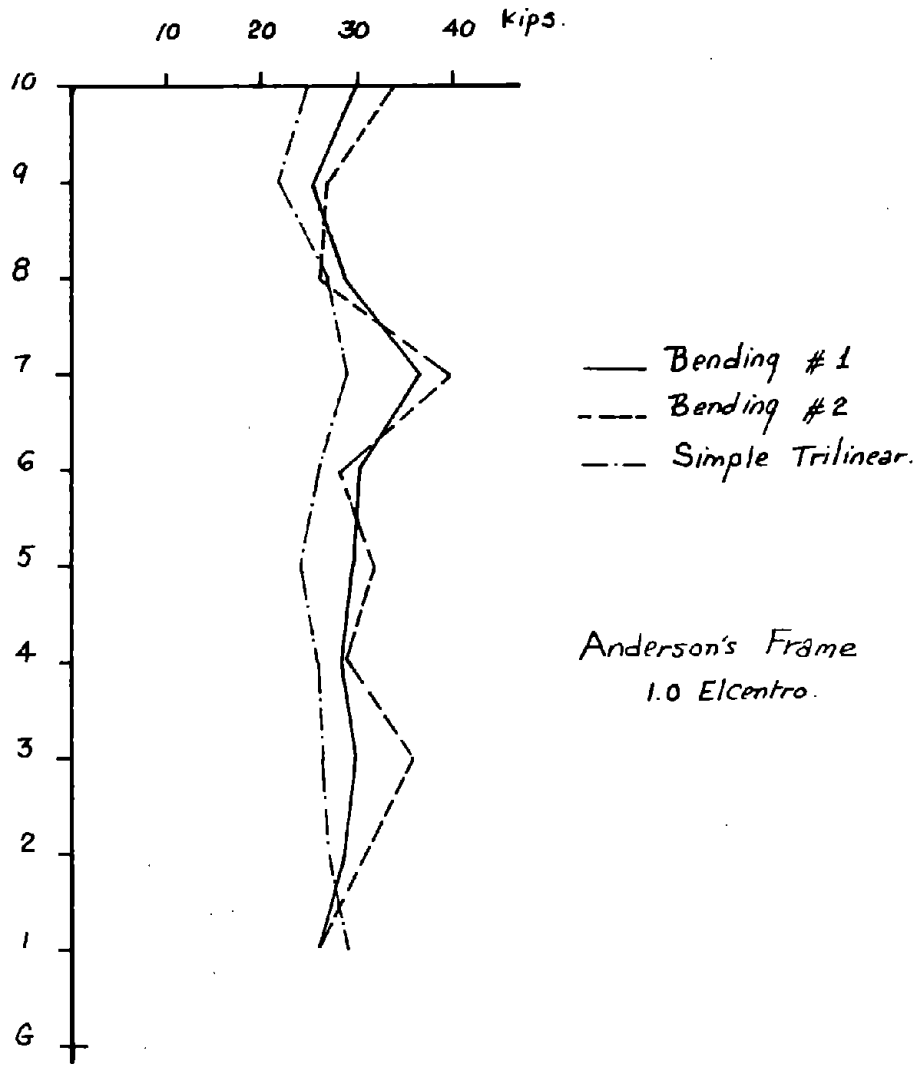

Fig 4.4 - Maximum Story Forces - Simple versus Bending

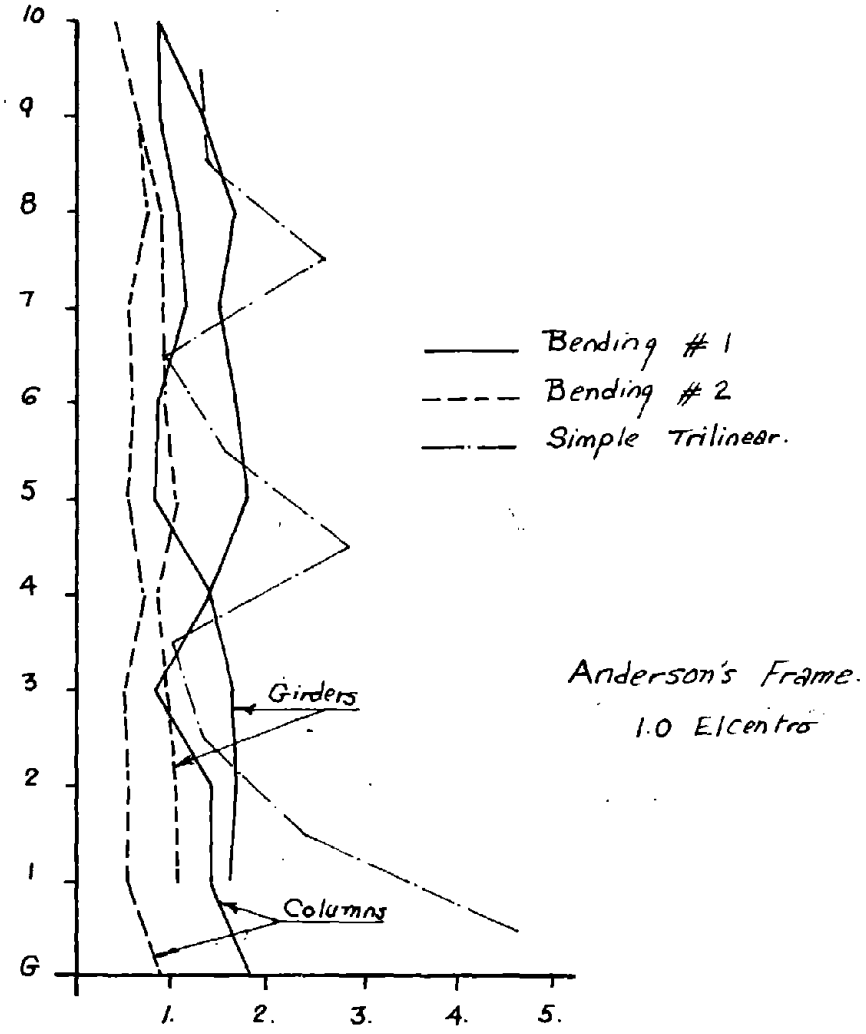

Fig. 4.5 Maximum Ductility - Simple versus Bending

Figs. 4.6 through 4.9 demonstrate the results obtained with the three models for a higher earthquake excitation. It is evident that while the two bending models become closer, the simple model moves far away from them. The simple model's ability to predict the interstory displacements at some levels is reasonably good, but it is relatively poor at other levels. Since ductility is defined differently for each model, it is very difficult to derive any conclusions from Fig. 4.9, but again the bending models seem to predict a more uniform distribution of ductilities with height.

Fig. 4.10 shows the different time histories of the roof displacements of the three previously studied models.

Table 4.1 summarizes the maximum base shears and the maximum overturning moments for the three models under the two levels of excitation. Generally speaking, one can conclude that the error introduced by the simple model as used here is of the order of 35 percent.

4.4 CASE STUDY II - KAMIL'S FRAME - 1972

The next frame studied is that designed by Kamil, 1972.[39] The frame is a 10-story 3-bay frame and has the properties and dimensions shown in Fig. 4.11. The frame has been subjected to the same two earthquake excitations discussed before, and the results are reported

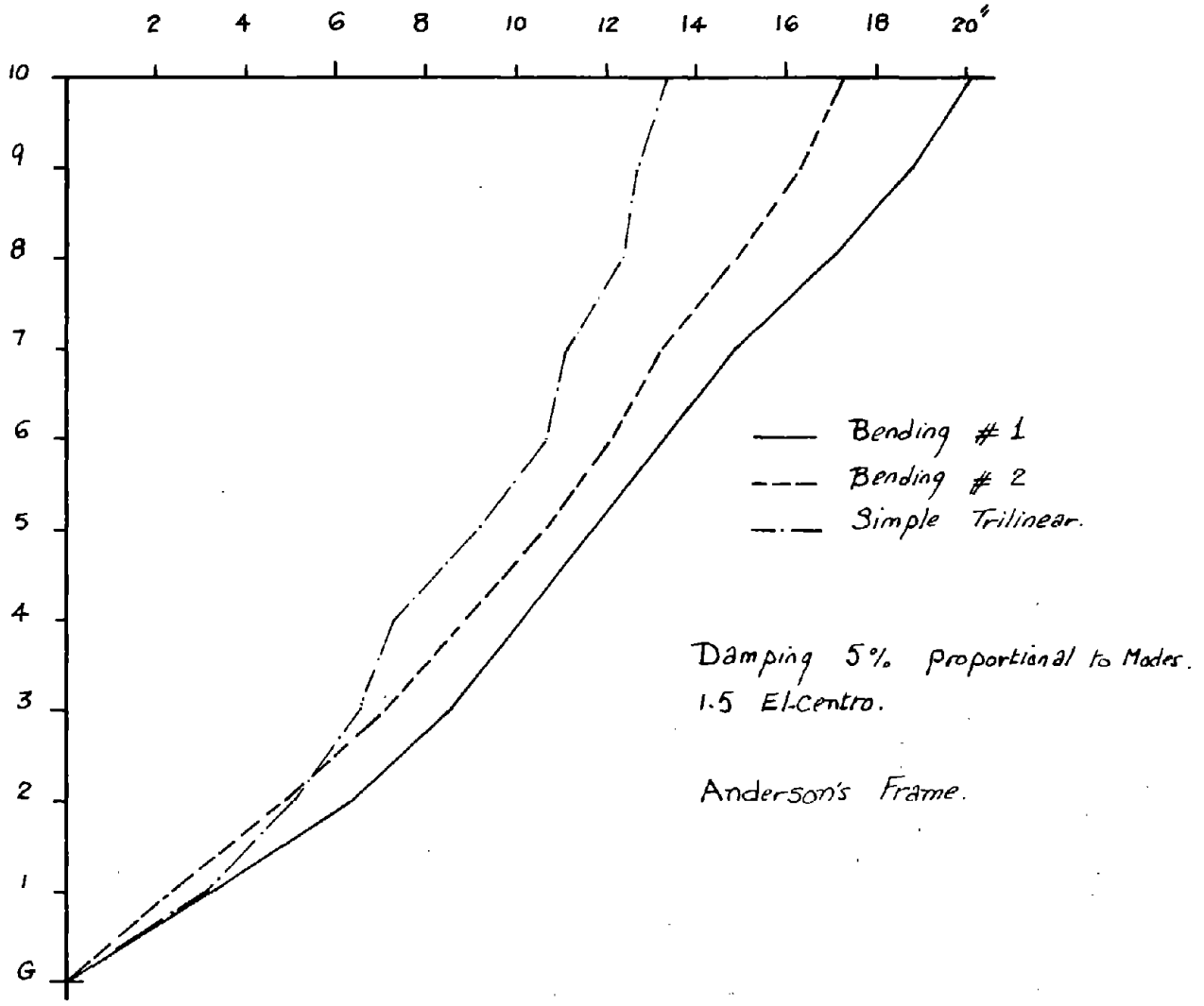

Fig 4.6 - Maximum Displacements - Simple versus Bending

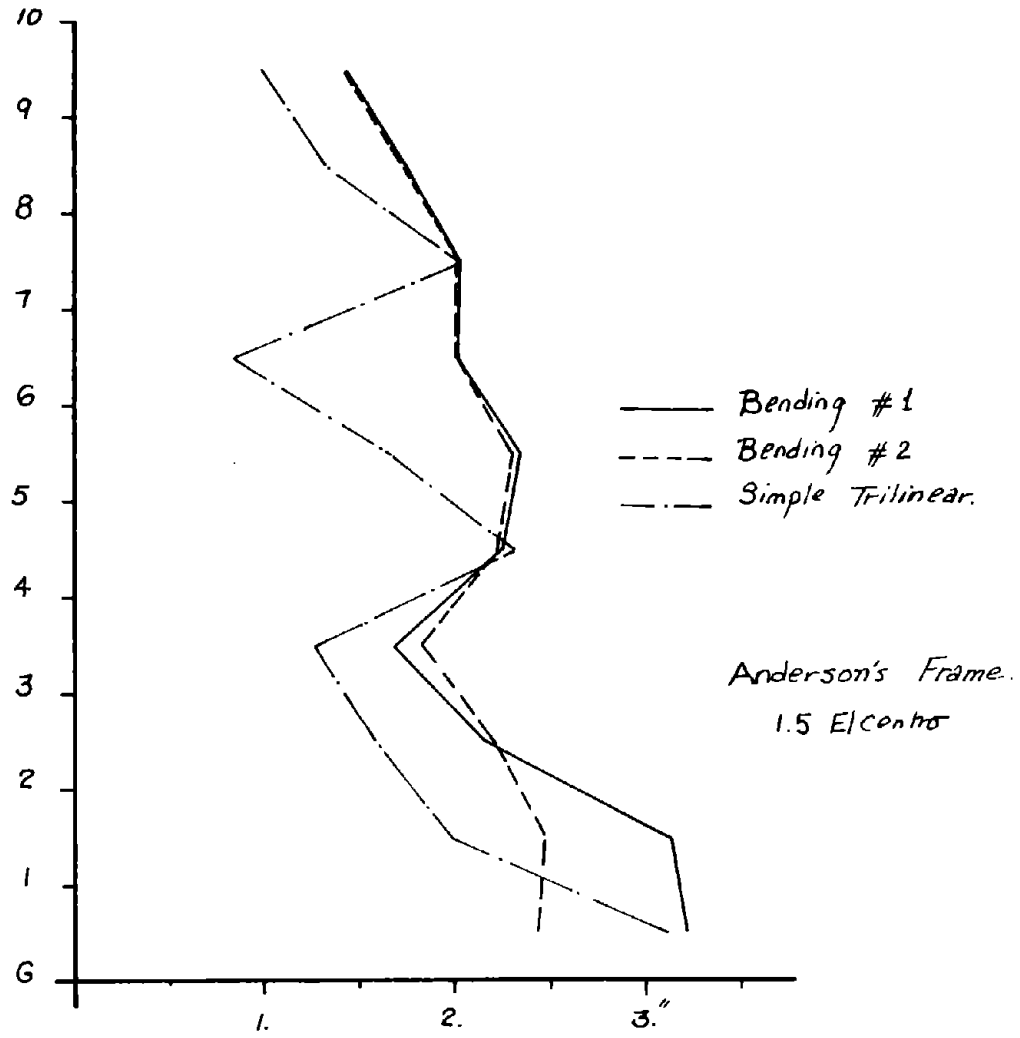

Fig. 4.7 - Maximum Interstory Displacements - Simple versus Bending

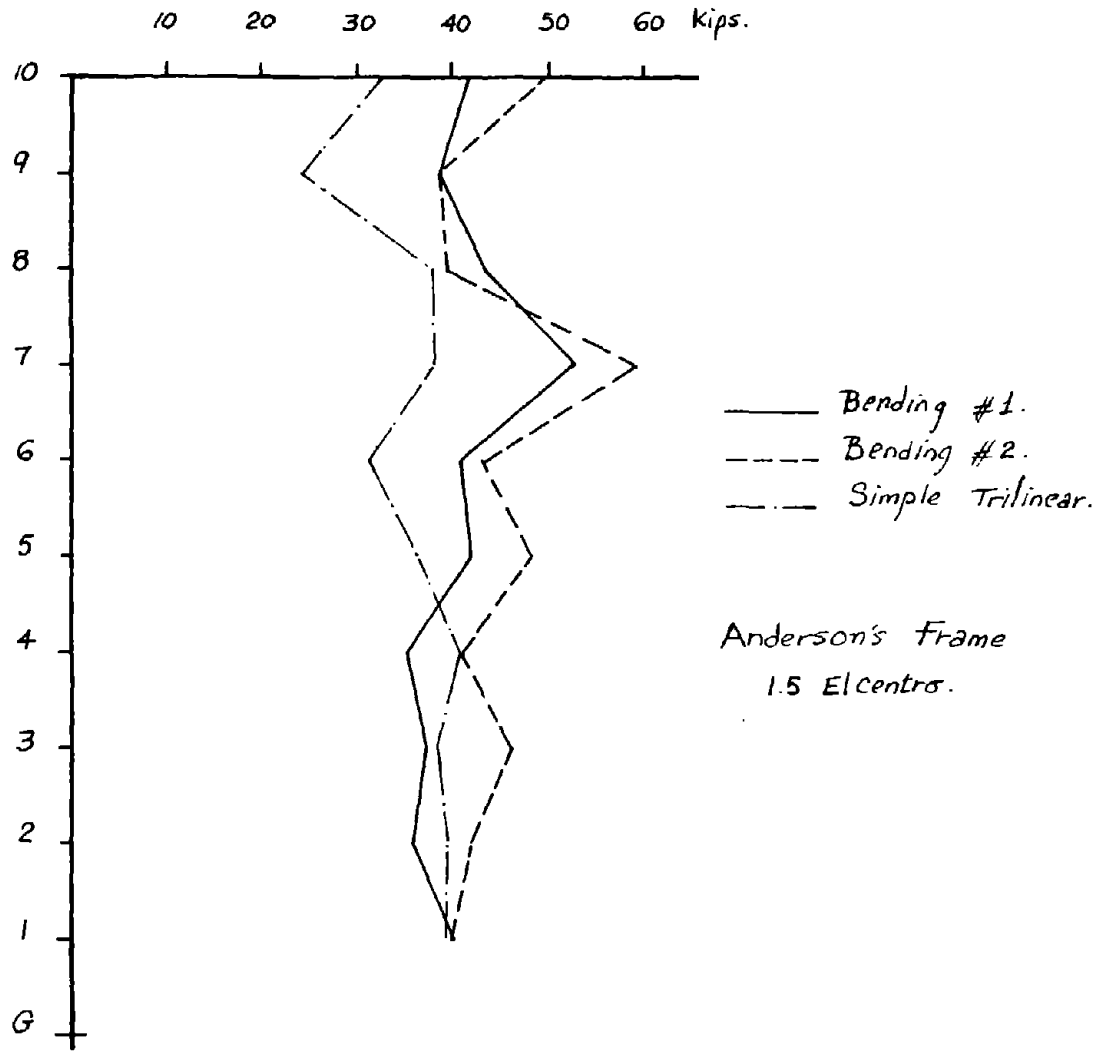

Fig. 4.8 - Maximum Story Forces - Simple versus Bending

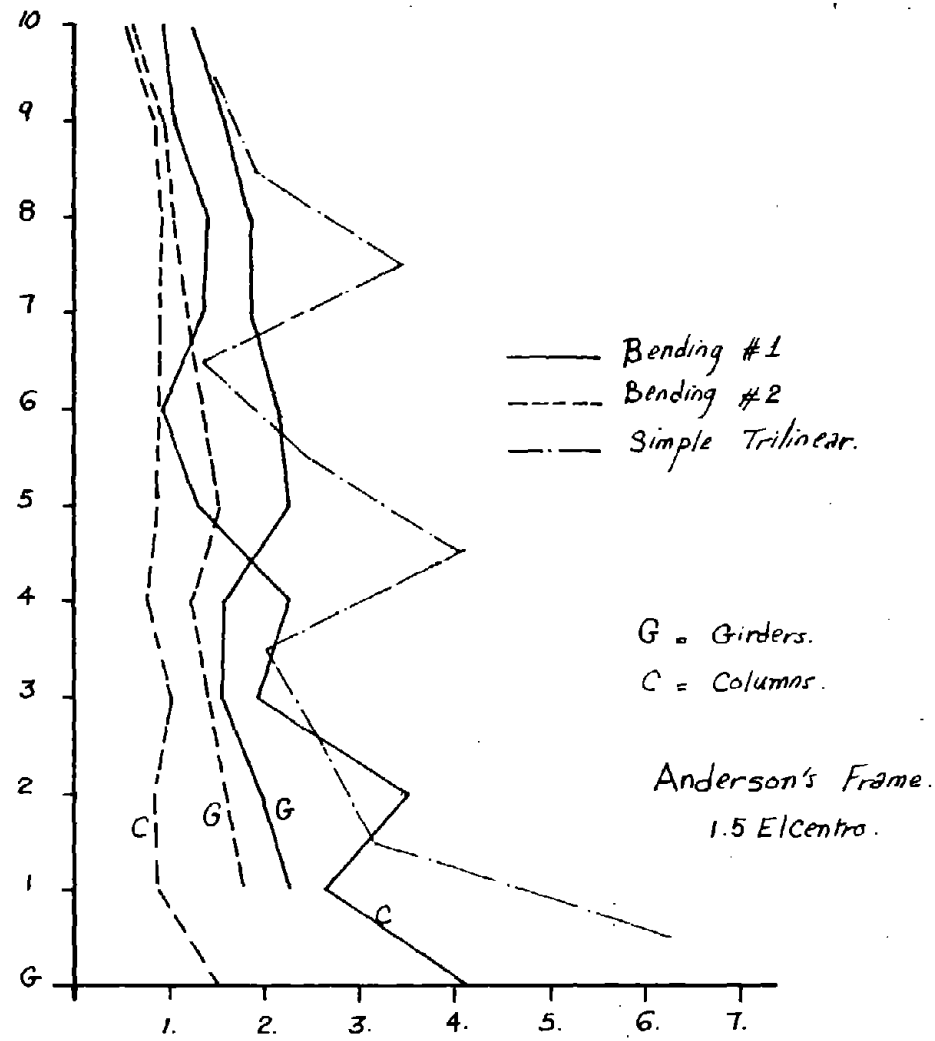

Fig. 4.9 Maximum Ductility - Simple versus Bending

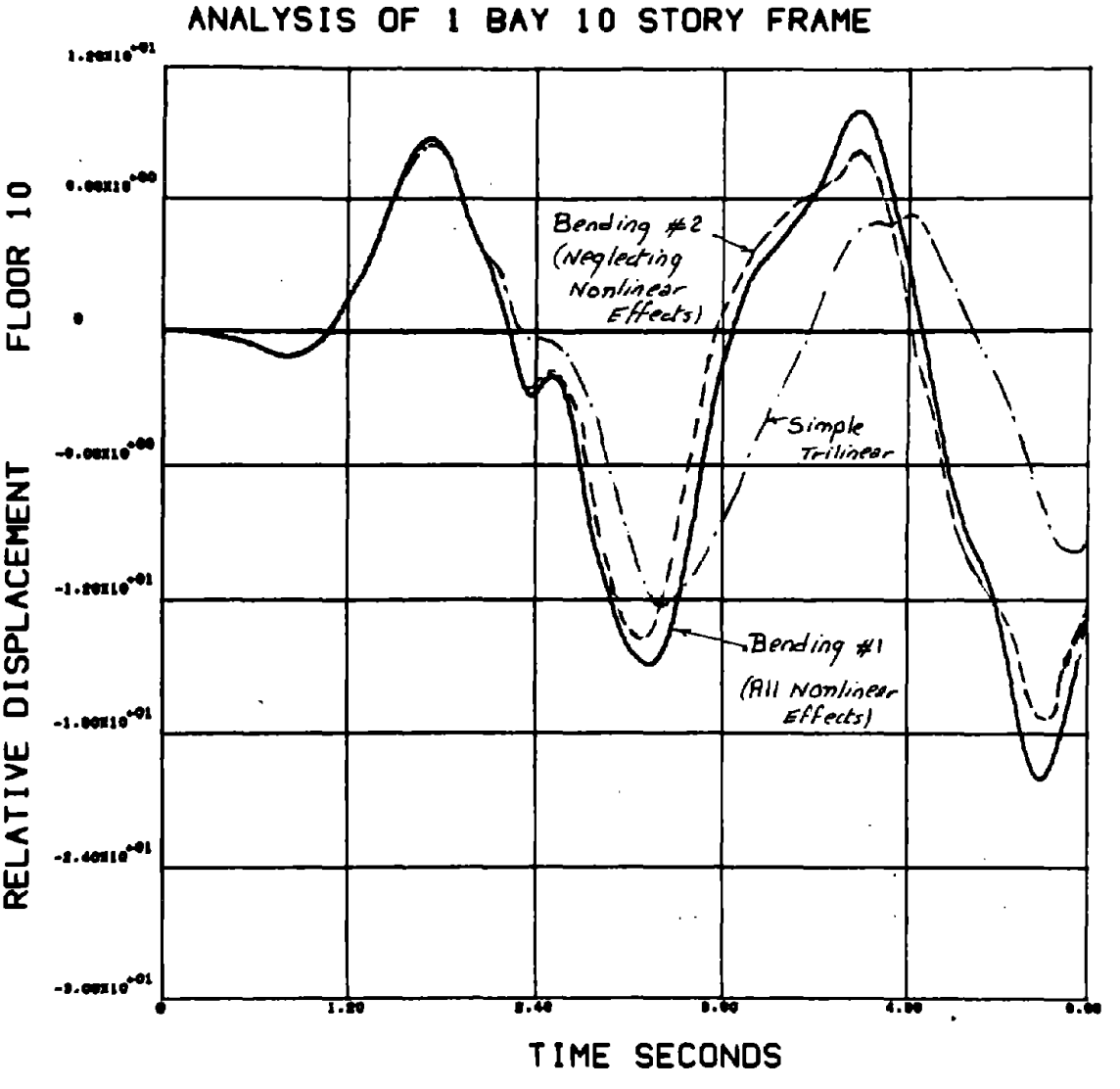

Fig. 4.10 - Comparison of Simple versus Bending Models
Anderson's Frame - 1.5 El-Centro

Table 4.1

Base Shears and Overturning Moments of Anderson's Frame

Earthquake	Model	Base Shear (kips)	% *	Overturning Moment (in.kips)	% *
1.0 EL CENTRO	Simple (Trilinear)	88.61	67.0	71154.2	64.0
	Bending (All nonlinear effects)	132.62	100.0	116878.9	100.0
	Bending (Neglecting nonlinear effects)	148.03	111.8	111401.2	101.0
1.5 EL CENTRO	Simple (Trilinear)	107.37	68.5	85780.44	63.3
	Bending (All nonlinear effects)	156.89	100.0	135821.87	100.0
	Bending (Neglecting nonlinear effects)	200.82	128.0	151544.44	111.1

* % of bending with all nonlinear effects.

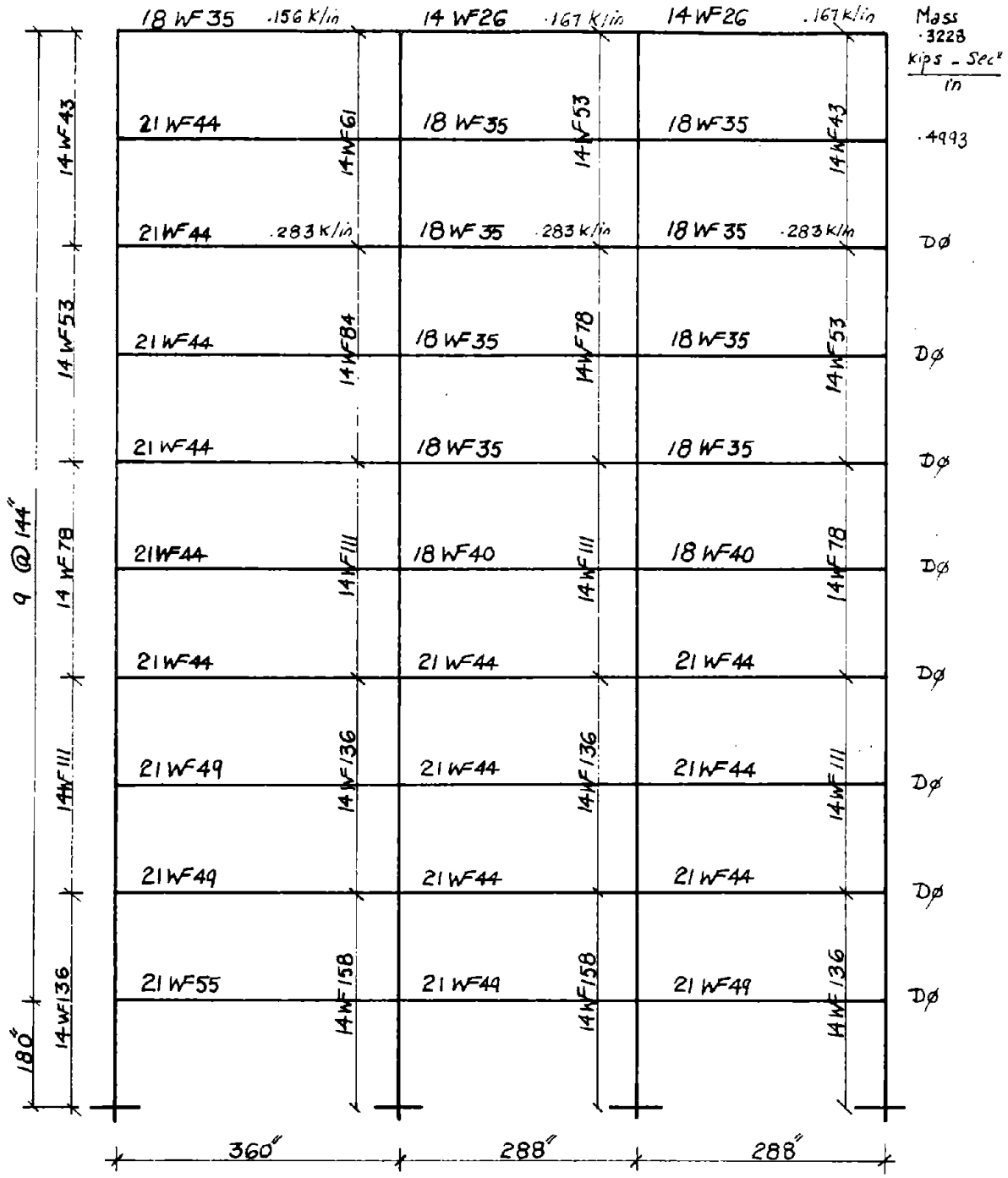

Fig. 4.11 - Kamil's Frame

in Figs. 4.12 through 4.18. From these figures the following observations can be made:

1. Under both levels of excitation the simple model tends to give reasonable results up to a certain height; then it deviates from the other two models.

2. The different nonlinear and analysis effects helped in this case to reduce the response of the frame by almost 15%. This type of behavior is observed for both El Centro and a higher excitation like 1.5 El Centro.

3. The simple model underestimates the story forces in the upper stories (Fig. 4.14) and the interstory displacements in the intermediate floors (Figs. 4.13 and 4.17). The order of the discrepancies does not seem to change much with the level of excitation.

4. The simple model predicts again a larger variation in floor ductilities along the height of the building than the variation in member ductilities resulting from the bending models. The largest ductility from the simple model occurs again at the bottom story. When comparing the actual ductility values one should still keep in mind that ductilities are defined in different ways for both models.

5. The simple model predicts again base shears and overturning moments of the order of 60% - 70% of the exact values. Table 4.2 summarizes the different base shears and overturning moments for different models and is self-explanatory.

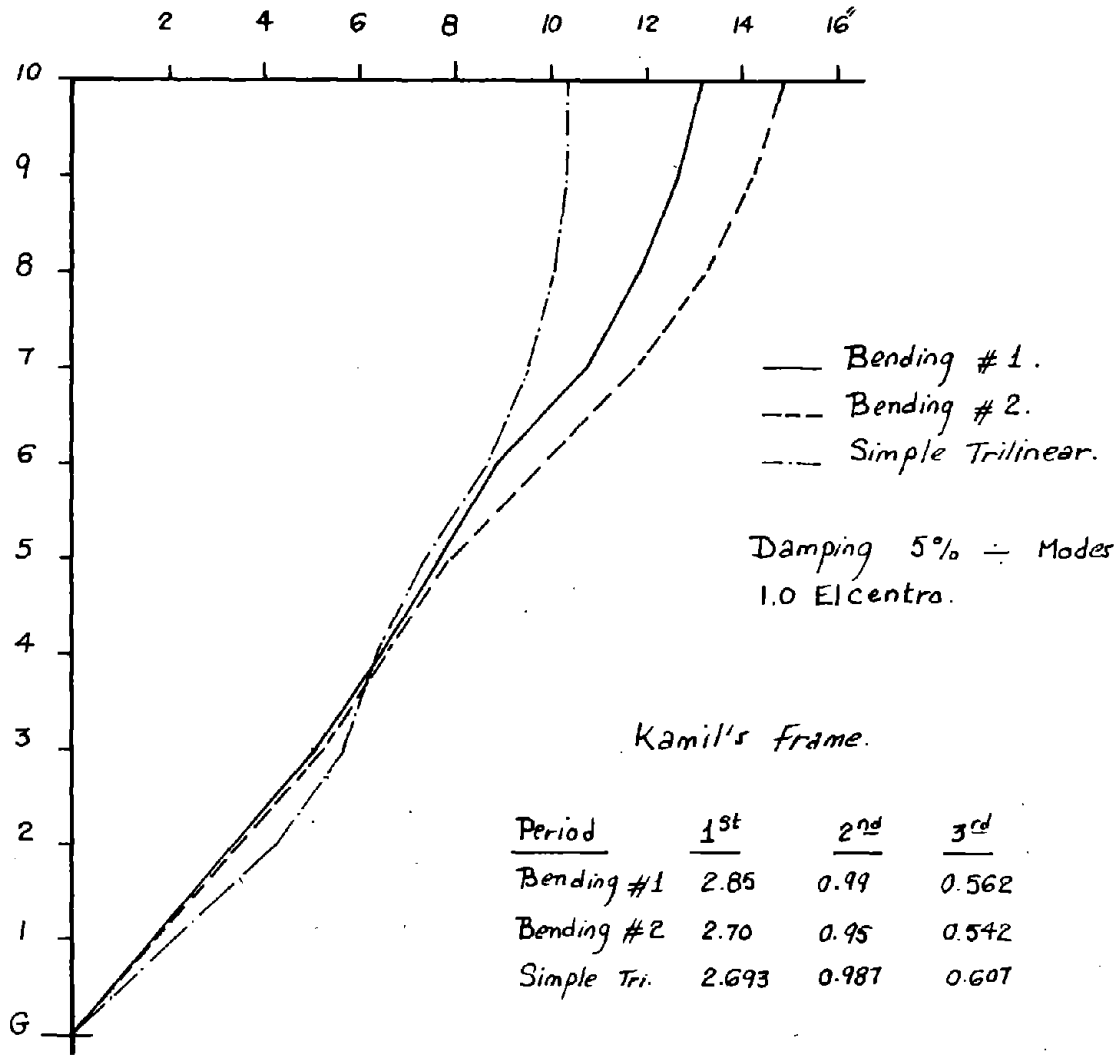

Fig. 4.12 - Maximum Displacements

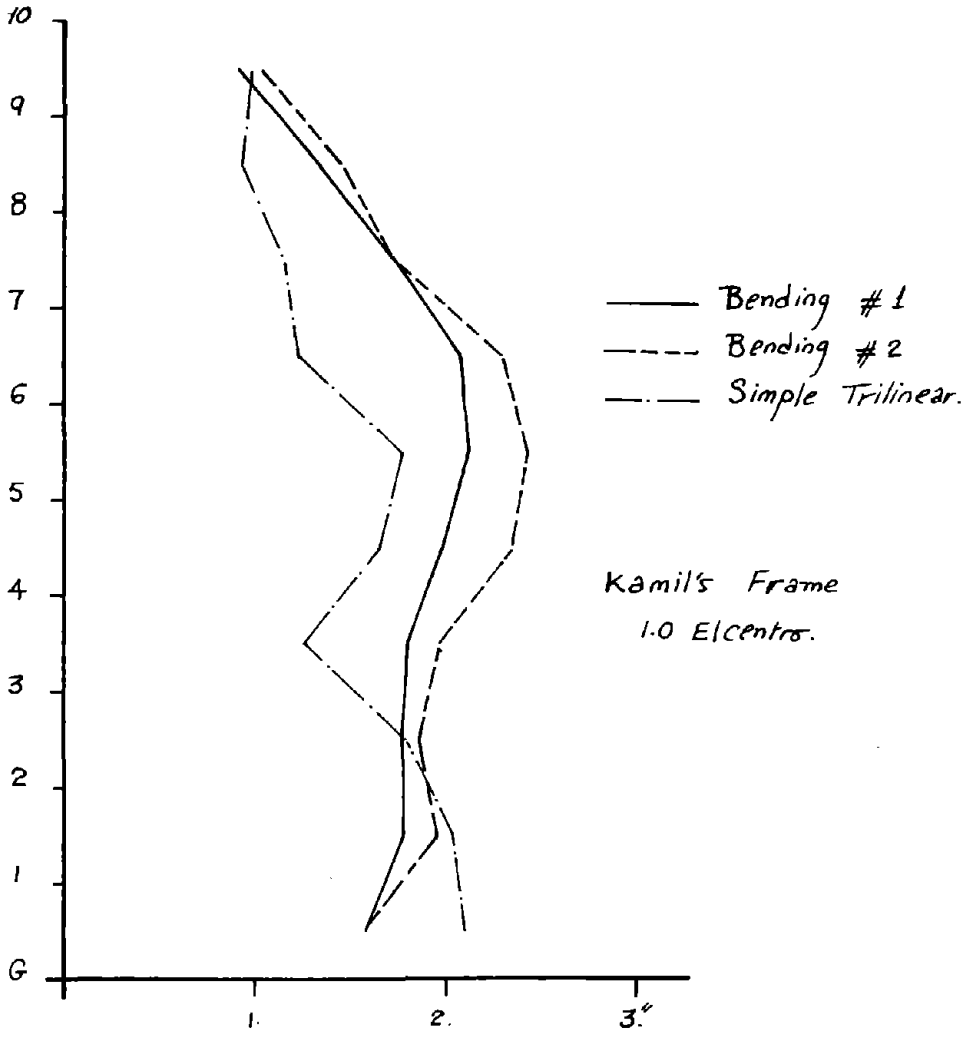

Fig. 4.13 - Maximum Interstory Displacements

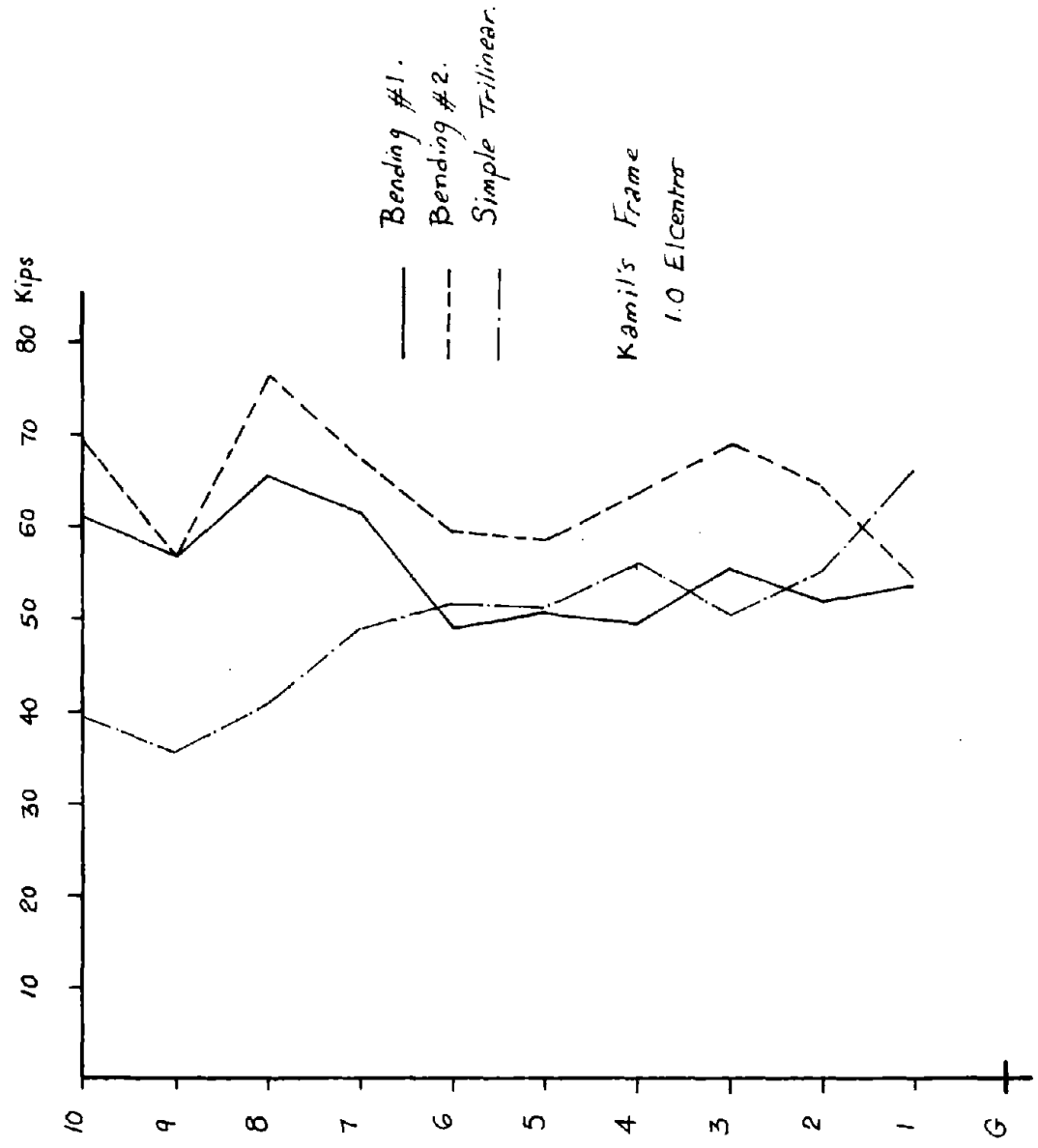

Fig.4 .14 - Maximum Story Forces

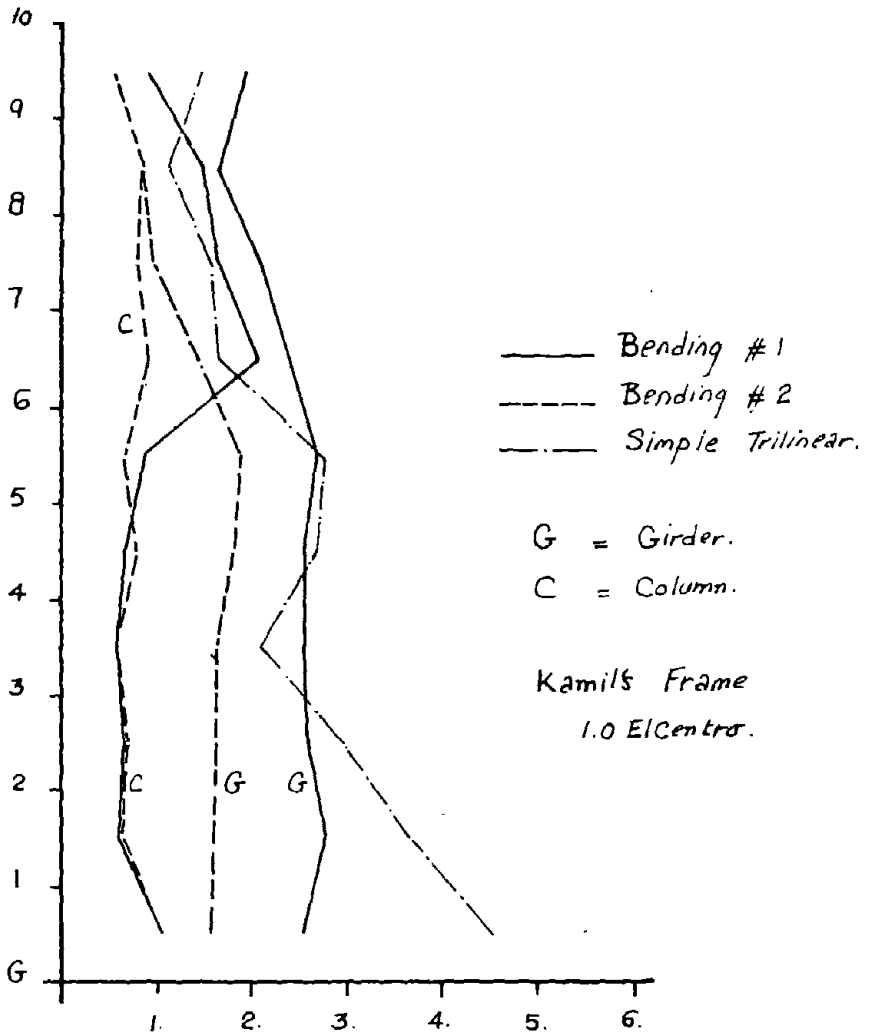

Fig. 4.15 - Maximum Ductility

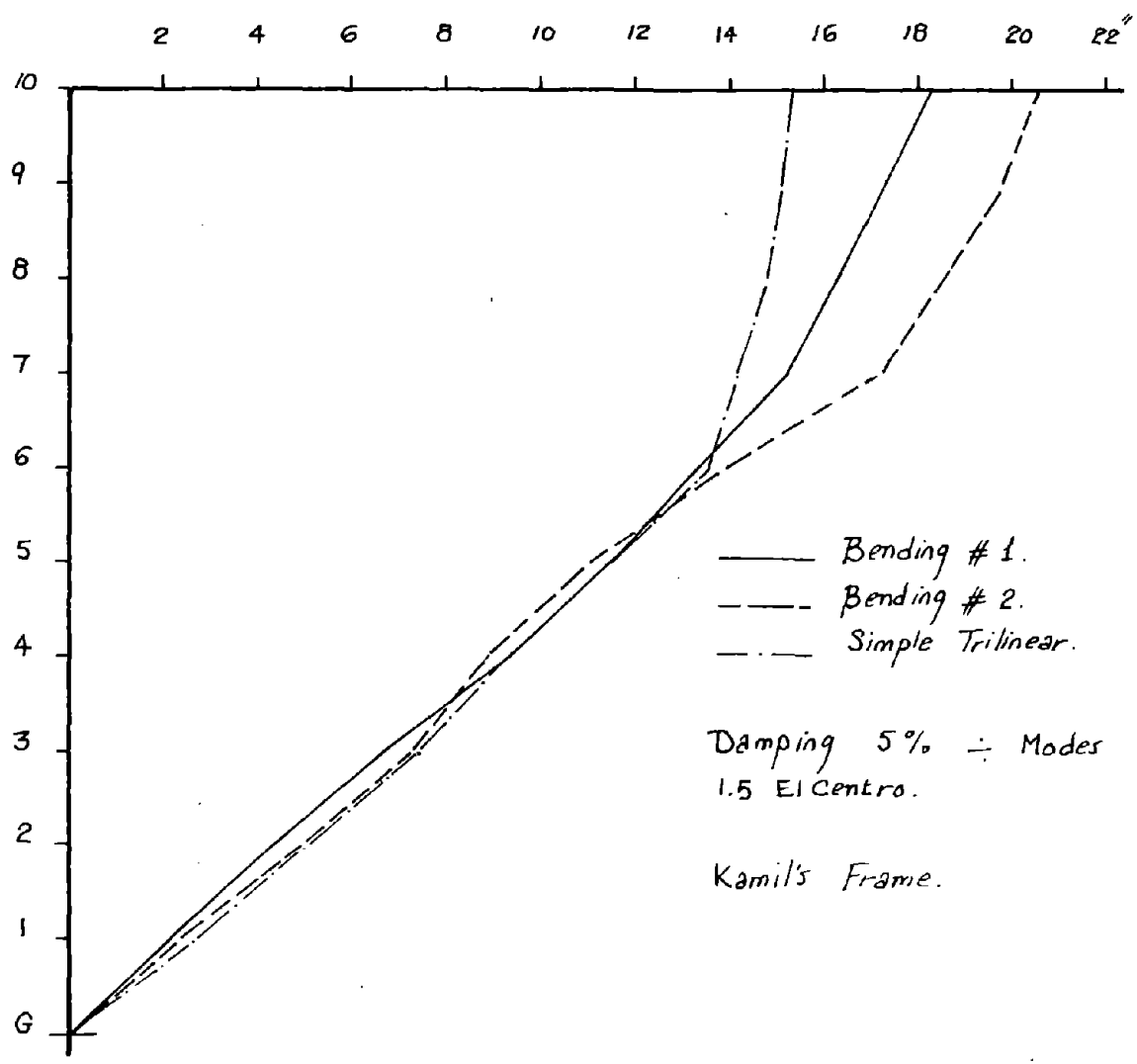

Fig. 4.16 - Maximum Story Displacements

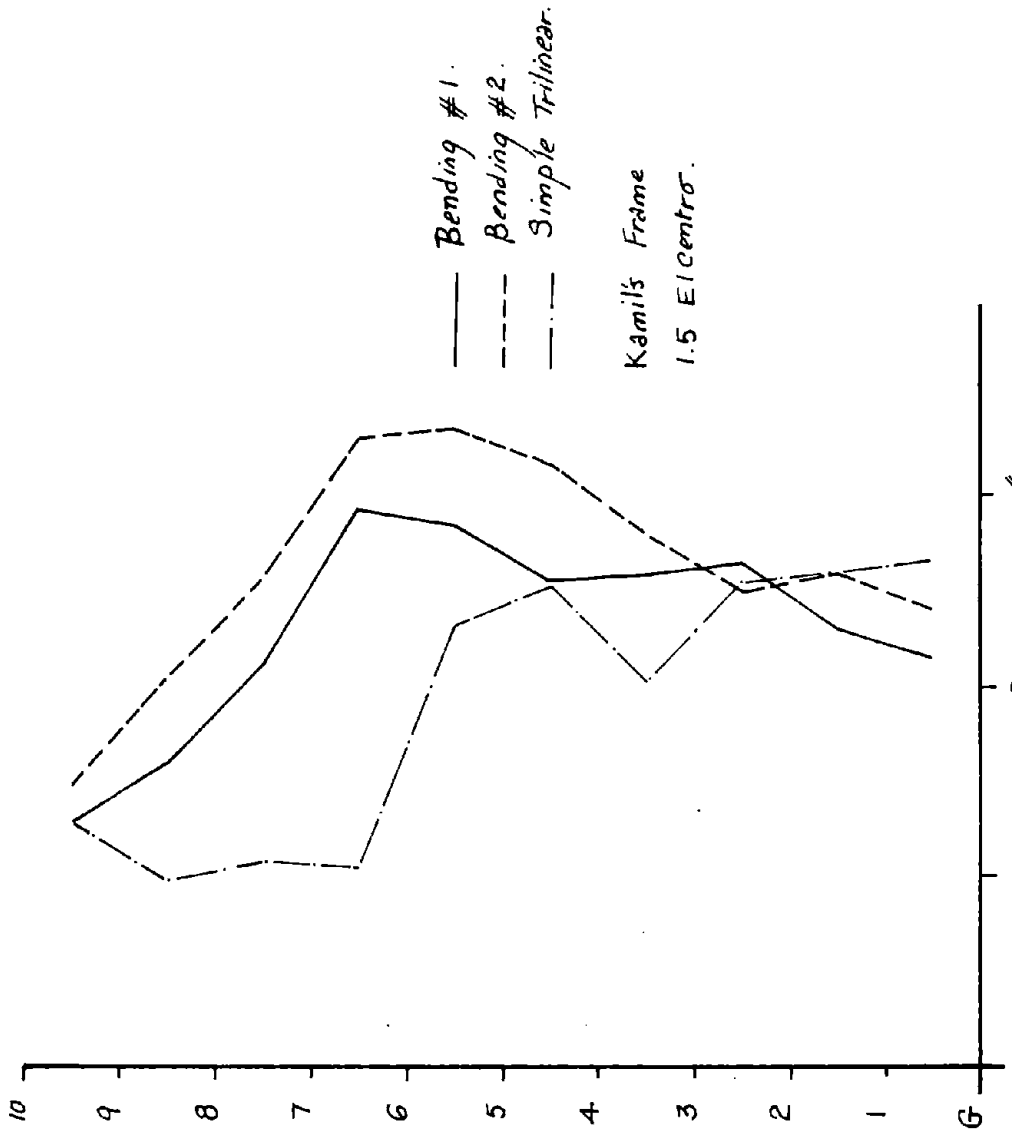

Fig. 4.17 - Maximum Interstory Displacements

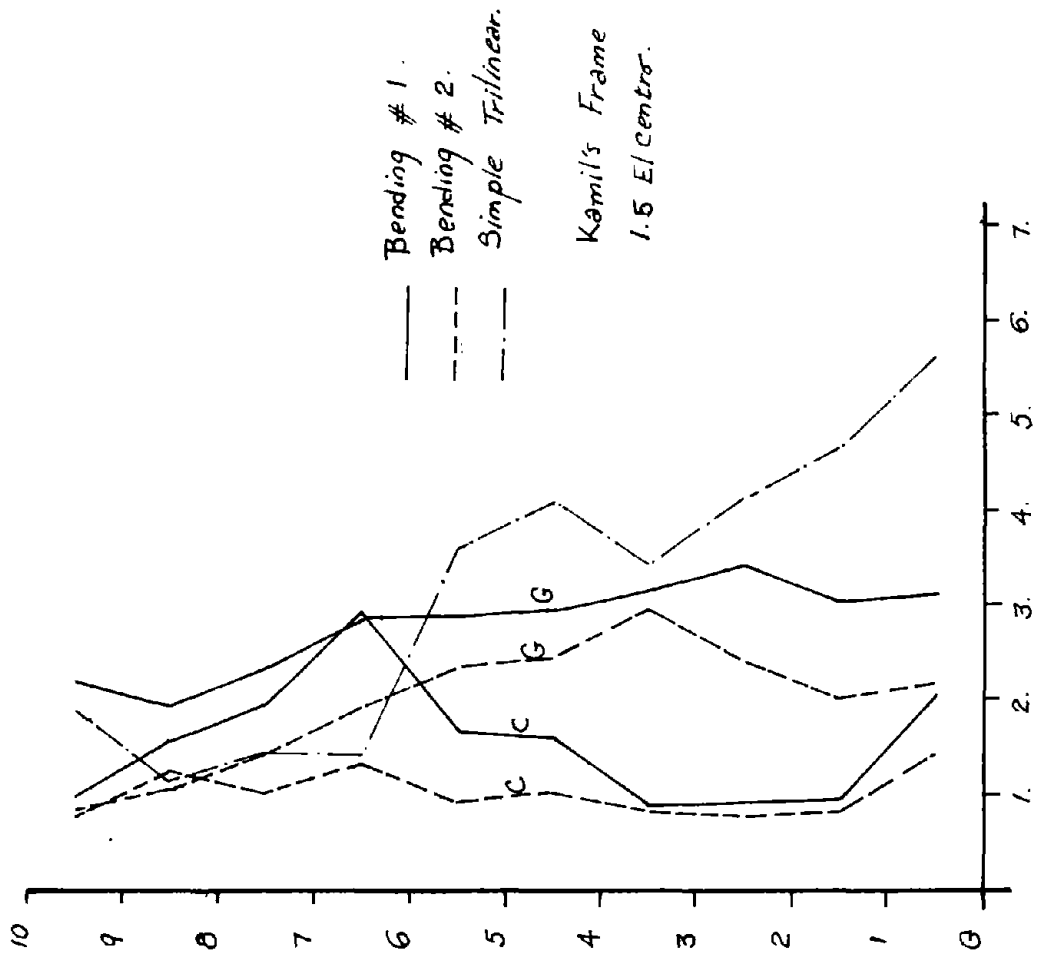

Fig. 4.18 - Maximum Ductility

Table 4.2

Base Shears and Overturning Moments of Kamil's Frame

Earthquake	Model	Base Shear		Overturning Moment	
		kips	%*	in.kips	%
1.0 EL CENTRO	Simple (Trilinear)	130.18	64.	112744.9	73.
	Bending (All nonlinear effects)	202.99	100.	154232.5	100.
	Bending (Neglecting all nonlinear effects	285.36	140..	189768.75	123.
1.5 EL CENTRO	Simple (Trilinear)	151.76	65.6	124378.00	72.
	Bending (All nonlinear effects)	230.96	100.	173127.87	100.
	Bending (Neglecting all nonlinear effects)	322.69	140.	229775.87	132.2

* % of bending with all nonlinear effects.

4.5 CASE STUDY III - GOEL'S FRAME - 1973

Another frame available in the literature, designed by Goel in 1973, was studied using the three different models. The geometry and the properties of the frame are shown in Fig. 4.19. The frame has 10 stories and is one-bay-wide. The frame has been subjected to the same two levels of excitations used in the previous cases. Figs. 4.20 through Fig. 4.27 show the results from the three models; the following observations can be made.

1. The simple and the bending models predict similar results up to a certain height, then they start to deviate.

2. The simple model underestimates, however, the displacement of the upper stories, since it is not capable of reproducing a bending-type behavior caused by axial deformation of the columns.

3. The average ductilities predicted by the simple model tend again to vary along the height in a more pronounced way than the member ductilities predicted by the bending model.

4. The simple model predicts base shears which are roughly 50% lower than the correct values, and it predicts also overturning moments which are 60% - 80% of the correct values.

Table 4.3 summarizes the base shears and the overturning moments obtained by the different models.

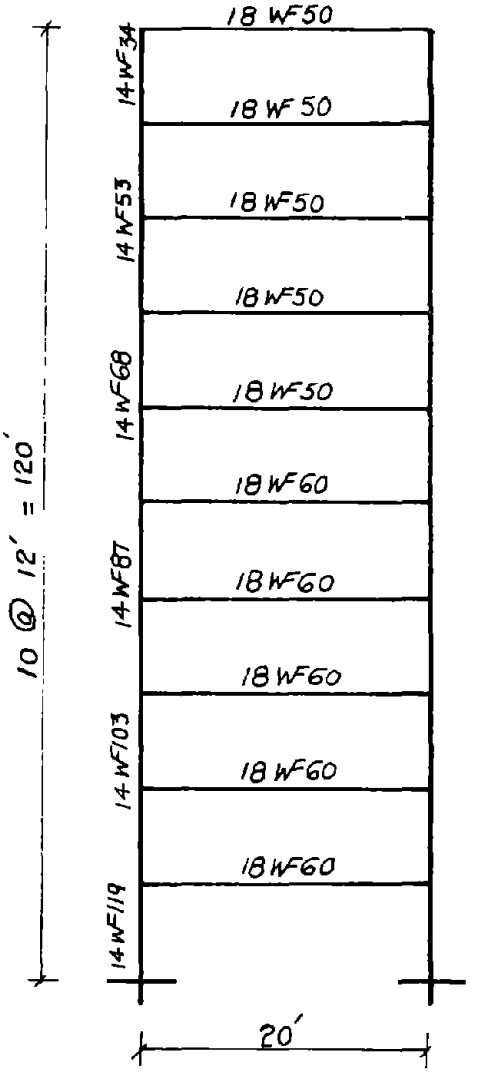

Mass per floor = 0.1144
D.L " " = 44.k
L.L per floor = 32.k.

Fig. 4.19 Goel's Frame

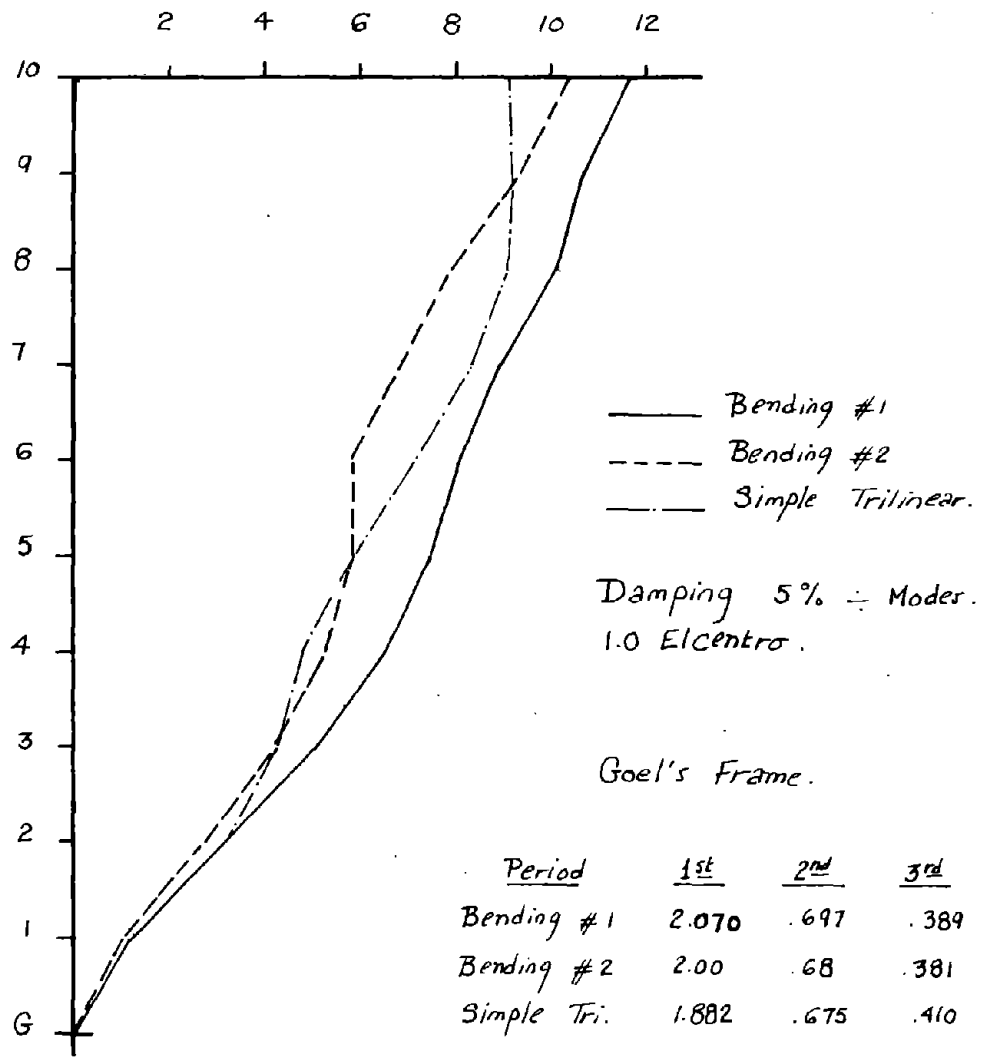

Fig. 4.20 - Maximum Story Displacements

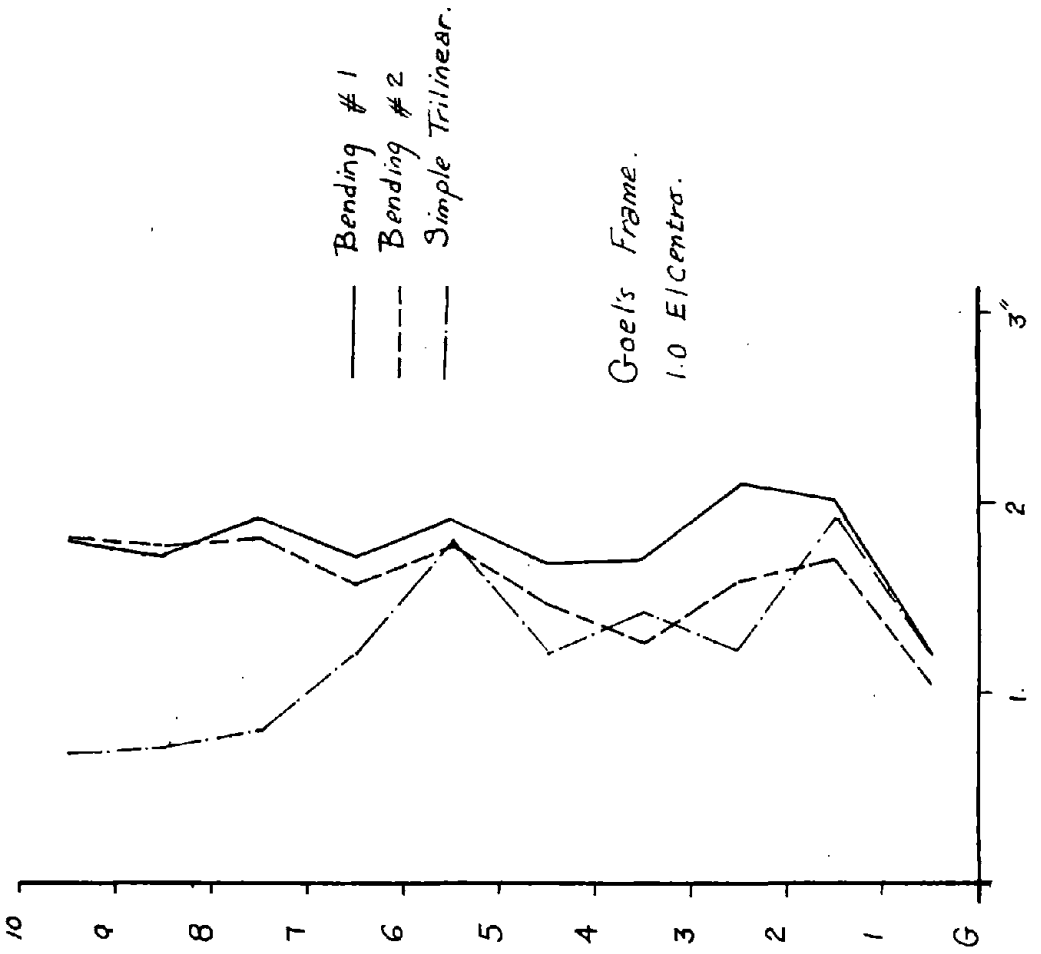

Fig. 4.21 - Maximum Interstory Displacements

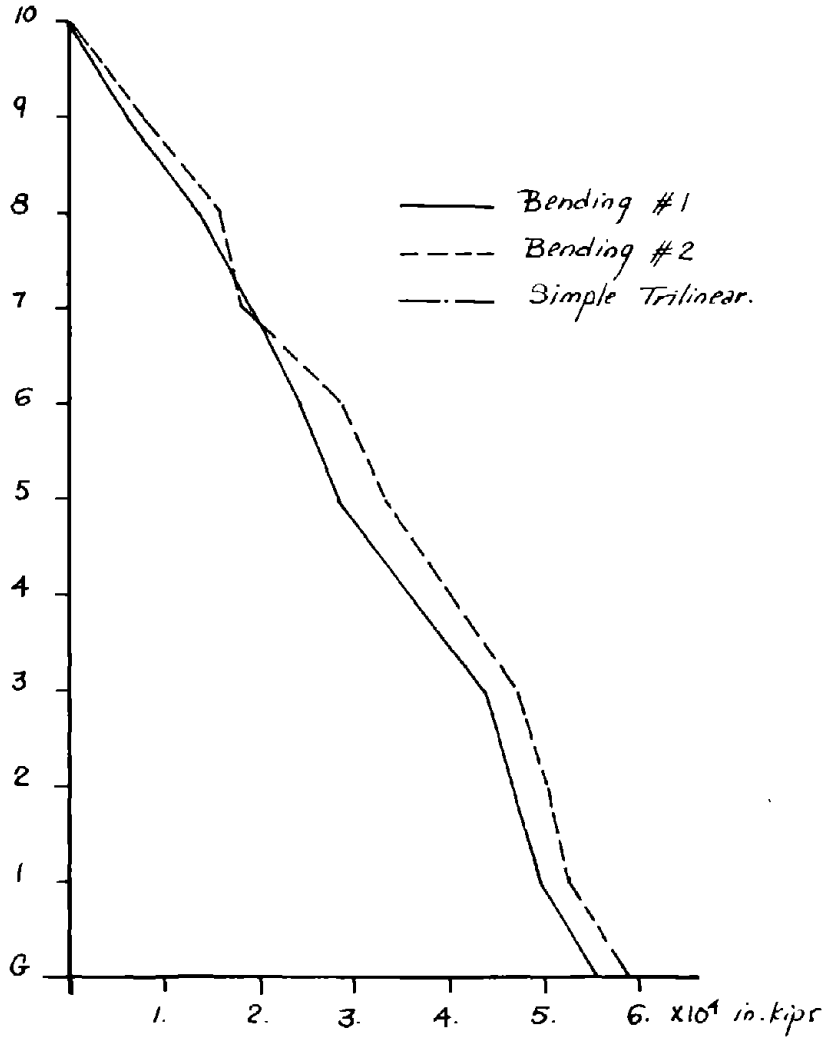

Fig. 4.22 - Maximum Overturning Moments

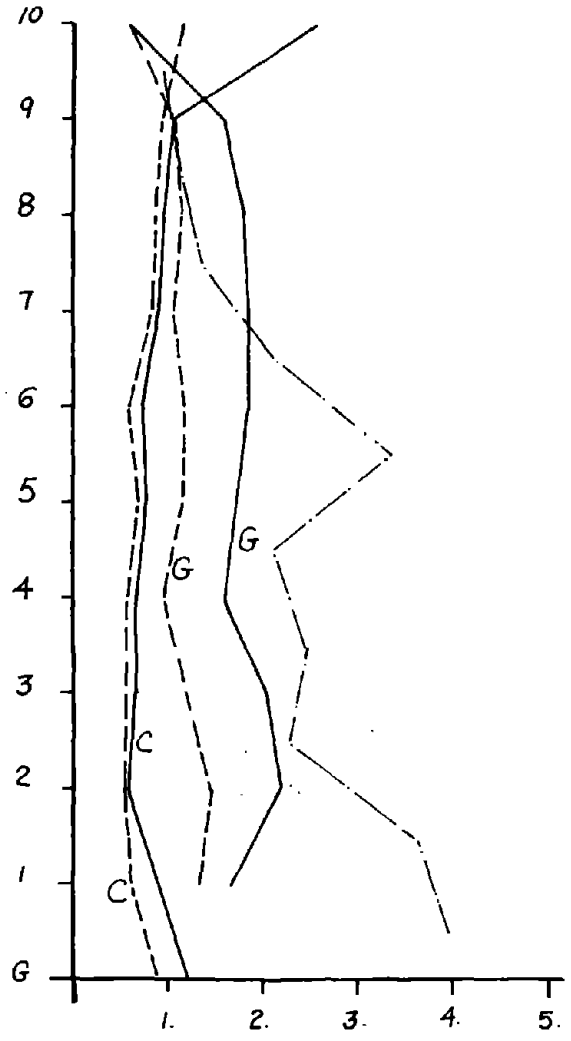

Fig. 4.23 - Maximum Ductility

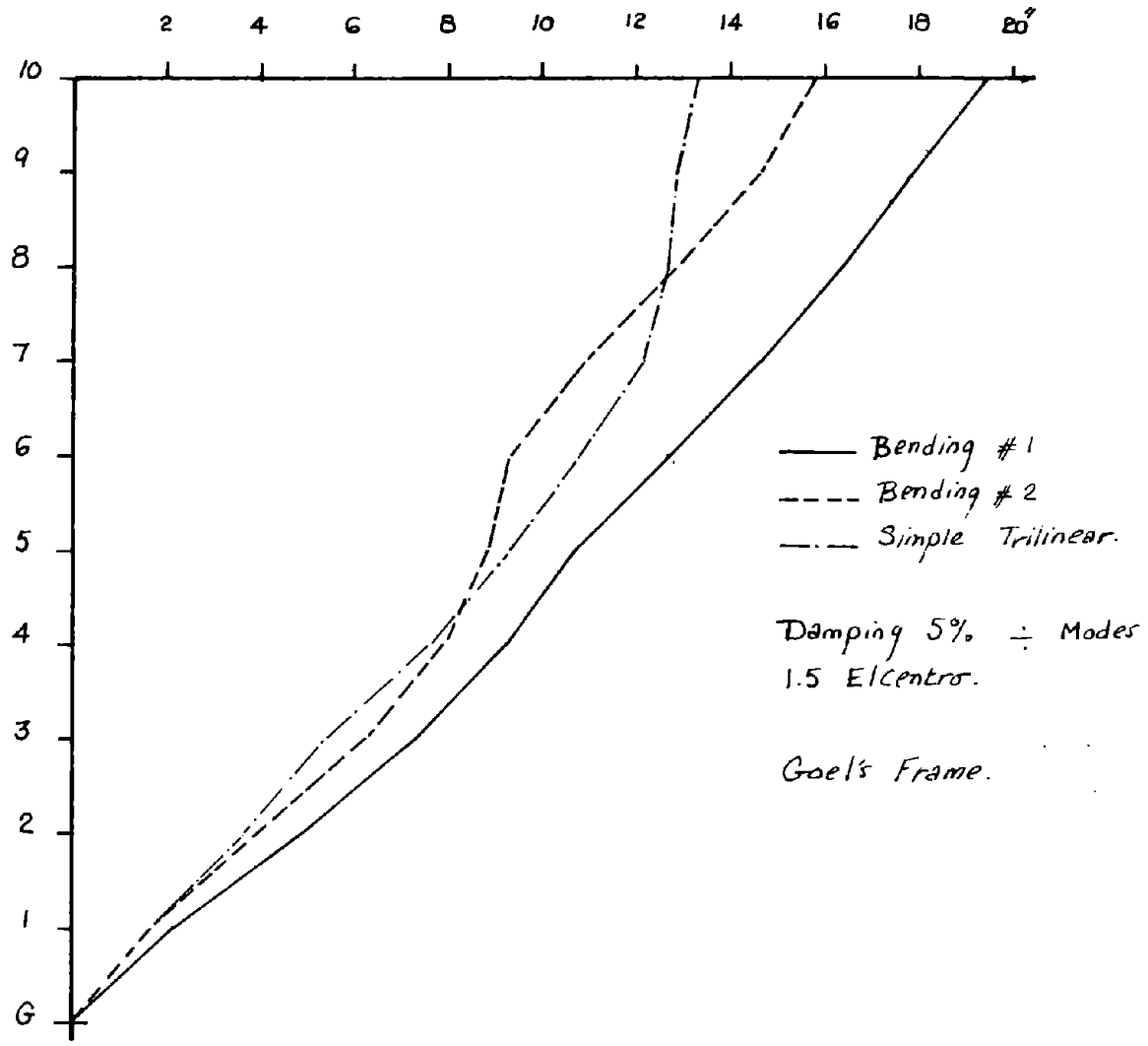

Fig. 4.24 - Maximum Displacements

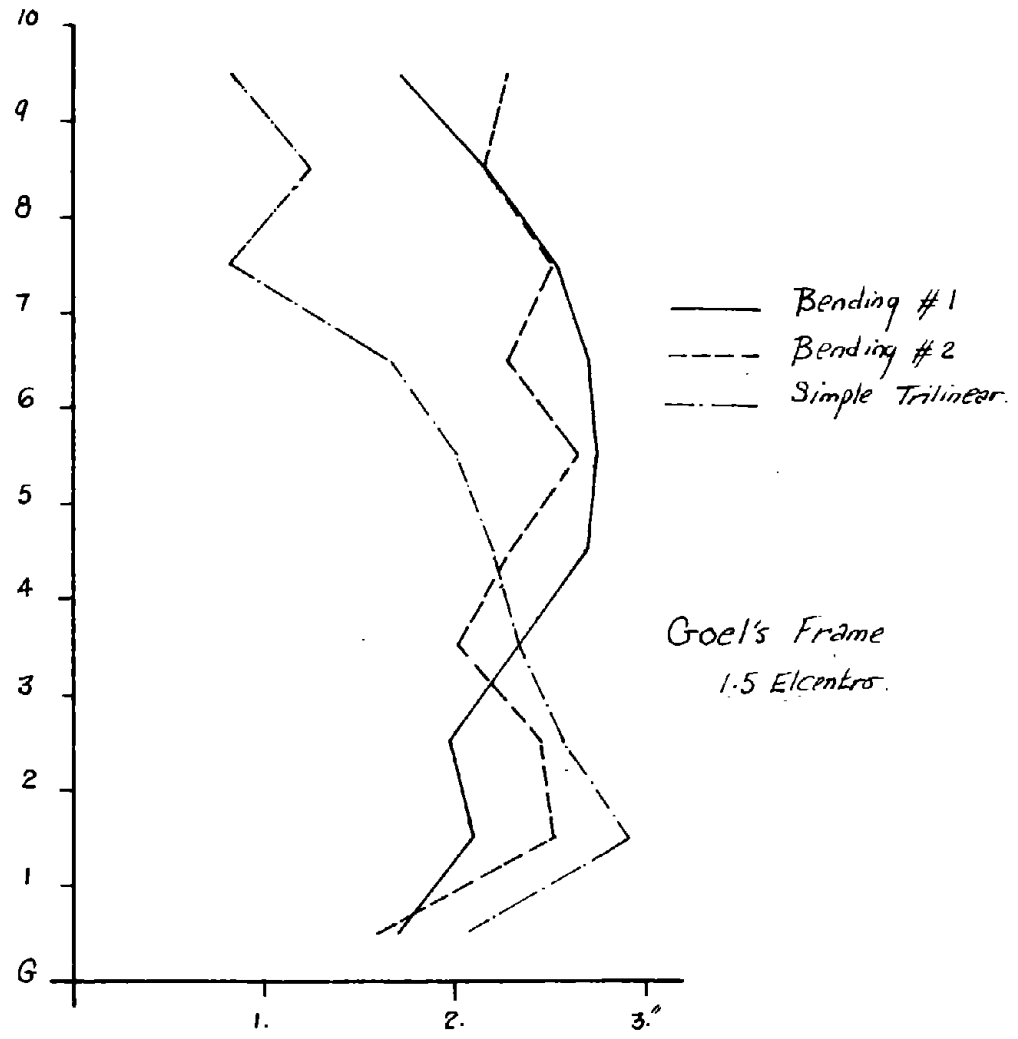

Fig. 4.25 - Maximum Intersory Displacements

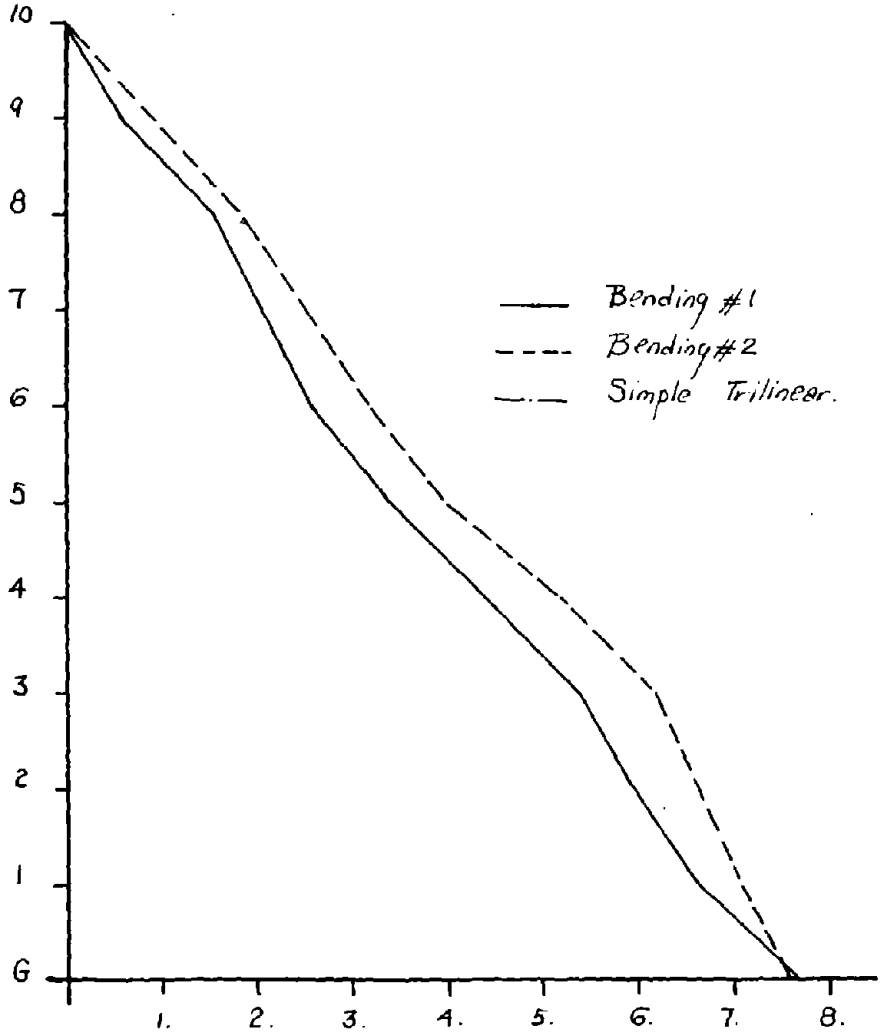

Fig. 4.26 - Maximum Overturning Moments

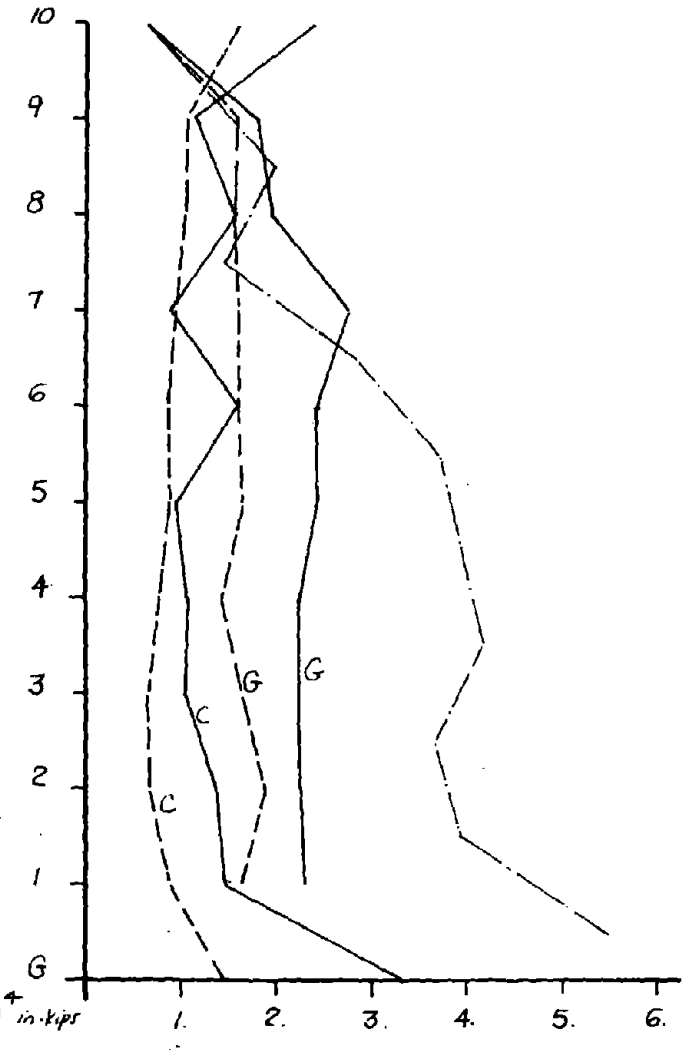

Fig. 4.27 - Maximum Ductility

Table 4.3

Base Shears and Overturning Moments of Goel's Frame

Earthquake	Model	Base Shear kips	Base Shear % *	Overturning Moment in.kips	Overturning Moment % *
1.0 EL CENTRO	Simple (Trilinear)	49.08	41.7	43153.15	77
	Bending (All nonlinear effects)	117.71	100..	56076.79	100.
	Bending (Neglecting all nonlinear effects)	118.57	101.	59739.86	106.4
1.5 EL CENTRO	Simple (Trilinear)	58.27	42.6	46662.43	60.5
	Bending (All nonlinear effects)	136.60	100.	77082.50	100.
	Bending (Neglecting all nonlinear effects)	161.56	118.	76039.75	99.

* % of bending with all nonlinear effects.

4.6 CLOSING REMARKS

In this Chapter an attempt has been made to evaluate the ability of simple models to predict the behavior of a building frame. Results of the simple model were compared with those obtained from the most realistic bending model which accounts for all the nonlinear effects and with those provided by a simplified bending model which does not account for some nonlinear effects. The results of the study indicate that the simple model as used may predict the correct behavior up to a certain level. Its ability to predict the behavior of the upper stories is impaired when overall bending due to axial deformation of the columns is important. The study demonstrated also that the nonlinear effects might be sometimes favorable, while in other cases they are unfavorable. Conceptually it may be possible to find properties for simple models which lead to a final response which matches better the correct ones. It is necessary, however, to do more work in order to find simple rules to derive the spring parameters for each story. Of particular significance is the fact that ductilities as predicted by the bending model seem to be much more uniform than the corresponding quantities resulting from the simple model.

CHAPTER V

INELASTIC ANALYSIS VIA A COUPLED NONLINEAR MODEL

5.1 GENERAL

By describing the equilibrium and compatibility equations in incremental form and combining these with the incremental constitutive equations, a unified solution procedure can be formulated for problems with combined geometric and material nonlinearities. This solution procedure is recognized as the "Finite Deflection Theory" of structural analysis.

In this Chapter the objective is to develop and present different complex analytical models which are capable of performing a "theoretically exact" nonlinear analysis under a static or dynamic loading. The words "theoretically exact" are used here to indicate the fact that an exact model is still subject to numerical errors.

These models are theoretically a refinement over all the models presented before. In particular they are able to take into consideration the following points:

1. The fact that inelastic deformations are spread over part of the member and are not localized at a section.

2. The coupling of axial and bending effects when a section yields.

3. The fact that under different loads the member might suffer from both local and global inelastic stability.

From the numerical point of view, two different approaches can be followed in the solution of any model.

The first approach is a tangent incremental solution which introduces small errors at each step, since equilibrium may not be perfectly satisfied. Special attention must be paid to avoid excessive propagation of these errors.

The second approach is a secant formulation which is usually expensive but allows through iteration the guarantee that equilibrium is satisfied.

In both approaches the results are stepped through either the time domain or the load domain. In the tangent-type models, piecewise linearization of the properties is used. In the secant-type models, iteration is used to arrive at the correct secant.

Generally speaking, the models can be divided into different levels: fiber models, section models, member models, story models, and frame level models.

Fiber models at one end of the spectrum are attractive from the theoretical point of view, while story models on the other end of the spectrum are attractive from the practical point of view for their economical features.

From the theoretical point of view it is not easy to compare two models of two different families. For example, it is hard to find a section model which matches exactly a fiber one, since the properties for both are specified differently. This becomes clear when one

tries to determine a strain-hardening factor to use in an analysis. In the presence of nonlinear effects, a small value of strain hardening becomes a crucial problem, since the presence of any small strain hardening might prevent the dynamic collapse of the model completely, while its absence, combined with a certain type of ground motion, might lead to a free body motion.

However, from the practical point of view one expects that some parameters can be reasonably chosen to arrive at comparable models.

5.2 COMPARATIVE STUDIES FOR FIBER MODELS VERSUS GENERALIZED BENDING MODELS.

In the fiber model one starts by specifying the stress-strain curve of the material from which one can obtain the inelastic stiffness coefficients as presented in Ref. 40, and consequently the stiffness of an inelastic member. Appendix "A" gives the expressions for the stiffness of a member obtained by integrating the inelastic stiffness coefficients. Whatever integration scheme is used, there is usually a numerical error involved in the analysis. The error is dependent on the increment size used to step the model through the load or the time domain, and also on the shape of the stress-strain diagram. For well-defined yield materials the errors might accumulate and lead to fictitious results.

In this Section, comparison is made between the GSCM models studied in previous chapters and complex models at the fiber level.

Four different models were used to evaluate the response of the one-bay three-story frame shown in Fig. 5.1. This frame has been previously used by Latona[40]. The frame might not represent a typical three-story building in seismic intensity 3; but it suits the purpose of the current analyses. The properties of the different models and their nature are defined as follows.

Model A - Interaction Model

In this model the effect of interaction is taken by the AISC formula, while stability is introduced by the stability functions. Initial axial forces are assumed in the columns as shown in Fig. 5.1. A strain-hardening factor of 0.001% is used in the analysis, with a damping value of 0.0%.

Model B - Pure Bending

In this model the interaction, initial axial forces, and stability effects are neglected. The other properties are identical to model A.

Model C - Seven Fiber Model

In this model the members are segmented into fibers. Seven fibers are used to simulate each section, and sections are taken along the member. The strain-hardening factor at the fiber level is taken as 0.00001 (simulating an almost elasto-plastic material). Initial axial forces and the stability effects are considered and properly accounted for in this model.

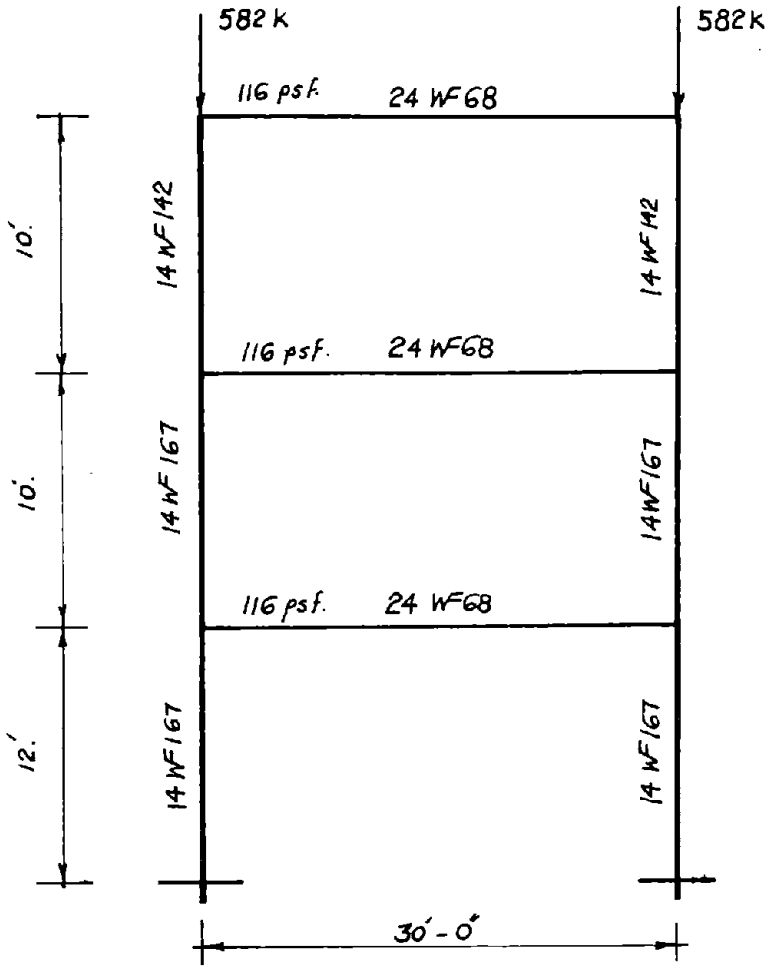

Fig. 5.1 - Three Story One Bay Frame

Model D - Elastic Nonlinear Model

In this model a pure elastic solution is performed. The P-Δ effect is introduced by using the stability functions.

The different models were subjected to the N.S. 1940 component of El Centro, magnified by 1.5. The version used is that designated as version (1) in Chapter III.

In order to investigate first the adequacy of the time step of integration for the fiber model, two runs were performed with Δt = 0.01 and 0.005 second. As indicated by figure 5.2, the results were almost identical.

Table 5.1 lists the fundamental periods of the different models, while Table 5.2 summarizes the base shears and the overturning moments obtained. The time histories of displacements at the top of the structure for the four models are presented in Figs. 5.3 through 5.6. Figs. 5.7 to 5.10 show a comparison of different response parameters.

The following observations can be made:

1. The 7-fiber model - which is theoretically the most exact - gives very similar results to the interaction model with all the nonlinear effects accounted for. The order of difference of their prediction is of the order of 10%, which can be expected considering the variation in the moment rotation relationships. This observation is confirmed by comparing the time histories in Figs. 5.3 and 5.5.

2. The earthquake forces for the inelastic models are much smaller than those of the corresponding elastic model.

3. Gravity effects and P-Δ effects do not seem to lead to any dynamic collapse for the case studied.

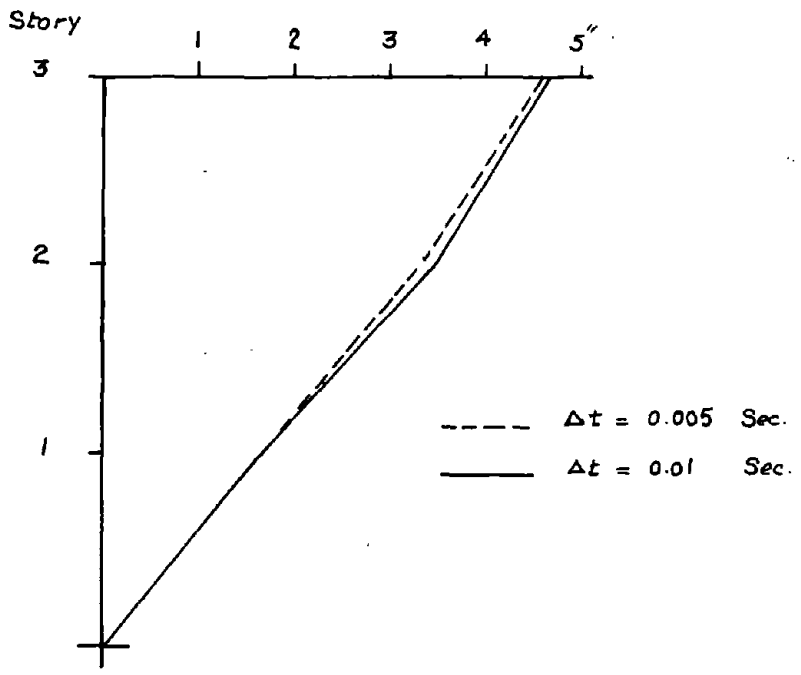

Fig. 5 .2 - Effect of Increment Size on the Behavior of a Fiber Model

Table 5.1

Fundamental Periods of Different Models

	Model	First	Second	Third
A	Interaction	.508	.140	.068
B	Pure Bending	.490	.137	.067
C	7-Fiber	.484	.135	.066
D	Elastic Nonlinear	.508	.140	.068

Table 5.2

Summary of Total Base Shear and Moments

	Model	Base Shear	Overturning Moment
A	Interaction	207.8	54559.9
B	Pure Bending	232.20	71248.3
C	7-Fiber	182.95	53686.3
D	Elastic Nonlinear	366.7	106857.2

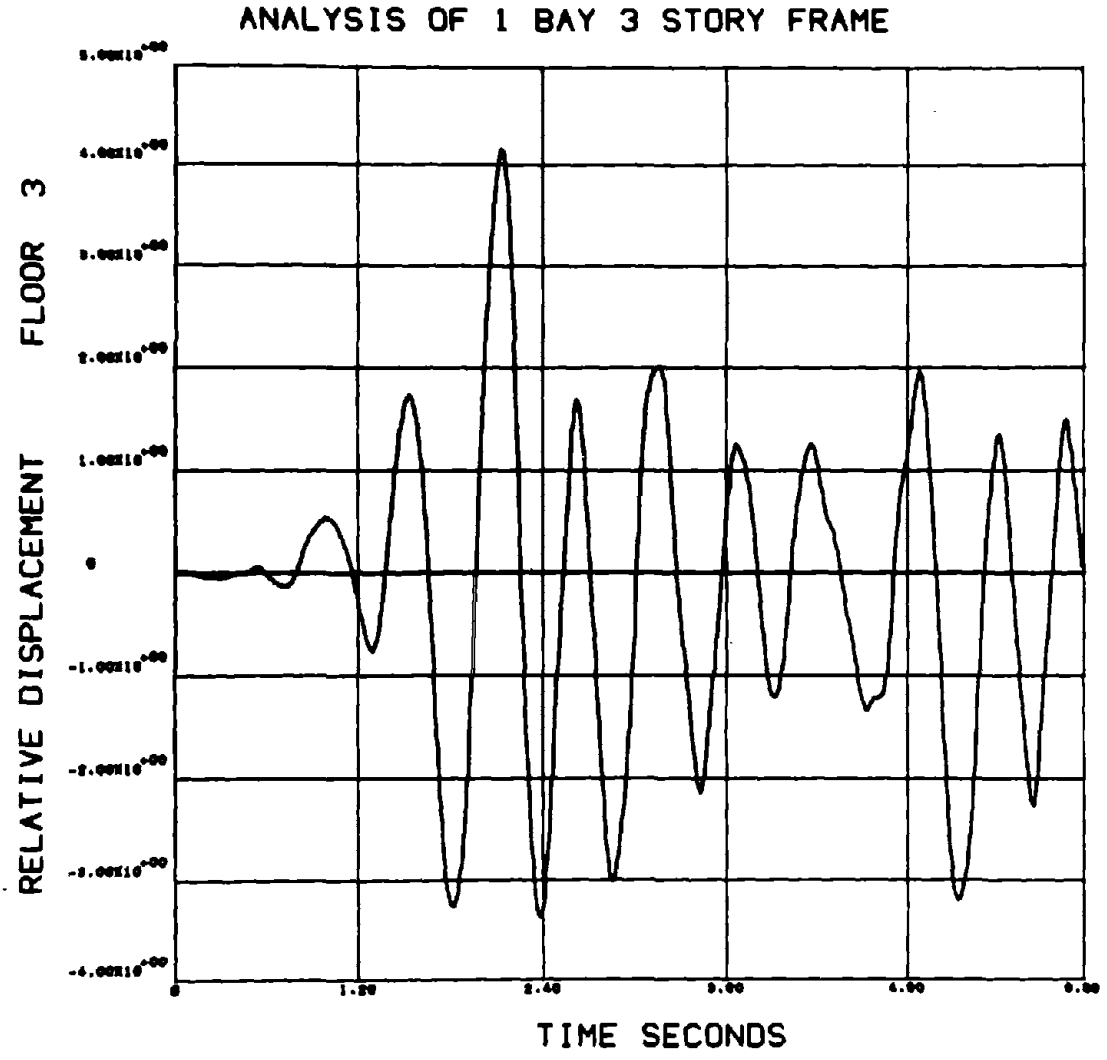

Fig.5 .3 - Behavior of the Interaction Model (Model A)

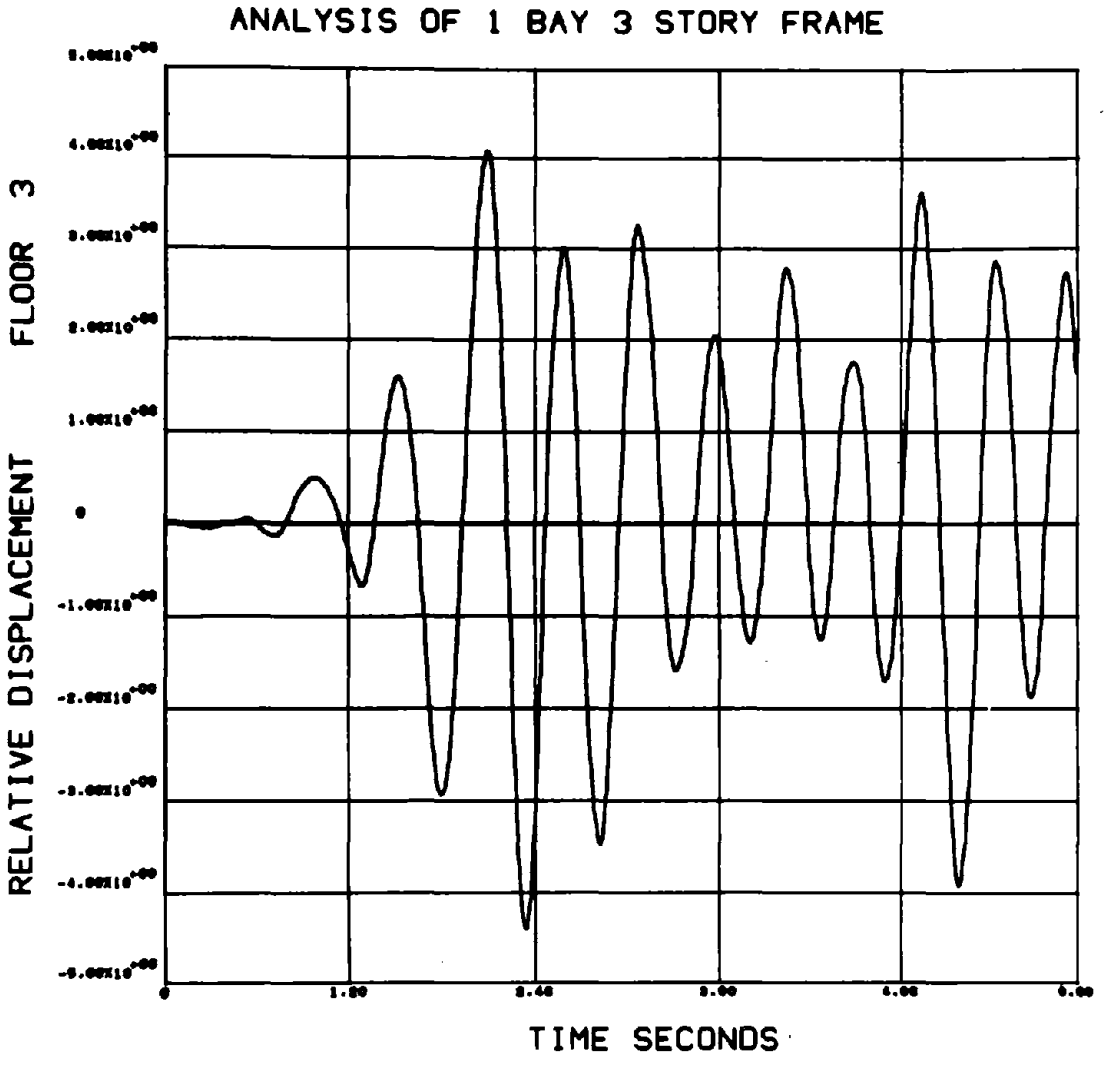

Fig. 5.4 - Behavior of the Bending Model (Model B)

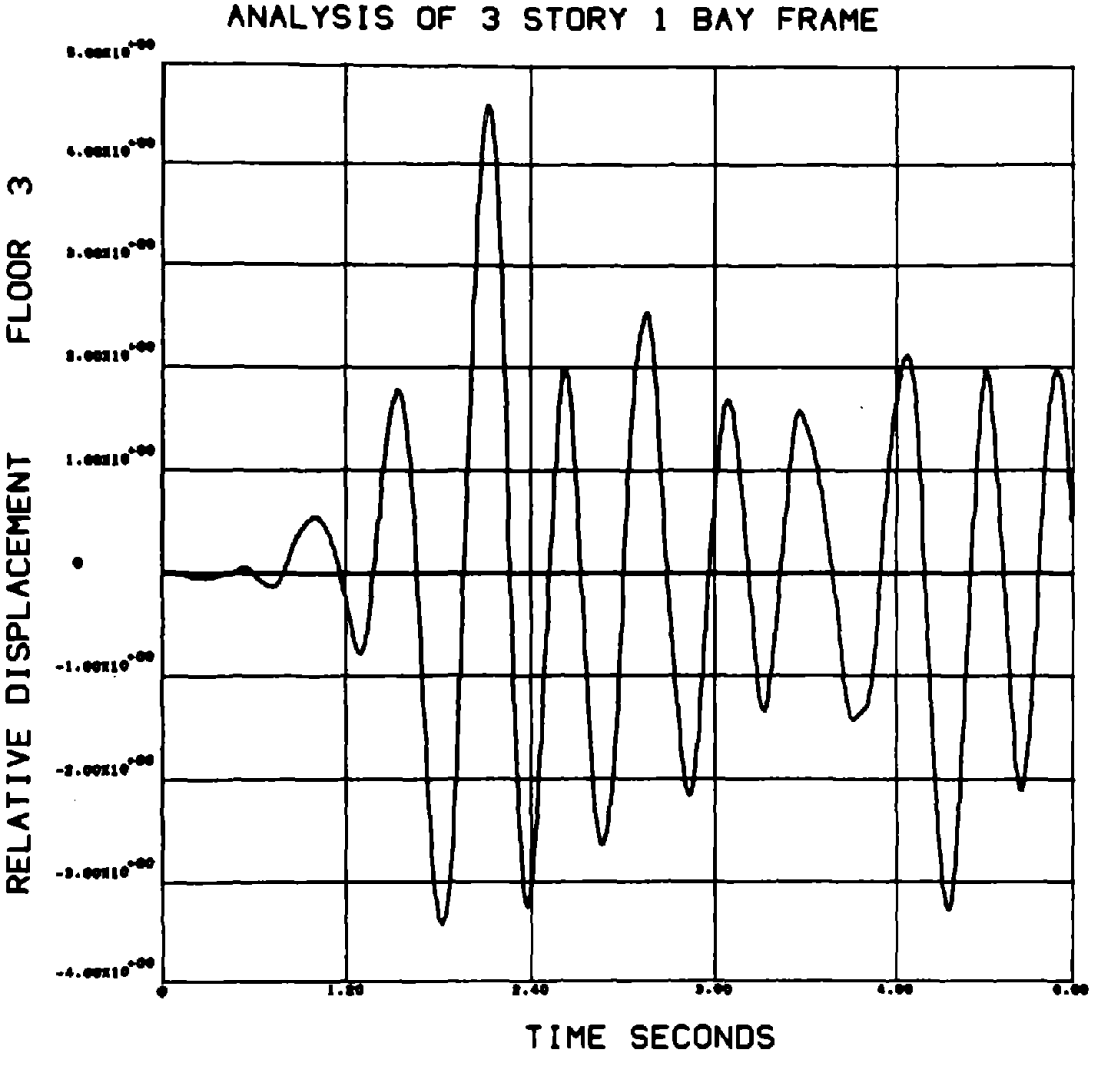

Fig. 5.5 - Behavior of the 7-Fiber Model (Model C)

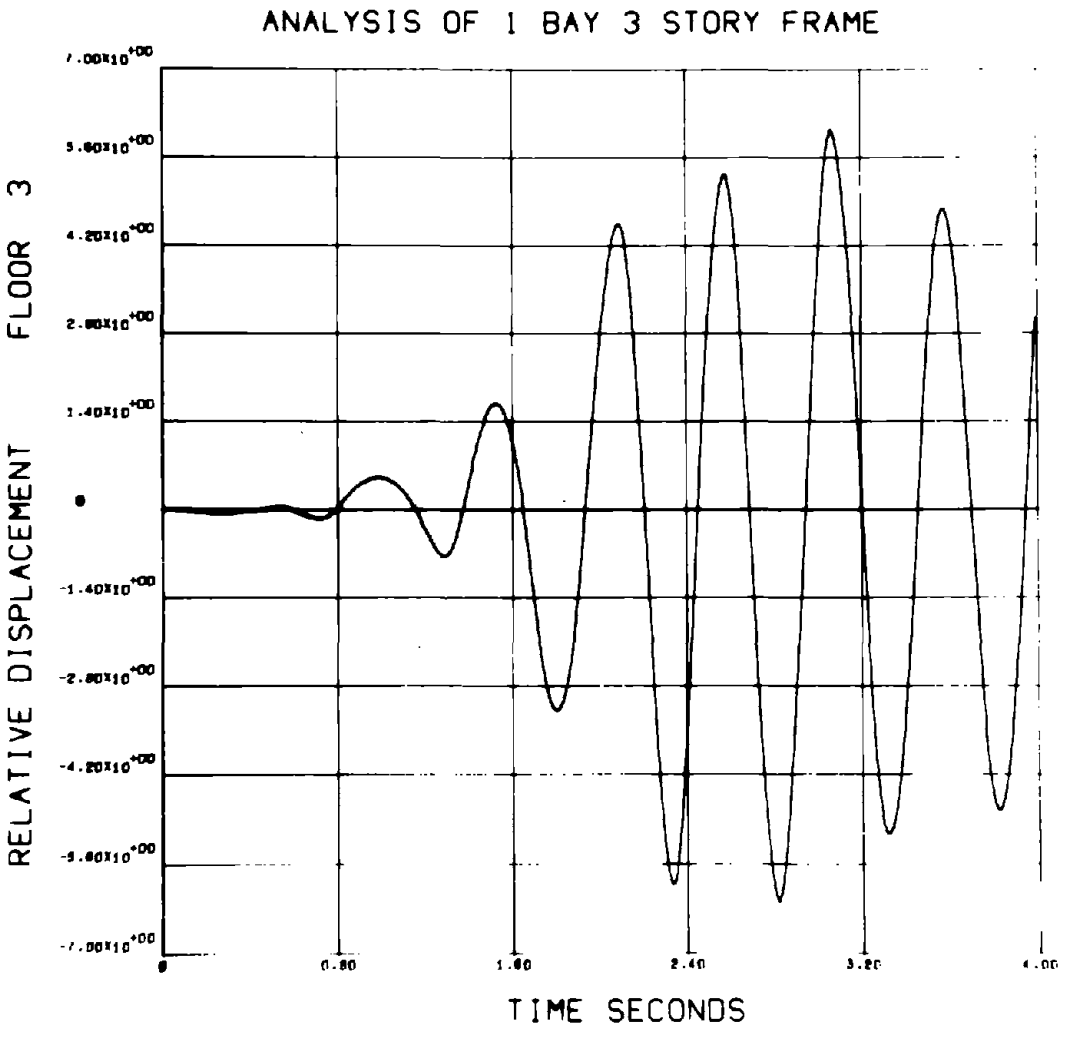

Fig. 5.6 - Behavior of the Elastic Nonlinear Model(Model D)

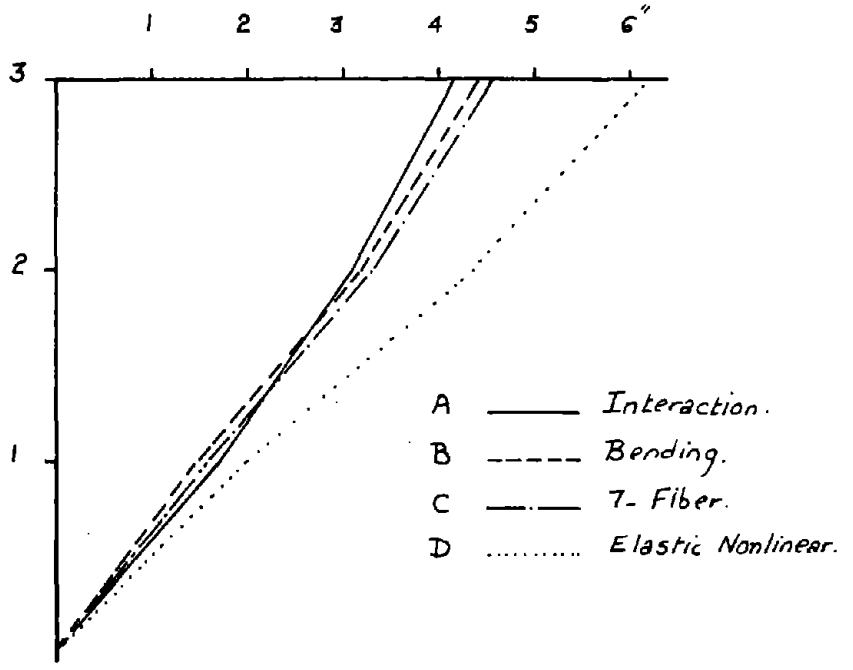

Fig. 5.7 - Maximum Displacements Relative to Ground for Different Models

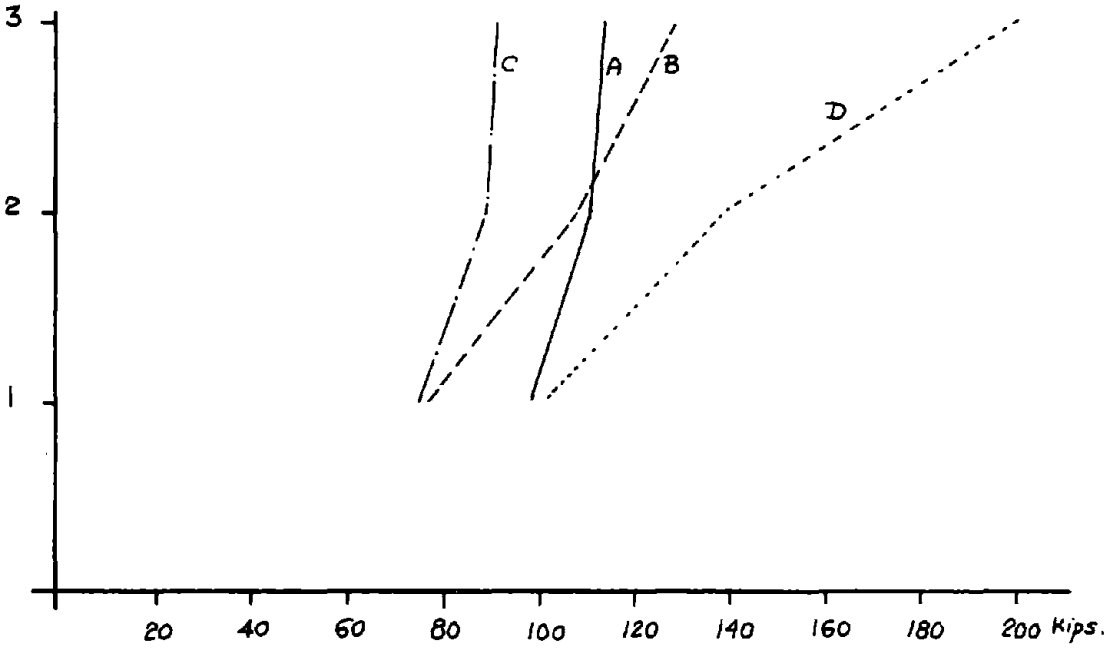

Fig. 5.8 - Maximum Story Forces for Different Models

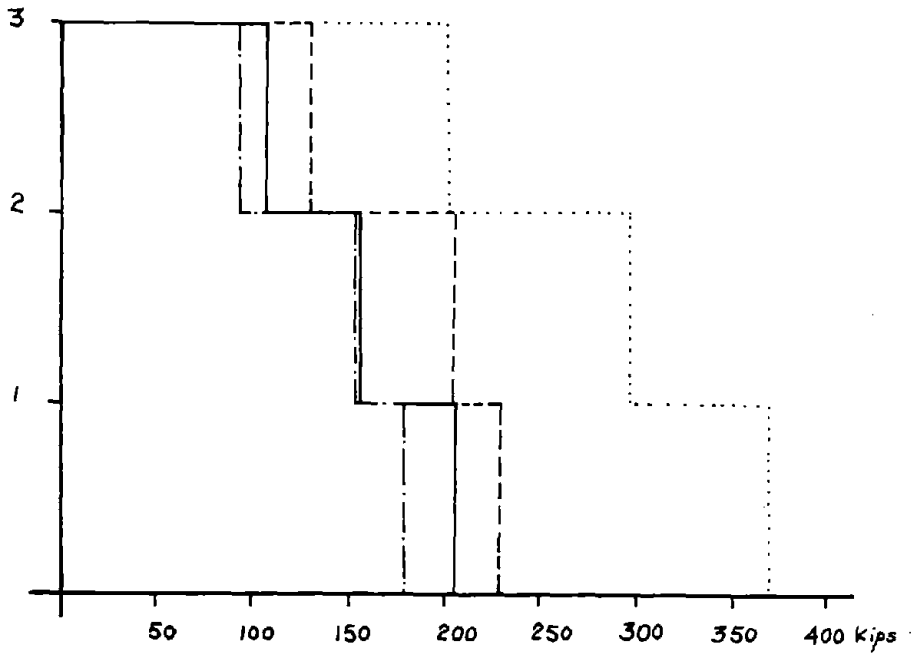

Fig. 5.9 - Story Shears for Different Models

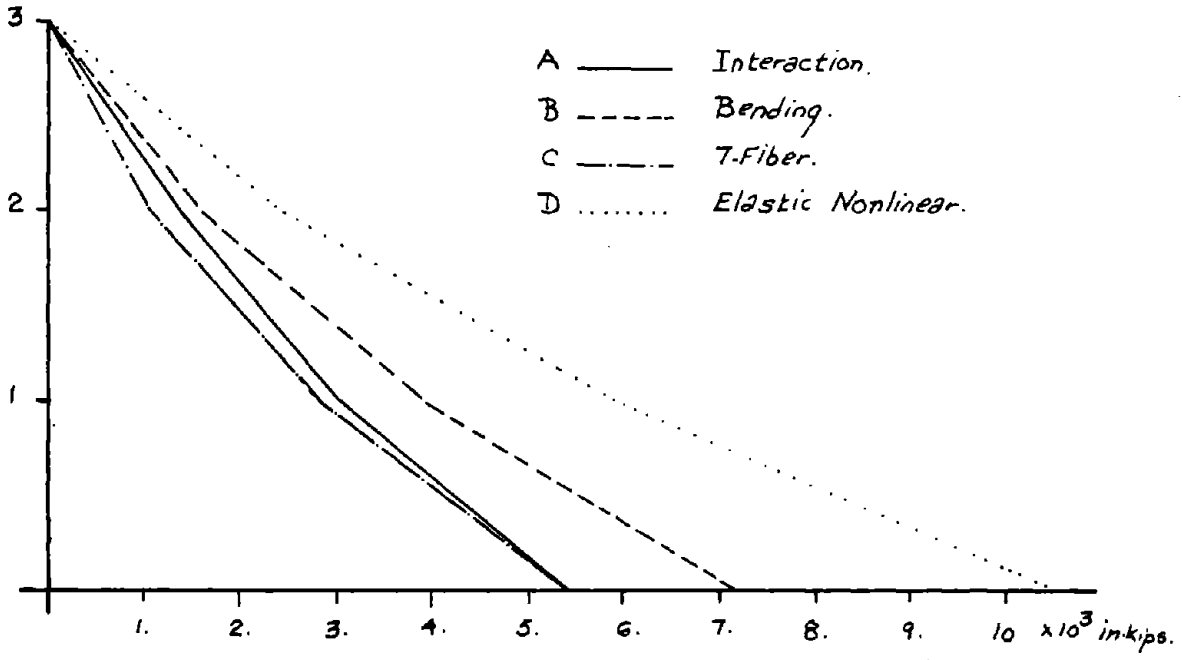

Fig. 5.10 - Overturning Moments for Different Models

CHAPTER VI

SUMMARY AND CONCLUSIONS

6.1 SUMMARY

In the current work attempts have been made to clarify some of the basic points associated with inelastic analysis of building frames.

The study is preceded by a review of the basic work done in the area, focusing on the features of each contribution and what factors it introduced in the analysis. Three levels of analytical models were discussed and compared: a simple model resulting in a close coupled system, where each story of a frame is replaced by an equivalent non-linear spring; intermediate models where point hinges are assumed to occur at the joints or at the ends of the members when the moment capacity is exceeded; and complex models, such as the fiber model, where account is taken of the spreading of yielding and of the coupling of axial and bending effects. The intermediate, point hinge or bending models are the ones most commonly used today and most of the work in this study was devoted to study their sensitivity to various assumptions. Simple models are particularly attractive from a practical point of view because of their reduced cost: in this work they were used in a standard form without any attempt to improve on the selection of the spring parameters (which may be a key point in ensuring their applicability). Fiber models are far too expensive for practical applications, but may be of value in resolving important questions, such as the best definition of ductility.

In Chapter II a formulation for the inelastic dynamic analysis of building frames has been presented. The formulation is general enough to take into consideration different nonlinearities which might occur in a building frame on a selective basis. The objective thus was to study the importance of each nonlinear effect separately and to point out those effects which may be more important than others. The types of nonlinearities studied can be grouped into two broad categories; those due to material behavior and those due to geometry changes.

Since the relative importance of each nonlinear effect is dependent on the shape of the building frame studied, some results may not be generalized and applied directly to other unusual configurations. Thus the objective here was only to demonstrate the relative importance of different effects for some building frames (a one-bay 10-story frame previously reported in the literature in particular). Ductility considerations as defined by fiber ductiliy, joint ductility, member ductility, and frame ductility were discussed. The need for a more general and consistent definition of ductility must be stressed.

Numerical problems like the overshooting and the backtracking were studied, and the effect of the time step for the integration of the nonlinear equations of motion was established. Comparisons between a general single component model "GSCM" and a dual component model "DCM" were conducted for the cases where they may be comparable. The study demonstrated that although a theoretical perfect match for both models is not possible, the results obtained will be very similar in cases

where both are applicable.

Different stability schemes were compared for some frames. The first-order solution scheme based on corrective terms added to the stiffness matrix proved to give almost identical results to a more accurate analysis using stability functions.

The relative importance of P-Δ effects in the analysis was also investigated. Based on the cases studied, it is concluded that P-Δ effects tend to increase both the displacements of the frame and the interstory displacements. It seems, however, to reduce the story shears. The P-Δ effects seem to put impact on ductility requirements in both columns and girders. The increase is more pronounced for the lower stories. It tends to increase joint distortions and member forces, but this might not cause physical collapse of the structure. The study demonstrated that under normal conditions the P-Δ effects are not as serious as might have been expected from some of the work reviewed, and in a code type approach for design, equivalent static forces might be determined to introduce such effects in the analysis. Currently codes are evolving, and it might be possible through more extensive studies for typical frames to push this approach forward in a rational way.

The effect of gravity loads proved to affect the response in several ways. Gravity loads on the structure may reduce substantially the elastic limit under lateral loads, due to earlier formation of inelastic action. It can introduce a considerable reduction in the

overall stiffness of the structure. Since the effective yield moments of the columns depend on the axial-flexural interaction, it is expected that gravity loads have more significant effect on these members. The effect may be magnified by the additional moments introduced due to the P-Δ effects. Considering gravity leads to larger ductility requirements for both girders and columns. It seems, however, that as far as the overall behavior is concerned, using a simplified bending model with reduced plastic moments due to the static initial axial forces in the columns gives results very similar to those of a more accurate interaction model.

Studies on the effect of axial deformation in the columns demonstrated that it might lead to an increase in the elastic period of the structure, which in turn may change the dynamic response. The accumulated effect of column distortions leads to an increase in the upper-story displacements, and also to an increase in the drift (and thus to a magnification in the P-Δ effects). An increase in plastic deformations and thus ductility requirements for both columns and girders is observed when axial deformations in the columns are properly taken into account.

Two factors which have opposite effects are the joint size and joint flexibility. The study showed that each one of them separately can produce an important variation in the results, affecting the fundamental period of the structure even in the elastic range. Further research should be directed towards a better understanding of the mech-

anism of deformation inside the beam-column overlap (panel zone).

From studies on the effect of damping, it was concluded that damping schemes used can be as important as many of the other nonlinear effects. Further research should also be directed to establish both the value and the mathematical form of damping to be used in dynamic analysis.

From the limited cases studied for soil-structure interaction effects through a nonlinear lumped model for the soil under the structure, it seems that soil-structure interaction has very little effect on the dynamic response of the type of frames studied.

In Chapter IV comparisons are made between the prediction of the most general bending model which includes all the nonlinear effects and the prediction of the least general bending model which neglects all the nonlinear effects. Different frames which appeared in the literature were used as working material for the comparative study. The two models were then used as yardsticks for evaluating simple approximate models based on the assumption of shear-type behavior of the frame. The study showed that the bending models seem to lead to more uniform variations of ductility through height than the simple model. The ability of the simple model to predict displacements is relatively good up to a certain story level, but deteriorates for the upper stories. As a result, interstory displacements are also poorly predicted in the upper part of the building.

Conceptually it may be possible to find properties for simple models which lead to a final response which matches better the correct ones. It is necessary, however, to do more work in order to find simple rules to derive spring parameters for each story.

The study demonstrated that sometimes the different nonlinear and gravity effects helped the frame to yield earlier, resulting in a reduction of its seismic forces and displacements.

In Chapter V different complex analytical models capable of performing a "theoretically exact" nonlinear analysis under a static or dynamic loading were discussed. These models are theoretically a refinement over the models presented before, but they may be more sensitive to numerical errors and require a smaller integration step.

Of particular importance in comparing results with these models is the need to define consistently the strain-hardening factor. In the presence of nonlinear effects, a small value of strain hardening becomes a crucial parameter, since it might prevent the dynamic collapse of the model, while its absence, combined with a certain type of ground motion, might lead to a free body motion.

The fiber model was compared with the interaction model. While a perfect match should not be expected, since many variables are defined in a different way, for the cases presented the two models gave almost identical results.

7.2 CONCLUSIONS

From the studies performed in this thesis, it would appear that for typical building frames a generalized bending model including all the nonlinear effects will yield results which are realistic and physically reasonable. Some additional work may be necessary to refine the way joint size and panel zone flexibility are accounted for and to determine the most realistic type of damping to use. Fiber models can theoretically be more exact, but they are also more sensitive to numerical errors. For the cases studied, use of these complex and expensive models does not seem justified. The difference in predictions reported by Latona for the three-story frame studied in Chapter V was not found in this study (the strain-hardening factor used by Latona was not known).

Simple models, while attractive because of their economy, need, however, further study to arrive at convenient and accurate determination of the stiffness characteristics of each story. Use of these models with some standard spring for each story will not yield satisfactory results, particularly in the upper part of the building.

References

1. Alvarez and Birnstiel, "Inelastic Analysis of Multistory Multi-bay Frames," Journal of the Structural Division, ASCE, Nov. 1969.

2. American Society of Civil Engineers, Commentary on Plastic Design in Steel, New York, 1961.

3. Anagnostopoulos, S.A., "Nonlinear Dynamic Response and Ductility Requirements of Building Structures subjected to Earthquakes," a Thesis submitted in partial fulfillment of the requirements for the degree of Doctor of Science, Sept., 1972.

4. Anderson, J.C., "Seismic Behavior of Multistory Frames Designed by Different Philosophies, Ph.D. Thesis, University of California, Berkeley, Dept. of Civil Engineering, 1969.

5. Anderson & Bertero, "Seismic Behavior of Multistory Steel Frames," Symposium on Earthquake Engineering, Indian Society of Earthquake Technology, Nov. 14-16, 1970.

6. Anderson & Gupta, "Earthquake-Resistant Design of Unbraced Frames," Journal of the Structural Division, ASCE, Nov. 1972.

7. Archer, J.S., "Consistent Mass Matrix for Distributed Systems," Journal of the Structural Division, ASCE, Aug. 1963.

8. Aziz, T.S., "Nonlinear Inelastic Analysis of Steel Frames," a Thesis submitted to Carleton University, Ottawa, Canada in partial fulfillment of the requirements for the degree of Master of Engineering, 1971.

9. Baron, Frank, and Benkateson, Mahadeva, S., "Inelastic Response for Arbitrary Histories of Loads," Journal of the Engineering Mechanics Division, ASCE, June 1969.

10. Basic Design Criteria of the Recommended Lateral Force Requirements and Commentary, ASCE, Journal of the Structural Division, Sept. 1972.

11. Berg, Glen V., and DaDeppo, Donald A., "Dynamic Analysis of Elastoplastic Structures," Journal of the Engineering Mechanics Division, ASCE, April 1960.

12. Ohile, J. Vasquez, Popov, E.P., and Bertero, V.V., "Earthquake Analysis of Steel Frames with Non-Rigid Joints," Fifth World Conference on Earthquake Engineering, Rome, 1973.

13. Blume, J.A., Newmark, N.M., and Corning, L.H., Design of Multistory Reinforced Concrete Buildings for earthquake Motions, Portland Cement Association, Skokie, Illinois, 1961.

14. Bolotin, V.V., The Dynamic Stability of Elastic Systems, Holden-Day, Inc., San Francisco, 1964.

15. Caughy, T.K., "Classical Normal Modes in Damped Linear Dynamic Systems," Journal of Applied Mechanics, ASME, June 1960.

16. Clough, Ray W., and Benuska, K.L., "FHA Study of Seismic Design Criteria for High-Rise Buildings," HUD ST-3, August 1966.

17. Clough, Ray W., and Benuska, K.L., "Nonlinear Earthquake Behavior of Tall Buildings," Journal of the Engineering Mechanics Division, ASCE, June 1967.

18. Clough, R.W., and Johnston, S.B., "Effect of Stiffness Degradation on Earthquake Ductility Requirements," Proceedings of the Japan Earthquake Engineering Symposium, 1967.

19. Clough, Benuska & Wilson, "Inelastic Earthquake Response of Tall Buildings," Third World Conference in Earthquake Engineering, New Zealand, 1969.

20. DiMaggio, Frank L., "Dynamic Elasto-Plastic Response of Rigid Frames," Journal of the Engineering Mechanics Division, ASCE, July 1958.

21. Fintel, M., and Kahn, F.R., "Shock-Absorbing Soft Story Concept for Multistory Earthquake Structures," Journal of the American Concrete Institute, May 1969.

22. Giberson, M.F., "The Response of Nonlinear Multistory Structures Subjected to Earthquake Excitation," thesis submitted to the California Institute of Technology at Pasadena in partial fulfillment of the requirements for the degree of Doctor of Philosophy, 1967.

23. Girijavallabhan,"Analysis of Shear Walls with Openings," Journal of the Structural Division, ASCE, Oct. 1969.

24. Girijavallabhan, "Buckling Loads of Nonuniform Columsn," Journal of the Structural Division, ASCE, Nov. 1969.

25. Goel, S.C., "Inelastic Behavior of Multistory Building Frames Subjected to Earthquake Motions," thesis submitted to the University of Michigan in partial fulfillment of the requirements for the degree of Doctor of Philosophy, 1967.

26. Goel, S.C., "P- and Axial Column Deformation in Aseismic Frames," Journal of the Structural Division, ASCE, August 1969.

27. Graham Powell, "Theory of Nonlinear Elastic Structures," Journal of the Structural Division, ASCE, Dec. 1969.

28. Gulkan, P., and Sozen, M.A., "Response and Energy-Dissipation of Reinforced Concrete Frames subjected to Strong Base Motions," Civil Engineering Studies, Structural Research Series No. 377, University of Illinois, 1971.

29. Guru, B.P., and Heidebrecht, A.C., "Factors Influencing Inelastic Response," Proceedings, 4th World Conference on Earthquake Engineering, Chile, 1969.

30. Hanson, R.D., and Alnati, A.M., "Post-Elastic Response of Mild Steel Structures," Proceedings of the 3rd Japan Earthquake Engineering Symposium, 1970.

31. Heidebrecht, Arthur C., Lee, Seng-Lip, and Fleming, John F., "Dynamic Analysis of Elastic-Plastic Frames," Journal of the Structural Division, ASCE, April 1964.

32. Horne, M.R., and Merchant, W., The Stability of Frames, Pergamon Press, New York, 1965.

33. Husid, Raul, "Gravity Effects on the Earthquake Response of Yielding Structures," Ph.D. Thesis, California Institute of Technology, 1967.

34. Jennings, P.C., "Equivalent Viscous Damping for Yielding Structures," Journal of the Engineering Mechanics Division, ASCE, Feb., 1968.

35. Jennings, P.C., "Response of Simple Yielding Structures to Earthquake Excitations," Thesis submitted to the California Institute of Technology at Pasadena in partial fulfillment of the requirements for the degree of Doctor of Philosophy, 1963.

36. Kaldjian, M.J., and Fan, W.R., "Earthquake Response of a Ramberg-Osgood Structure," Journal of the Structural Division, ASCE, Oct. 1968.

37. Kaldjian, Mouses, J., and Fan, W.R., "Earthquake Response of a Ramberg-Osgood Structure," Journal of the Engineering Mechanics Division, ASCE, Feb., 1969.

38. Kaldjian, Mouses J., "Moment-Curvature of Beams as Ramberg-Osgood Functions," Journal of the Structural Division, ASCE, Oct. 1967.

39. Kamil, H., "Optimum Inelastic Design of Unbraced Multistory Frames under Dynamic Loads," Ph.D. Thesis, University of California, Berkeley, June 1972.

40. Latona, R.W., "Nonlinear Analysis of Building Frames for Earthquake Loading," a Thesis submitted to the Massachusetts Institute of Technology in the partial fulfillment of the requirements for the Doctor of Philosophy Degree, 1970.

41. Lehigh University, Plastic Design of Multistory Frames, Lecture Notes Vols. 1 and 2, Bethlehem, Pennsylvania, August 1965.

42. Lionberger, Steve R., and Weaver, William Jr., "Dynamic Response of Frames with Nonrigid Connections," Journal of the Engineering Mechanics Division, ASCE, Feb. 1969.

43. Nielson, W.N., and Imbeault, F.A., "Validity of Various Hysteretic Systems," Proceedings of the 3rd Japan Earthquake Engineering Symposium, 1970.

44. Nigan, N.C., "Aseismic Design of Structures in the Inelastic Range," Symposium on Earthquake Engineering, Indian Society of Earthquake Technology, Nov. 14-16, 1970.

45. Otani, S., and Sozen, M.A., "Behavior of Multistory Reinforced Concrete Frames during Earthquakes," Civil Engineering Studies, Structural Research Series No. 392, University of Illinois, 1972.

46. Penzien, J., "Dynamic Response of Elasto-Plastic Frames," Journal of the Structural Division, ASCE, July 1960.

47. Pérez, Fernando, "Comportamiento Plástico de Pórticas Bajo Cargo Dinámica," Engineering Thesis, Universidad Católica de Chile, Santiago, Chile, 1968.

48. Popov and Pinkroy, "Cyclic Yield Reversal in Steel Building Connections," Journal of the Structural Division, ASCE, March 1969.

49. Saul, W.E., Fleming, J.F., and Lee, S.L., "Dynamic Analysis of Bilinear Inelastic Multiple Story Shear Buildings," Proceedings of the Third World Conference on Earthquake Engineering, Vol. II, New Zealand, 1965.

50. Veletsos, A.S., "Maximum Deformation of Certain Nonlinear Systems," Proceedings of the Fourth World Conference on Earthquake Engineering, Santiago, Chile, January 1969.

51. Veletsos, A.S., and Newmark, N.M., "Effect of Inelastic Behavior on the Response of Simple Systems to Earthquake Motions," Proceedings, 2nd World Conference on Earthquake Engineering, Japan, 1960, Vol. II.

52. Walpole, Warren R., and Shepherd, Robin,"Elasto-Plastic Seismic Response of Reinforced Concrete Frame," Journal of the Structural Division, ASCE, Oct. 1969.

53. Wen, R.K., Janssen, J.G., "Dynamic Analysis of Elasto-Inelastic Frames," Proceedings, 3rd World Conference on Earthquake Engineering, New Zealand, 1965, Vol. II.

54. Whetstone, "Computer Analysis of Large Linear Space Frames," Journal of the Structural Division, ASCE, Nov. 1969.

55. Whitman and Richart, "Design Procedures for Dynamically Loaded Foundations," Journal of the Soil Mechanics Division, ASCE, June 1967.

56. Yura and Lu, "Ultimate Load Tests on Braced Multistory Frames," Journal of the Structural Division, Oct. 1969.

57. Timoshenko, S.P., and Gere, J.M., Theory of Elastic S tability, 2nd Ed., McGraw-Hill Book Company, New York, 1961.

58. Livesely, R.K., Matrix Methods in Structural Analysis, Pergamon Press, 1964.

59. Roesset, J.M., Unpublished Lecture Notes on Stability of Structures, Massachusetts Institute of Technology, Cambridge, Massachusetts.

60. Archer, J.S., "Consistent Mass Matrix for Distributed Systems," Proceedings of the ASCE, Structural Division, Vol. 89, Aug. 1963, p. 161.

61. Archer, J.S., "Consistent Matrix for Formulation for Structural Analysis Using Finite Element Techniques," AIAA Journal, Vol. 3, No. 10, Oct. 1965. P. 1910.

62. Parelee, R.A., Perelman, D.S., Lee, S-L, and Keer, L.M., "Seismic Response of Structure-Foundation Systems," Journal of Engineering Mechanics Division, ASCE, Vol. 95, No. EM6, pp. 1295-1315, 1968.

63. Bycroft, G.N., Arnold, R.N., and Warburton, G.B., Journal of Applied Mechanics, Vol. 22, No. 3, 1955, pp. 391-400.

64. Biggs, J.M., and Grace, P.H., "Seismic Response of Buildings Designed by Code for Different Earthquake Intensities," Report R73-7, Structures Publication No. 358, M.I.T. Dept. of Civil Engineering, Jan. 1973.

65. Isbell, J.E., Biggs, J.M., "Inelastic Design of Building Frames to Resist Earthquakes," Report R74-36, Structures Publication No. 393, M.I.T. Dept. of Civil Engineering, May 1974.

APPENDIX A

STIFFNESS MATRIX OF A FIBER MODEL

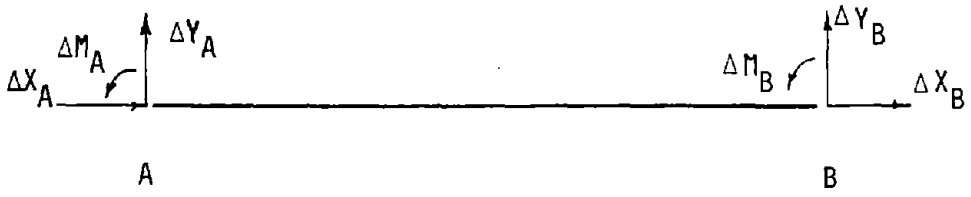

$$\Delta F_A = \begin{bmatrix} \Delta X_A \\ \Delta Y_A \\ \Delta M_A \end{bmatrix} \qquad \Delta U^* = \begin{bmatrix} \Delta U_A - \Delta U_B \\ \Delta V_A - \Delta V_B + L\Delta\theta_A \\ \Delta\theta_A - \Delta\theta_B \end{bmatrix}$$

$$\Delta U^* = F \cdot \Delta F_A$$

$$\begin{bmatrix} \Delta N \\ \Delta M \end{bmatrix} = \begin{bmatrix} K_{11} & K_{12} \\ K_{21} & K_{22} \end{bmatrix} \begin{bmatrix} \Delta\epsilon \\ \Delta\phi \end{bmatrix}$$

$$\begin{bmatrix} \Delta\epsilon \\ \Delta\phi \end{bmatrix} = \begin{bmatrix} f_{11} & f_{12} \\ f_{21} & f_{22} \end{bmatrix} \begin{bmatrix} \Delta N \\ \Delta M \end{bmatrix}$$

$$F_{11} = \int_0^L f_{11}\, dx$$

$$F_{12} = -\int_0^L x\, f_{12}\, dx$$

$$F_{13} = \int_0^L f_{12}\, dx$$

$$F_{21} = \int_o^L (L-x)\, f_{21}\, dx = L \cdot F_{13} + F_{12}$$

$$F_{22} = -\int_o^L x(L-x)\, f_{22}\, dx$$

$$F_{23} = \int_o^L (L-x)\, f_{22}\, dx = L \cdot F_{33} + F_{32}$$

$$F_{31} = \int_o^L f_{21}\, dx$$

$$F_{32} = -\int_o^L x \cdot f_{22}\, dx$$

$$F_{33} = \int_o^L f_{22}\, dx$$

$$\underset{\sim}{K} = \begin{bmatrix} K_{ii} & K_{ij} \\ K_{ji} & K_{jj} \end{bmatrix}$$

$$K = F^{-1}$$

$$K_{ii} = K\, T_i$$

$$K_{ij} = -K_{ii}$$

$$K_{ji} = T_j\, KT_i = T_j\, K$$

$$K_{jj} = -T_j\, K$$

$$T_i = \begin{bmatrix} 1 & 0 & 0 \\ 0 & 1 & L \\ 0 & 0 & 1 \end{bmatrix} \qquad \text{and} \qquad T_j = \begin{bmatrix} -1 & 0 & 0 \\ 0 & -1 & 0 \\ 0 & L & -1 \end{bmatrix}$$

50272-101

REPORT DOCUMENTATION PAGE	1. REPORT NO. NSF/RA-761665	2.	3. Recipient's Accession No. PB296609

4. Title and Subtitle
Inelastic Dynamic Analysis of Building Frames

5. Report Date
August 1976

6.

7. Author(s)
T.S. Aziz

8. Performing Organization Rept. No.
R76-37

9. Performing Organization Name and Address
Massachusetts Institute of Technology
School of Engineering
Department of Civil Engineering
Cambridge, Massachusetts 02139

10. Project/Task/Work Unit No.
Order No. 554

11. Contract(C) or Grant(G) No.
(C)
(G) GI43106

12. Sponsoring Organization Name and Address
Applied Science and Research Applications (ASRA)
National Science Foundation
1800 G Street, N.W.
Washington, D.C. 20550

13. Type of Report & Period Covered

14.

15. Supplementary Notes

16. Abstract (Limit: 200 words)

The nonlinear dynamic behavior of building frames is considered. The study covers basic points associated with inelastic dynamic analysis procedures. A formulation for the inelastic analysis of a building frame is presented. The formulation is general enough to take into consideration different nonlinearities which might occur in a building frame on a selective basis. Two types of nonlinearities are studied: those due to material behavior and those due to geometry changes. The importance of each nonlinear effect is studied separately and those effects which might be more important than others are pointed out. Among the different effects studied are the P-Δ and stability effects, the presence of gravity loads, axial deformations in the columns, joint size and nonlinear joint behavior, damping, and nonlinear soil-structure interaction. Comparisons are made between different complex, intermediate, and simple models for inelastic dynamic analysis. From the studies performed, it would appear that for typical building frames a generalized bending model including all the nonlinear effects will yield results which are realistic and physically reasonable. Complex models can be theoretically more exact, but they are also more sensitive to numerical errors. For the cases studied, use of these complex and expensive models does not seem justified.

17. Document Analysis a. Descriptors

Dynamic loads
Dynamic structural analysis
Structural analysis
Elastic properties
Hysteresis

b. Identifiers/Open-Ended Terms

Nonlinear inelastic planar frames

c. COSATI Field/Group

18. Availability Statement	19. Security Class (This Report)	21. No. of Pages
NTIS		230
	20. Security Cl.	

(See ANSI-Z39.18) See Instructions on Reverse

(Formerly NTIS-35)
Department of Commerce

CAPITAL SYSTEMS GROUP, INC.
5110 EXECUTIVE BOULEVARD
SUITE 250
ROCKVILLE, MARYLAND 20852